THE UNIVERSITY OF HULL

SOME ASPECTS OF INTERNAL AERATION IN WETLAND PLANTS

being a thesis submitted for the degree of

DOCTOR OF PHILOSOPHY

in the University of Hull

by

THOMAS JOSEPH GAYNARD, B.Sc.

May, 1979

ACKNOWLEDGEMENTS

I would like to express my most sincere appreciation to Dr.W.Armstrong, for his advice and guidance throughout this investigation, and to Professor J.Friend, for making available to me the facilities in the Department of Plant Biology.

I am extremely grateful to all the members of the technical staff of the Plant Biology Department, but in particular I would like to thank the following: Miss S.Lythe, for much technical advice and assistance, and for preparing many of the figures; Mr.E.J.Wright, for designing and building the polarographic equipment, and for constructing the electrical analogue; Mr.P. Meaker, Mr. K. Anderson and the late Mr.P. Smith, for help with the photography; Miss K.A. Braithwaite and Mr.V.Swetez, of the University Botanic Gardens, for cultivating the experimental plants.

I am also indebted to Mr. P. B. Cashman, for advice on certain of the mathematical aspects, and to Miss J. Walton, for typing the thesis.

Finally, I wish to express my gratitude to my parents and family, for their interest and support during the course of this study, and throughout the years before.

CONTENTS

CHAPTER 1

INTRODUCTION

This thesis is concerned with certain factors relating to the ability of wetland plants to exploit soils devoid of molecular oxygen.

In unsaturated soils the aerobic metabolism of soil organisms is facilitated by the presence in the soil of non-capillary pores, which provide a low resistance pathway for gas exchange with the atmosphere. This aeration process is chiefly diffusive, though under certain circumstances (eg. during rapid temperature fluctuations) mass flow may occur (Grable, 1966; Wood and Greenwood, 1971). In the unsaturated soil diffusion will take place largely in the gas phase and owing to the high diffusivities of the atmospheric gases in air it is likely to be fairly rapid. However, soil organisms, including roots, are invariably surrounded by water films, hence the last stage in the aeration pathway will take place in the liquid phase. In the case of oxygen, the diffusion coefficient in water is some 10,000 times less than in air (2.267×10^{-5} and $0.205\ cm^2 s^{-1}$ respectively). In addition the concentration of oxygen undergoes a 29-fold drop in passing from gas to liquid phase. Consequently the greatest physical impedance to the diffusive flow of oxygen in a soil is that provided by water.

The high resistance to oxygen diffusion offered by the water path may be illustrated by use of an equation derived by Kristensen and Lemon (1964); by means of this equation the thickness of water film which will allow a root to remain wholly aerobic may be predicted. The equation is:

$$\log \left(\frac{r_r}{b}\right) = \frac{D_{e,w}}{D_{e,r}} - \frac{2\, D_{e,w} C_w}{M_e r_r^2} \qquad (1.1)$$

where

r_r = the root radius (cm)

b = the critical radial distance from centre of root to the outer boundary of the water film at which the root remains just wholly aerobic (cm)

$D_{e,w}$ = the effective diffusion coefficient for oxygen within the water film ($cm^2 s^{-1}$)

C_w = the equilibrium oxygen concentration at the outer boundary of the water film ($g\ cm^{-3}$)

$D_{e,r}$ = the effective radial diffusion coefficient for oxygen within the root ($cm^2 s^{-1}$)

M_r = the rate of root oxygen consumption ($g\ cm^{-3} s^{-1}$)

For example, in the case of a root of radius 0.05cm and respiratory rate 100ng O_2 $cm^{-3} s^{-1}$ the critical water film thickness ($b - r_r$) would be only 0.0423cm, even if the outer surface of the water film was at air-saturation ($D_{e,w}$ and $D_{e,r}$ taken as 1×10^{-5} and 7×10^{-5} $cm^2 s^{-1}$ respectively - Armstrong, 1978).

If oxygen sinks were not present within a soil there would be no net diffusive flux of oxygen and the soil would remain at air saturation regardless of the magnitude of the physical diffusion barriers. The presence of aerobically-respiring organisms may be said to effectively magnify the resistance to oxygen diffusion, and the aeration status of a soil will depend upon the rate of oxygen supply on the one hand and the rate of its depletion on the other. This synergism between physical diffusion barriers and oxygen sink activities may be considered as "effective resistance" to oxygen diffusion. An increase in either or both components of effective resistance will result in a decrease in the aeration status of the soil. Anaerobiosis will ensue if effective resistance becomes infinite. Clearly, excessive soil water will increase the diffusive impedance, and waterlogging is a sure way to produce infinite resistance. Unless the soil is flushed by running water it will become anaerobic in all but a shallow surface layer (Armstrong and Boatman, 1967; Ponnamperuma, 1972). This may be illustrated by use of an equation derived by Greenwood (1967b):

$$L = \frac{D_{e,soil}\ C_{o,a}}{M_{soil}} \quad cm \qquad (1.2)$$

where:

$D_{e,soil}$ = the effective diffusion coefficient of oxygen in waterlogged soil ($cm^2 s^{-1}$)

$C_{o,a}$ = the concentration of oxygen in air ($g\ cm^{-3}$)

M_{soil} = the rate of soil oxygen consumption ($g\ cm^{-3} s^{-1}$)

L = the depth at which the O_2 concentration falls to zero (cm).

For example, if $D_{e,soil}$ is 1×10^{-5} $cm^2 s^{-1}$ (Greenwood and Goodman, 1967) and M_{soil} is 5.27×10^{-8} $g\ cm^{-3} s^{-1}$ (Teal and Kanwisher, 1961), oxygen will penetrate the soil to a depth of only 0.057cm.

Plant organs situated in waterlogged soil are subject to a number of physiological stresses arising directly or indirectly from the absence of oxygen in the rooting medium.

Some Characteristics of Waterlogged Soils

Water displaces air from soil pores, and although waterlogged soil may contain up to about 10% gas-filled pore space (Grable and Siemer, 1968) this will be discontinuous. Oxygen present within the gas-filled pores and dissolved in the soil water is rapidly depleted by the aerobic respiration of soil organisms and its concentration falls quickly to zero. This has been demonstrated by Scott and Evans (1955) who monitored the fall in oxygen concentration in air-dried soil after flooding with air-saturated water. They found that the oxygen concentration became zero after only 6-10h. Greenwood and Goodman (1967) used a polarographic method to show that the oxygen concentration fell from air-saturation at the surface to zero within 0.2cm inside saturated soil spheres. They found also that the diffusion coefficient of oxygen in such spheres was a factor of 2×10^4 less than its value in air.

It is of importance to note that in unsaturated soils also oxygen supply to the root surface may fall below that optimum for respiration, particularly when the root lies within a localised anaerobic zone. Greenwood (1968) has suggested that unsaturated soils consist of water-

saturated pockets surrounded by gas-filled unsaturated regions. Direct observations on the distribution of water in translucent porous materials tend to confirm this (Williams, 1967). Intra-crumb capillary pores become water-filled before the larger inter-crumb pores and Currie (1961, 1962) has shown theoretically that anaerobic zones may occur within saturated crumbs which are above a critical radius even though the inter-crumb pores may be gas-filled. Since roots are often situated within the intra-crumb pores (Currie, 1961) they may be embarrassed by low oxygen levels even though the gas-filled fraction of the soil as a whole may be considerable.

Exhaustion of soil oxygen following waterlogging results in the quiescence or death of obligate aerobic microorganisms and the proliferation of facultative or obligate anaerobes. Using organic matter as substrate and various oxidised soil components as electron acceptors the microbes effect drastic chemical changes within the soil environment. Ponnamperuma (1972) lists these as: (a) decrease in redox potential, (b) increase in the pH of acid soils and decrease in the pH of alkaline soils, (c) changes in specific conductance and ionic strength, (d) shifts in mineral equilibria, (e) cation and anion exchange reactions, (f) sorption and desorption of ions. Among the more important changes in inorganic equilibria are the following reductions: $NO_3^- \longrightarrow N_2$, $Mn^{4+} \longrightarrow Mn^{2+}$, $Fe^{3+} \longrightarrow Fe^{2+}$, $SO_4^{2-} \longrightarrow H_2S$, $CO_2 \longrightarrow CH_4$, $N_2 \longrightarrow NH_3$, $H^+ \longrightarrow H_2$. In addition many organic compounds accumulate, including lower fatty acids, alcohols and ethylene. Amongst the numerous products of reduction are many substances of proven phytotoxicity (see Rowe and Beardsell, 1973).

The reduction process proceeds in a stepwise manner and its intensity is reflected in a sequential lowering of the soil redox potential. The sequence is basically that predicted by thermodynamics (Ponnamperuma, 1972). For example, experiments by Turner and Patrick (1968) indicate that nitrate reduction is the first to follow (or accompany) the depletion

of oxygen, and the presence of nitrate prevents reduction of other soil components, maintaining the redox potention (E_7) at between 0.2 and 0.4V. Release of exchangable manganese, due to reduction of insoluble MnO_2, follows the disappearance of NO_3^-. Reduction of iron is associated with redox potentials of around 0.15V, high concentrations of soluble Fe^{2+} compounds being present at -0.15V. Sulphate reduction is probably associated with a redox potential of zero volts, whilst methane formation may commence only at the lower value of -0.15V (Takai and Kamura, 1966).

The reduced components, together with facultative anaerobes, constitute a latent oxygen sink within the soil (Scott and Evans, 1955; Teal and Kanwisher, 1961) and soils of low redox potentials may be considered to be "negatively aerated". However, no constant relationship between redox potential and soil oxygen regime has been reported, though at low oxygen levels redox potential shows a rapid increase for a very small rise in oxygen concentration (Scott and Evans, 1955; Armstrong 1967a; Turner and Patrick, 1968).

Adverse Effects of Soil Waterlogging

The subterranean organs of plants growing in permanently waterlogged soil are faced with two potential causes of physiological disturbance: anoxia itself and the presence of soil phytotoxins. There is much interspecific variation in tolerance to soil waterlogging. A large assemblage of plants are endemic to wetland sites whilst others may suffer drastically if subjected to soil anoxia; between these extremes are varying degrees of tolerance. According to their ability to withstand waterlogging plants may be roughly divided into "wetland" and "non-wetland" species; in general the latter suffer impeded growth when subjected to low oxygen levels in the rooting medium. There is abundant evidence in the literature to illustrate this and the following are but a few examples.

Yu et al. (1969) observed the responses of barley, corn, sunflower, tomato and wheat plants subjected to various degrees of soil waterlogging

and found that full flooding produced decreased growth rates and dry weights in all species. Similarly, Sojka et al. (1975) found that decreasing soil oxygen levels between 21% and zero reduced total, root and top dry weights, leaf area and tillering in wheat. Geisler (1967) found that root growth in barley and pea declined at soil oxygen concentrations below 7 and 14% respectively. Healy (1975), also working with pea, found that primary root elongation in liquid medium continuously bubbled with nitrogen was much slower than that in air-bubbled medium; root growth ceased in the N_2-bubbled medium after four days (root length 5.8cm) whilst roots in air-bubbled medium continued their growth unchecked. There was also a reduction in shoot growth in the plants subjected to nitrogen bubbling.

Armstrong and Boatman (1967) found that Molinia caerulea (L.) Moench. grew well on valley bog soils only where the soil was "flushed" with running water; they suggested that this was a consequence of the increased soil oxygen levels in comparison to the unflushed parts of the bog. Summerfield and Rieley (1974) similarly concluded that increased productivity of Narthecium ossifragum (L.) Huds. on areas of mire with lateral water movement was at least in part a consequence of improved aeration.

Root growth of pine and spruce seedlings was found by Leyton and Rouseau (1958) to fall rapidly when the roots were subjected to a liquid phase oxygen concentration corresponding to 10% in the gas phase; if completely deprived of oxygen the seedlings died within two days. Boggie (1972) grew Pinus contorta Loud. on deep peat having various heights of water table and found that root growth was severely restricted to aerobic horizons. Working with sitka spruce on upland peaty gleys Armstrong et al. (1976) showed that the largest and most stable trees were found on areas having improved soil aeration. They concluded that high water tables were a cause of poor tree growth. Adams et al. (1972) had previously arrived at a similar conclusion.

Precise Physiological Effects of Anoxia

Although the precise manner in which soil waterlogging causes retarded growth is not yet fully understood, the following have been suggested as contributing factors.

1. Formation of Autotoxic Substances

In roots completely deprived of oxygen aerobic respiration will cease and anaerobic respiration will ensue. Various end products of anaerobic metabolism have been reported and some of these are potentially phytotoxic (Fulton and Erickson, 1964; McManmon and Crawford, 1971; Rowe and Beardsell, 1973). Crawford (1966) and McManmon and Crawford (1971) showed a positive correlation between ethanol accumulation and sensitivity to waterlogging in species of Senecio. However, it has been assumed, rather than shown, that ethanol accumulates within plants to toxic levels. In fact Rowe (1966) showed a self-regulating mechanism for ethanol production in roots of peach, plum and pear. Several other species, including Iris pseudacorus L. (Boulter et al., 1963) and Nyssa sylvatica (Walt.) Sarg. (Hook et al., 1971) have been shown to produce ethanol without apparent ill-effects.

Rowe and Beardsell (1973) have reviewed work which shows that cyanide may be an important autotoxic substance produced in certain plants. When the roots of peach, apricot and plum, for example, were subjected to anaerobiosis, the hydrolysis of cyanogenic glycoside released phytotoxic amounts of HCN. This lead to inhibition of respiration and eventual root death.

Rowe and Beardsell (1973) cite work by Kawase (1972) in which ethylene production was apparently induced by waterlogging in cuttings, roots and bulbs of several horticultural species. More recently other workers have obtained an apparent correlation between flooding damage symptoms and increased ethylene concentration in flooded plants (El-Beltagy and Hall, 1974; Jackson and Campbell, 1975a,b). Ethylene may therefore be regarded as an autotoxic substance, but its role has not yet been determined.

2. Water Absorption and Membrane Permeability

A common feature of waterlogging injury is the wilting of leaves. Rowe and Beardsell (1973) review work by various authors which indicates that oxygen is necessary for uptake and transport of water.

Inhibitors of metabolism, such as cyanide and H_2S, produce effects similar to waterlogging and Slatyer (1967) suggests that the energy depletion resulting from anoxia causes decreased membrane permeability and reduced water uptake. Weakened osmotic gradients due to a reduction in ion absorption (q.v.) may enhance the effect of lowered membrane permeability.

3. Uptake and Transport of Nutrients

The uptake of nutrients by the root is at least in part an active process (Kramer, 1966; Etherington, 1975). Therefore, it may be expected that a drastic reduction in the energy output of the root system, such as that caused by the onset of anaerobic respiration, will result in reduced nutrient absorption. There are many examples in the literature which show this to be the case and Rowe and Beardsell (1973) have reviewed several of these. The uptake of nitrogen, phosphorus, potassium and calcium is especially dependent upon adequate root aeration.

4. Synthetic Activites and Hormone Imbalance

It is known that in various species organic nitrogen, sulphur and phosphorus compounds are synthesised in the roots and pass into the xylem. Kramer (1966) suggests that reduced synthesis of such compounds due to inadequate root aeration may reduce shoot growth.

Roots also produce hormones and it is likely that certain of the symptoms of waterlogging, such as leaf epinasty, are due to hormone imbalance brought about by anoxia in the root system (Kramer, 1966; Rowe and Beardsell, 1973).

5. Susceptibility to Pathogens

Soil waterlogging may increase the susceptibility of plants to pathogenic organisms (eg. Zentmyer, 1966). The root systems themselves

may become more susceptible to attack or the shoot system can become the centre of infection due to metabolic disorders in the anoxic roots. Rowe and Beardsell (1973) list possible reasons for the increased activity of pathogenic phycomycetous fungi in waterlogged conditions; these include: the dependence of zoospore production and dispersal on free water, the ability of the fungi to tolerate impeded gas exchange, weakening of the host due to root asphyxiation, and increased fungal substrate exudations from the host under anaerobiosis.

6. Disruption of cell ultrastructure

Vartapetian (1973) and Vartapetian et al. (1970) have obtained evidence of mitochondrial damage in the roots of various species when subjected to anoxia. Their results suggest that in this respect wetland plants may be the more sensitive. Mitochondrial damage was evident in meristematic cells of detached rice roots after only 4 to 5h of nitrogen-bubbling, whilst after 7h mitochondrial disruption was extensive and apparently irreversible. On the other hand in pumpkin, bean and tomato the mitochondrial ultrastructure remained intact at 24h but was irreversibly damaged at 50h.

Adaptation to the Wetland Environment

There appear to be two basic adaptive mechanisms which enable higher plants to grow in permanently waterlogged soil; these are metabolic modifications, and the facility for the internal transport of substantial quantities of oxygen within the plant body.

1. Metabolic Adaptations

The supposition that alcoholic fermentation may lead to the accumulation of lethal levels of ethanol in submerged organs has prompted a search for alternative metabolic pathways in flood-tolerant species. For example, relatively non-toxic shikimic acid has been shown to accumulate during anaerobic metabolism in rhizomes of Iris pseudacorus L. and Nuphar lutea (L.) Sm. (Boulter et al. 1963; Tyler and Crawford, 1970).

Crawford (1966, 1967, 1969), and McManmon and Crawford (1971) have

suggested that flood-tolerant species accumulate non-toxic malate rather than ethanol. The suggestion is based on the inability of these workers to detect malic enzyme in tolerant species; in intolerant species malic enzyme catalyses the decarboxylation of malate to pyruvate, which contributes to ethanol accumulation.

However, the scheme proposed by Crawford and co-workers is open to criticism. Evidence already cited (p. 7) suggests that although the capacity for ethanol production exists the product may not rise to lethal levels. In addition malic enzyme has now been detected in several flood-tolerant species (Davies et al, 1974) including species studied by McManmon and Crawford (1971). Furthermore, John and Greenway (1976) found increased levels of alcohol dehydrogenase (which catalyses the conversion of acetaldehyde to ethanol) in rice roots subjected to anaerobiosis. This result is at variance with the suggestion by Crawford and co-workers that increased levels of this enzyme under anaerobiosis are confined to flood-intolerant species.

In terms of energy yield anaerobic respiration is an inefficient process compared with aerobic respiration. Because of this the former may be regarded more as a means of sustaining viability rather than an aid to normal growth activities.

2. Internal Oxygen Transport

For many years it had been generally assumed that the high level of gas space provision in wetland plants served an aerating function (Arber, 1920), but research proper into internal plant aeration began in the 1930s. Conway (1937), Laing (1940b) and van Raalte (1941, 1944) clearly demonstrated the continuity of the gas space in the shoot and roots of wetland plants, and the dependence of the submerged root upon the shoot for its oxygen supply. In his 1941 paper van Raalte stated that "In the normal rice plant oxygen penetrates the aerial parts and is transported to the roots. By this transport the roots are capable of living in a medium which is nearly completely devoid of oxygen."

There is a correlation between the extent of the gas space system and the degree of tolerance of waterlogged soils (Arikado and Adachi, 1955; Martin, 1968). Thus, the tissues of non-wetland species are usually of low porosity, whilst wetland plants are characterised by the possession of specialised "aerenchymatous" tissue and may be up to 60% porous. In aerenchyma the "intercellular spaces" take the form of large gas-filled chambers called "lacunae" (see p.40). The available evidence suggests that unless a species either possesses, or has the ability to develop, an extensive gas-space system its potential for withstanding prolonged periods of soil submergence is severely restricted. For example, Arikado and Adachi (1955) found that Kentucky-31-fescue,with its well-developed lacunar system, was resistant to waterlogging whereas Gange, which lacks the capacity for lacunae development, was highly susceptible. Yu et al. (1969) subjected several non-wetland species to varying degrees of soil waterlogging (full-flooded, half-flooded and drained). In the full-flooding treatment roots of corn (of porosity 15-18%) and sunflower (porosity 11%) penetrated to depths of 17 and 15cm respectively. Barley roots, though only 3.5% porous, attained 12cm depth but Pato wheat, with a porosity of 15%, rooted to only 5cm. Yu et al. concluded that enhanced root growth was a consequence of the better internal aeration associated with higher porosities; the apparent exceptions of barley and wheat were due respectively to exceptionally low and unusually high respiration rates.

Root porosity has been shown to vary depending upon the degree of waterlogging to which a species is subjected. For example, Armstrong (1971a) found that lacunae formation was more extensive in roots of rice grown in waterlogged, compared with those grown in non-waterlogged, soil; Das and Jat (1977) obtained a similar result. Yu et al. (1969) showed increased root porosities in several non-wetland species when grown in full-flooded, rather than half-flooded or drained soils.

Although certain factors (eg. temperature and barometric fluctuations, diffusive inequalities of the atmospheric gases) may cause mass-flow

(Arber, 1920; Sifton, 1945; Scholander et al., 1955; Wood and Greenwood, 1971), it is generally accepted that oxygen moves through the gas space system chiefly by diffusion. The existence of oxygen concentration gradients between aerial and submerged parts has been abundantly demonstrated (Conway, 1937; Laing 1940a,b; Vallance and Coult, 1951; Coult and Vallance, 1958; Barber, 1961; Teal and Kanwisher, 1966). Oxygen diffusion through the plant body has also been demonstrated numerous times, not only in wetland plants, but also in certain mesophytic and woody species (van Raalte, 1941; Brown, 1947; Barber et al., 1962; Armstrong 1964, 1967b; Greenwood, 1967a,b; Armstrong and Read, 1972; Healy and Armstrong, 1972).

Besides providing for the respiratory requirements of organs situated in anaerobic soil oxygen transported internally may diffuse across the root wall into the surrounding medium. This radial oxygen loss (R.O.L.) is most pronounced in wetland species (van Raalte, 1941, 1944; Armstrong 1964, 1967b) and may account for an amount of oxygen as high as a third to twice that consumed in root respiration (Teal and Kanwisher, 1966). However, it also occurs in mesophytic species (Greenwood, 1967a,b; Healy and Armstrong, 1972) and in woody plants (Armstrong, 1968; Armstrong and Read, 1972).

There is an increasing volume of evidence to indicate that R.O.L. is necessary for plant survival in permanently waterlogged soil. Oxygen leakage has been shown to contribute to the formation around the root of an oxidised zone in an otherwise reduced soil. Within this zone reduced toxins are nullified by their re-oxidation (Molisch, 1926; Ponnamperuma, 1955; Jeffery, 1961; Armstrong 1967b, 1970; Engler and Patrick, 1975; Green and Etherington, 1977) and are thus rendered harmless to the plant. Although other substances diffusing from roots have been shown to affect soil oxidation it seems that these are effective only in the presence of molecular oxygen (Yamada and Ota, 1958; Armstrong, 1967c).

Species differ in their capacity for rhizosphere oxidations (Yu and

Li, 1956; Doi, 1952; Armstrong, 1964, 1967b,c, 1970) and those with the greatest capacity appear the more tolerant of intense soil reduction (Fukui, 1953; Bartlett, 1961; Armstrong and Boatman, 1967; Boatman and Armstrong, 1968; Martin, 1968). Root oxidising activity has also been correlated with resistance to injury by soil phytotoxins such as sulphide and ferrous iron (eg. Goto and Tai, 1957; Baba et al, 1967; Armstrong, 1969).

The magnitude of R.O.L. has been shown by Armstrong (1972) to be markedly influenced by root porosity. Using an "artificial root" constructed from glass capillary and silicone rubber tubing he demonstrated that R.O.L. was still increasing significantly when the root porosity was as high as 25%. Williams and Barber (1961) apparently neglected to take into account the importance of R.O.L. to plant survival when they suggested that the function of the gas space system of wetland plants is not primarily one of oxygen transport, but is rather to provide a reduction in respiring tissue.

Objectives of the Present Study

Internal oxygen transport is now widely recognised as the most important mechanism enabling higher plants to successfully exploit permanently waterlogged soils. It is not surprising, therefore, that plant aeration, particularly that of wetland species, has been the subject of much research. However, the analysis is far from complete, and several aspects of the process remain obscure. In particular the part played by the leaves and stem in controlling the internal oxygen supply to the subterranean organs has been neglected, whilst the possible role of the gas space system as an oxygen reservoir has as yet been no more than speculated upon. The precise internal oxygen concentrations necessary to maintain complete aerobic respiration have never been determined, neither has the influence of anaerobic soil upon the internal oxygen regime of the roots been investigated. The major part of the present study was an attempt to elucidate these important points: the main

objectives were as follows:

1. To assess the importance of the lacunar system as an oxygen store.
2. To quantify the diffusive resistance to oxygen entry into the plant.
3. To determine the sites and magnitude of the resistance to oxygen diffusion within the plant body.
4. To assess the influence of respiration on oxygen transport within the various organs.
5. To determine the critical oxygen pressures for respiration in the intact plant and to assess the growth responses of the roots of plants held at, above or below these critical pressures.
6. To determine the extent to which photosynthesis may influence the internal oxygen regime.
7. To assess the effectiveness of soil oxygen demand as a factor influencing the internal oxygen regime of the root.

Two easily cultivated wetland species were chosen for this investigation: Eriophorum angustifolium Honc. (cotton grass) and Oryza sativa L. (rice).

CHAPTER 2

GENERAL METHODS

I. The Cylindrical Platinum Electrode Technique for Monitoring Radial Oxygen Diffusion From Roots.

The use of polarography to measure oxygen diffusion from roots in anaerobic media has been described by Armstrong (1967b) and Armstrong and Wright (1975). The method involves the electrolytic reduction of oxygen at cylindrical platinum electrodes through which the roots are inserted. The magnitude of the current flowing in the polarographic circuit is directly related to the amount of oxygen diffusing to the platinum surface, which in turn reflects the internal oxygen regime of the plant.

The importance of the cylindrical platinum electrode technique as a tool in the study of plant oxygen relationships is now well established (Armstrong, 1964, 1967b,c, 1968, 1969, 1971a,b, 1972; Martin, 1968; Read and Armstrong, 1972; Healy and Armstrong, 1972; Armstrong and Read, 1972). However, since the method has been used to obtain much of the experimental data presented in this thesis, and since certain modifications have been made to the equipment and procedure originally described by Armstrong, a detailed account of the technique will be given.

A. PRINCIPLES OF POLAROGRAPHY

If a solution of electro-reducible or electro-oxidisable substances is electrolysed between suitable indicator and reference electrodes the relationship between the applied E.M.F. and the current flowing in the system has unique characteristics. The "current-voltage" curve so produced enables both the identity and concentration of the substances in the solution to be determined.

Jaroslav Heyrovsky, who developed the technique of polarographic chemical analysis in the 1920s, employed the dropping mercury cathode as indicator electrode and named the determination of current-voltage

curves "polarography". The instrument developed by Heyrovsky and Shikata (1925) to record automatically current-voltage curves was named a "polarograph", and the curves so produced were termed "polarograms".

Kolthoff and Laitinen (1940) suggested that the term "polarography" should, in fact, be applied to the technique only when a dropping electrode in conjunction with automatic equipment is used. They advocated that the more general term "voltammetry" should be adopted when electrodes other than the dropping mercury cathode are used or when the current-voltage curves are produced manually. They felt that "voltammetry" was more descriptive since the two quantities measured are voltage and current - the former yielding information concerning the identity of a substance, the latter information concerning its concentration.

However, the term "polarography" has been widely retained to describe the general technique. It is used throughout this thesis where it complies, at least in part, with the "criteria" laid down by Kolthoff and Laitinen, for although solid platinum cathodes have replaced the dropping mercury electrode, current-voltage curves have been obtained automatically.

B. THE POLAROGRAPHIC ASSAY OF OXYGEN USING A PLATINUM CATHODE

It has long been recognised that dissolved oxygen is reduced by electrolysis. For example, Daneel was studying the electrolytic reduction of oxygen at platinum electrodes as long ago as 1897, but perhaps the earliest application of the technique to biological systems was made by Vitek (1933) who used polarography to study grass respiration.

1. Circuit and current-voltage curves

The basic circuit required for polarographic oxygen analysis is extremely simple (Fig.2.1). It comprises a source of variable electrical potential together with devices to measure current and applied E.M.F.. A typical current-voltage curve due to oxygen reduction at a Pt cathode (Ag/AgCl reference electrode) is shown in Fig.2.2.(b). The curve has

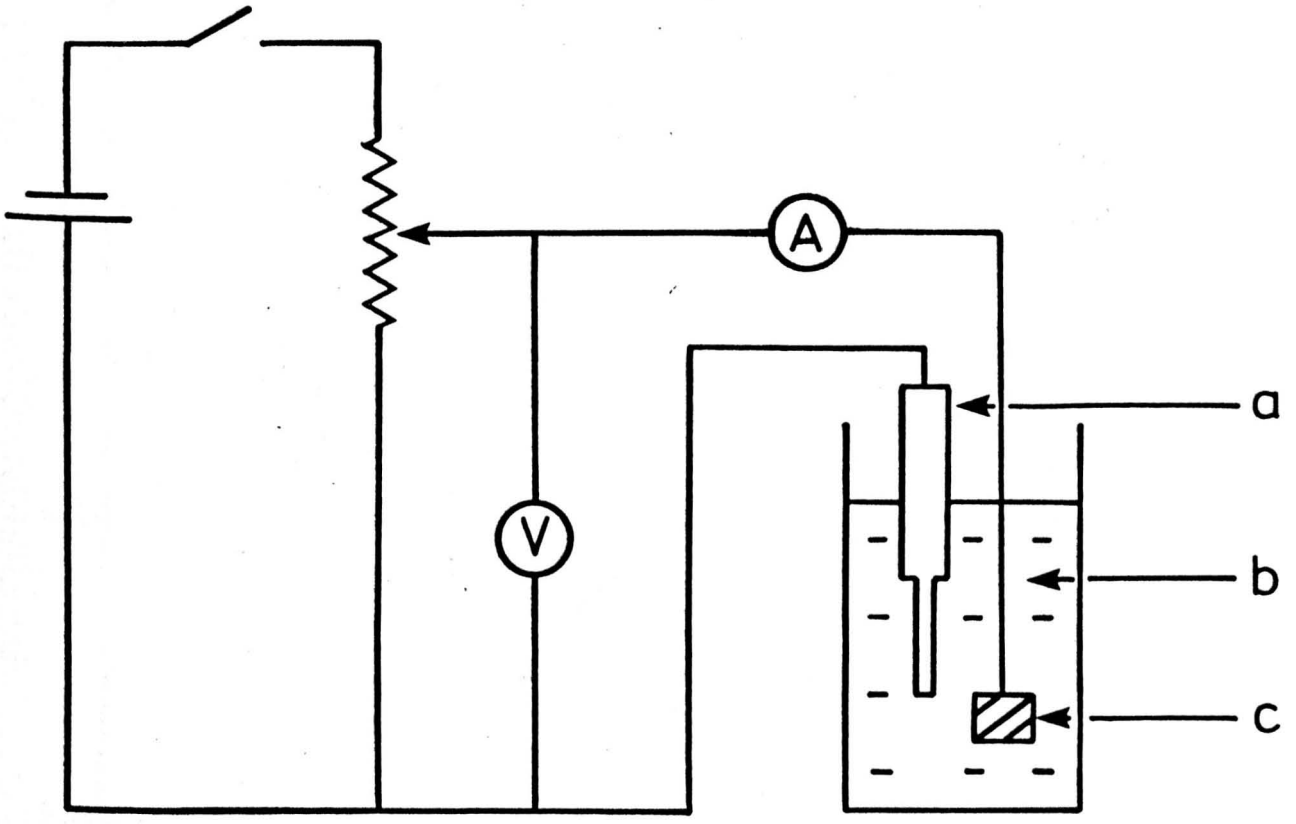

FIG. 2.1 Basic circuit for polarographic determination of dissolved oxygen.

a. Silver-silver chloride anode

b. Oxygen solution

c. Platinum cathode

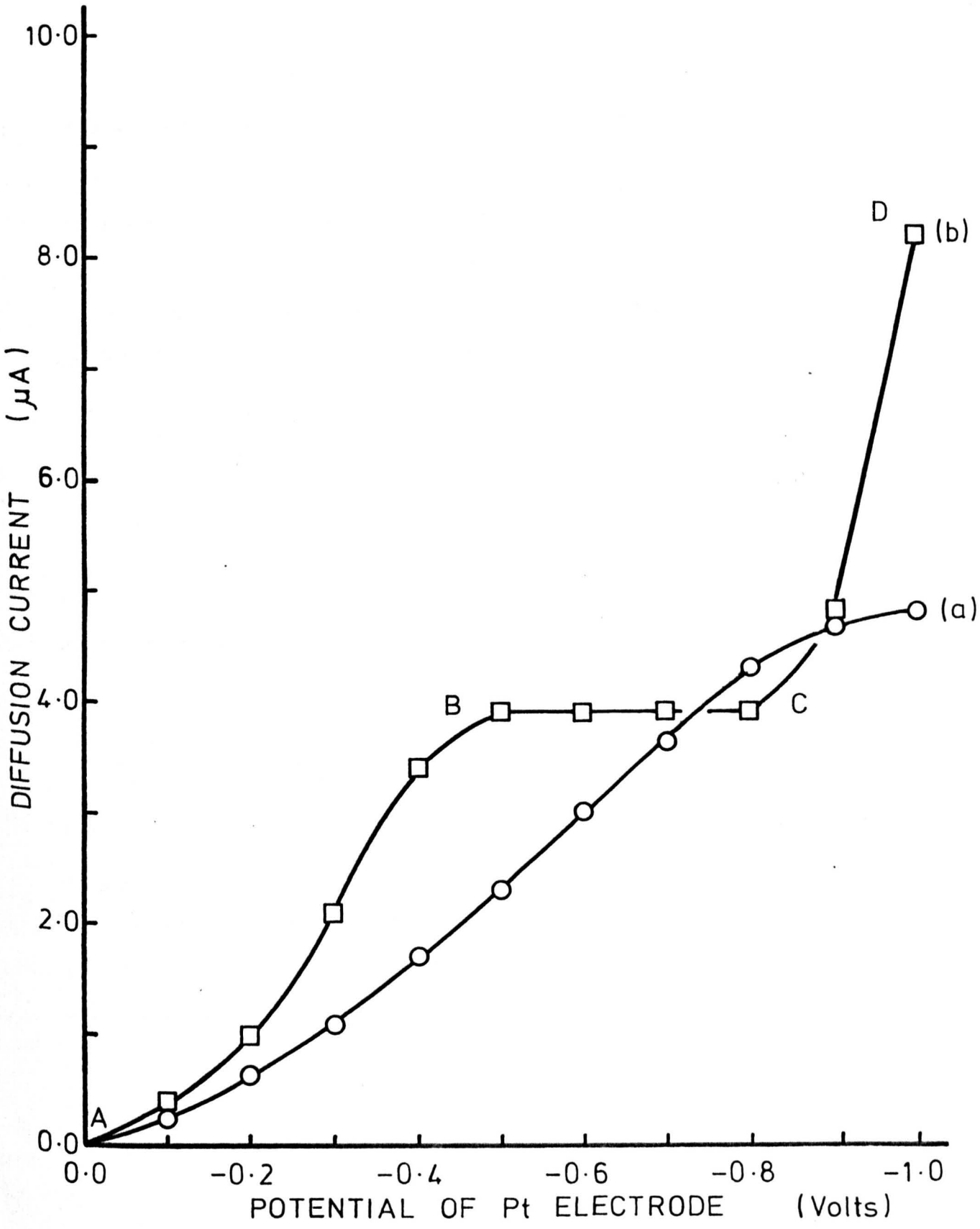

FIG. 2.2 Current-Voltage curves for air-saturated water at 23°C

(a) 150cm^3 de-ionised water

(b) As (a) with addition of 0·3cm^3 saturated KCl

several distinct portions. Between A and B the current increases as more negative cathode potentials cause the reduction of greater amounts of oxygen. At point B, however, the curve assumes a distinct plateau. The potential of the cathode has become sufficiently negative for all oxygen molecules to be reduced as soon as they reach the platinum surface. The current in the plateau region, B–C, is, therefore, independent of applied E.M.F. It is governed by the rate of oxygen diffusion to the cathode, which is said to be in a state of "concentration polarisation" (i.e. the current is governed by the oxygen concentration in the solution and not by the imposed cathode potential). The current in the plateau region is aptly termed "limiting" or "diffusion" current. It is the direct dependence of the diffusion current upon the solute concentration which is the fundamental principle upon which polarographic analysis depends.

The final part of the curve, C–D, is a sudden and rapid rise in current. This is the result of a second electrode reaction, namely the reduction of hydrogen ions to hydrogen gas ("hydrogen discharge").

2. <u>The electrode reaction</u>

The nature of the electrolytic reduction at the platinum cathode is not fully understood. Depending upon the pH of the system the net reactions are thought to be:

In acid media:

$$O_2 + 4H^+ + 4e^- \longrightarrow 2H_2O \qquad (a)$$

In alkaline media:

$$O_2 + 2H_2O + 4e^- \longrightarrow 4OH^- \qquad (b)$$

(See McIntyre, 1970)

Both reactions involve the transfer of four electrons for each molecule of oxygen reduced.

Oden (1962) considers that reaction (b) is dominant at pH values above 3.5, the range encountered in the present study. Two substantially different courses have been proposed to account for the net reaction (Williams, 1966). The first occurs in two steps and involves the production of hydrogen peroxide, followed by its reduction:

$$\left.\begin{array}{l} O_2 + 2H_2O + 2e^- \longrightarrow 2OH^- + H_2O_2 \\ H_2O_2 + 2e^- \longrightarrow 2OH^- \end{array}\right) \quad (c)$$

$$O_2 + 2H_2O + 4e^- \longrightarrow 4OH^-$$

The second reaction sequence involves three steps and depends on the formation, and subsequent decomposition, of metal oxides at the electrode surface:

$$\left.\begin{array}{l} O_2 + 2M \longrightarrow 2MO \\ 2MO + 2H_2O + 2e^- \longrightarrow 2MOH + 2OH^- \\ 2MOH + 2e^- \longrightarrow 2M + 2OH^- \end{array}\right) \quad (d)$$

$$O_2 + 2H_2O + 4e^- \longrightarrow 4OH^-$$

There is evidence to indicate that H_2O_2 is produced during cathodic oxygen reduction. Laitinen and Kolthoff (1941) found that, after prolonged oxygen reduction at a platinum cathode, H_2O_2 was detectable in the solution. Bockris and Huq (1956) also detected H_2O_2, although they estimated that the amount produced was only one-thousandth of that expected had all the oxygen been reduced to H_2O_2. This evidence, together with the fact that the current-voltage curve produced using a dropping mercury electrode consists of two waves of equal height, tends to confirm the two-step reaction sequence (c).

However, some evidence has been put forward which favours sequence (d). For example, Lingane (1961) and Riddiford (1961), from analyses of various data, concluded that H_2O_2 was not produced at all during electrolytic oxygen reduction. However, Hoare (1968) makes clear the unreliability of using non-detection of H_2O_2 as evidence. He states that H_2O_2 is always formed, but at current densities less than 10^{-4} Amperes cm^{-2} it is reduced so rapidly that its detection is impossible.

The results of Muller and Nekrassow (1965) suggest that the answer to the problem lies between the two proposed alternatives. They found that whereas oxides of platinum actually retarded the reduction of oxygen to H_2O_2 they did, in fact, accelerate further reduction of the peroxide by catalytically decomposing it to OH^- ions. Rickman et al. (1968) also favour the catalytic effect of the metal oxide and state that though H_2O_2 is formed regardless of the state of oxidation of the electrode, its subsequent decomposition is dependent on the presence of an "active oxide". Davies (1962) suggests that the catalytic effect of the oxide may explain the absence of a second wave in the current-voltage curve using a platinum cathode, if it enables the H_2O_2 to be reduced at less negative potentials.

C. THEORY

1. Oxygen diffusion from a root to a cylindrical platinum electrode

With the limiting potential applied and the electrode reaction at equilibrium the oxygen concentration at the electrode may be considered as effectively zero. In a planar system this equilibrium state would be described by Fick's first law, as:

$$f_{x=o,t} = -D\left(\frac{dC}{dx}\right), \; x = o,t \qquad (2.1)$$

where:

$f_{x=o,t}$ = the rate of transfer of oxygen per unit cross-sectional area of diffusion path (A) at distance x from the electrode surface at time t (eg. moles cm^{-2} s^{-1}); also termed 'oxygen flux', and given by $\frac{Q}{tA}$, where Q is the quantity (eg. moles) of oxygen transfered in time t.

D = the diffusion coefficient of oxygen in the medium concerned (cm^2 s^{-1}) .

$\frac{dC}{dx}$ = the oxygen concentration gradient between source and electrode surface (linear in an equilibrated system).

In the case of radial diffusion, such as in the root-cylindrical electrode system, a modified form of equation 2.1, based on cylindrical coordinates, is required. The general diffusion equation in cylindrical coordinates is:

$$\frac{1}{r}\frac{d}{dr}\left(r\, D\, \frac{dC}{dr}\right) = 0 \qquad (2.2)$$

With D constant, integration gives:

$$C = A + B \log r \qquad (2.3)$$

The constants A and B may be determined from the boundary conditions appropriate to the root-electrode system (Fig.2.3):

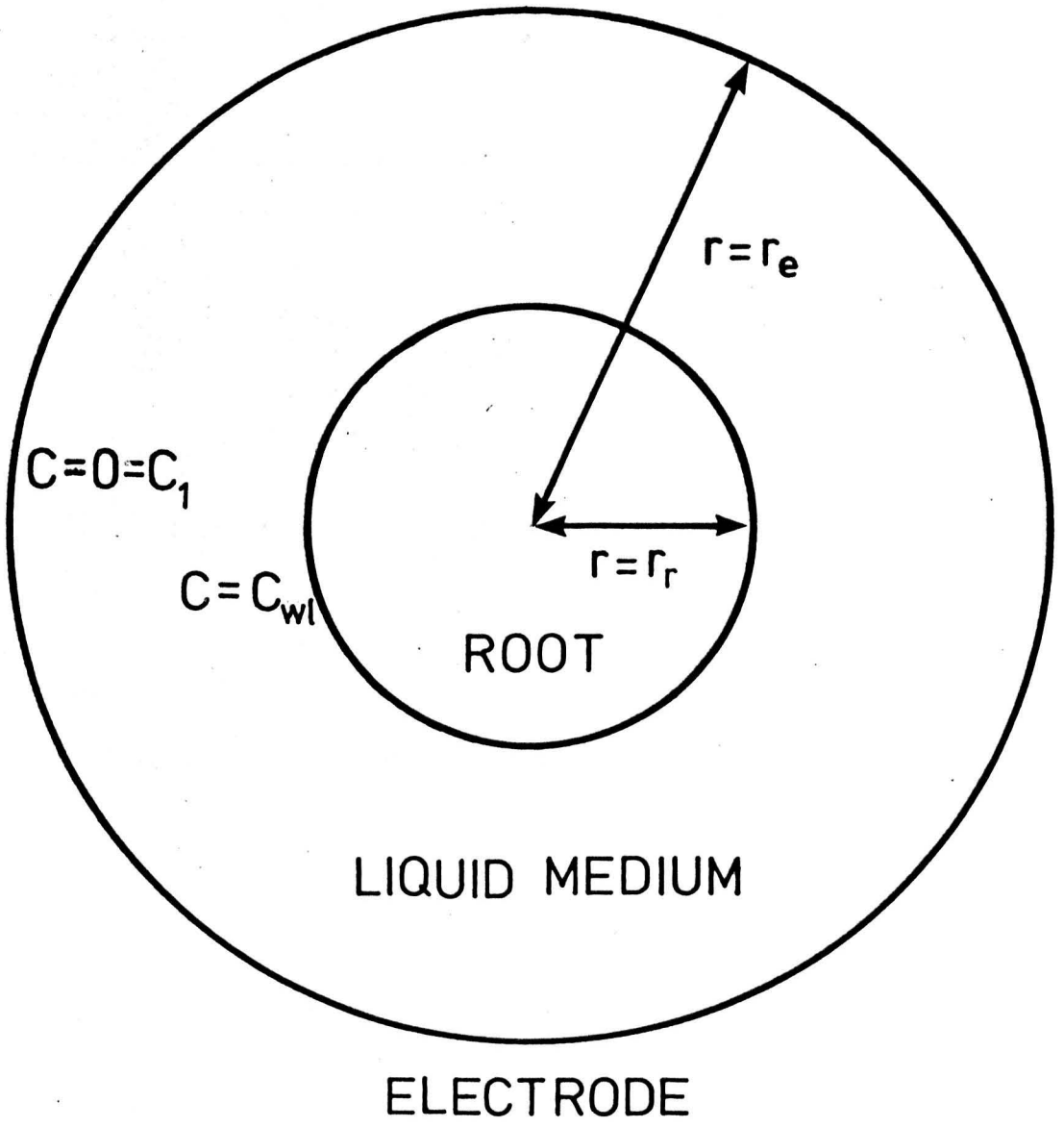

FIG. 2.3 Oxygen diffusion from a root to a cylindrical Pt electrode.
Diagram to show the boundary conditions at the root and electrode surfaces.

$C = C_{wl}$ (O_2 concentration at the root wall) on

$r = r_r$ (the root radius), and

$C = C_1$ on $r = r_e$ (electrode radius).

Hence, $$B = \frac{-(C_{wl} - C_1)}{\log(r_e/r_r)}$$

and $$A = \frac{(C_{wl} \log r_e - C_1 \log r_r)}{\log (r_e/r_r)}$$

Substitution for A and B in equation 2.3 gives:

$$C = \frac{C_{wl} \log (r_e/r) + C_1 \log (r/r_r)}{\log (r_e/r_r)} \qquad (2.4)$$

and differentiating with respect to r:

$$\frac{dC}{dr} = \frac{1}{\log(r_e/r_r)}\left(-\frac{C_{wl}}{r} + \frac{C_1}{r}\right) \qquad (2.5)$$

For the radial system the analogue of equation 2.1 is:

$$\frac{Q}{tA} = -D.\frac{dC}{dr} \qquad (2.6)$$

and substitution from equation 2.5 gives:

$$\frac{Q}{t\,A} = -D.\frac{1}{\log(r_e/r_r)}\left(-\frac{C_{wl}}{r} + \frac{C_1}{r}\right) \qquad (2.7)$$

which re-arranges to:

$$\frac{Q}{t\,A} = D.\frac{(C_{wl} - C_1)}{r \log(r_e/r_r)} \qquad (2.8)$$

In the root-cylindrical electrode system we are concerned with oxygen diffusion from the surface of the root, radius $r = r_r$. If the oxygen concentration at the electrode surface, C_1, is considered as effectively zero, the equation describing the system becomes:

$$\frac{Q}{t\,A_r} = \frac{D.\,C_{wl}}{r_r \log(r_e/r_r)} \qquad (2.9)$$

where A_r = the surface area of the segment of root within the electrode.

2. Conversion of diffusion current to oxygen flux

Kolthoff and Lingane (1952) have related diffusion current to flux incident upon an electrode by the following equation:

$$i_t = n.F.A_e.f_{x=o,t} \qquad (2.10)$$

where:

i_t = the diffusion current at time t (amperes)

n = the number of electrons involved in the reduction of one molecule of oxygen (taken as 4)

F = the "Faraday" (96,500 Amp.s)

A_e = the surface area of the electrode (cm^2)

$f_{x=o,t}$ = the flux (moles s^{-1} cm^{-2} electrode surface).

Rearrangement of equation 2.10 gives:

$$f_{x=o,t} = \frac{i_t}{n.F.A_e} \qquad (2.11)$$

Diffusion current is conveniently measured in microamperes. If the right hand side of equation 2.11 is multiplied by the factors 32(M.W.of O_2), 60(s to min), and 10^9, the flux will be in nanogrammes (ng) min^{-1} cm^{-2} electrode surface.

To express the radial oxygen diffusion <u>from</u> roots the surface area of that portion of root within the cylindrical electrode (A_r) is substituted for electrode surface area, A_e, in equation 2.6. The equation in its final form is:

$$f_{x=o,t} = \frac{i_t.60.32.10^{-6}.10^9}{4.\ 96,500.A_r} \text{ ng } cm^{-2}min^{-1} \qquad (2.12)$$

which simplifies to:

$$f_{x=o,t} = \frac{4.974\ i_t}{A_r} \text{ ng } cm^{-2}min^{-1} \qquad (2.13)$$

D. FACTORS INFLUENCING MEASUREMENTS

1. Supporting electrolytes

The forces acting upon electroreducible substances during electrolysis are of two types. There is the diffusive force, mentioned earlier, which is proportional to the concentration gradient between the electrode surface and bulk solution, and an electrical force, dependent on the applied potential or electrical gradient. The limiting current is a function of these two forces.

If an excess of an indifferent (i.e. non-reducible) electrolyte is added to the solution the electrical forces acting on the reducible species are nullified. Virtually all the current is then carried by the ions of the added salt (or "supporting electrolyte") and the limiting current becomes effectively the diffusion current, governed solely by the diffusion rate of the reducible species to the cathode.

Fig.2.2a is the current-voltage curve for air-saturated de-ionised water. On the addition of supporting electrolyte the curve assumes the characteristic form depicted in Fig.2.2b. In this case, and throughout the present study, the solution concentration of supporting electrolyte (KCl) was 6.94×10^{-4} g cm^{-3}, giving to the solution an electrical conductivity of approximately 1.980×10^{-3} mho cm^{-1} at 23°C.

2. Applied Potential

Current is directly proportional to oxygen concentration only in the plateau region of the current-voltage curve. Consequently the applied cathode potential must correspond with the plateau voltage.

It has been found that a change in dissolved oxygen concentration is accompanied by a shift in plateau potential (Fig.2.7 and Armstrong, 1967a). Hence, current-voltage curves were always obtained prior to oxygen determinations to enable the correct cathode potential to be applied in each experiment.

3. Equilibration

On application of the plateau potential there is an initial current decay as oxygen adjacent to the cathode surface is rapidly reduced. An equilibrium value is eventually reached which is governed by the diffusion rate of oxygen in the system concerned. Accurate results are possible only if the current taken is this equilibrium value. In the present study equilibration was followed using a chart recorder.

4. Temperature

Change in temperature may significantly affect oxygen diffusion current since it alters the solubility of oxygen, its concentration in air, and its diffusivity in gases and liquids (Table 2.1). In the root-cylindrical electrode system the situation is complicated by temperature effects on metabolism. For these reasons care was taken to minimise temperature fluctuations during experiments, which were carried out at 23° or $3^{\circ}C$.

5. Electrode poisoning

The poisoning of Pt electrodes with surface deposits, resulting in a change in the electrode reaction, has been reported. For example, Birkle et al. (1964) claimed that solid Pt microelectrodes are prone to poisoning, especially if left embedded in soil for longer than two weeks. On the other hand, Armstrong (personal communication) has found no evidence of poisoning of soil electrodes even after two months' burial.

In the present study electrodes were immersed in relatively pure medium during measurements for periods not exceeding 2-3 days and poisoning as such was not a problem. However, Rickman et al. (1968) found that an irreversibly-formed oxide can exist on clean platinum due to ageing and this may interfere with the catalytic decomposition of H_2O_2. In view of this electrodes were cleaned frequently using the mildly abrasive detergent "Pyroneg" applied with a moist pipe cleaner; this was followed by thorough rinsing in distilled water. Frequently, electrodes were checked using standard "artificial roots" (see p.54) of known diffusive resistance (calculable by equation 7.1) to ensure that the measured flux

TABLE 2.1: OXYGEN: FRACTIONAL VOLUMES IN AIR, SOLUBILITIES AND DIFFUSION COEFFICIENTS

Temperature (^{o}C)	Fractional volume in moist air at N.P.	Concentration in moist air at N.P. (10^{-6}g cm^{-3})	Solubility in pure water from moist air at N.P. (10^{-6}g cm^{-3})	Diffusion coefficient in air (cm^{2}s^{-1})	Diffusion coefficient in water (10^{-5}cm^{2}s^{-1})
0	0.2086	297.9	14.63	0.178	0.99
* 3	0.2083	294.2	13.46	0.181	1.16
10	0.2074	285.6	11.28	0.189	1.54
20	0.2050	272.8	9.08	0.201	2.10
*23	0.2041	268.7	8.57	0.205	2.267
30	0.2011	258.7	7.57	0.214	2.67

* Indicates data most frequently referred to in this thesis

(Figures compiled by Armstrong, unpublished)

agreed with that predicted using equation 4.4.

6. Residual current

Diffusion current is a composite quantity, being composed of two contributing currents. These are:

a) the current due to electroreduction of the substance under investigation, in this case oxygen

b) the current due to the reduction of electroreducible impurities.

The latter, termed the "residual current", should normally be subtracted from the diffusion current (Kolthoff and Lingane, 1952). In the present study oxygen assays were carried out in anaerobic medium (p. 27) and residual currents, which were almost certainly due to traces of dissolved oxygen, were usually extremely small and were ignored. Even if the residual currents had been larger it is doubtful whether they would have affected diffusion current since with a root in position the relatively high concentration of oxygen within the electrode, compared with that in the deoxygenated medium, would favour diffusion out of, rather than into, the platinum cylinder. Nevertheless, residual currents were always measured to check for any abnormality in the system such as persistent air bubbles in the electrode or ineffective deoxygenation of the experimental medium.

E. APPARATUS

1. The cylindrical platinum cathode

The electrodes were as shown in Fig.2.4(a) and were constructed as follows.

A thermo-pure platinum cylinder (length 6cm, inner radius 0.1125cm - Armstrong, 1967b) was marked off in 0.5cm (occasionally 1.0cm) sections. Perspex tubing (inner radius 0.325cm, outer radius 0.475cm) was marked in a similar manner and a hole of a size sufficient to accommodate a sleeved copper lead (length 50cm, radius 0.050cm) was drilled through the mid-point of each section. A lead was passed through each hole and along

FIG. 2.4 Electrodes used in the polarographic assay of oxygen diffusing from roots.

(a) Cylindrical platinum cathode

(b) Silver-silver chloride anode

a celluloid guide

b perspex tube

c platinum cylinder

d epoxy resin

e root through electrode

f solder joint

g araldite

h sleeved copper wire

i copper wire - Ag/AgCl junction

j Ag/AgCl core

k saturated KCl solution

l polythene extension

m glass tube with fibre plug

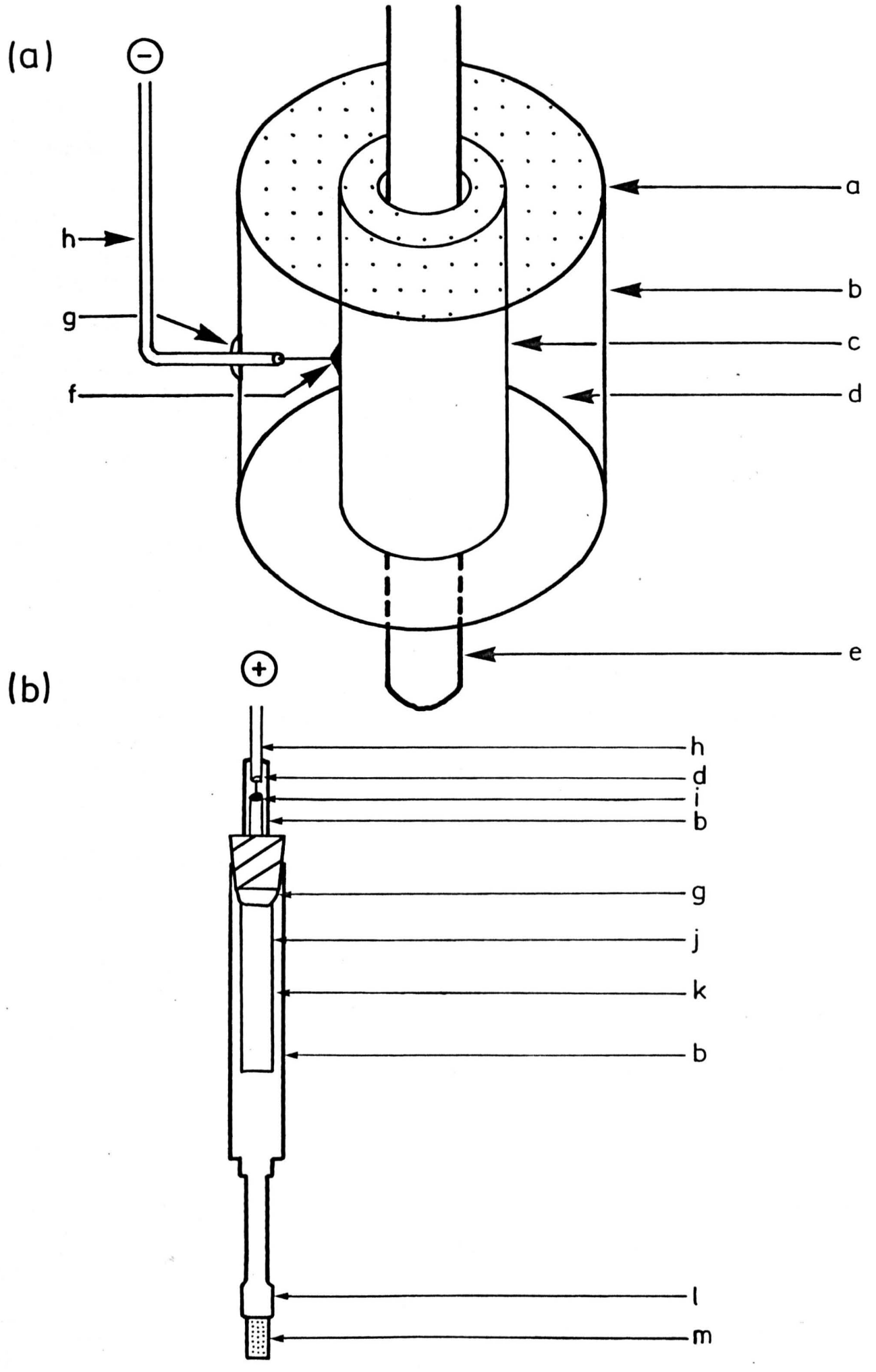
(a)
⊖
a
h
b
g
c
f
d
e
(b)
⊕
h
d
i
b
g
j
k
b
l
m

the perspex tube so that all leads emerged from the same end of the perspex cylinder; one lead was then soldered to the mid-point of each section of the marked platinum tube. Care was taken to remove the "flux" from the soldered Cu-Pt junction since this was found to prevent the adherence of the epoxy-resin insulation; chloroform proved to be a satisfactory solvent for the flux. The platinum cylinder was then manoeuvered to lie centrally inside the perspex tube and the leads sealed into the perspex with household "Araldite".

One end of the concentric cylinders was blocked with plasticine and the space between the platinum and perspex was filled with Spurr's low viscosity resin (Spurr, 1969), care being taken to eliminate air bubbles. The resin was hardened at 60°C for 24h and the cylinders sawn through at the marks to yield the individual electrodes. The ends of each electrode were sanded smooth and parallel, and the inner surface of the platinum thoroughly cleaned (p. 24). Finally, celluloid guides were cemented with perspex glue to each end of the electrodes to ensure that roots would pass centrally through the platinum cylinders.

2. The silver-silver chloride anode

All silver-silver chloride electrodes used were constructed in the laboratory. The main features are illustrated in Fig.2.4(b).

The silver-silver chloride core was made by electrolysis in saturated potassium chloride solution using very pure silver sheet as anode and platinum wire as cathode. Migration of chloride ions to the silver results in their deposition on the surface of the electrode as insoluble silver chloride, which is visible as a brownish coating. When the coating was seen to be complete the electrolysis was stopped and the silver-silver chloride sheet allowed to age for a few days in distilled water before use.

Such an electrode maintains its potential for long periods, after which its efficiency deteriorates due to crystal growth on the Ag-AgCl core (Shoemaker et al., 1974). When this occurs the old silver chloride

coat may be removed with ammonia and a fresh coating applied for continued use.

3. The polarograph

The polarograph (Plate 2.1) used throughout this study was that developed by Armstrong and Wright (1976a) for the large-scale sampling of soil oxygen flux in the field; the instrument may be used with equal success in the laboratory. Whilst retaining the basic features required in a polarographic circuit (Fig.2.1) the polarograph had the additional facilities of an automatic system for plotting current-voltage curves and the provision for the simultaneous polarisation of several cathodes.

Details of the instrument and its operation are given in Appendix 2.

F. GENERAL PROCEDURE FOR THE ASSAY OF OXYGEN DIFFUSING FROM ROOTS

1. Preparation of the anaerobic medium

Throughout this study oxygen diffusion measurements were made with roots and electrodes immersed in an anaerobic medium prepared as follows.

A small quantity of Davis standard agar was added to de-ionised water so that the concentration was 0.05% w/v. After stirring, the mixture was placed in a steamer for a minimum of 2h. Most of the dissolved oxygen was expelled from the medium during this process. The supporting electrolyte was then added ($1.0cm^3$ saturated KCl per $500cm^3$).

To remove the remaining traces of oxygen from the medium oxygen-free nitrogen was bubbled through the liquid for at least 24h. A plug of moist cotton wool was inserted into the mouth of the container (usually a one-litre measuring cylinder) to prevent air re-entering the medium during the nitrogen-bubbling.

The dilute agar medium, whilst retaining the diffusional characteristics of pure water, was sufficiently viscous to prevent convection due to normal laboratory temperature differentials.

2. Oxygen measurement

Although individual experiments necessarily differed in certain

PLATE 2.1: The polarographic measurement of radial oxygen loss from the root apex of Eriophorum angustifolium.

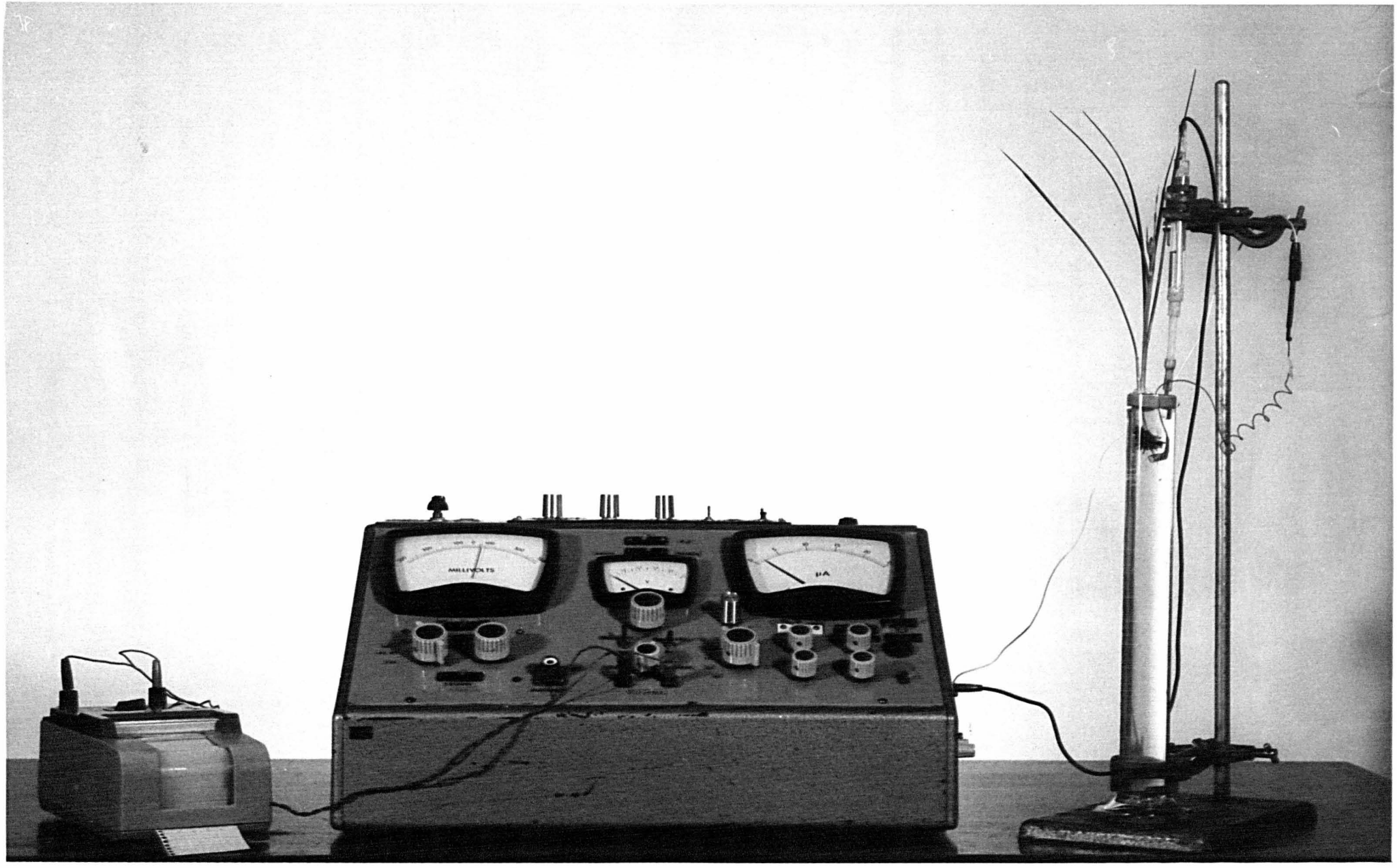
MILLIVOLTS
μA

respects, each followed the same general procedure.

A measuring cylinder ($250cm^3$) provided a convenient vessel for the anaerobic medium. A thin rubber bung with holes of the required size was used to support the plant and cylindrical cathode, whilst allowing access for the Ag/AgCl anode (Fig.2.5).

Agar medium was poured gently into the measuring cylinder to within 1 to 2cm of the mouth and the cylinder clamped firmly at its base. The cathode was thoroughly wetted in the medium and checked to ensure that no air bubbles remained trapped within the platinum cylinder. Persistent bubbles were easily removed by withdrawing the electrode and gently blowing through it. The electrode was then suspended beneath the bung by passing its lead through the corresponding hole.

The plant under investigation was washed free of soil debris and any cut rhizomes were sealed with lanolin. It was then positioned in the bung, its hole being lined with moist cotton wool to hold the plant steady and to prevent tissue damage. Then without delay the basal portions of the plant, together with the electrode, were submerged by gently lowering the bung beneath the surface of the agar medium (Fig.2.5). Finally, the anode was positioned with its fibre-plugged tip just below the liquid.

At this stage the root was left free from the cathode, since the residual current first required measurement. The electrode leads were connected to the primary polarising circuit of the polarograph (See Appendix 2). At this point an opportunity was provided for a last check on the apparatus. If functioning correctly connection of the electrodes to the polarograph produces a very brief positive swing of the microammeter needle. This is due to the electrode potential of the platinum cathode being initially more negative than that of the Ag/AgCl anode. A persistent negative deflection of the microammeter indicates a fault, usually associated with liquid creep to the copper lead - platinum junction of the cathode.

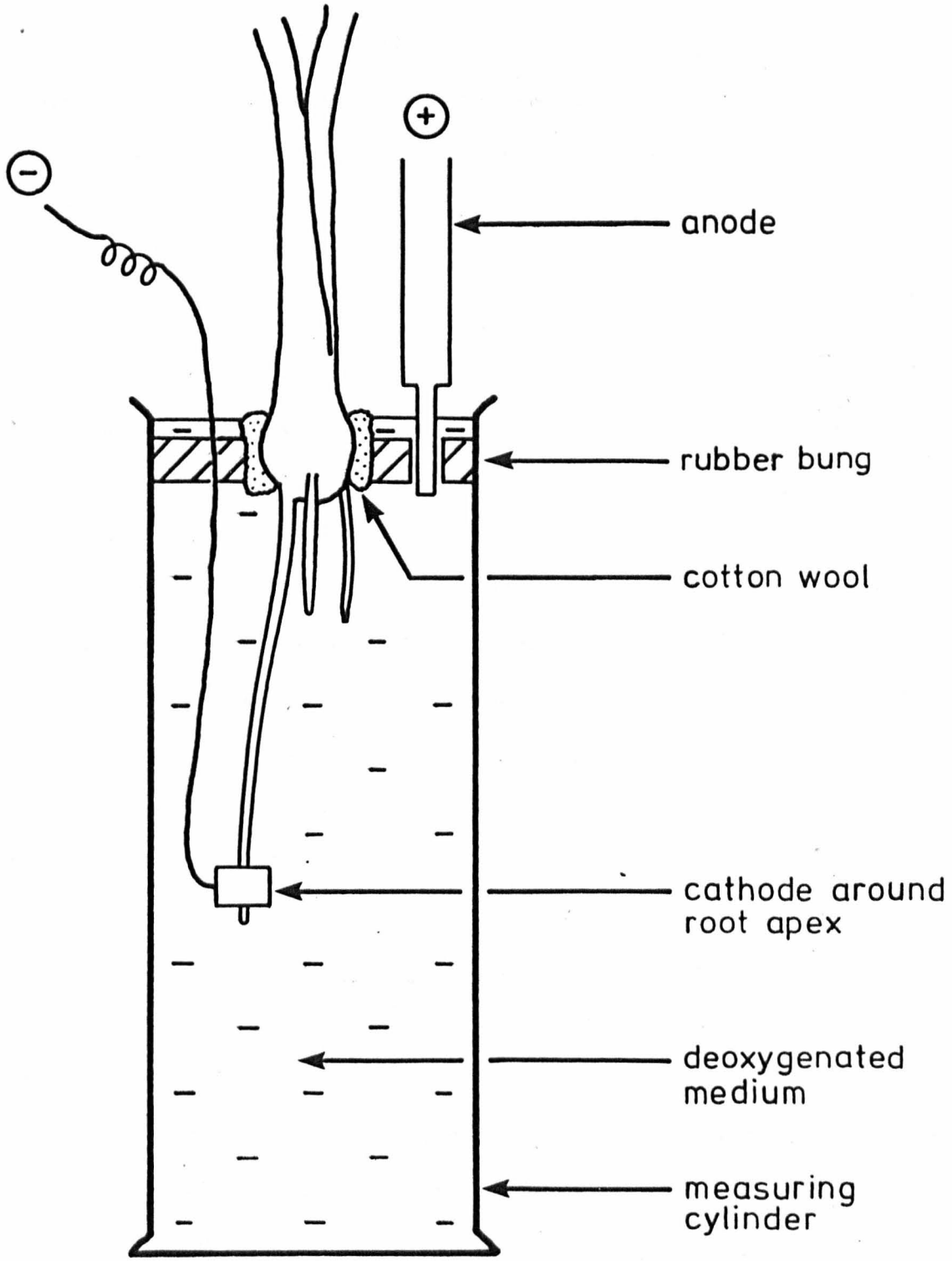

FIG. 2.5 Basic experimental assembly for the measurement of radial oxygen loss from roots .

If the equipment was functioning correctly the voltage regulator was set on automatic and the polarograph allowed to plot the residual current-voltage curve (Fig.2.6a). With the plateau voltage then reset and held the residual diffusion current was allowed to equilibrate and its value determined from the microammeter. The polarising voltage was then returned to zero.

A healthy root was then inserted through the cathode. This was most easily done with the aid of the bent end of a thin metal rod passed through the anode hole in the bung. In most experiments R.O.L. from the apical region of the root was measured, hence the cathode was usually positioned around the root apex; this part of the root is also associated with greatest R.O.L. (Fig.2.7). A current-voltage curve was then obtained (Fig.2.6b) and the diffusion current due to R.O.L. from the root measured.

At the end of each experiment the length and apical radius of the experimental root were accurately measured using a travelling microscope.

It must be mentioned that although the method outlined above was common to most of the investigations it usually formed the basis of a more complex procedure; details are given in the subsequent descriptions of the individual experiments.

II. An Electrical Analogue to Simulate Root Aeration in the Wetland Condition

A. MODELLING OF BIOLOGICAL SYSTEMS

The use of mathematical or working models to simulate biological systems has increased during the past few years as the advantages of this method of research have been realised. Information may be gained from models which would be difficult, or even impossible, to obtain by experiment.

In the field of plant aeration emphasis has tended towards mathematical rather than working models. For example, Luxmoore *et al.* (1970a,b,c,d) and Luxmoore and Stolzy (1972a,b) have successfully derived and applied equations to describe various aspects of root aeration. Armstrong (1970) has used a

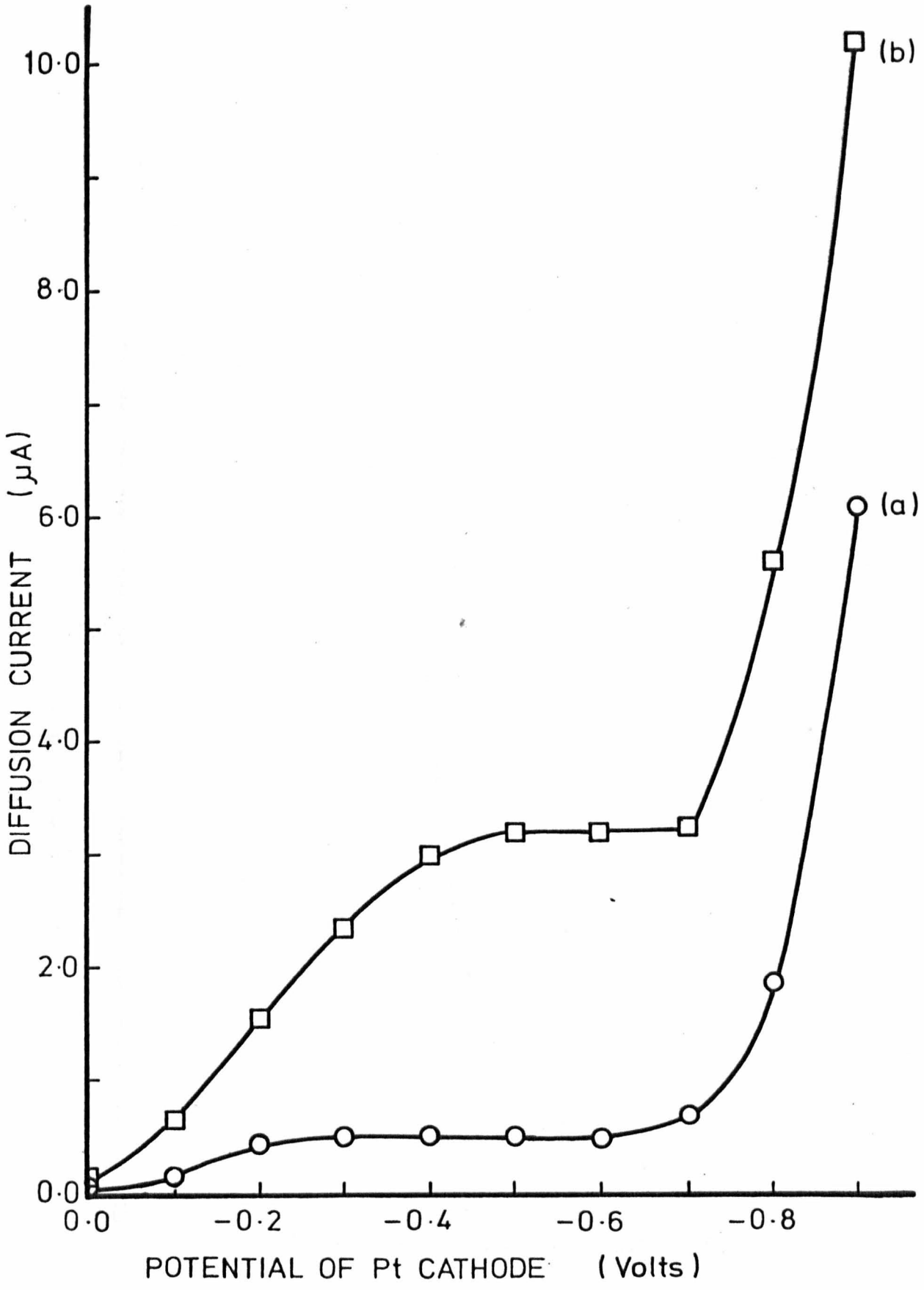

FIG. 2.6 Current - Voltage curves for E. angustifolium at 23°C

(a) Cathode free in deoxygenated medium

(b) Cathode around root apex.

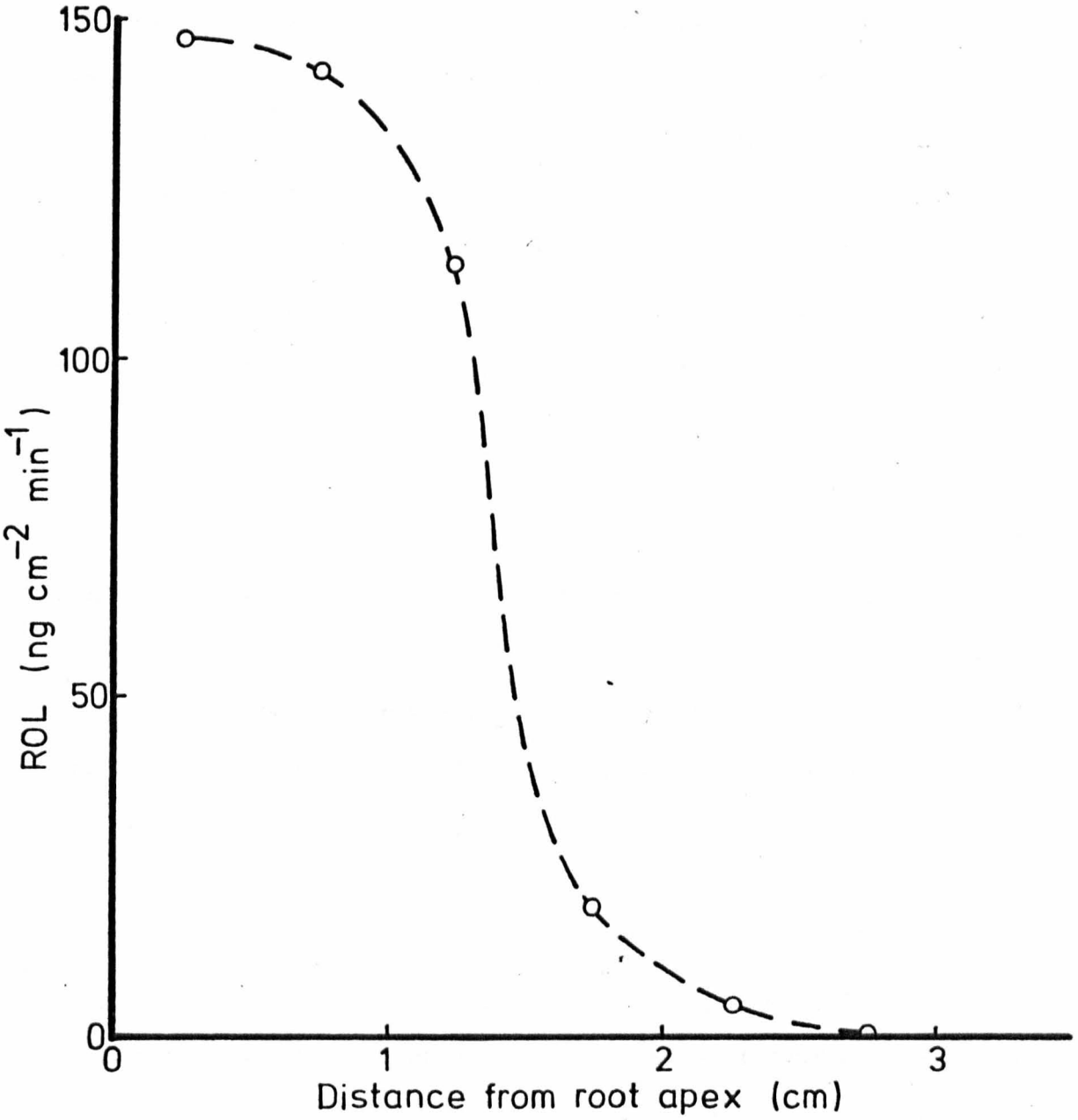

FIG. 2.7 Variation in ROL along a root of E. angustifolium

mathematical treatment to predict the dimensions of the oxygenated rhizosphere produced by radial loss of oxygen from roots. Lemon (1962), Lemon and Wiegand (1962), Covey and Lemon (1962) and Kristensen and Lemon (1964) have analysed mathematically the relationships between soil oxygen supply and root oxygen demand.

However, as the number of variables is increased, mathematical models become necessarily very complex, and often the equations can be solved only by computer (e.g. Luxmoore et al. 1960a); under these circumstances working models may be employed to advantage. Individual variables may be programmed independently and their interaction determined by direct observation. An example of such a model is the electrical analogue developed by Sanders et al. (1970) and Baldwin et al. (1972) which was used successfully to study the diffusion of nutrients to multiple root systems in soil.

In this study use was made of the electrical root-aeration analogue developed by Armstrong and Wright (1976b); a brief description follows. During the investigation certain amendments were made to the original model and these are described in this chapter. In addition, part of the present study involved the development of a more realistic device for simulating the oxygen sink due to the soil and a full account of the method adopted is given in Chapter 9.

B. THEORY

1. The basis of the electrical modelling of diffusion systems

Oxygen transport through a root situated in waterlogged soil is a process involving diffusion of the gas from a source (the internal atmosphere of the aerial organs) to a sink (tissue respiratory sites, and the soil in the case of R.O.L.). In the steady-state (i.e. in the case of a constant oxygen concentration gradient) the system is describable by Fick's first law written in the form:

$$J = - \frac{D_e A \Delta C}{L} \qquad (2.14)$$

where: J = the oxygen diffusion rate ($g\ s^{-1}$)

D_e = the effective diffusion coefficient of oxygen in the system ($cm^2\ s^{-1}$) (see p.126)

A = the area over which the oxygen diffuses (cm^2)

ΔC = the oxygen concentration difference ($g\ cm^{-3}$) between two points L(cm) apart.

The diffusive resistance, R, in the system is given by:

$$R = \frac{L}{D_e A} \quad s\ cm^{-3} \qquad (2.15)$$

Oxygen flow along a diffusion gradient may be likened to an electrical system in which current is induced along a conductor by a difference in electrical potential. The electrical analogue of equation 2.14 is embodied in Ohm's law, viz.:

$$I = \frac{V}{R'} = V\left(\frac{A}{sL}\right) \qquad (2.16)$$

where:

I = the rate of current flow (coulombs s^{-1} or amperes).

A = the cross sectional area of the conductor (cm^2)

L = the length of the conductor (cm)

V = the potential difference between the ends of the conductor (volts)

s = the specific resistance of the conducting material (ohm cm)

$\frac{sL}{A} = R'$ = the electrical resistance of the conductor (ohms)

Comparing equations 2.14 and 2.16 it is apparent that:

I is analogous to J

ΔC is analogous to V

$R = \frac{L}{D_e A}$ is analogous to $R' = \frac{sL}{A}$

It is this fundamental similarity between the electrical and diffusion laws which is the basis for the electrical modelling of diffusion systems.

2. Factors influencing root aeration and their analogue equivalents

Factors which influence the aeration status of a root in wet soil include:

(i) Diffusion path length, internal porosity, tortuosity of the gas space system and permeability of the root wall. These contribute to the internal diffusive resistance (Chapter 7) which is represented in the analogue by electrical resistors.

(ii) Respiratory and soil oxygen demand. These are the oxygen sinks, and are represented by electrical resistors with leakage to earth.

(iii) Oxygen concentration gradient - represented by potential difference.

Suitably scaled voltmeters and ammeters enable oxygen concentration and diffusion rate to be monitored.

C. BASIC CIRCUIT AND CONDITIONS GOVERNING E.M.F. AND RESISTOR VALUES

For convenience Armstrong and Wright (1976b) divided the root-wet soil system into short segments, each represented by a circuit unit. Fig.2.8 illustrates the construction of the basic unit which represents the oxygen diffusion paths, resistances and sinks present in segments of root-wet soil system; additional circuit details are given in Appendix 3. The analogue was made up of twenty such units connected in series, the resistor and E.M.F. values being such as to fulfil the following conditions:

(i) Root unbranched and open at the base

(ii) Root length variable between one and twenty centimetres (i.e. one circuit unit per centimetre segment)

(iii) Root radius originally constant at 0.05cm, but later variable between 0.01 and 0.10 cm (see Chapter 9)

(iv) Oxygen concentration at the root base variable between zero and 269×10^{-6} g cm^{-3} (20.41%), and measurable between these values in each segment.

FIG. 2.8 Electrical analogue : Basic circuit

R'_p	Resistors controlling pore space resistance
R'_R	Resistors controlling respiratory oxygen consumption
R'_{wl}	Resistors controlling root wall resistance
R'_s	Resistance of external liquid path
V	Field effect transistorised voltmeters for monitoring oxygen concentration
mA1	Milliameters monitoring R.O.L.
mA2	Milliameters monitoring respiratory oxygen consumption

For further details see Armstrong and Wright, 1976b.

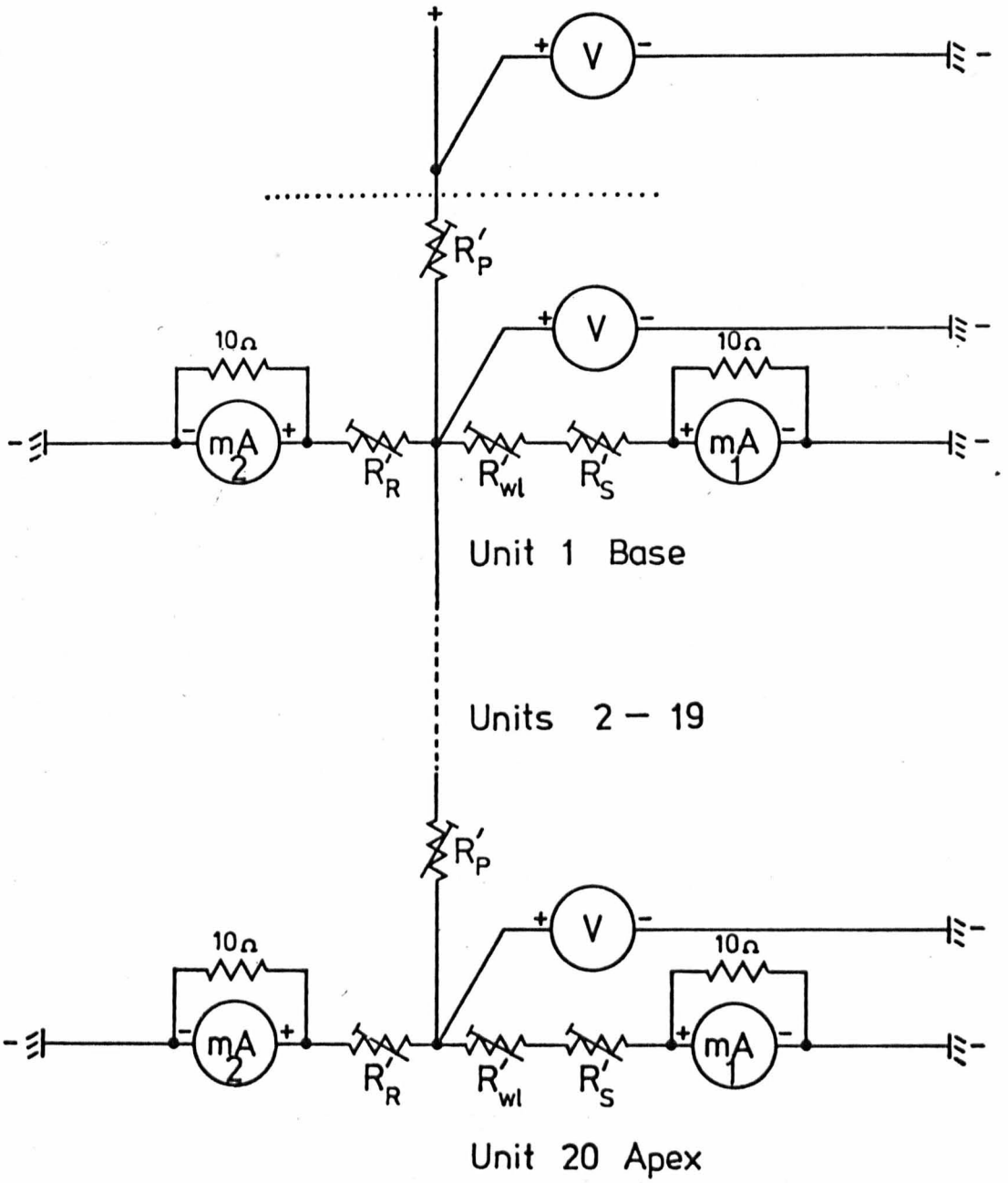
+
V
-
R'_P
10Ω
mA 2
R'_R
R'_{wl}
R'_S
10Ω
mA 1
Unit 1 Base
Units 2 – 19
R'_P
Unit 20 Apex

(v) Porosity in each segment variable between 0.7 and 100%.

(vi) Respiratory oxygen uptake variable between zero and 1.66×10^{-7} g s^{-1} cm^{-3} root. However, more conveniently monitored in the equivalent units zero to 250ng min^{-1} cm^{-2} root surface.

(vii) Root wall permeability variable between zero and 100% in each segment.

(viii) Potential soil oxygen demand ("soil sink"):

Armstrong and Wright (1976b) simulated the oxygen demand outside the root by considering each root segment to lie centrally within a cylindrical ' water shell (r = 0.1125cm) with the shell boundary maintained at zero oxygen concentration. Luxmoore et al. (1970a) employed a similar method to apply external sink activity in their mathematical model, and the amount of oxygen consumed by the sink varied with the internal oxygen concentration of the root. In the present study the analogue was modified to allow the modelling of specified rates of soil oxygen consumption between zero and 10.0×10^{-5} cm^3 cm^{-3} s^{-1}. Full details of the modifications are given in Chapter 9.

(ix) Radial oxygen loss measurable between zero and 250ng cm^{-2} min^{-1} (78.5ng min^{-1} per segment).

(x) Temperature normally 23°C but readily variable.

D. PROGRAMMING

The analogue was programmed on a per centimetre segment basis.

1. Internal diffusive resistance

Diffusive resistance, either calculated from porosity data (equation 7.4; Luxmoore et al., 1970b; Armstrong, 1971a; Chapter 3) or obtained experimentally (Chapter 7) was converted to electrical resistance as described by Armstrong and Wright (1976b) and as outlined on p.176 Internal and wall resistances were set prior to respiration.

2. Respiration

Respiration rate programmed in any segment must be appropriate to

the oxygen concentration in that segment. However, results presented in Chapter 4 (see also Armstrong and Gaynard, 1976) suggest that respiration will be at a maximum above an internal oxygen concentration of about 2%. Since respiratory activity in the model is expressed in ng $cm^{-2}min^{-1}$ it was necessary to convert experimental data to these units.

In the original analogue described by Armstrong and Wright correct respiratory programming required several adjustments of the respiratory controls because of the interdependence of the segment activities. With the incorporation of "constant current devices" (see p.35) it became necessary to adjust each respiratory control once only.

E. AMENDMENTS TO THE ORIGINAL ANALOGUE

1. Placing of resistors controlling respiration and R.O.L.

In the original analogue the currents representing the oxygen consumed in respiration and that lost by leakage (R.O.L.) were "tapped" at the base of each centimetre segment (Fig.2.8). During the course of this investigation it was realised that this was not an entirely satisfactory analogue of the living condition since it fails to take proper account of the distribution of respiration and leakage along the whole root, or even along an individual segment. In unit length of root, having uniformly distributed respiration and R.O.L., an entirely accurate simulation would be one in which an infinite number of equal tappings, of total current equal to that lost per segment, were taken along the porosity resistor. However, it is impossible to construct such an analogue and a compromise must be reached.

Consider a 20Ω linear resistor, R', with a source of potential, V, of 40 volts applied at one end. Let the current, i, taken by each of a finite number, n, of tappings set equidistant along R' be such that the total current taken, $\sum_{1}^{n} i$, be 2 amperes.

The voltage drop, ΔV, across R' may be calculated by summing the

individual voltage drops across the n components of R'. For example, if n = 5, then V = 24 volts. This same voltage drop would be realised also if the current $\sum_1^n i$ had been taken from a single point R'_{eff} along R'. The value of R'_{eff} is given by

$$\frac{\Delta V}{\sum_1^n i}$$

and in this case is $24 \div 2$, or 12Ω. The ratio R'_{eff}/R' is 0.6 when n = 5; if n is less than 5 the ratio increases, whilst for values of n greater than 5 it diminishes.

The relationship between n and the ratio R'_{eff}/R' is given in Fig.2.9. The curve is a hyperbola and its equation (found by plotting 1/n against R'_{eff}/R') is:

$$R'_{eff}/R' = (0.5/n) + 0.5$$

From this equation it is evident that as $n \to \infty$, then R'_{eff}/R' tends to 0.5. In other words, provided that the major concern is with total concentration drop along unit length of root rather than with the concentration profile, the best representation of the living condition is made if respiration and R.O.L. are tapped mid-way along the segment. In practice this was achieved without alterations to the basic circuit by programming the porosity resistors, R'_p, as shown in Fig.2.10 (i.e. effectively connecting the ammeters and voltmeters at 0.5, 1.5, 2.5cm etc. from the root base). The voltages V_1, V_2, V_3 etc at 1.0, 2.0, 3.0cm etc were then obtained as shown in Fig.2.10.

2. Constant current devices to simulate respiration

In the basic circuit (Fig.2.8) respiratory oxygen demand was simulated by adjusting the variable resistors, R'_R, in order to take the required current. Any change in internal oxygen concentration (voltage) altered the current through R'_R, which therefore required readjustment. Certain of the analogue investigations in this study required that respiration be kept constant despite a continuously diminishing internal oxygen regime (Chapter 5). This necessitated the incorporation of constant current

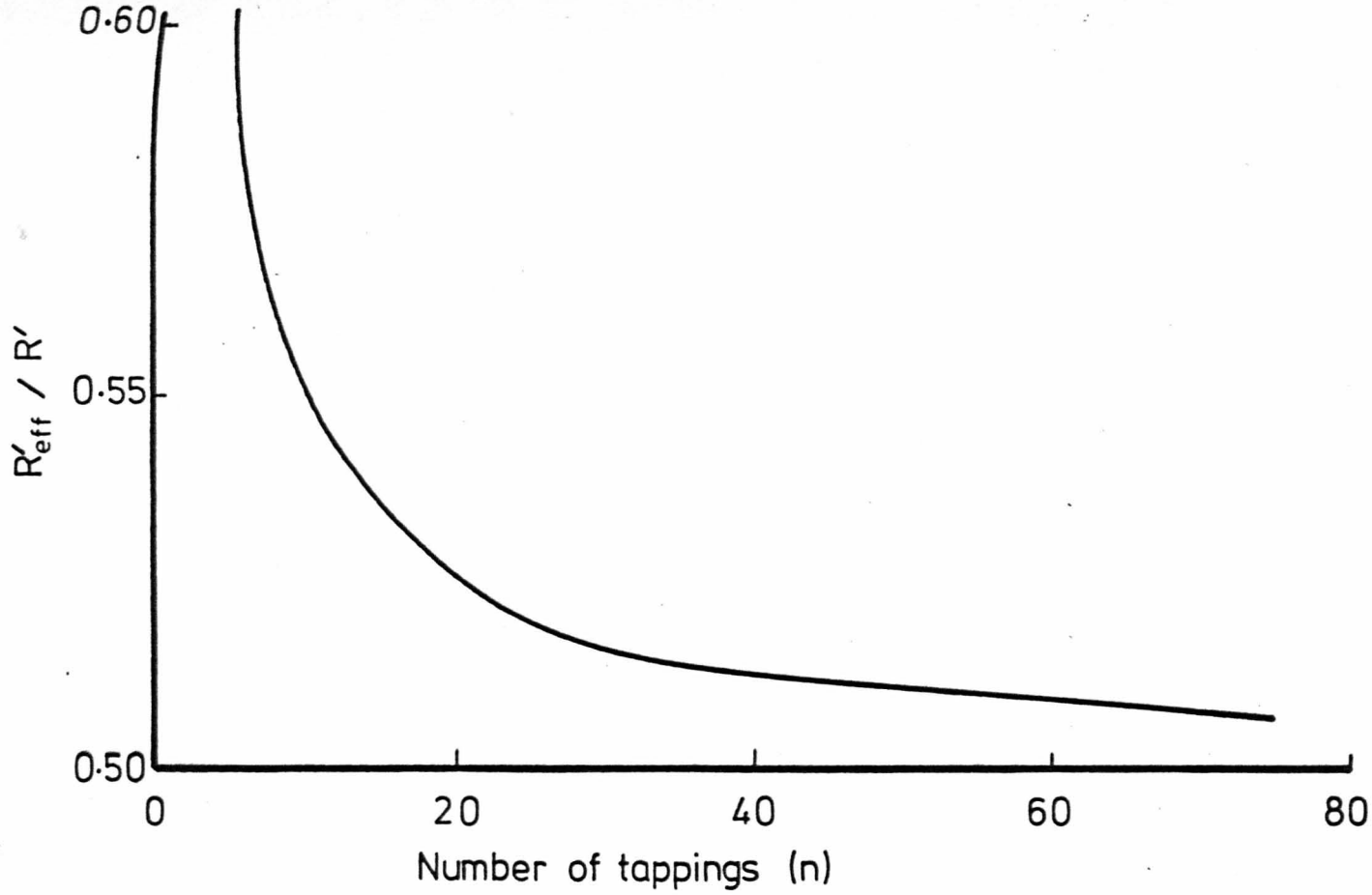

FIG. 2.9 · For explanation see p.35

$$\frac{R'_{eff}}{R'} = \frac{0{\cdot}5}{n} + 0{\cdot}5$$

FIG. 2.10 Electrical analogue : Showing the method of programming the pore space resistors ($R'p$) to effectively tap respiration and R.O.L. mid-way along each segment (ie 0·5, 1·5, 2·5cm etc from the base).
Oxygen concentration at the end of each segment (boxed) is derived from the voltmeter readings as shown.

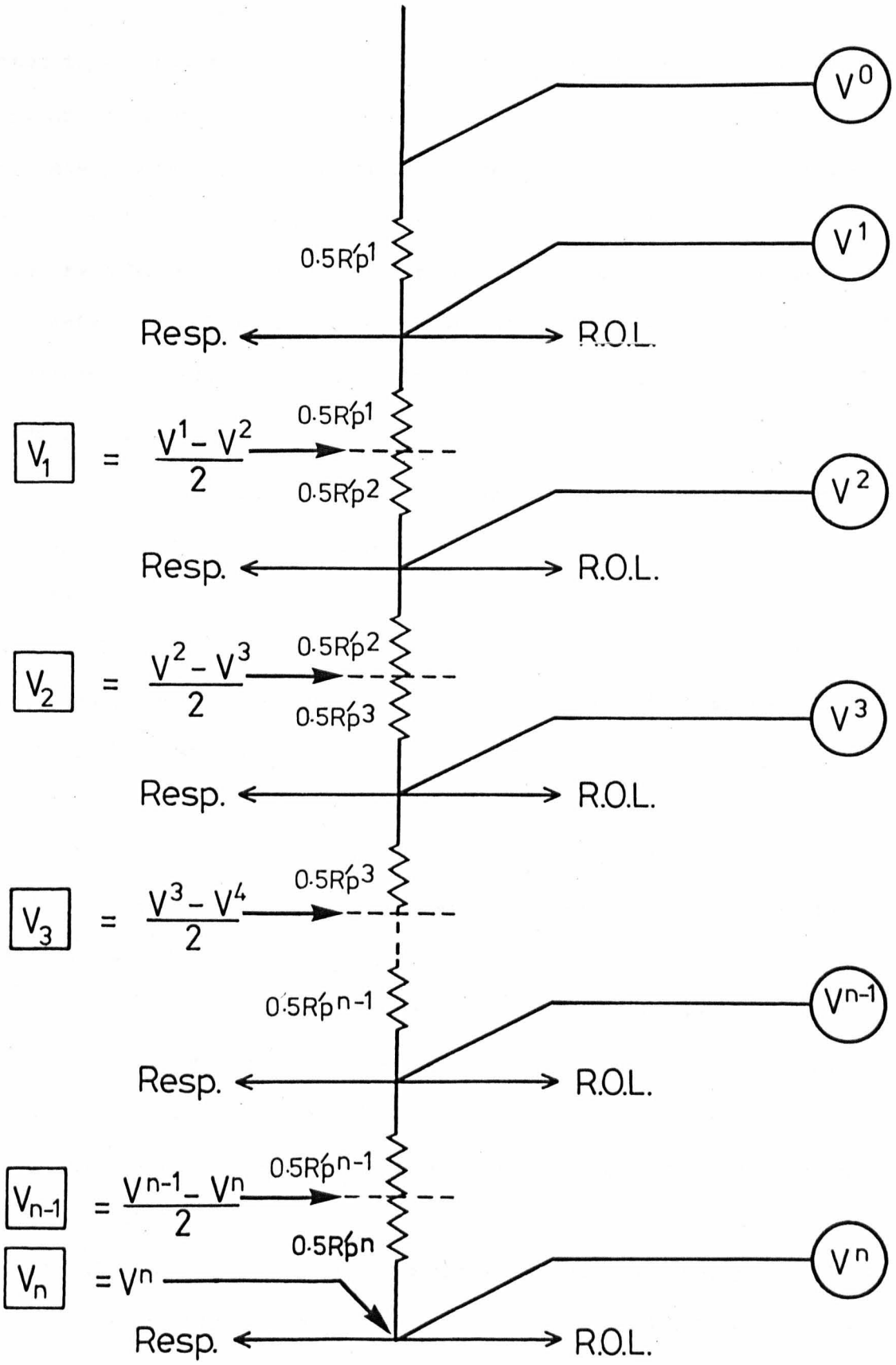
V^0
V^1
$0.5R'p^1$
Resp.
R.O.L.
$V_1 = \frac{V^1 - V^2}{2}$
$0.5R'p^1$
$0.5R'p^2$
V^2
Resp.
R.O.L.
$V_2 = \frac{V^2 - V^3}{2}$
$0.5R'p^2$
$0.5R'p^3$
V^3
Resp.
R.O.L.
$V_3 = \frac{V^3 - V^4}{2}$
$0.5R'p^3$
$0.5R'p^{n-1}$
V^{n-1}
Resp.
R.O.L.
$V_{n-1} = \frac{V^{n-1} - V^n}{2}$
$0.5R'p^{n-1}$
$0.5R'p^n$
$V_n = V^n$
V^n
Resp.
R.O.L.

devices to replace the simple variable resistors, R'_R; circuit details are given in Appendix 3. These devices allowed the desired respiration rate, once programmed, to remain independent of internal oxygen concentration until a pre-set value was reached, or until the oxygen concentration fell below that required for the efficient operation of the instruments (0.3 - 0.4%). The constant current devices also facilitated respiratory programming along the length of the root.

III. Microscopy

Plant material required for both light and transmission electron microscopy was prepared as follows.

Tissue segments were fixed in 3% glutaraldehyde in phosphate buffer (pH 7.3). The tissue was first infiltrated with the glutaraldehyde solution under vacuum and then left to stand in the fixative for 5h on a rotator. This was followed by overnight washing in two changes of buffer.

The tissue was then double-fixed in 1% osmium tetroxide in buffer for 2½h followed by a 15 min buffer-wash. It was then dehydrated in an ethanol series (30% to absolute).

The dehydrated tissue was embedded in Spurr's low viscosity resin (Spurr,1969). This involved impregnation for 2½h by a mixture of equal parts resin and absolute alcohol followed by overnight impregnation by pure resin. Finally the tissue was embedded in resin which was polymerised overnight at 70°C.

The material was sectioned on a Huxley ultra-microtome using glass knives. Sections for light microscopy were cut at 1.0μm thickness and stained in 1% toluidene blue in 1% borax. Specimens were photographed using a Zeiss photomicroscope.

Sections for electron microscopy were cut at 0.09 - 0.15μm thickness (i.e. gold off the knife). They were stained in uranyl acetate and lead

citrate and examined in a J.E.M. 7A electron microscope at 80 Kv accelerating voltage.

IV. Plant Material

1. Eriophorum angustifolium Honck.

Typical of wetland species E.angustifolium is adapted to growth in anaerobic soils largely by virtue of its well-developed oxygen transport system. The rate of radial oxygen loss from the roots is high, rendering the species an ideal subject for investigation by the cylindrical platinum electrode technique.

Stock plants were grown in large buckets of waterlogged peat-loam mix (3:1). They were started under glass and then transferred to a growth room having the following conditions: temperature, 20 $\pm$ 1°C; day length, 16h; photosynthetically active radiant flux density at the soil surface, 100μE $m^{-2}s^{-1}$ (provided by cool fluorescent lights). The water table was maintained at 1-2cm above the soil surface with distilled water, and soil pH under these conditions was about 7.0. Vegetative propagation was prolific, and plants were continuously available in a variety of sizes.

Individual plants were easily extracted by gently pulling them from the soil and severing any attached rhizomes. The root system was immersed in clean water to remove the soil, any stubborn soil particles being loosened with a soft brush. Finally the ends of cut rhizomes were sealed with lanolin to prevent flooding.

2. Rice

Husked seeds of rice (Oryza sativa L., var. Norin 36 or 37) were coated with a mercury-based fungicidal dressing, placed on moist blotting paper in a shallow tray, covered with a transparent polythene sheet and germinated in the dark at 25°C. After seven days roots and shoots were well-developed and the tray was transferred to a 25°C growth room; illumination was as for Eriophorum. After a further two days the seedlings were planted in wet peat-loam mix (3:1) and left for three days to become

established; the soil was then waterlogged as for the Eriophorum. Tillering commenced at about 2-3 weeks and plants were removed for use at the two tiller stage (about 6 weeks).

CHAPTER 3

MORPHOLOGICAL, ANATOMICAL AND RESPIRATORY CHARACTERISTICS OF ERIOPHORUM ANGUSTIFOLIUM

Most of the experimental work described in this thesis was performed on Eriophorum angustifolium, whilst the greater part of the mathematical and electrical modelling was based on this species also. As a preliminary to the main part of the study, therefore, it was necessary to obtain certain morphological, anatomical and respiratory data pertinent to the investigation of internal aeration in Eriophorum.

A. GENERAL MORPHOLOGY

Much of the morphology and anatomy of E.angustifolium has been described by Phillips (1953, 1954 a,b) and Metcalfe (1971). The major vegetative features of the plant are shown in Plate 3.1. The species is perennial, spreading by means of rapidly growing rhizomes. The rhizome bears scale-leaves but lacks buds and roots save at the end, where it turns upwards to produce a swollen stem bearing foliage leaves, roots and buds. Axillary buds on the stem elongate to produce daughter rhizomes, forming a sympodial system. The inflorescence forms terminally, usually during the third season of growth of the shoot; after flowering the shoot dies.

The foliage leaves are normally divisible into three distinct regions. These are a narrow, pointed tip, of triangular cross-section; a channelled blade, of approximately v-shaped cross-section; and a sheathing base, crescentric in cross-section. The adaxial surface of the leaf base bears a large membranous ligule, which extends laterally from the leaf margin to tightly envelope the inner leaves and effectively extend the sheath region some distance along the leaves. In the present study this membrane has been referred to as the "leaf sheath".

Stomata, which are restricted to the abaxial surface, are few or absent in the sheath region but increase markedly in number beyond (Chapter 6).

PLATE 3.1: Eriophorum angustifolium; vegetative features.

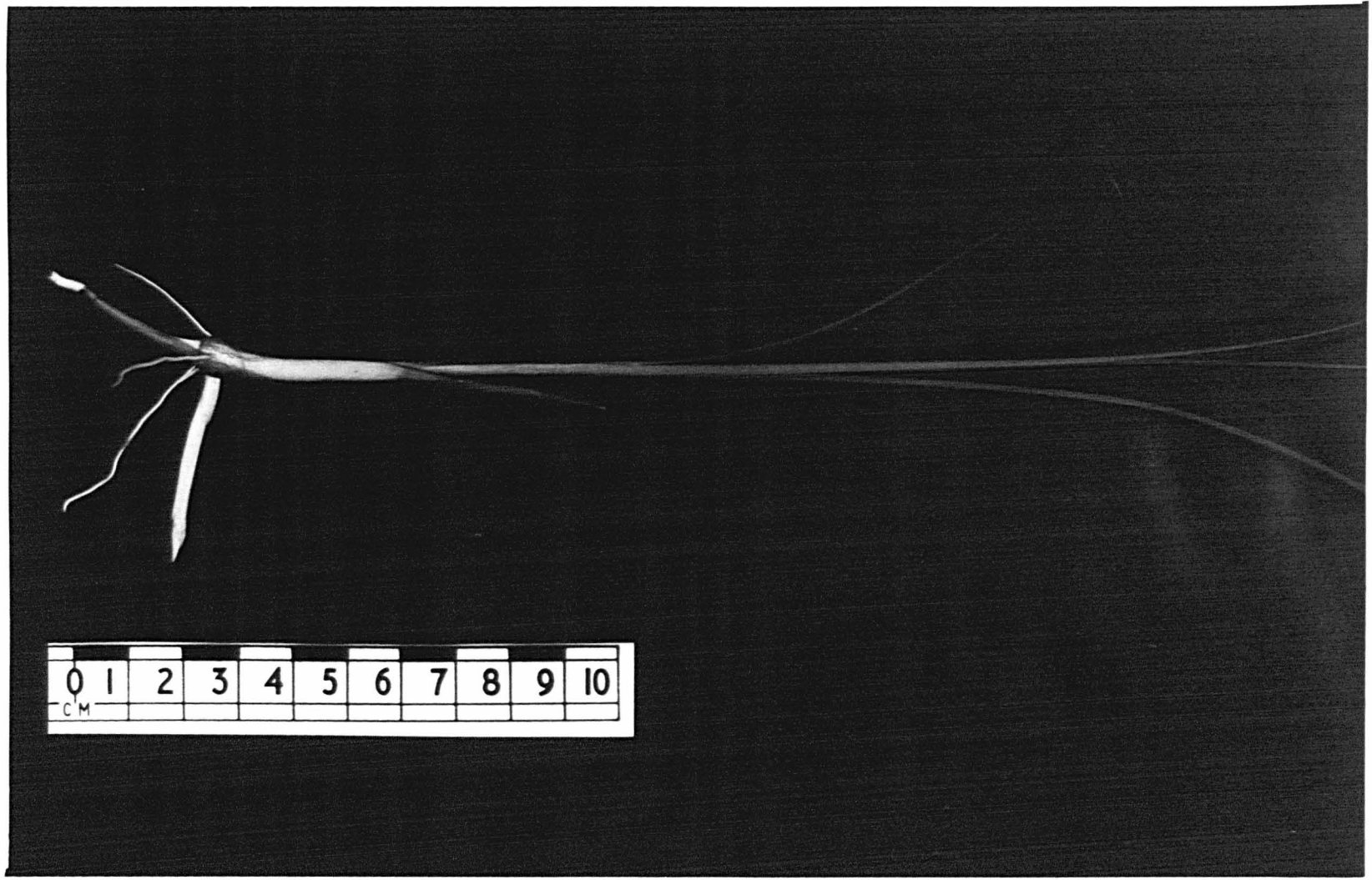
0 1 2 3 4 5 6 7 8 9 10
CM

In addition to the normal foliage leaves shorter, outer leaves occur which are not included in the main leaf group (Plate 3.1). These "free leaves" are less distinctly divisible into tip, blade and base and tend to wither at an early stage of growth. They rarely extend beyond the main sheath region but, as shown in Chapter 6, they may be of importance in the internal aeration of the root system.

B. THE GAS SPACE SYSTEM

1. Introduction

Intercellular gas spaces occur to some degree in all higher plants. Their size ranges from the tiny structures formed immediately behind apical meristems to the large chambers or lacunae in the aerenchymatous tissue of aquatic and semi-aquatic plants. Plate 3.2 shows tangential longitudinal sections through root apices of Eriophorum (a) and rice (b); in the former, intercellular spaces were observed to within 28μm (three cell layers) of the root tip proper (i.e. excluding the root cap) whilst in the latter they occurred to within 19μm (four cell layers) of the tip. In transverse section the apical intercellular spaces of Eriophorum (ca. 35μm from the root tip) and rice (20μm from the root tip) are as shown in Plate 3.3 a and b respectively. Aerenchymatous lacunae in the basal regions of the Eriophorum root are shown in Plate 3.7 c and d.

Intercellular spaces are found in both primary and secondary tissues. In the former they occur mainly in extrastelar ground tissues, for example the cortical parenchymas of stem and root, and the mesophyll and palisade tissues of leaves. In all cases an interconnecting network is formed, and in herbaceous species the labyrinth of gas-conducting channels may form a continuum between the ground tissues of leaves, stem and roots (see p. 10). In general gas space tissue in secondary tissues tends to be less extensive. The term "aerenchyma" was first used to describe the gas space tissue which forms from secondary cambia in some species (Schenck,

PLATE 3.2: Tangential longitudinal sections through root apices of:

(a) E. angustifolium (x 725)

(b) Rice (x 290)

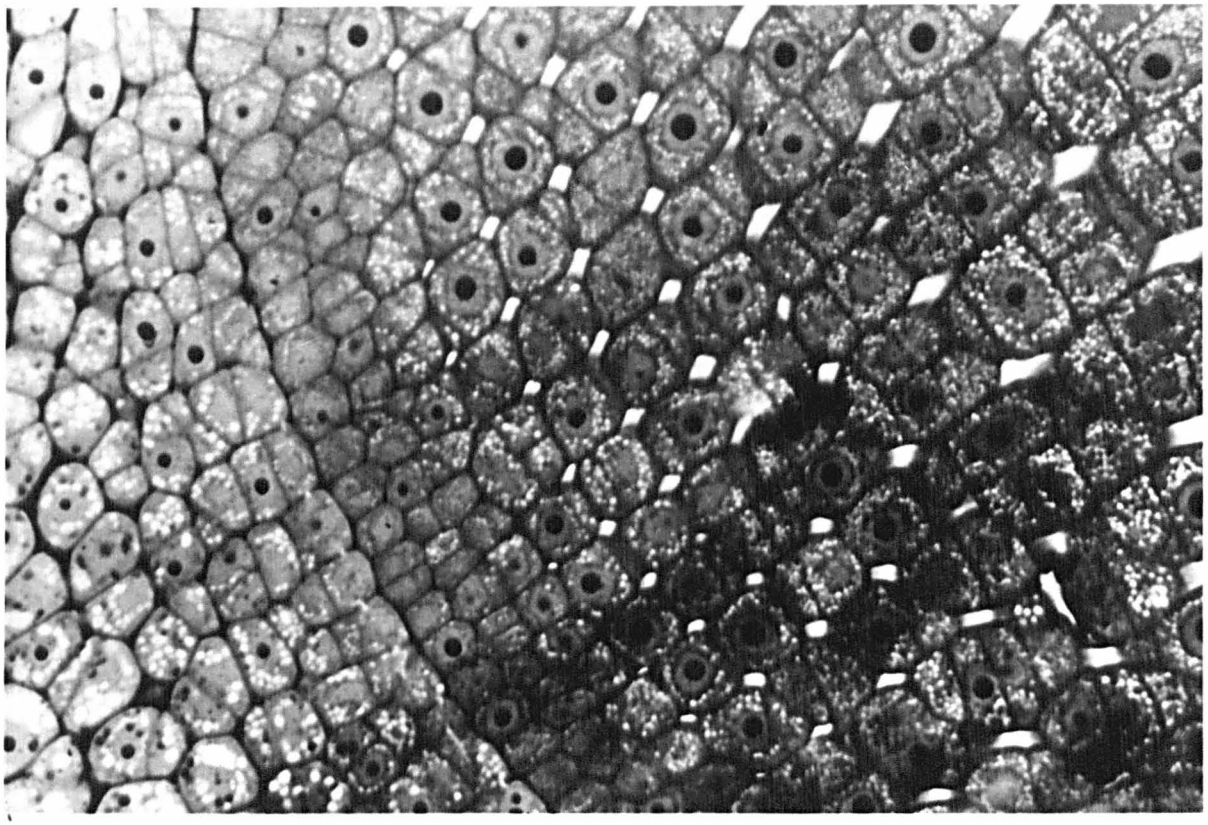

a

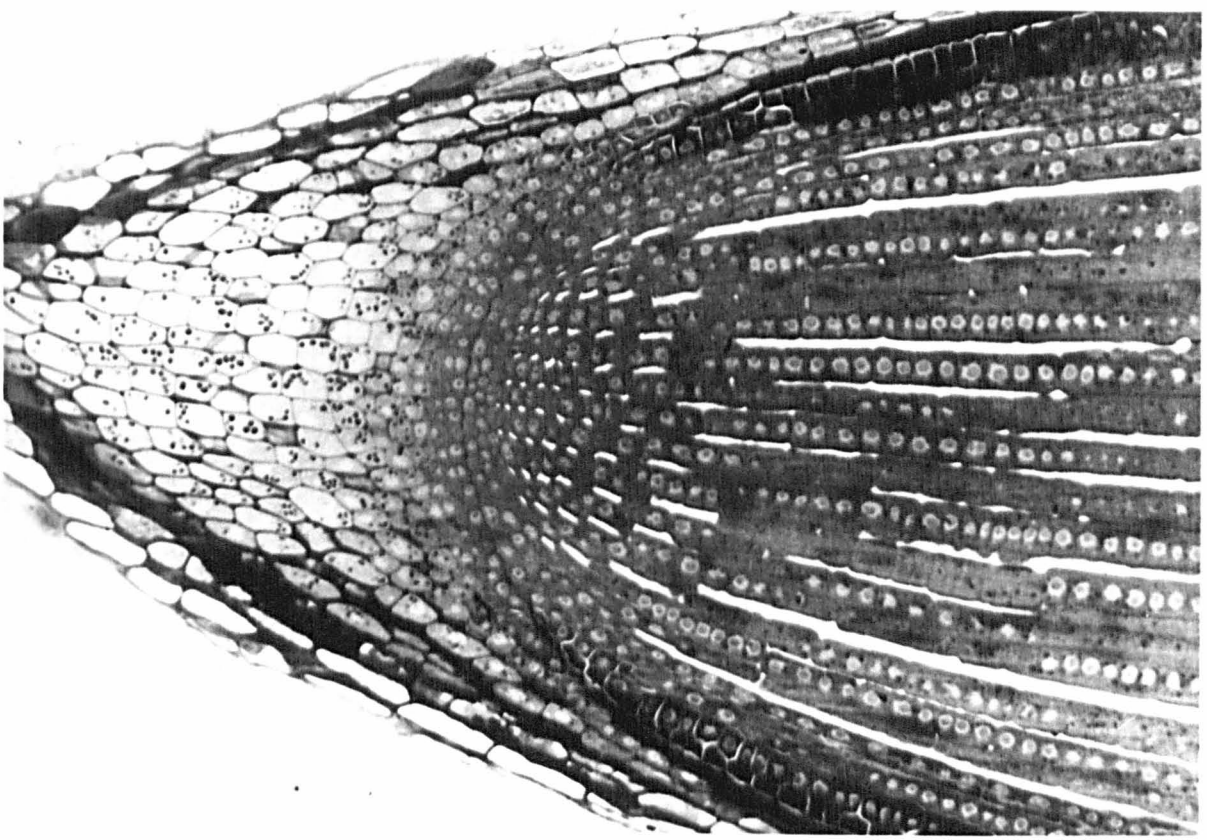

b

PLATE 3.3: Transverse sections through roots of:

(a) E.angustifolium at 35μm behind the root tip (x 240)

(b) Rice at 20μm behind the root tip (x 230)

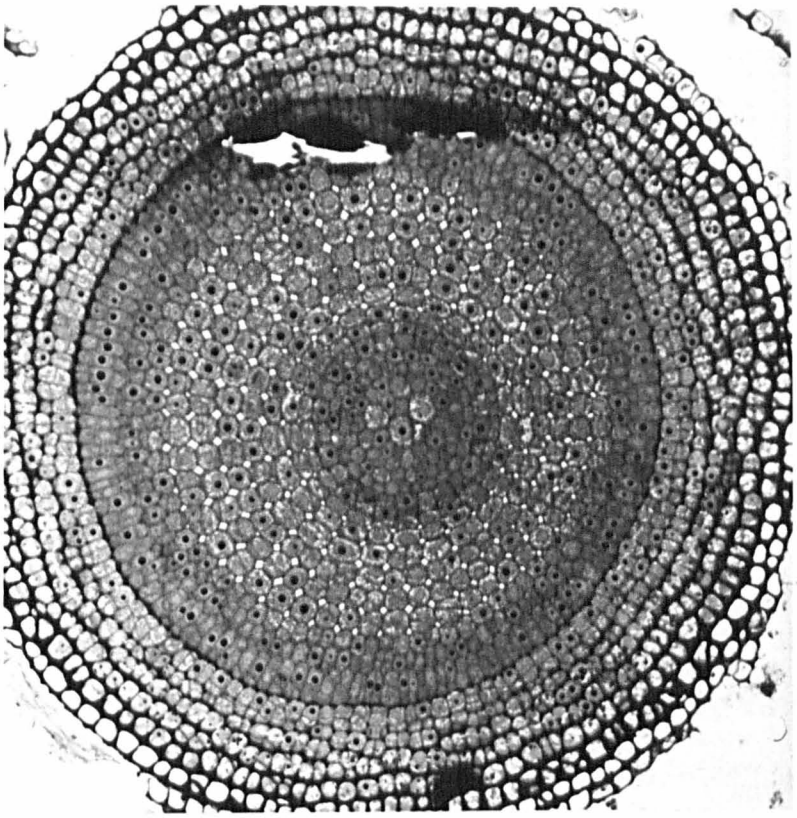

a

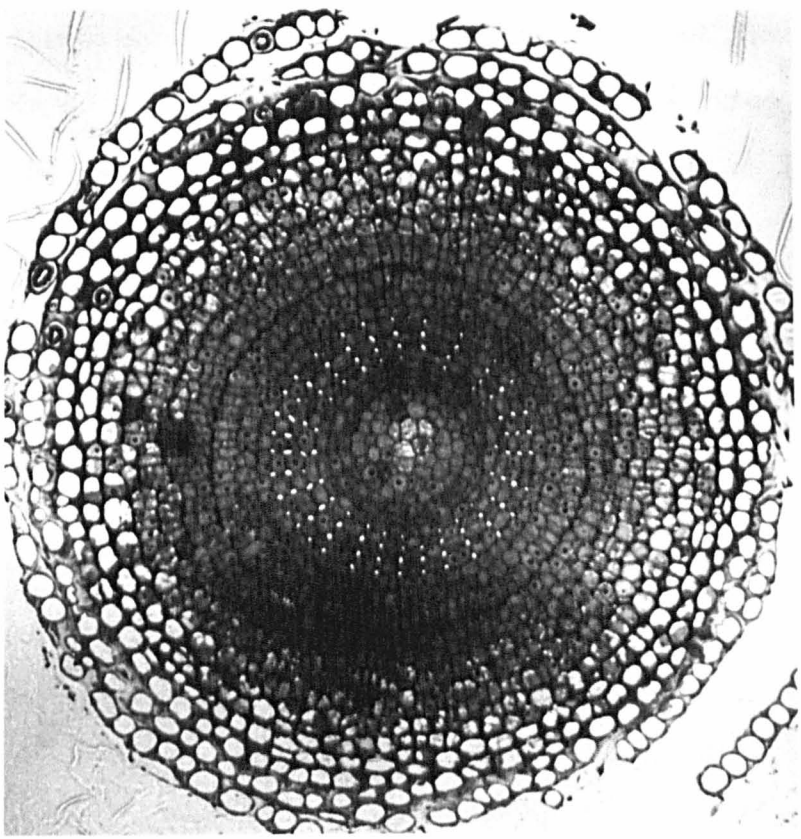

b

1889), but the word is now applied to any tissue containing large gas-conducting channels, whether primary or secondary in origin.

The tiny apical intercellular spaces appear to be the forerunners of all primary gas spaces (Sifton, 1945). Martens (1937, 1938), cited by Esau (1965), described the formation of these structures: when a cell divides the new middle lamella is separated from the old one surrounding the parent cell by the cell wall. The free ends of the new middle lamella thicken to form a mass within which develops a cavity. The parent cell wall adjacent to the expanding daughter middle lamella breaks down and the old and new middle lamellae fuse. The cavity thus becomes an intercellular space lined with lamellar substance. Although this view of intercellular space formation is widely held it may not be invariably true: Plate 3.4 a and b show the development of intercellular spaces at about 30μm from the rice root apex. It can clearly be seen that in this case the middle lamellae have fused before cavity formation commences. This is in agreement with the description of intercellular space formation given by Robards (1970). Fully-formed spaces at about 0.15cm from the root apex are shown in Plate 3.5. In some cases a waxy substance may be deposited on the pectic material of the lamella lining the intercellular space (Sorokin, 1967).

Further development of the intercellular spaces may continue in one of two ways. De Bary (1884) has described these as follows:

(a)... "by separation of <u>permanent</u> tissue-elements, as the result of their unequal surface-growth in different directions, the original common walls splitting, while the common limiting layer which was originally present is - perhaps always - dissolved."

(b)... "by disorganisation, dissolving, or in many cases rupture of certain <u>transitory</u> cells, or groups of cells, which are surrounded by permanent tissues."

The former process is termed "schizogeny", the latter "lysigeny".

Schizogenous enlargement of the first-formed intercellular spaces has

PLATE 3.4: Electron micrographs showing the development of intercellular spaces at about 30μm behind the rice root tip.
Note the fusion of the middle lamellae prior to cavity formation.

(a) x 36,550

(b) x 18,450

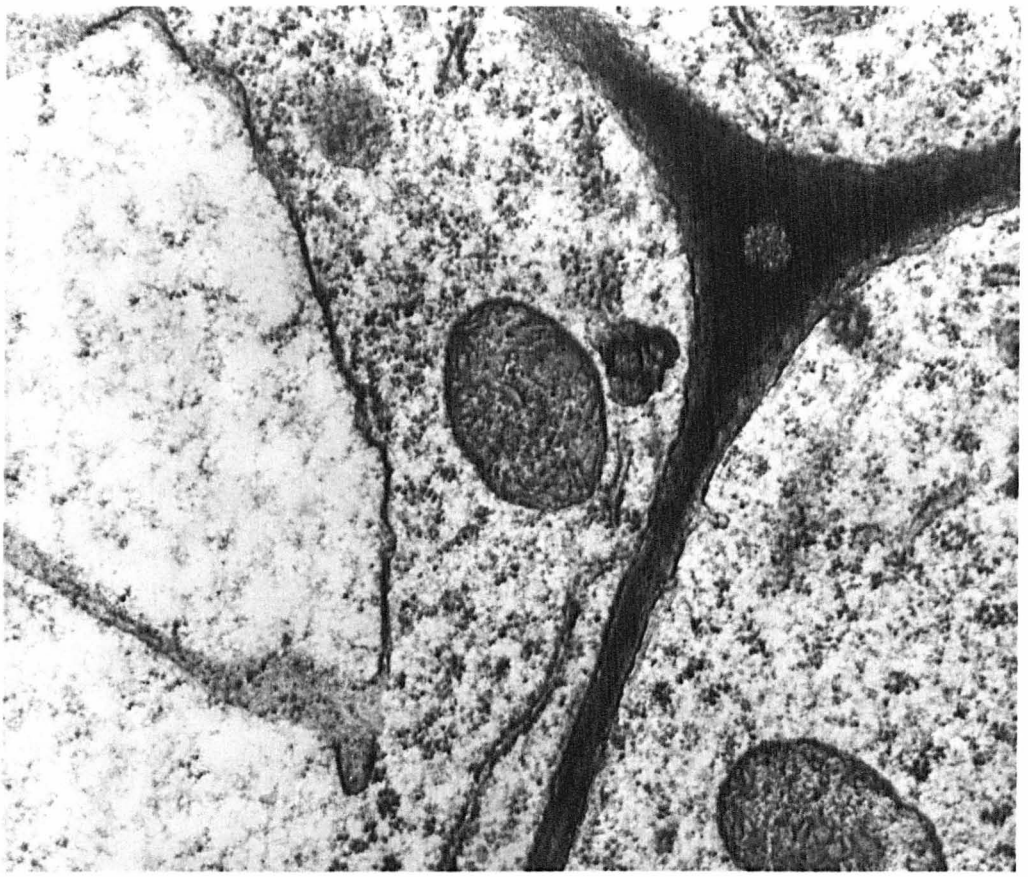

a

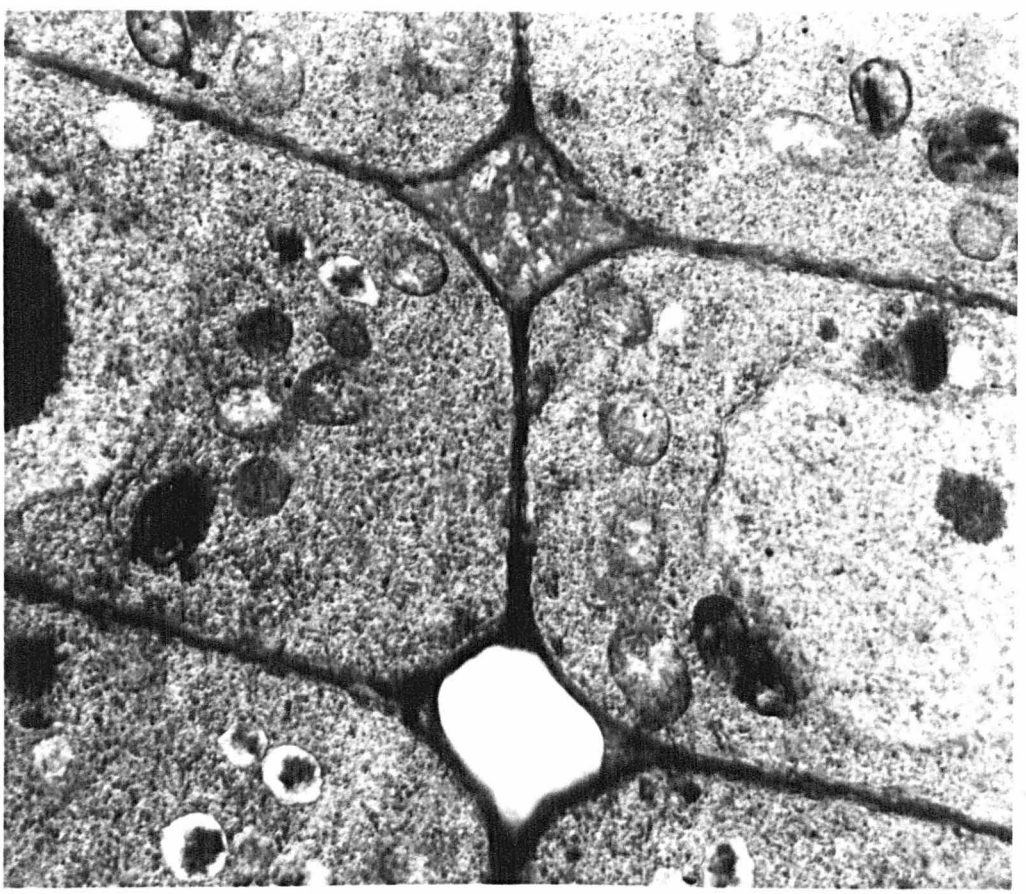

b

PLATE 3.5: Electron micrograph showing fully-formed intercellular spaces at 0.15cm behind the rice root tip (x 5,150).

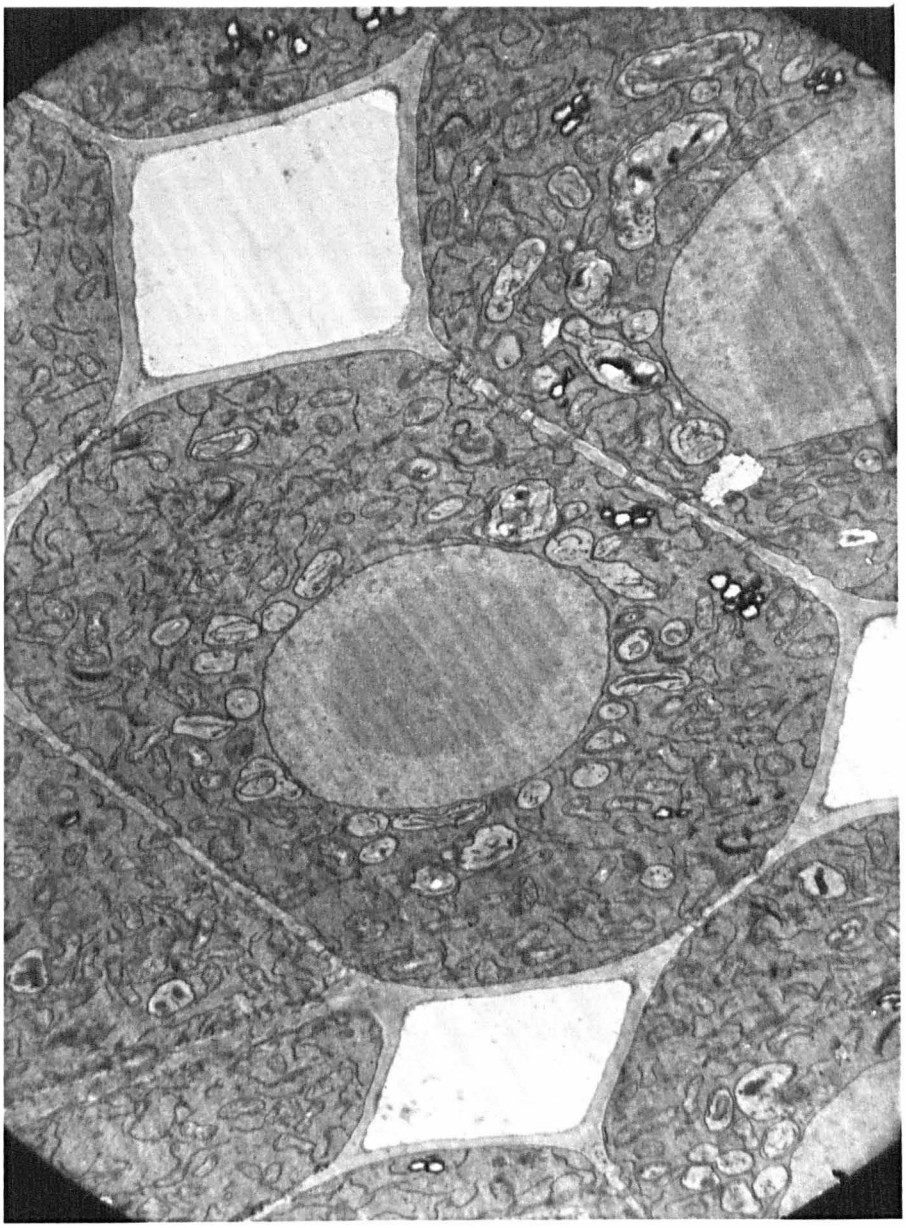

been followed by Arber (1914) in the root of Stratiotes aloides L. The cortical cells are arranged in radial plates, and in their early stages divide rapidly at right angles to the long axis of the root. This results in elongation of the plates in the direction of growth, but at a rate greater than that of the other root tissues. Consequently, the cell plates are thrown into undulations, an increase in root diameter allowing for their separation at intervals in the form of schizogenous gas spaces.

In many species development ceases at this stage, but in others, particularly in the aerial parts of wetland plants, much larger schizogenous spaces may develop; cell walls become drawn in at points not in contact with neighbouring cells, the spaces become rounded, and the result is a network of irregularly-shaped cells maintaining contact by means of arms projecting in various directions (Sifton, 1945).

Lysigeny is a process common in the roots of wetland plants. Cell collapse may be so extensive as to leave only thin partitions or septa between lacunae, and a few layers of cells adjacent to the endodermis and epidermis; gas-filled porosity may reach 60%. The basipetal development of lysigenous gas spaces in the root of E.angustifolium is shown in Plate 3.7.

The primary gas channels in the aerial parts of wetland plants are not continuous structures but are interrupted at intervals by perforate septa called diaphragms. These assume a variety of forms, but in all cases they are permeable to gases but impermeable to water. They therefore serve the important role of preventing the flooding of the entire lacunar system through injury.

In most species diaphragms have a definite tissue form, being composed of one, two or occasionally several cell layers (Sculthorpe, 1967). Pores form where cells draw apart at their corners, and in some cases separation occurs also at points along contact faces to give rise to cells of stellate shape and to increase the number of pores (Sifton, 1945). Plate 3.6a is a transverse section of a leaf of E.angustifolium showing a diaphragm across

PLATE 3.6: Lacunar diaphragms in the leaf of E.angustifolium.

(a) Transverse section through a leaf showing the gross appearance of a diaphragm across one of the gas channels (x 240).

(b) Transverse section through a diaphragm showing the intercellular pores (x 1,960).

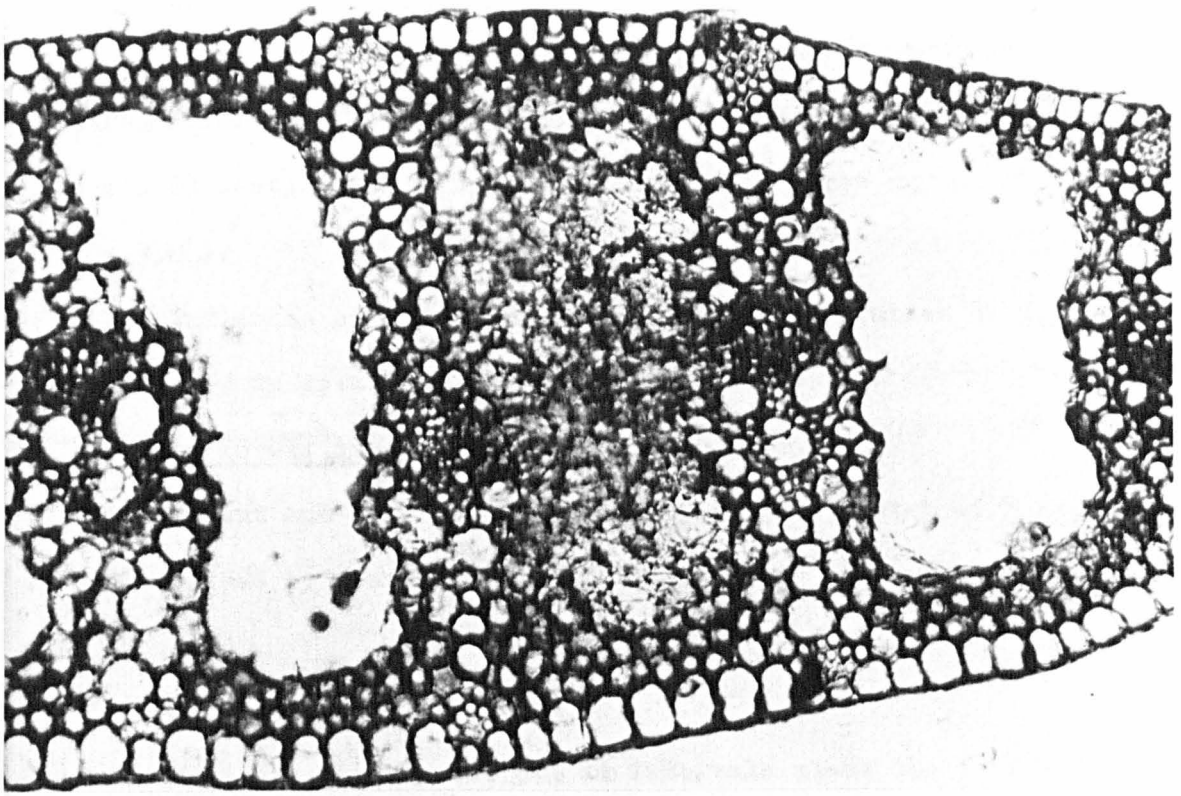

a

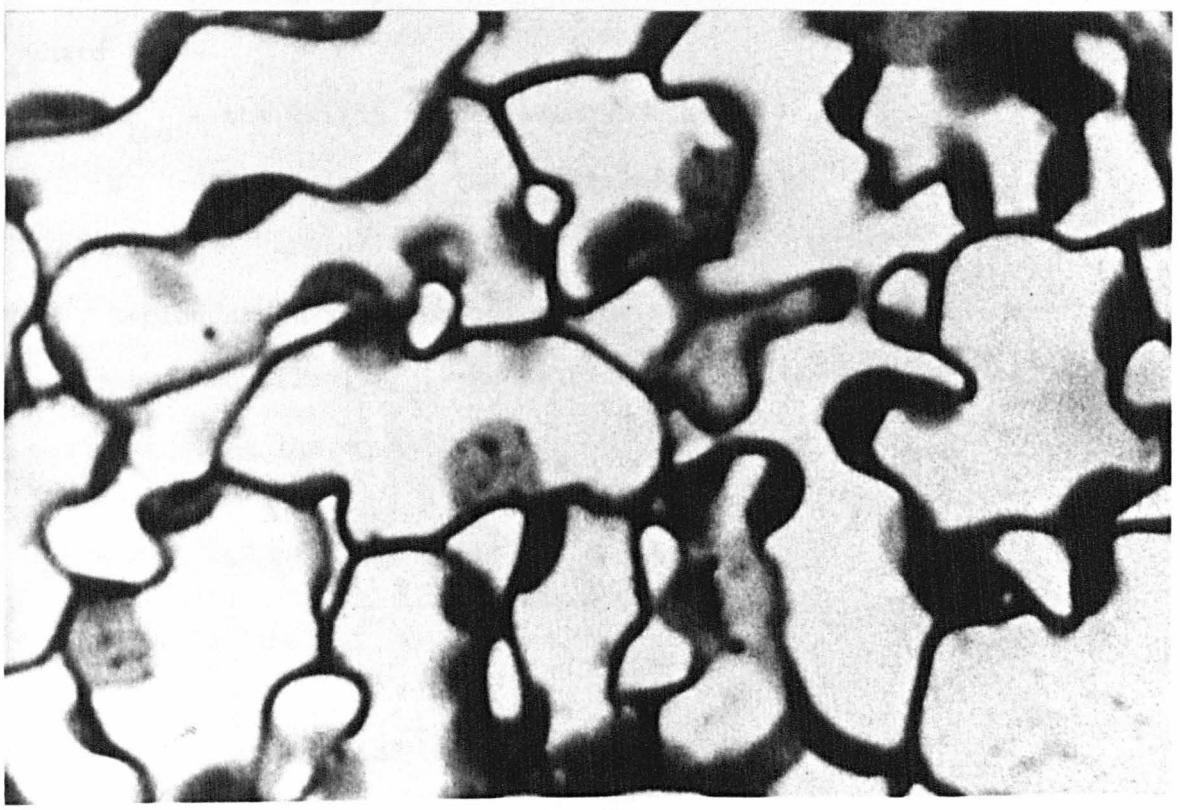

b

one of the gas channels. In surface view and at low magnification the diaphragm, which is several cells thick, has an amorphous appearance. However, in section the cellular structure and pores may be clearly seen (Plate 3.6b).

The influence of diaphragms on the internal aeration of E.angustifolium is considered in detail in Chapter 7.

2. Porosity levels in E.angustifolium

The extent and distribution of the gas space system of E.angustifolium were determined by measuring gas-filled porosity throughout the plant.

(a) Methods

(i) Leaves

Transverse sections were cut at intervals along the leaf and photographed using a Zeiss photomicroscope. The air cavities were clearly visible in the enlarged photographs (Plate 3.6a). Fractional porosity, ϵ_l, was given by:

$$\epsilon_l = \frac{W_{lac}}{W} \times 100 \quad \% \qquad (3.1)$$

where

W_{lac} = the weight of the lacunae (g)

W = the weight of the entire section (g)

(ii) Roots

Beginning at the apex transverse sections were cut at intervals along the root. Porosity, ϵ_r, was determined from enlarged photographs of the sections using the equation:

$$\epsilon_r = \frac{\left[(W_{ct} - W_{lac}) \frac{W_{ac}}{W_c}\right] + W_{lac}}{W} \times 100 \quad \% \qquad (3.2)$$

where:

W = the total weight of the section

W_{ct} = the total weight of the cortex

W_{lac} = the weight of the lacunae

W_c = the weight of cortex over area A

W_{ac} = the weight of the cortical intercellular spaces in area A

(iii) Stem

Due to its structure the stem did not lend itself to porosity determinations by photography. The vascular bundles are scattered through dense ground tissue within the central endodermis, whilst the outer parenchymatous tissue comprises starch-filled cells with apparently few large intercellular spaces. The method adopted to determine the porosity of the stem was based upon the pycnometer technique of Jensen et al. (1969). The modified procedure was as follows.

A pycnometer (capacity 25cm^3) was filled with boiled distilled water and weighed (W_w). Several stems, with leaf and root bases and rhizome removed, were surface dried and weighed as quickly as possible (W_s). They were then cut into slices approximately 0.1cm thick and placed in the pycnometer, which was filled with water and re-weighed (W_{s+w}). At this point the method differed from that of Jensen et al. In order to remove the gas from the intercellular spaces these workers employed an homogeniser. In the present study, however, it was found that errors were introduced due to incomplete transference of the homogenate between the homogeniser and pycnometer. This was avoided by removing the gas from the tissues by placing the pycnometer and contents under vacuum (0.6cm Hg) in a vacuum desiccator for about ten minutes. The vacuum was applied several times and then the pycnometer was topped-up with distilled water and re-weighed (W_a).

The fractional porosity of the stem tissues, ϵ_{sm}, was obtained as follows:

Let V_{sm} be the total volume of stem tissue. Then:

$$W_{s+w} = W_w + W_s - \rho V_{sm}$$

or

$$V_{sm} = (W_w + W_s - W_{s+w}) \div \rho$$

where ρ = the density of water (g cm^{-3})

If v is the gas space volume in the stems:

$$W_a = W_{s+w} + \rho v$$

or

$$v = (W_a - W_{s+w}) \div \rho$$

now, $$\epsilon_{sm}(\%) = \frac{v}{V_{sm}} \times 100$$

ie. $$\epsilon_{sm} = \frac{W_a - W_{s+w}}{W_w + W_s - W_{s+w}} \times 100 \ \% \qquad (3.3)$$

Care was taken to thoroughly dry the outside of the pycnometer before each weighing and to ensure that all distilled water used was at the same (laboratory) temperature. The pycnometer was always handled with forceps to prevent moisture from the skin adhering to the glass.

(b) Results

Gas-filled porosity in a 30cm long leaf of E.angustifolium is shown as a function of distance from the apex in Fig.3.1. The porosity remains fairly constant at about 30% over the apical 10cm, but then rises steadily to about 60% in the basal regions of the leaf.

Porosity in the root varied with distance from the apex as shown in Fig.3.2. There is a sharp increase from about 15% at 0.25cm to about 23% at 0.5cm. The porosity remains constant to 3.0cm but then rises abruptly again to 53% at 6.0cm and appears to remain at this value in the more basal regions of the root. Further work, however, showed a marked decrease in porosity of the root cortex in the region of the root-shoot junction, where the aerenchyma seems to be absent (see Plate 7.2).

The variation in porosity along the Eriophorum root is strikingly similar to that in the rice root (Armstrong, 1971a). However, root porosity in Eriophorum is in general higher than that in rice which is, for example, 6 to 7% porous at 0.5cm and 46% porous at 6.0cm from the apex when grown in waterlogged soil. The situation in both these wetland species contrasts strongly to that in mesophytes. For example Luxmoore et al.

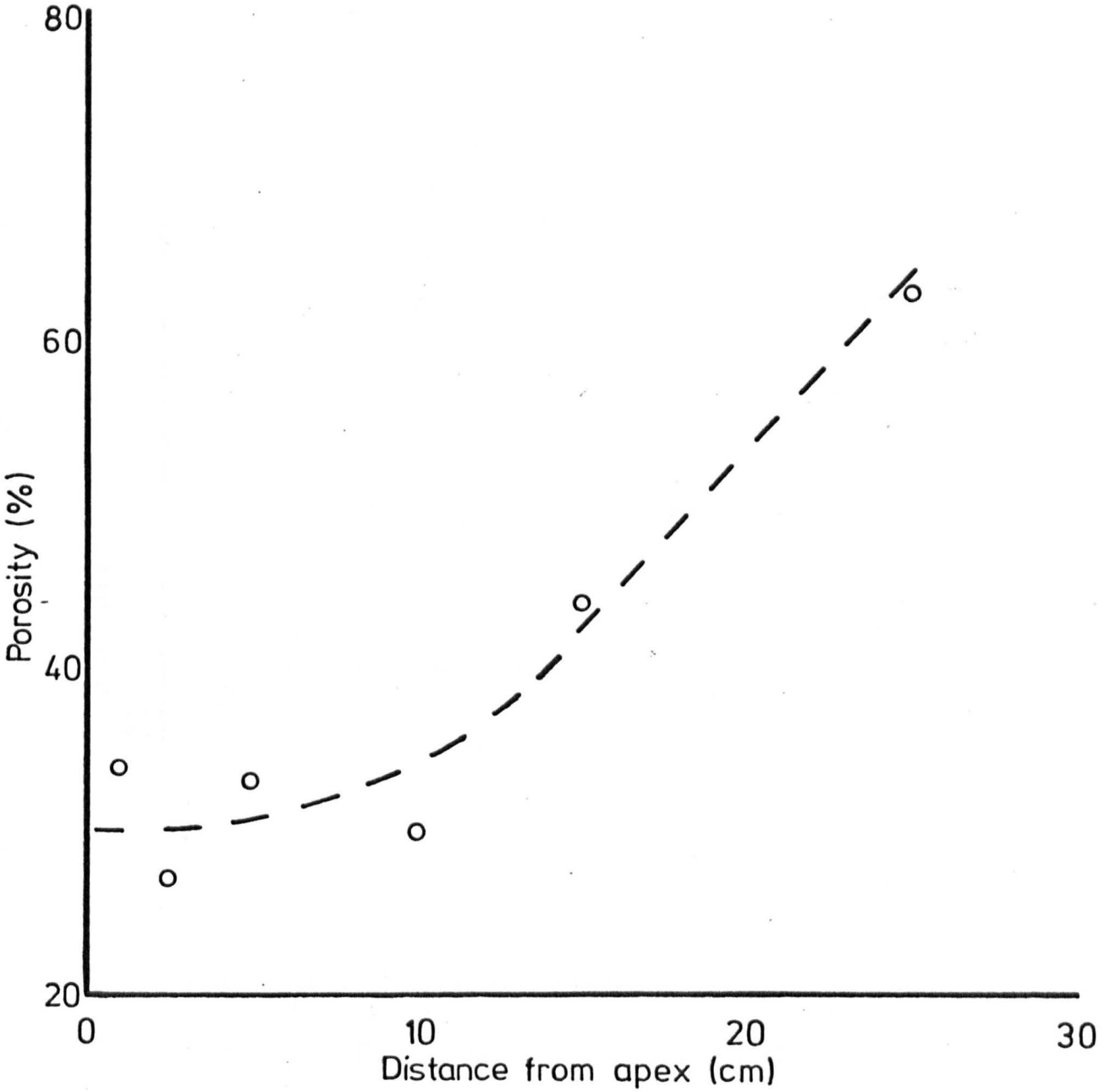

FIG. 3.1 Gas-filled porosity along a leaf of E. angustifolium

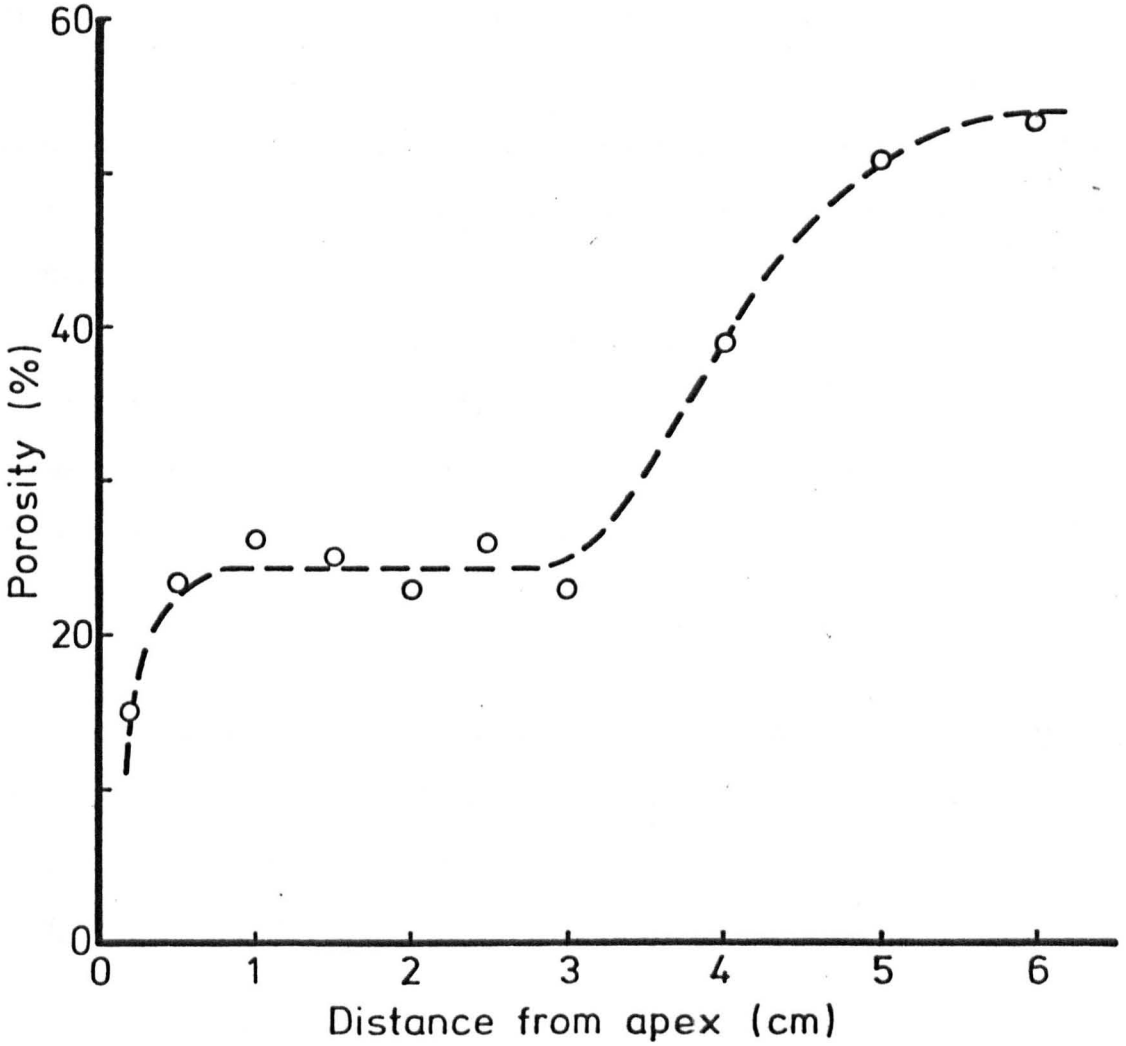

FIG. 3.2 Change in gas-filled porosity along a root of E. angustifolium.

(1970b) measured a porosity of about 9% at 6cm from the apex of the maize root, whilst in pea the gas-filled porosity, which is constant along the length of the root, is as low as 3.8% (Armstrong, unpublished).

The basipetal increase in porosity along the roots of E.angustifolium is illustrated in Plate 3.7 by transverse sections at 0.2, 2.0, 4.0 and 6.0cm from the apex. The high porosity in the basal regions of the roots is associated with lysigenous gas space formation.

Gas-filled porosity in the stem was found to be 10.4%, S.D. $\pm$ 0.55%. This figure was unexpectedly high since in gross appearance the tissues of the stem seem very compact. However, on microscopic examination the stem cortex is seen to have a surprisingly porous structure (Plate 7.2).

In Chapter 5 an evacuation technique is described by which whole plant porosity was determined. There is a curvilinear relationship between porosity and plant volume (Fig.5.2), the percentage of gas space increasing from about 25% in the smallest plants to about 48% in the expanded adults.

C. RESPIRATORY CHARACTERISTICS

Respiration rates were measured using commercial oxygen electrode systems in conjunction with the polarographic equipment described in Chapter 2. Measurements were made on leaf, stem and root tissues.

1. Tissue preparation

(a) Leaf

(i) Apex

Ten one-centimetre apical segments were used for each determination, care being taken to avoid leaves with dead (reddened) tissues.

The pyramidal segments were quickly weighed and the surface area calculated from measurements of the height and base of each of the triangular faces. The total volume of each segment was determined from the formula:

$$V = 1/3\ A\ h \quad cm^3$$

PLATE 3.7: Basipetal development of lysigenous gas spaces in the root of E.angustifolium.

(a) - (d) : transverse sections at 0.2, 2.0, 4.0, 6.0 cm from the root tip respectively. (x 100).

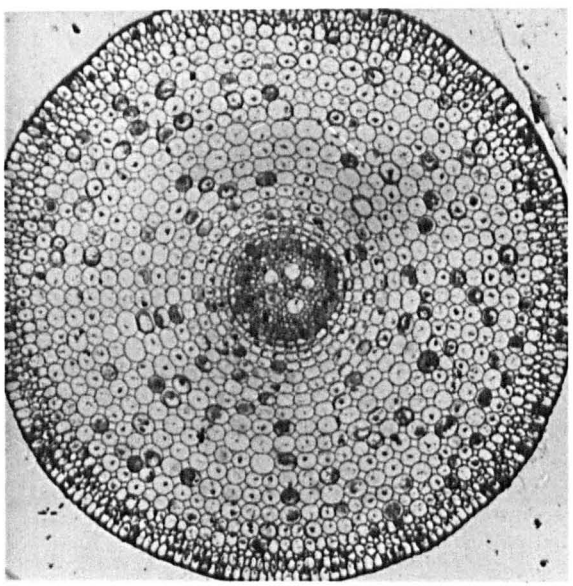

a

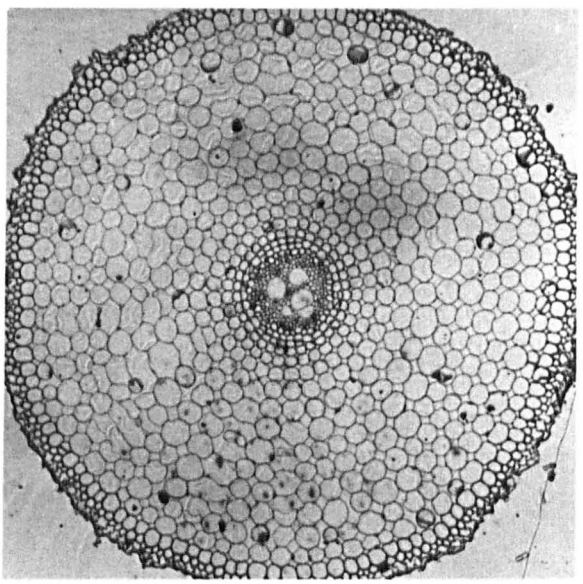

b

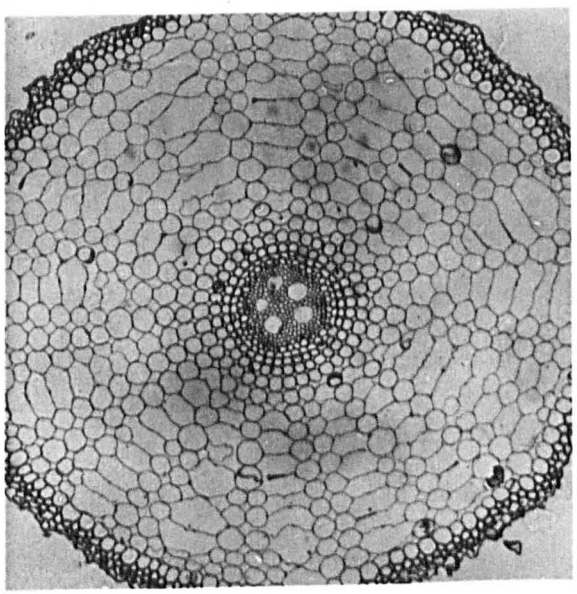

c

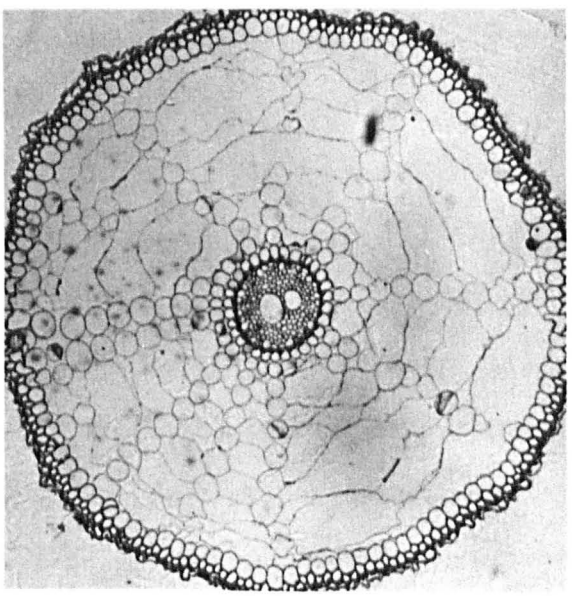

d

where:

A = the area of the triangular base (cm^2)

h = the perpendicular height (cm)

(ii) Mid-leaf and base

One-centimetre segments, taken from the mid-point or the base of three healthy leaves, were used in each determination. The segments were weighed, and the volume and surface area of each were calculated from scale drawings of transverse sections.

(iii) Stem

A cubical block of stem tissue, of side approximately 0.5cm, was used in each determination, no attempt being made to separate the various tissues. The blocks were quickly weighed, and their volumes calculated from the linear dimensions.

(iv) Roots

Beginning with the apical centimetre the respiration rate of consecutive one-centimetre segments was measured, ten segments from each region being used in each determination. The diameter of each segment was measured at the ends and mid-point, and the mean used in calculating the volume and surface area.

2. Procedure

Tap water ($3.0cm^3$) was pipetted into the incubation chamber of the oxygen electrode and stirred continually by means of a magnetic stirrer and "flea". Temperature was maintained at $23^{\circ}C$ by means of a circulating water jacket around the incubation chamber. With a potential difference of 0.6V between the platinum (-ve) and Ag-AgCl (+ve) electrodes the dissolved oxygen concentration was allowed to equilibrate with that of the atmosphere, equilibrium being detected as a levelling of the recorder trace of oxygen diffusion current.

The tissue under investigation was cut into thin slices and transferred to the incubation chamber. This was usually followed by a slight fall in diffusion current due, presumably, to a small reduction in stirrer speed.

When the current had re-equilibrated the lid was inserted into the incubation chamber. Utilisation of the dissolved oxygen in tissue respiration resulted in a fall in diffusion current. When leaf tissue was being investigated measurements were performed in the dark to prevent photosynthetic oxygen production.

At the end of each determination a test was made for residual current by adding a few crystals of sodium dithionite ($Na_2S_2O_4$) to the contents of the incubation chamber to remove all dissolved oxygen. In most cases this resulted in a fall in current to zero. Where a residual current was detected its value was subtracted from the experimental current readings.

3. Calculations

The magnitude of the diffusion current is directly proportional to the concentration of dissolved oxygen in the electrode solution. This value is known for the initial equilibrium current and at 23°C is 8.57×10^{-6} g cm^{-3}. Since the volume of liquid is also known (3.0cm^3) the initial weight of dissolved oxygen is 25.71×10^{-6}g. Other current values may be converted to values of dissolved oxygen by direct proportionality. Therefore, by selecting to current values on the initial linear portion of the recorder trace (i.e. respiration not limited by oxygen concentration - Chapter 4) the weight of oxygen consumed in a known time is easily calculated. The respiration rate is then given by:

$$\text{Resp.Rate} = \frac{W_o}{M\,t} \text{ eg. } gO_2 \text{ cm}^{-3} \text{ tissue } S^{-1} \qquad (3.4)$$

where:

W_o = the weight of oxygen consumed in time t (g)

M = the weight, volume or surface area of the tissue (g ; cm^3 ; cm^2)

4. Results

Respiration rates of leaf and stem tissues are given in Table 3.1; root respiration is shown in Fig.3.3.

The results show that respiration rate in tissues of lower porosity (eg. stem, leaf apex, root apex) is higher than that in the more porous tissues (mid-leaf, leaf base, root base). This indicates that not only

TABLE 3.1: RESPIRATION RATES IN LEAF AND STEM OF ERIOPHORUM ANGUSTIFOLIUM

Tissue	Respiration Rate (Mean, Standard Deviation and No. Experiments)		
	$ngO_2\ g^{-1}\ s^{-1}$	$ngO_2\ cm^{-3}\ s^{-1}$	$ngO_2\ cm^{-2}$ surf. s^{-1}
Leaf apex	131.6 ± 6.4 (4)	92.0 ± 4.7 (4)	1.85 ± 0.10 (4)
Mid-leaf	91.1 ± 10.0 (5)	57.5 ± 9.6 (5)	1.03 ± 0.14 (5)
Leaf base	51.0 ± 9.3 (5)	26.7 ± 6.1 (5)	0.69 ± 0.17 (5)
Stem	138.0 ± 8.2 (4)	122.6 ± 17.0 (4)	- - -

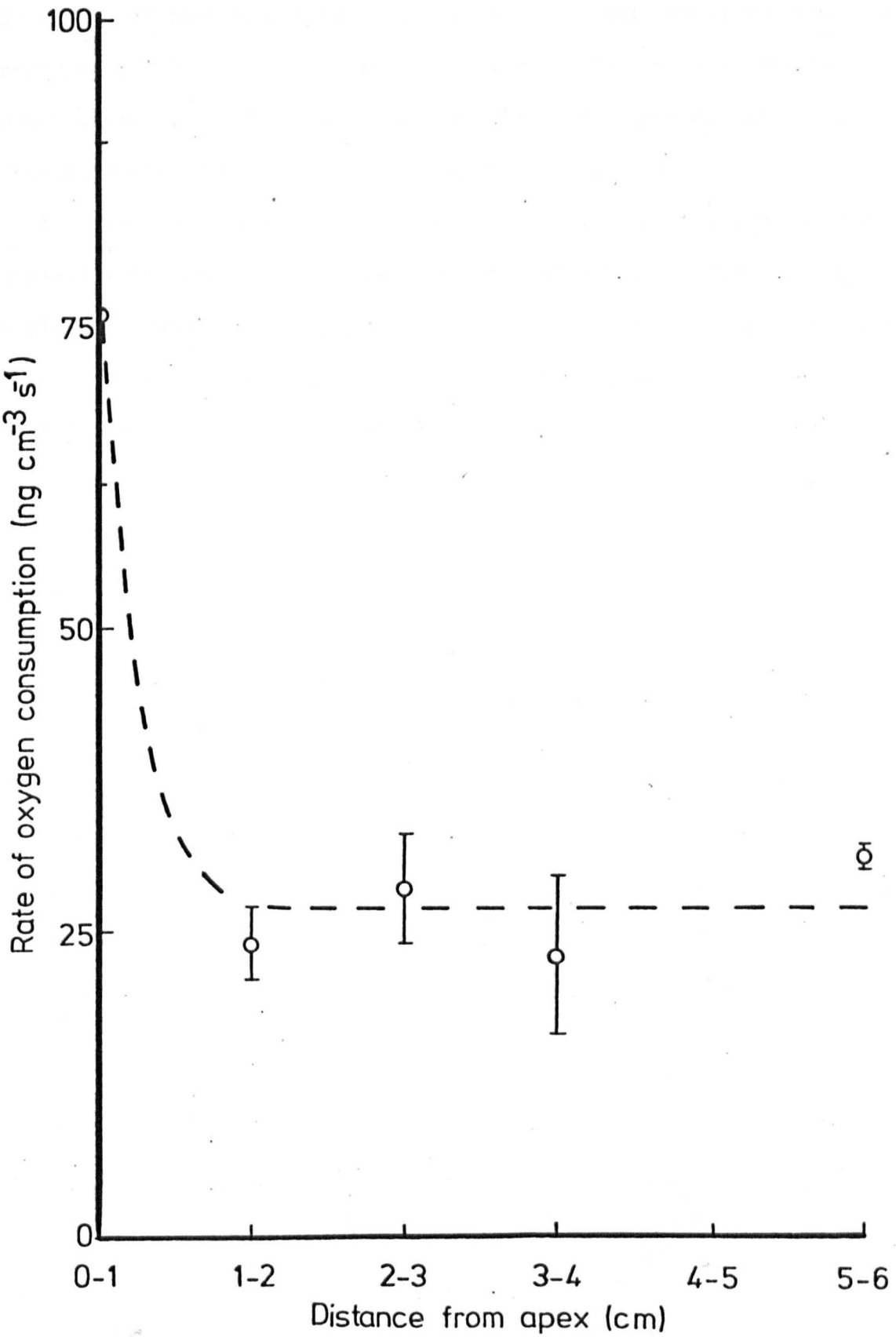

FIG. 3.3 Root respiration in E.angustifolium as a function of distance from the apex.

Bars indicate standard deviation.

does the aerenchymatous structure reduce respiratory demand by lowering the volume of respiring tissue (Williams and Barber, 1961) but that the respiratory rate of the tissues themselves is also lower in the highly porous regions. In the root apex the active processes of cell division and elongation will contribute to the high respiration rate.

The graph of root respiration against distance from the apex (Fig.3.3) is similar to that for rice given by Luxmoore et al. (1970b) although the respiratory rates in the Eriophorum root are in general only about one-fifth of those in rice. This may, in part, be a consequence of the higher porosity of the Eriophorum roots (p. 45).

CHAPTER 4

CRITICAL OXYGEN PRESSURE IN THE INTACT PLANT : ITS MEASUREMENT AND EFFECT ON ROOT GROWTH

I. MEASUREMENT

A. INTRODUCTION

There is abundant evidence that by means of internal aeration relatively high oxygen levels can be maintained in the roots of wetland species; apical oxygen concentrations may often exceed 10% (eg. Chapter 7; van Raalte, 1941; Armstrong, 1967b). However, oxygen concentrations of this magnitude are not in themselves proof of the adequacy of internal aeration; it is necessary also to determine whether longitudinal oxygen transport can satisfy the respiratory demands of the plant.

Unfortunately, oxygen uptake by intact plants is rarely studied and the bulk of respiratory information available in the literature has been obtained using tissue slices in manometric and membrane electrode systems. In these circumstances the rate of oxygen uptake with increasing oxygen pressure rises in the classical hyperbolic manner until a point is reached at which respiration rate becomes constant. Berry and Norris (1949) called this point the "critical oxygen pressure" (C.O.P.).

Although the major terminal oxidases are known to be unaffected in their activity even at extremely low oxygen concentrations (Winzler, 1941; Yocum and Hackett, 1957) the C.O.P. recorded for tissue respiration is rarely lower than 0.10 atm. Berry and Norris (1949) have attributed this discrepancy to the excessive diffusive impedance within the tissues caused by flooding of the intercellular spaces during the *in vitro* assay procedures. In these circumstances elevated oxygen pressures at the periphery of the samples will be necessary to sustain maximum respiratory activity at the centre. Results of Yocum and Hackett (1957) support this view; for thick slices of aroid spadix suspended in liquid the pO_2 for half maximum respiration was 0.15 atm, but when moist slices were used

the value fell to 0.002 atm.

In intact plants, particularly wetland species, the gas space system greatly enhances oxygen diffusivity. Consequently the C.O.P. measured in the in vivo condition should be substantially lower, and therefore represent a truer value, than that determined in vitro. In the case of wetland species, rooting in oxygen deficient soil, a low C.O.P. may be distinctly advantageous.

With these points in mind two methods were devised to assess C.O.P. in intact wetland plants. The first (polarographic method) was based upon the indirect measurement of internal root oxygen concentration from flux values obtained by the cylindrical Pt electrode technique; this allowed C.O.P. to be assessed in the root apex - ie. the part of the plant most remote from the atmosphere and therefore probably that most likely to experience oxygen stress. The second (gas analysis) method relied on the analysis of gas samples extracted from the leaves of submerged plants and enabled C.O.P. to be measured in the aerial parts.

B. POLAROGRAPHIC METHOD

1. Theory

Where oxygen is supplied only from the aerial parts by diffusion the radial oxygen flux from the apex of a submerged root to an ensheathing electrode can be quantified by two expressions. The first (equation 2.9) relates the flux to the concentration of oxygen at the root surface:

$$f = \frac{Q}{tA_r} = \frac{D\,C_{wl}}{r_r \log(r_e/r_r)}$$

If the root wall offers an effectively negligible resistance to oxygen diffusion across it, the gas space oxygen concentration, C_{ias}, will be that in equilibrium with the solution concentration C_{wl}. C_{ias} may be calculated by substitution of measured flux into the above equation.

If root wall resistance is significant, the value of C_{ias} obtained using equation 2.9 will require correction as described on p. 58 and in Chapter 7.

The second equation takes account of the diffusive resistance along the diffusion path between the oxygen source (atmosphere) and the electrode. Assuming the oxygen concentration at the electrode surface to be zero, the equation is:

$$\frac{Q}{tA_r} = \frac{C}{A_r(R_p+R_{wl}+R_s)} - \text{Resp.} \qquad (4.1)$$

where:

C = the concentration of oxygen at the source ($g\ cm^{-3}$)

R_p = the non-metabolic (pore space) resistance of the plant ($s\ cm^{-3}$) (see Chapter 7)

R_{wl} = the non-metabolic resistance in the root wall ($s\ cm^{-3}$)

R_s = the diffusive resistance offered by the liquid shell between root and electrode ($s\ cm^{-3}$)

and "Resp." is a quantity determined by the intensity and distribution of the respiratory activity of the plant (not respiratory rate sensu stricto, but taking units of $gO_2\ s^{-1}\ cm^{-2}$ surface area).

Assuming that for the duration of the experiments the quantity $(R_p + R_{wl} + R_s)A_r$ is constant equation 4.1 can be used to predict the form of the relationship between oxygen flux and atmospheric oxygen pressure at varying levels of respiratory consumption. Several types of relationship are possible:

a) When respiration is zero the equation predicts a linear relationship between f and C (Fig. 4.1a).

b) When respiration is significant and increases linearly in rate with C, f v. C will be again a straight line but will diverge from, and lie below, the non-respiratory plot (Fig.4.1b).

c) If an initial linear increase in respiration is followed by constant respiratory rate above some limiting atmospheric oxygen concentration

FIG. 4.1 Assumed changes in the oxygen flux (f) from roots as the oxygen concentration (C) of the atmosphere increases from zero.

Root respiration assumed to be:-

(a) zero

(b) a linear function of (C)

(c) initially a linear function of C but becoming constant at the critical oxygen pressure

(d) initially a curvilinear function of C but becoming constant at the critical oxygen pressure

(e) as (d) but decreasing curvilinearly at some higher oxygen pressure

NB. Ordinates and abscissae in arbitrary units.

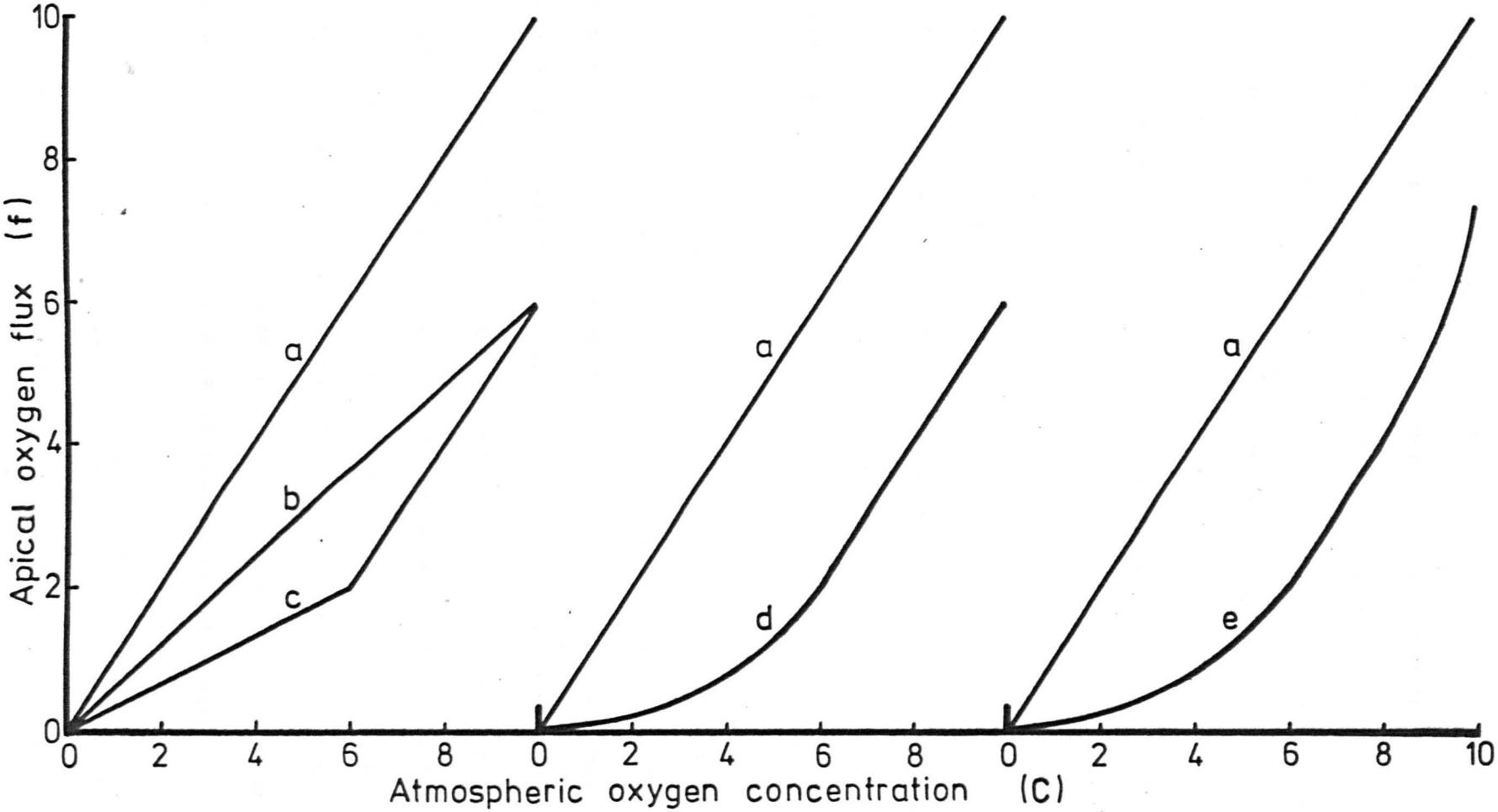
Apical oxygen flux (f)
10
8
6
4
2
0
a
b
c
a
d
a
e
0 2 4 6 8 0 2 4 6 8 0 2 4 6 8 10
Atmospheric oxygen concentration (C)

a bi-linear relationship is produced (Fig. 4.1c). It may be noted that once respiration has become constant the curve lies parallel with but below the non-respiratory condition.

d) A curvilinear relationship between f and C below the limiting oxygen concentration will produce the line in Fig.4.1d.

e) Finally, if at some value of C above the limiting value respiration becomes inhibited, the type of relationship shown in Fig.4.1e will result.

The above theory was tested using the electrical analogue and for short roots complete agreement obtained. In longer roots the combination of non-metabolic resistance and respiration produces an oxygen concentration gradient between base and apex. Where this occurs the analogue results indicated that type 4.1d curves will be obtained whether respiration rate varies linearly or curvilinearly with oxygen concentration below the limiting value.

At this point it must be emphasised that the expressions "limiting oxygen concentration" and "critical oxygen pressure" are not here used synonymously. The former term refers to the ambient oxygen concentration below which tissue respiration declines; the latter describes the corresponding concentration within the plant. Because of the oxygen concentration gradient between the atmosphere and the remote parts of the plant the value of the C.O.P. will depend upon the position along the internal diffusion path at which the measurements are made. In the present study C.O.P was taken to mean the limiting oxygen pressure within the intercellular spaces most adjacent to the sites of respiratory decline, and as such will always have a lower value than the ambient limiting oxygen concentration.

In view of the above theory it was apparent that if the f v. C relationship was determined experimentally the C.O.P. in the root cortex could be deduced by substituting the flux at the limiting oxygen concentration into equation 2.9.

2. Method

a) Calibration of Gas Mixtures

Commercial gas cylinders containing approximate oxygen-nitrogen mixtures were accurately analysed polarographically using "artificial roots" (Armstrong, 1972). These were constructed from lengths of glass capillary (bore radius 0.015cm) with an "apex" of oxygen-permeable silicone rubber tubing (outer radius 0.05cm). Using cylindrical Pt electrodes the diffusion current due to oxygen leakage from the apex was measured when the open base of the artificial root was exposed to the atmosphere and to the $O_2 - N_2$ mixtures. The oxygen concentration in the gas mixtures was then calculated from the equation:

$$[O_2] = \frac{20.99 i_{mix}}{i_{atm}} \quad \% \qquad (4.2)$$

where:

$i_{atm.}$ = the diffusion current with the root base exposed to the atmosphere (i.e. 20.99% O_2 for dry air - Humphries, 1926)

$i_{mix.}$ = the diffusion current with the root base exposed to the $O_2 - N_2$ mixture.

The percentage oxygen concentrations were: 3.0, 4.9, 7.2, 9.4, and 13.65 (pO_2 : 0.03, 0.49, 0.72, 0.94 and 0.1365 atm). Atmospheric oxygen was supplied by a small air pump.

b) Procedure

Plants (Eriophorum or rice) were prepared and arranged for analysis of R.O.L. as described in Chapter 2 but using a boiling tube (150 cm^3), rather than a measuring cylinder, as vessel for the anaerobic medium, the surface of which just covered the root bases. The leafy parts were enclosed within an inverted measuring cylinder (500 cm^3) which contained moist blotting paper and fitted over the mouth of the boiling tube. The oxygen-nitrogen mixtures were introduced in turn into the measuring cylinder through a gas line, and excess gas escaped through a "seal" of moist cotton wool between the boiling tube and rim of the measuring cylinder.

Equilibration between the internal atmosphere of the plants and each gas mixture was indicated when the oxygen flux from the root became constant. An oxygen polarograph was then taken and the flux recorded after further equilibration at the limiting potential.

When the experiment had been completed at room temperature (23°C) the root system was cooled to 3°C to curtail respiration and establish the "non-respiratory" relationship between f and C. The aerial parts were again exposed to the sequence of gas mixtures and the equilibrium fluxes recorded.

3. Manipulation of 3°C Flux Data

Low temperature, by virtue of its effect upon the physical constants diffusion coefficient (D) and oxygen solubility, alters the resistance to oxygen diffusion in the system. Therefore, it was necessary to manipulate the flux data obtained at 3°C in order to preduct the values which would be expected at 23°C with respiration curtailed. The method of manipulation was based on that described by Armstrong and Wright (1975) and is given below.

The resistance, R, to the oxygen flux, f, from base to apex of a root, and from the apex to an ensheathing electrode, may be considered as the sum of two series components:

R_r , the effective resistance of the root

R_s , the diffusive resistance of the liquid shell between root and electrode.

If C is the oxygen concentration at the root base and $f = f_1$ on $R_r = 0$, then

$$f_1 = \frac{C}{A_r R_s} \qquad (4.3)$$

If $f = f_2$ when $R_r > 0$, then

$$f_2 = \frac{C}{A_r (R_r + R_s)} \qquad (4.4)$$

Equations 4.3 and 4.4 may be combined with respect to C to give:

$$R_r = R_s \left(\frac{f_1}{f_2} - 1 \right) \qquad (4.5)$$

Under these circumstances f_1 is the oxygen flux from the surface of a root of zero internal and wall resistance and may be calculated from an equation similar to 2.9:

$$f_1 = \frac{D_w^t \; C_{wl}^t}{r_r (\log r_e / r_r)} \quad g \; cm^{-2} \; s^{-1} \qquad (4.6)$$

where

D_w^t = the diffusion coefficient for O_2 in water at t^o ($cm^2 \; s^{-1}$)

C_{wl}^t = the dissolved O_2 concentration at the root wall at t^o ($g \; cm^{-3}$)

For example, in the case of an air-filled root of radius 0.05cm within an electrode of radius 0.1125cm, the oxygen flux at 23°C ($D_w = 2.267 \times 10^{-5} cm^2 s^{-1}$ and $C_{wl} = 8.57 \times 10^{-6} g \; cm^{-3}$) calculates to $287.2 ng \; cm^{-2} min^{-1}$.

f_2, the flux from the root when internal and wall resistances are significant, is obtained experimentally, whilst the liquid shell resistance R_2, may be calculated from the equation:

$$R_s^t = \frac{r_r (\log r_e / r_r)}{D_w^t \; A_r} \cdot \frac{C_a^t}{C_{a-w}^t} \quad s \; cm^{-3} \qquad (4.7)$$

where:

C_a^t = the concentration of O_2 in moist air at t^o (eg. 268.7×10^{-6} $g \; cm^{-3}$ at 23°C - extrapolated from data of Humphries, 1926).

C_{a-w}^t = the concentration of O_2 in air-saturated water at t^oC (eg. $8.57 \times 10^{-6} g \; cm^{-3}$ at 23°C - Montgomery et al., 1964).

For the root-electrode system described above, and with electrode length 0.5cm, R_s at 23°C calculates to $3.57 \times 10^5 \; s \; cm^{-3}$.

The overall effective diffusive resistance of the root (R_r), which may be calculated by fitting values of f_1, f_2 and R_s into equation 4.5, is

a composite quantity, being a function of pore space resistance (R_p), root wall resistance (R_{wl}), and synergistic respiratory and oxygen leakage effects (see Chapter 7).

If the effective diffusion path length through the root wall is L_{wl}, the diffusive resistance of the wall at temperature t is given by an equation analogous to 4.7:

$$R^t_{wl} = \frac{(r_r - L_{wl}) \log[r_r/(r_r - L_{wl})]}{D^t_w \; A^1} \cdot \frac{C^t_a}{C^t_{a-w}} \quad s\ cm^{-3} \qquad (4.8)$$

where:

A^1 = the surface area of the cylinder of radius $r_r - L_{wl}$ (cm^2)

Oxygen leakage from sub-apical regions of wetland roots is small (see p. 134 and Fig.2.7) and if cooling the root to 3°C effectively curtails respiration the overall resistance at 3°C will be a function of pore space and apical root wall resistance only. Hence:

$$R^{3^o}_p = R^{3^o}_r - R^{3^o}_{wl} \quad s\ cm^{-3} \qquad (4.9)$$

$R^{3^o}_r$ may be determined by substitution of the experimental flux at 3°C ($f^{3^o}_2$) into equation 4.5, with $f^{3^o}_1$ and $R^{3^o}_s$ calculated using appropriate 3°C values for C_{wl} and D_w (13.46×10^{-6} g cm^{-3} and 1.16×10^{-5} $cm^2\ s^{-1}$ respectively) in equations 4.6 and 4.7. $R^{3^o}_{wl}$ may also be calculated using appropriate values of C_{wl} and D_w in equation 4.8. Finally the pore space resistance at normal temperature (ie. $R^{23^o}_p$) is given by:

$$R^{23^o}_p = R^{3^o}_p \cdot \frac{D^{3^o}_a}{D^{23^o}_a} \quad s\ cm^{-3} \qquad (4.10)$$

where:

$D^{3^o}_a$ = the diffusion coefficient for O_2 in air at 3°C (0.182 $cm^2\ s^{-1}$)

$D^{23^o}_a$ = the diffusion coefficient for O_2 in air at 23°C (0.205 $cm^2 s^{-1}$).

$R^{23^o}_p$ may then be used to predict the oxygen flux from the root at normal temperatures and minimal respiration. Thus:

$$f(\text{resp.minimal at } 23^{\circ}C) = \frac{C_a^{23^{\circ}}}{(R_p^{23^{\circ}} + R_{wl}^{23^{\circ}} + R_s^{23^{\circ}})A_r} \text{ g cm}^{-2}\text{s}^{-1} \qquad (4.11)$$

If root wall resistance is negligible:

$$f(\text{resp.minimal at } 23^{\circ}C) = \frac{C_a^{23^{\circ}}}{(R_p^{23^{\circ}} + R_s^{23^{\circ}})A_r} \text{ g cm}^{-2}\text{s}^{-1} \qquad (4.12)$$

Apical root wall resistance for rice was considered insignificant at $23^{\circ}C$ (see p. 145) whilst at $3^{\circ}C$ the value was based on the measured wall thickness and calculated from equation 4.8 assuming the effective diffusion coefficient across the wall to be that for water, ie. 1.16×10^{-5} cm^{-2} s^{-1}. Eriophorum, on the other hand, was found to have significant wall resistance at $23^{\circ}C$, and results for this species were corrected using the data presented in Chapter 7.

4. Results and Discussion

A typical example of the relationship found between leaf chamber oxygen concentration and apical oxygen flux at $23^{\circ}C$ is given in Fig.4.2. The linearity above a limiting oxygen concentration was as anticipated, but a lower curvilinear portion, which would be expected if respiration showed a curvilinear increase with oxygen concentration (Fig.4.1d), was replaced by a second linear relationship. This indicates linearity between respiration rate and oxygen concentration below the C.O.P., and is comparable with the prediction in Fig.4.1c. However, an important difference is apparent in that the experimental curve fails to pass through the origin. There were no exceptions to this bi-linear flux pattern, but the intercept with the abscissa varied within the range 1.4 to 4.6% O_2. Critical oxygen pressures (atm), calculated from the oxygen flux at the inflexion point, and their standard deviations were: rice (N.37), 0.026 $\pm$ 0.002 (5 plants); rice (N.36), 0.024 $\pm$ 0.001 (6 plants); E.angustifolium, 0.026 $\pm$ 0.003 (10 plants).

The manipulated $3^{\circ}C$ data gave a straight line relationship between flux and leaf chamber oxygen concentration (Fig.4.2), which ran parallel

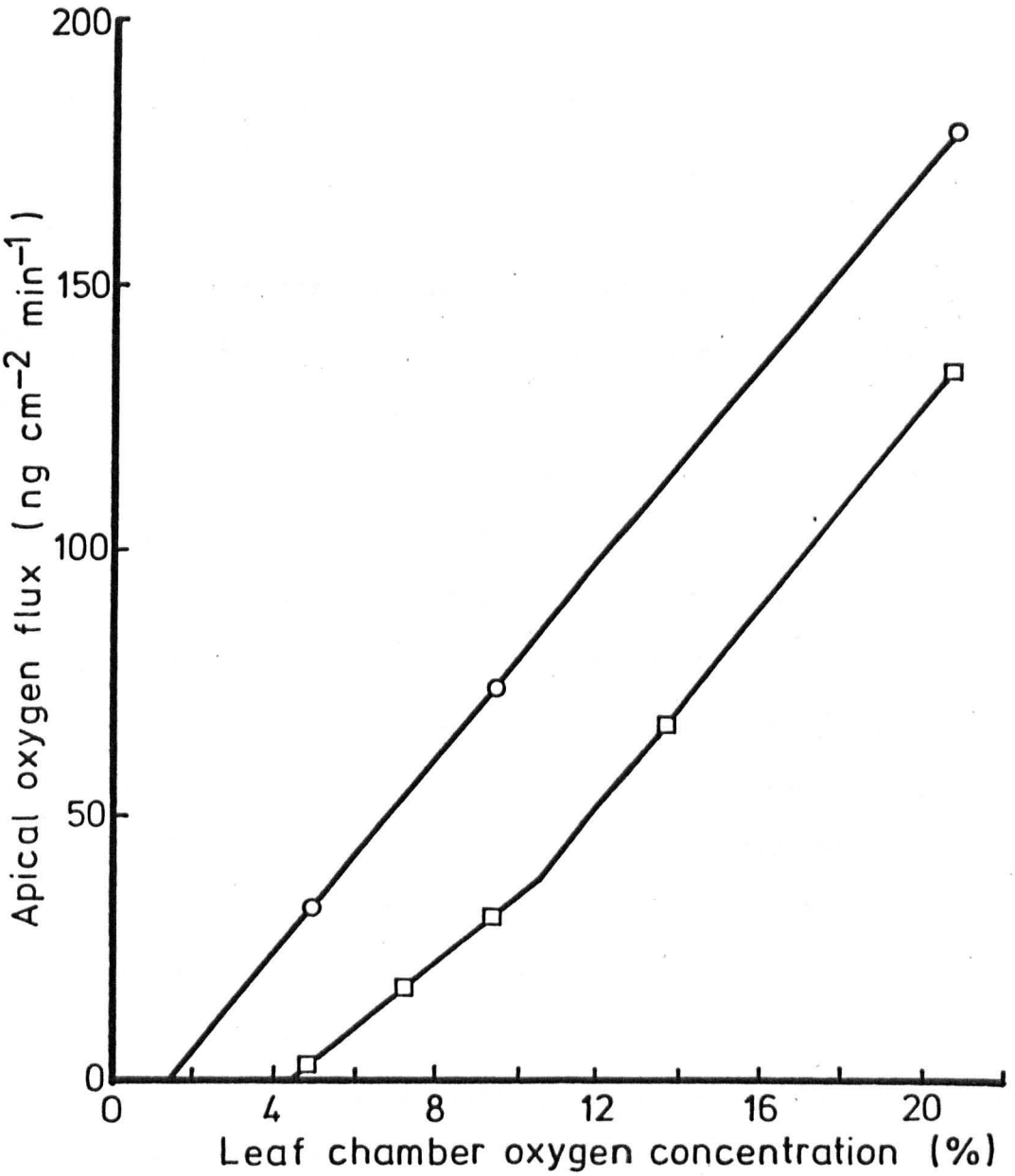

FIG. 4.2 Experimental relationships found between leaf chamber oxygen concentration and oxygen flux from the apex of a rice root at 3°C (o) and 23°C (□)

with the upper portion of the room temperature plot as predicted in Fig.4.1a. However, the extrapolated line failed to pass through the origin but intersected the abscissa at a leaf chamber oxygen concentration up to 1.5%. This was found to be due to respiration in the uncooled, astomatal leaf bases (see p.96). When the leaf bases were cooled to 3°C the line just failed to pass through the origin, but when the leaf system above the bases was excised the line ran directly into the origin as predicted in Fig.4.1a.

An explanation for the unexpected bi-linear form of the experimental 23°C plot, and its intersection with the abscissa, was sought using the electrical analogue which was programmed to simulate rice using input data from a number of sources (see Table 4.1). In order to reproduce the experimental results (Fig.4.3B) it was necessary to make certain assumptions. Firstly, that the C.O.P. was experienced in the apical 2cm of root only; secondly, that the respiration rate v. oxygen concentration curve for intact roots does not follow the hyperbolic form found in vitro (see Fig.4.4), but rather adheres to the type of relationship shown in Fig.4.3A. Here it was assumed that 45% of the total respiratory demand in the apical centimetre was accounted for by the low porosity stelar and meristematic tissues, whilst in the second centimetre the stele accounted for 8% of the respiratory demand. The assumption was made that the low effective diffusion coefficient in these tissues would lead to the production of anaerobic centres at the C.O.P.'s detected experimentally. The high porosity cortical tissue, however, which accounted for the remaining respiratory demand, was assumed to exhibit an extremely low C.O.P. ($\leqslant$ 0.001 atm) due to the close proximity of the cells with the gas phase. Work of Forrester et al. (1966) on dark respiration of whole leaves, and of Yocum and Hackett (1957) on the respiration of moist tissue slices support this assumption. Thus, at a C.O.P. of 2.4% the respiration rate in the apical centimetre fell from its maximum value of 360ng O_2 min^{-1} cm^{-2} root surface to 55% of this value at a very low oxygen concentration

TABLE 4.1 : ANALOGUE PROGRAMMING DETAILS USED TO REPRODUCE THE TYPE OF EXPERIMENTAL RESULT SHOWN IN FIG.4.2.

Distance from apex (cm)	Effective porosity (%)	Potential respiration ($ng\ cm^{-2}\ min^{-1}$)	Potential O_2 leakage through root wall (% max.)
0 - 1	6	360	100
1 - 2	9	150	95
2 - 3	12	135	73
3 - 4	16	109	56
4 - 5	24	99	0

FIG. 4.3 Analogue simulation of oxygen concentration vs. apical flux relationship.

(A) Relationships between root respiration and internal oxygen concentration used to programme the analogue in order to reproduce the experimental flux pattern

(B) Analogue - predicted relationships between leaf chamber oxygen concentration and apical oxygen flux for a cooled (o) and uncooled (□) root.

Programming details are given in table 4.1

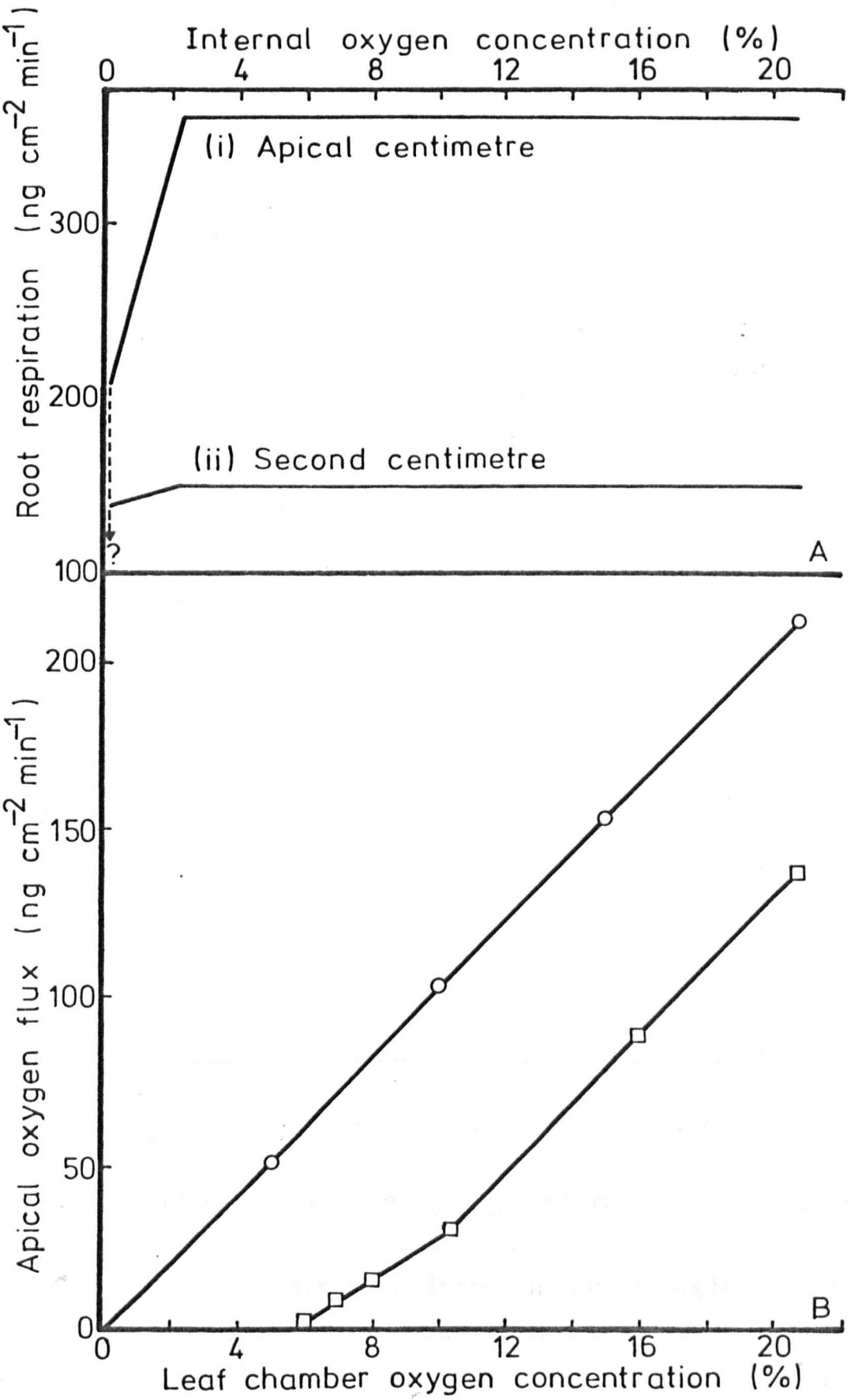
Internal oxygen concentration (%)
0
4
8
12
16
20
Root respiration (ng cm^{-2} min^{-1})
300
200
100
(i) Apical centimetre
(ii) Second centimetre
?
A
Apical oxygen flux (ng cm^{-2} min^{-1})
200
150
100
50
0
B
0
4
8
12
16
20
Leaf chamber oxygen concentration (%)

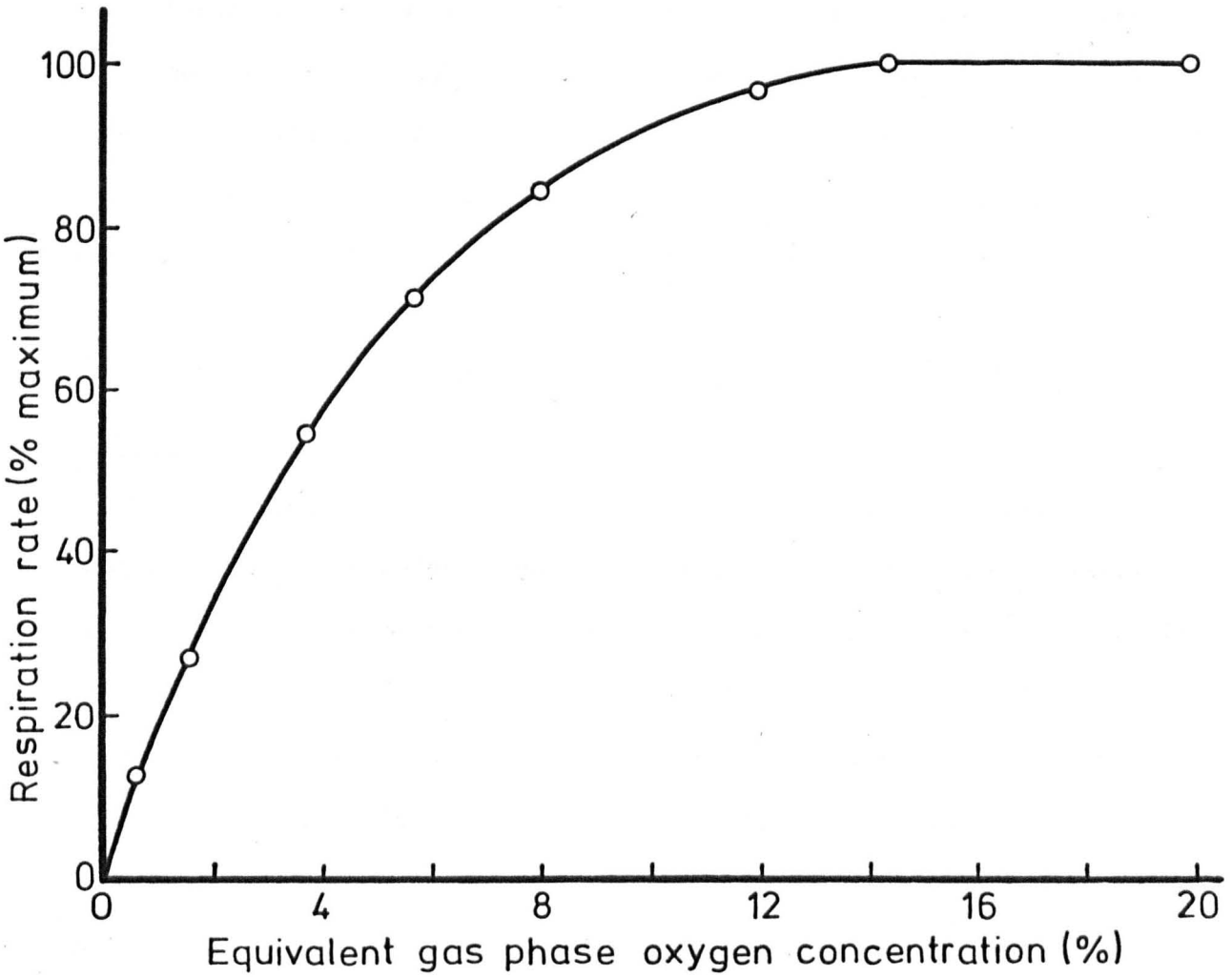

FIG. 4.4 Root respiration of E. angustifolium as a function of oxygen concentration. Measurements were made in vitro in a Rank membrane-electrode assembly using slices taken from 2cm apical segments.

(Fig.4.3Ai). Similarly, in the second centimetre, the respiratory rate fell by 8% of the maximum value of 150ng $O_2 min^{-1} cm^{-2}$ root surface (Fig.4.3Aii).

The final assumption made was that the volume of anaerobic tissue increased linearly as the oxygen concentration fell further below the C.O.P. (cf. Fig.4.1c).

If the above assumptions are correct, then the C.O.P.'s recorded experimentally are a property of low porosity tissue masses in the root such as the stele and meristematic zone, and not of the gas-filled tissues. The indications are that the C.O.P. for the intact cortical region is so low that it will be extremely difficult to detect.

C. GAS ANALYSIS METHOD

1. Theory

The concentration of oxygen within the intercellular spaces of a wetland plant is dependent upon the balance between the rate of oxygen supply and the rate of its depletion. During darkness oxygen is supplied by diffusion from the atmosphere, but in daylight photosynthesis may provide for the entire oxygen requirements of the plant (see Chapter 8). Consequently, if photosynthesis is prevented and the plant immersed in anaerobic medium, a fall in the internal oxygen status will follow. The rate of fall will be determined by respiratory rate and by leakage of oxygen from leaves and roots; during the depletion of the internal oxygen reservoir which follows submergence the balance between these factors will be reflected in the relationship internal oxygen concentration v. time. In theory several types of curve are possible and these are illustrated in Fig.4.5a-d. They may be interpreted as follows:

a) When the respiratory component is insignificant compared with leakage the predicted curve is exponential since the rate of oxygen loss is dependent upon internal concentration. Low respiration rate, or

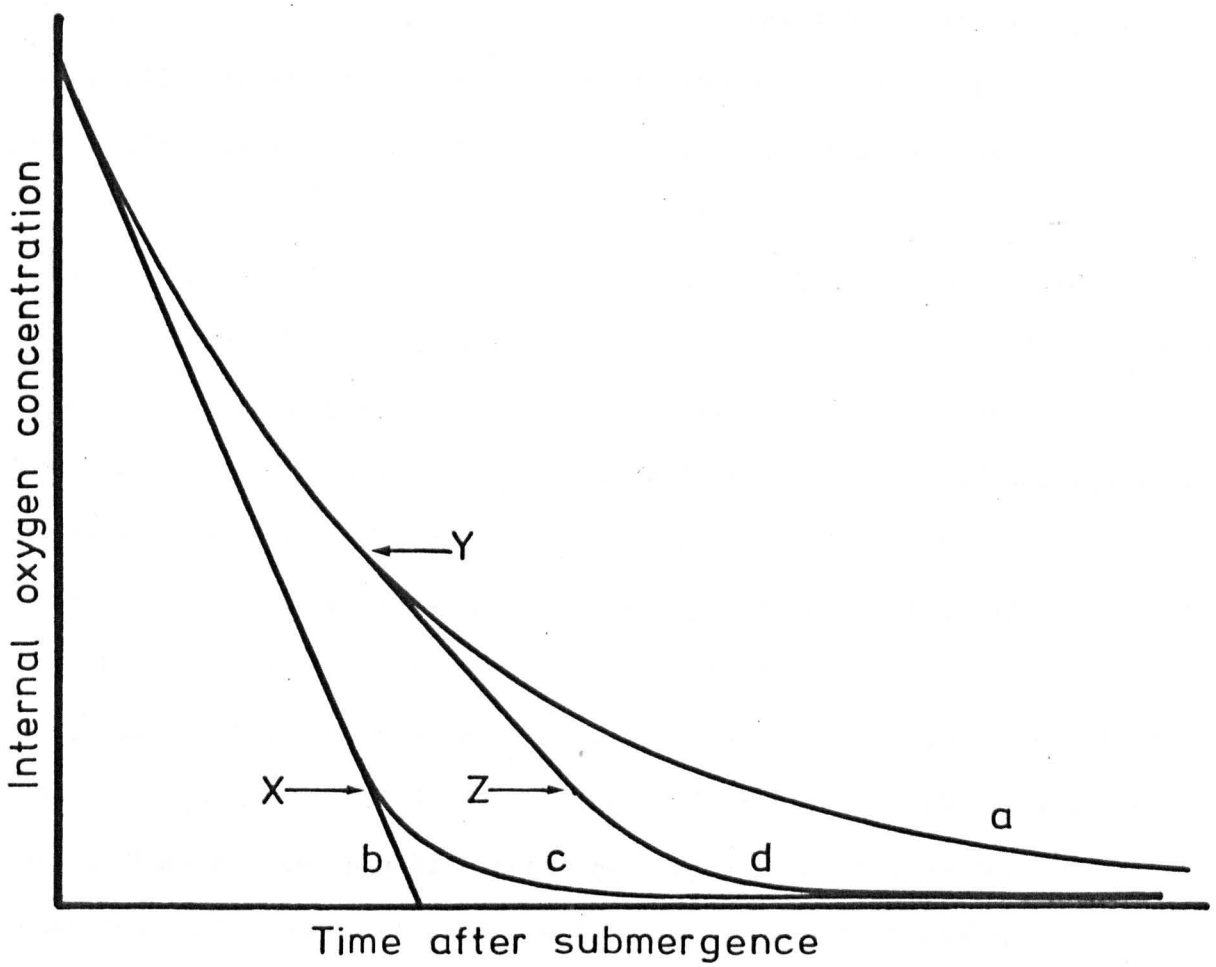

FIG. 4.5 Assumed changes in the internal oxygen regime of intact plants after submergence in anaerobic medium.

(a) no respiratory effect

(b) no leakage effect

(c) as (b) but respiration limited by COP at point "X"

(d) curve influenced by leakage to point "Y", below "Y" respiratory influence only, and respiration limited by COP at point "Z"

large exposure of leaf surface relative to the volume of respiring tissue, might produce this type of relationship.

b) Here the leakage component is insignificant. The constant slope indicates constant respiratory rate and the total linearity suggests that respiration is entirely independent of oxygen concentration. High respiration rate or a small exposure of leaf could give this curve.

However, it would seem that curves (a) and (b) may be no more than theoretical. The former is unlikely since the leakage component should rarely subdue the respiratory effect entirely, and its contribution will diminish as the oxygen concentration falls. The total linearity of (b) is also unlikely because, despite the very low Km values of the respiratory enzymes, significant C.O.P.'s should still arise due to the relatively long diffusion paths between gas-filled spaces and certain of the tissues.

c) When respiration becomes limited by oxygen concentration at point 'x' (ie. the C.O.P.) the curve ceases to be linear and falls more slowly to zero. The value of the C.O.P. will depend upon such factors as temperature, the diffusion path lengths between gas spaces and mitochondria, and the position in the plant at which measurements are made (p. 53).

d) Leakage is significant over the first part of this curve but later becomes obscured by the respiratory component at point 'Y'; the C.O.P. occurs at point 'Z'.

It follows from the above that if oxygen concentration at any particular point in a plant could be adequately recorded during the period after submergence the plot of oxygen concentration v. time might be suitable for assessing the C.O.P. In this case measurements were made at the leaf bases.

2. Method

With certain modifications the method followed that of Roughton and Scholander (1943) and Scholander et al., (1951).

(a) Gas Analyser

A diagram of the gas analyser is given in Fig.4.6. It consisted of

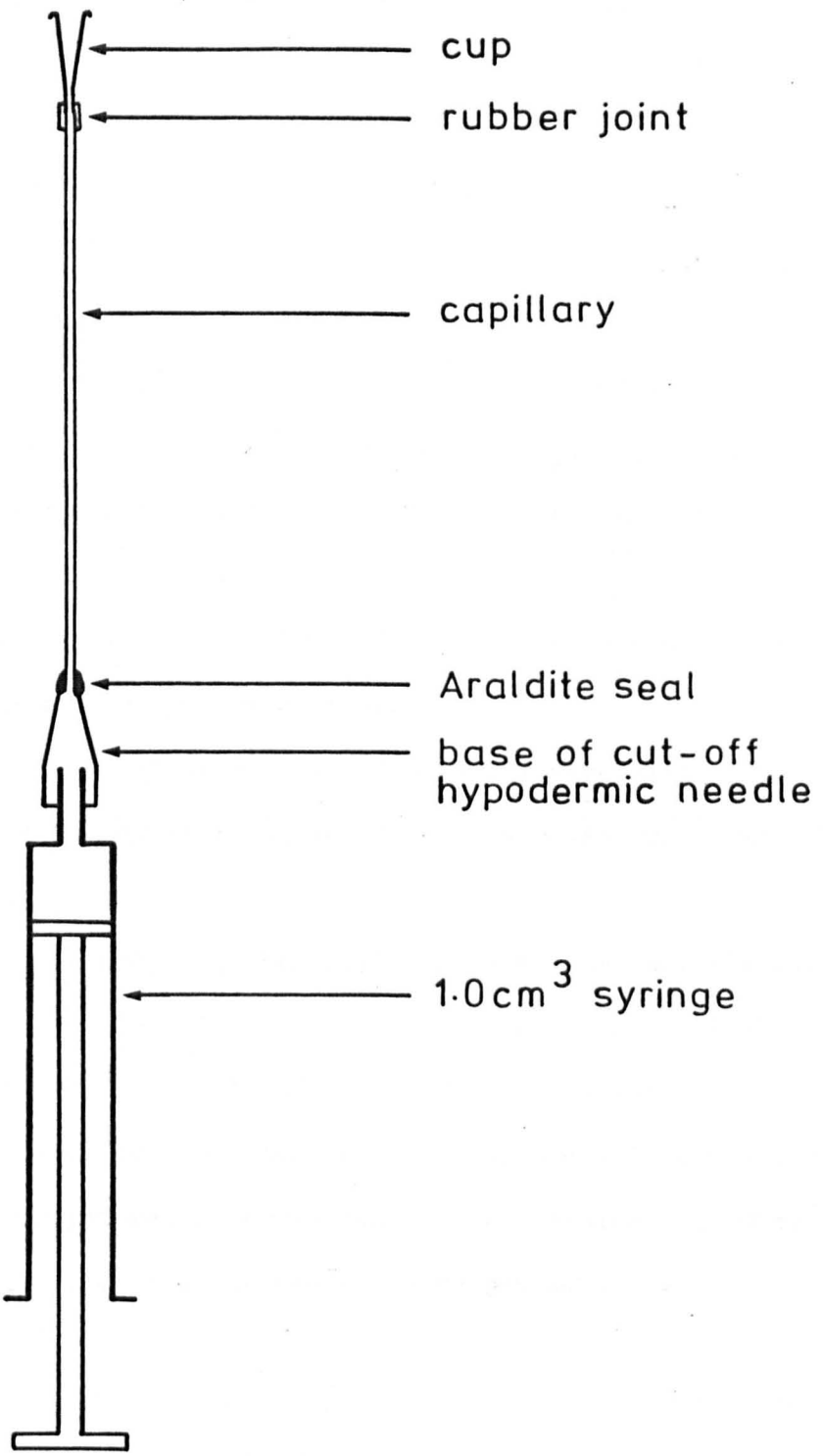

FIG. 4.6 Gas analyser (actual size)

a fine capillary, internal radius 0.025cm, sealed to the basal end of a cut-off hypodermic needle by means of household "Araldite". To the distal end of the capillary was attached a small, tapered glass cup (mouth radius 0.15cm). The needle base was fitted to a normal syringe of capacity 1.0cm^3.

(b) Reagents

The solutions used in the extraction and analysis of the gas samples were as follows:

Acid citrate (for extraction and storage of the gas samples): 70g sodium citrate ($Na_3C_6H_5O_7.2H_2O$) were dissolved in 100cm^3 water to which was added 3g citric acid. According to Scholander et al. (1951), this reagent absorbs negligible gas from the samples, even over a period of several hours.

Alkaline citrate (CO_2 absorber): 70g sodium citrate were dissolved in 120cm^3 water and 4g sodium hydroxide added.

Alkaline pyrogallol (O_2 absorber): 15g pyrogallol were dissolved in 100cm^3 20% sodium hydroxide by stirring gently with a glass rod under a layer of paraffin oil.

Sodium dithionite ($Na_2S_2O_4$)(O_2 absorber): in some later experiments acid citrate solution saturated with sodium dithionite replaced alkaline pyrogallol. The use of this reagent made prior CO_2 absorption unnecessary.

Acid rinsing solution (for removing traces of pyrogallol or dithionite from the analyser): 10mg potassium permanganate were dissolved in 500cm^3 water to which had been added 1cm^3 concentrated sulphuric acid.

(c) Procedure

(i) Gas extraction

In order to minimise changes to the internal oxygen regime it was necessary to extract only small gas samples from the plants. The use of a hypodermic syringe proved inconvenient since the small bubbles frequently became trapped in the needle base. A satisfactory substitute was found to be a finely drawn-out long-nozzled Pasteur pipette. The very fine point

caused negligible damage to the plants and the tapered bore facilitated the subsequent ejection of the bubbles. By controlling the pressure on the bulb the bubbles could be retained in the long nozzle, and by sealing the point with a small block of wax they could be stored until required for analysis.

Timing began with the submergence of the plant in deoxygenated medium in a shallow, light-proof dish. To determine as closely as possible the oxygen concentration within the plant prior to submergence the first gas sample was extracted immediately. The point of a drawn-out pipette, previously filled with acid citrate, was inserted into a lacuna of a leaf base and a few bubbles of gas drawn into the citrate. The pipette was withdrawn and the point immersed in a beaker of acid citrate. The last few bubbles collected, which may have become contaminated by contact with the deoxygenated agar medium, were ejected and replaced with citrate.

If it was necessary to store the sample prior to analysis a small block of wax was pushed over the point of the pipette, enabling pressure on the bulb to be released and leaving the bubbles stationary in the nozzle.

Subsequent samples were extracted at the same level on the leaf bases, working round the plant, and sampling was continued until oxygen could no longer be detected. Flooding of the gas-conducting system never occurred during sampling since the punctured lacunae were effectively sealed off from the remaining gas space by diaphragms.

(ii) Gas analysis

The analyser was filled with acid citrate and clamped in an inverted position with the cup submerged in citrate contained in a shallow beaker. A gas sample was injected into the cup and drawn into the capillary by careful adjustment of the plunger. Sufficient gas was introduced to give a bubble 1.0 to 1.5cm long.

At this stage the analyser was clamped with the cup uppermost and the length of the bubble between upper and lower menisci measured using a

travelling microscope. As much acid citrate as possible was then removed from the cup and from the capillary above the bubble using a fine pipette. If pyrogallol was to be used the empty cup was filled with alkaline citrate and the plunger carefully adjusted to bring the bubble into the cup. After two minutes the bubble was drawn back into the capillary and re-measured. Care was taken to adjust the position of the upper meniscus to its previous level in order to eliminate errors due to hydrostatic pressure. This procedure was repeated until the bubble length remained constant, indicating complete CO_2 absorption.

The alkaline citrate was then replaced by pyrogallol solution and the above operation repeated until all the oxygen had been absorbed.

Between analyses the fluid in the analyser was discarded and the apparatus flushed repeatedly with acid rinsing solution to oxidise any traces of pyrogallol. Finally the analyser was rinsed several times with distilled water.

The analyses were performed under very stable laboratory temperatures and no fluctuations in bubble volume due to temperature changes were observed. For this reason a constant temperature jacket round the analyser was considered unnecessary.

The oxygen concentration in a gas sample was given by:

$$[O_2] = \frac{r^2(L_2 - L_3)}{r^2(L_1 - 2a) + 4a^3/3} \times 100 \quad \% \qquad (4.13)$$

where:

L_1 = the initial length of the bubble (cm)

L_2 = the length of the bubble after CO_2 removal (cm)

L_3 = the length of the bubble after O_2 removal (cm)

a = the radius of the meniscus (assumed hemispherical) (cm)

r = the inner radius of the capillary (cm)

Measurements were confined to E.angustifolium.

3. Results and Discussion

The internal oxygen concentration v. time curves were of two types. During the earlier stages of the work there was a preponderance of the curvilinear relationship illustrated in Fig.4.7, which is similar in form to the predicted curve in Fig.4.5c (Armstrong and Gaynard, 1976). However, as further experiments were carried out it became clear that the totally linear relationship shown in Fig. 4.8 (c.f. Fig. 4.5b) was the more typical. In neither Fig.4.7 nor Fig.4.8 is a significant leakage component detectable and it is likely that this was due to the smallness of the experimental plants. In these the leaves were enclosed for much of their length within the apparently oxygen-impermeable membranous leaf sheath (see Chapter 3); hence diffusion from their surfaces was greatly reduced. Results of other experiments, in which R.O.L. was measured continually after total submergence (Chapter 5) indicated that significant leakage from the leaves of large plants would have given curves of type 4.5d.

The total linearity of the majority of the experimental curves was unexpected. The implication of this result is that C.O.P. in the leaf bases has a value sufficiently low to be beyond the limits of detection by the gas analysis method.

The reason why certain plants produced curvilinear relationships is not clear; however, there are several possible explanations. Prior to total submergence a gradient of oxygen concentration exists between the leaves and root apices; after submergence the gradient persists (see Chapter 5) and a C.O.P. almost certainly occurs first in the root tissues. It may be expected that the associated lowering of root oxygen demand should be reflected in a decline in the rate of oxygen loss from the leaves, with the production of an "apparent C.O.P." in the leaf bases which is in excess of the value measured in the root; analogue work described in Chapter 5 indicated this. Although the experimental plants were not obviously of different stature it may have been the case that

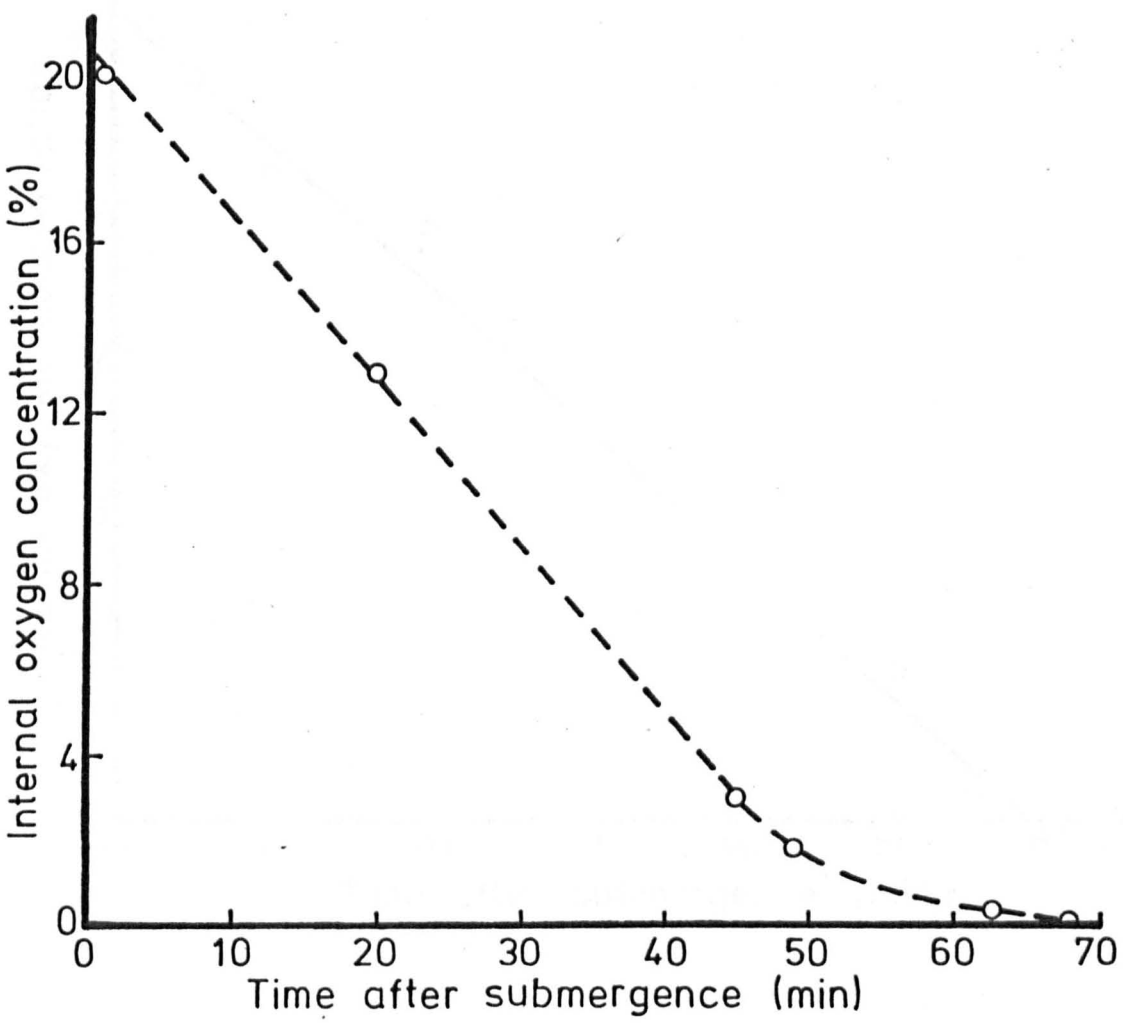

FIG.4.7 Internal oxygen concentration in the leaves of E. angustifolium following the submergence of the intact plant in anaerobic medium

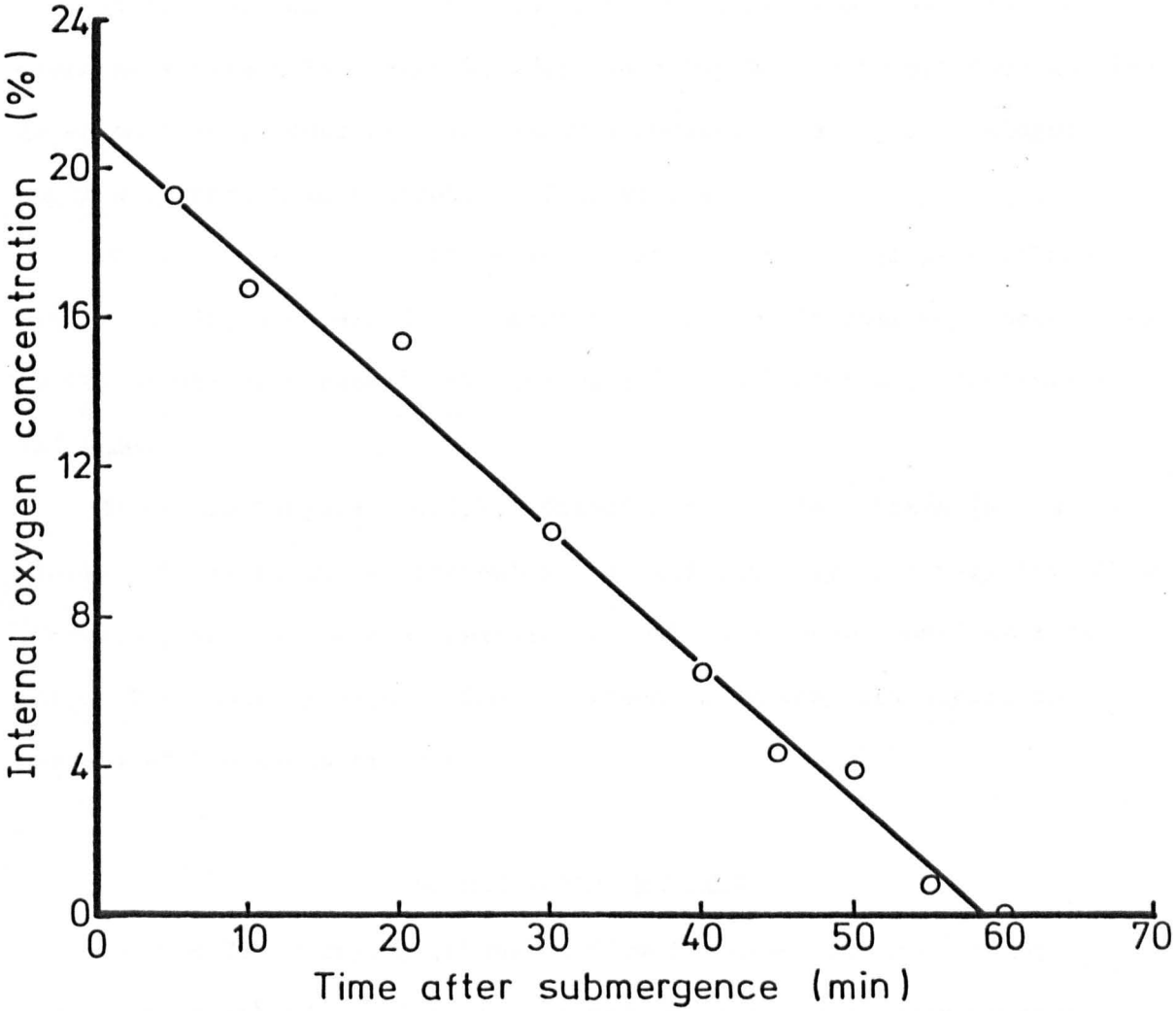

FIG. 4.8 Internal oxygen concentration in the leaves of E. angustifolium following submergence of the intact plant in anaerobic medium

$$y = -0.359x + 21.16$$

$$r = -0.995$$

in some the root material was sufficiently abundant to make this effect detectable. The C.O.P.'s so indicated ranged from 2.5 to 4.0%, being somewhat higher than the root C.O.P.'s obtained by the polarographic method.

It is also possible that C.O.P. in the tissues of the stem could cause an apparent leaf base C.O.P.; this may have been detected in plants in which stem tissues were unusually abundant. Once again analogue studies support this contention (Chapter 5).

Finally, the possibility exists that in certain plants blockage of gas-conducting channels during sampling may have in some way contributed to the curvilinear relationship between internal oxygen concentration and time.

Below the "apparent C.O.P." detected in the leaf bases (eg. 3% in Fig.4.7) internal oxygen concentration fell linearly to a very low value (Fig.4.9), indicating that respiratory rate had become constant once more. This again points to the occurrence of a very low C.O.P. in certain of the plant tissues.

D. CONCLUDING REMARKS

The results described above confirm the conclusions of other workers that the high C.O.P.'s obtained in _in vitro_ studies of higher plant respiration are a consequence of the resistance to oxygen diffusion offered by flooded intercellular spaces. For example Luxmoore _et al._ (1970b) obtained a C.O.P. for rice root respiration in excess of 0.2075 atm. In the present study the values determined by the polarographic method ranged from 0.016 to 0.033 atm, and since these data are based on analyses of the gas phase oxygen concentration within the intact roots they are likely to be a truer estimate of the C.O.P. for root respiration than _in vitro_ measurements. Berry and Norris (1949) concluded that the respiratory rate of onion root segments could be limited by the rate of oxygen diffusion into the tissue. It seems certain that the C.O.P.

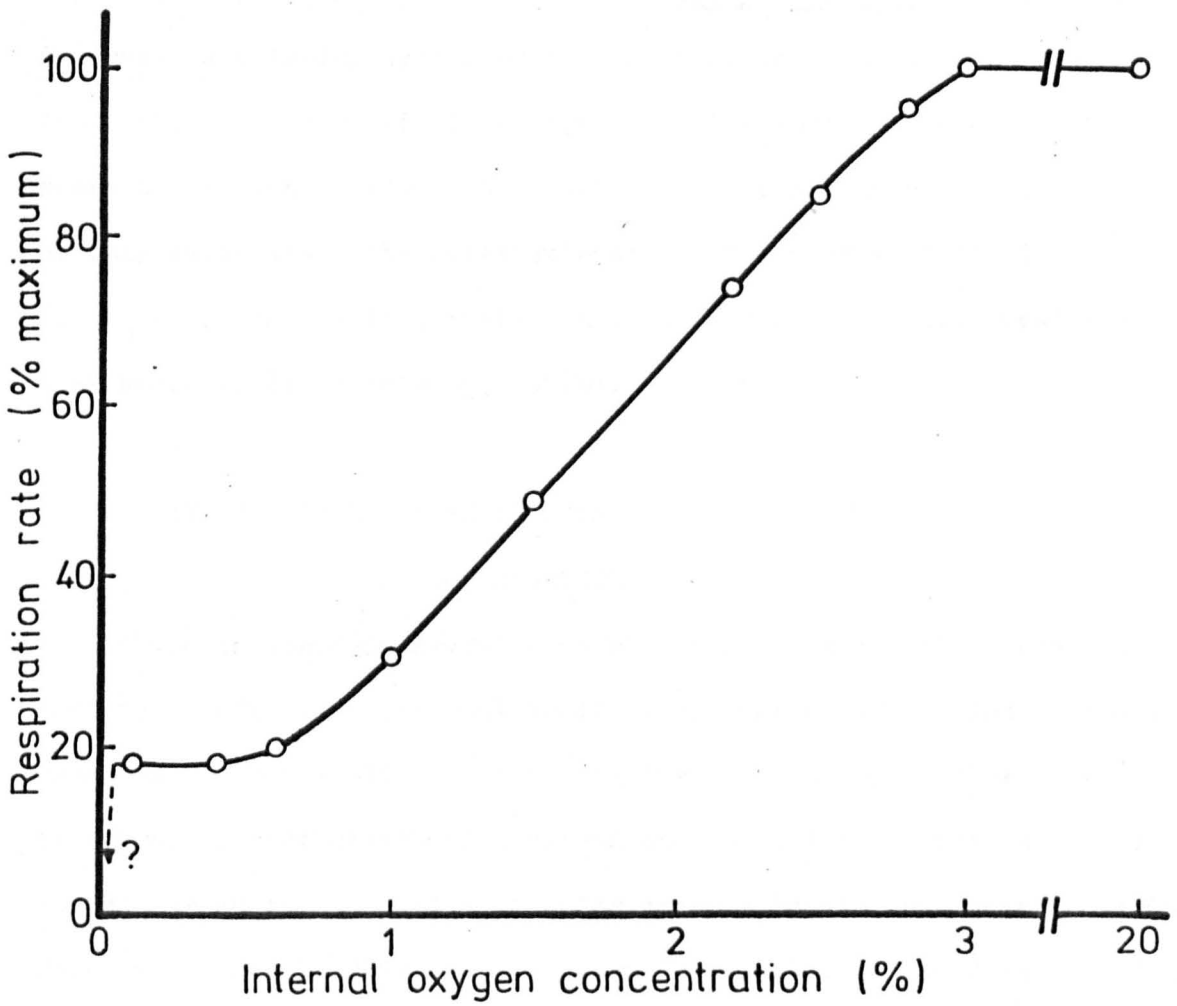

FIG. 4.9 Whole plant respiration as a function of internal oxygen concentration in submerged E. angustifolium (calculated from Figure 4.7)

values recorded in the present study are a function of the diffusive impedence offered by certain low-porosity tissues, in particular those of the meristem and stele (Plate 4.1). The indications are that the C.O.P. for the intact, high porosity cortex is so low as to be virtually undetectable.

The implication of the data presented in this chapter is that for unrestricted respiratory metabolism in E.angustifolium and rice the internal ventilating system must be such as to maintain the oxygen concentration in the cortical gas spaces of the root apices above about 2.5%. There is abundant evidence that internal oxygen concentrations in excess of this value are a characteristic of the roots of wetland plants (Chapter 7; van Raalte, 1941; Vallance and Coult, 1951; Teal and Kamwisher, 1966; Armstrong, 1967b).

II. CRITICAL OXYGEN PRESSURE AND ROOT GROWTH

A. INTRODUCTION

There is abundant evidence to show that root growth in species lacking an efficient internal ventilating system is retarded by low oxygen pressures in the rooting medium (Chapter 1). Various workers have attempted to correlate root growth with oxygen concentration external to the roots in soil or culture solution (see for example Banath and Monteith, 1966). However, it can be difficult, or even impossible, to use data so obtained to estimate the oxygen pressure within the root at which growth becomes impeded. Oxygen levels measured in bulk soil or culture medium are not necessarily identical to those at the root surface (eg. Greenwood, 1969). Also, internal transport of oxygen may elevate the oxygen pressure within the root above that recorded in the rooting medium. Consequently, the precise internal oxygen pressures which limit root growth have never been determined.

In the first part of this chapter it was concluded that the critical oxygen pressure in intact plants may well be a property of the meristematic

PLATE 4.1: Eriophorum angusifolium root;

(a) Radial longitudinal section through the apex showing the dense tissue in the meristematic region (x 870).

(b) Transverse section at about 0.2cm from the tip. Note the scarcity of intercellular spaces in the stele (x 650).

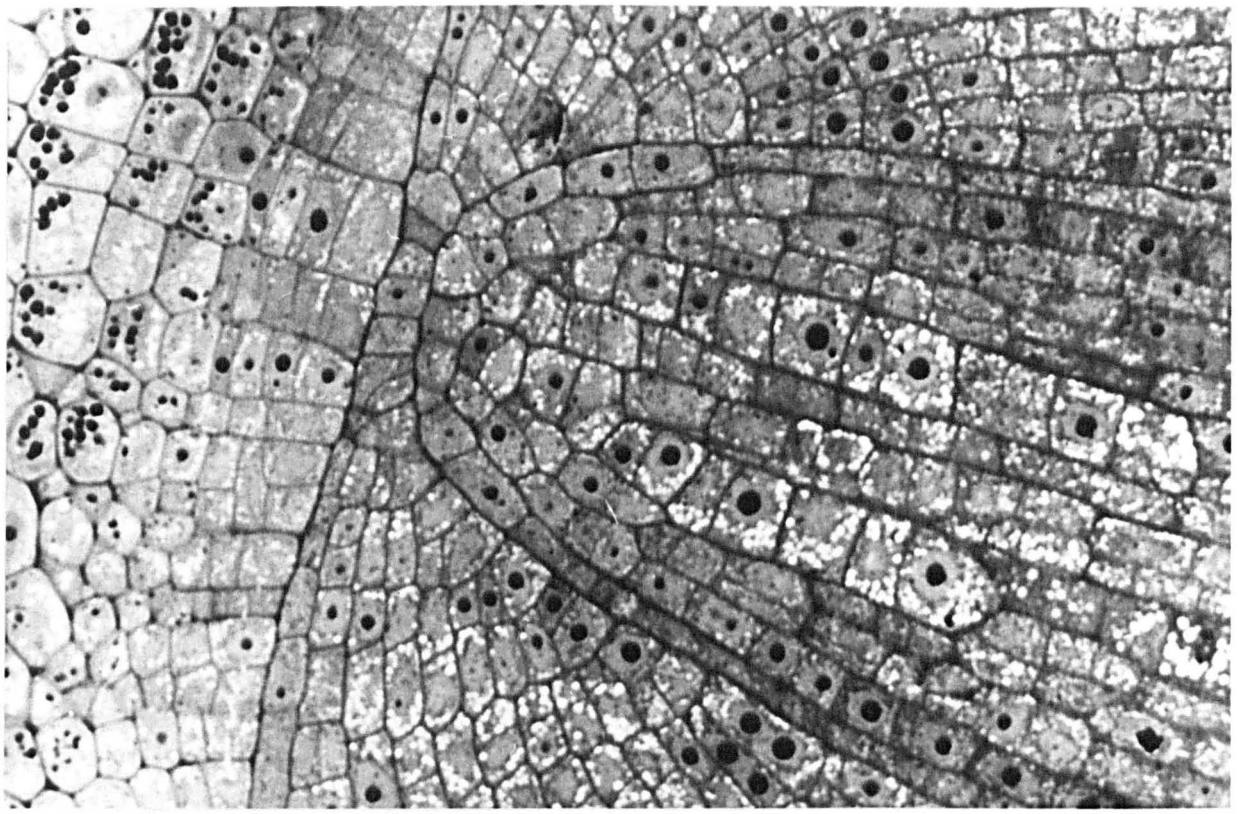

a

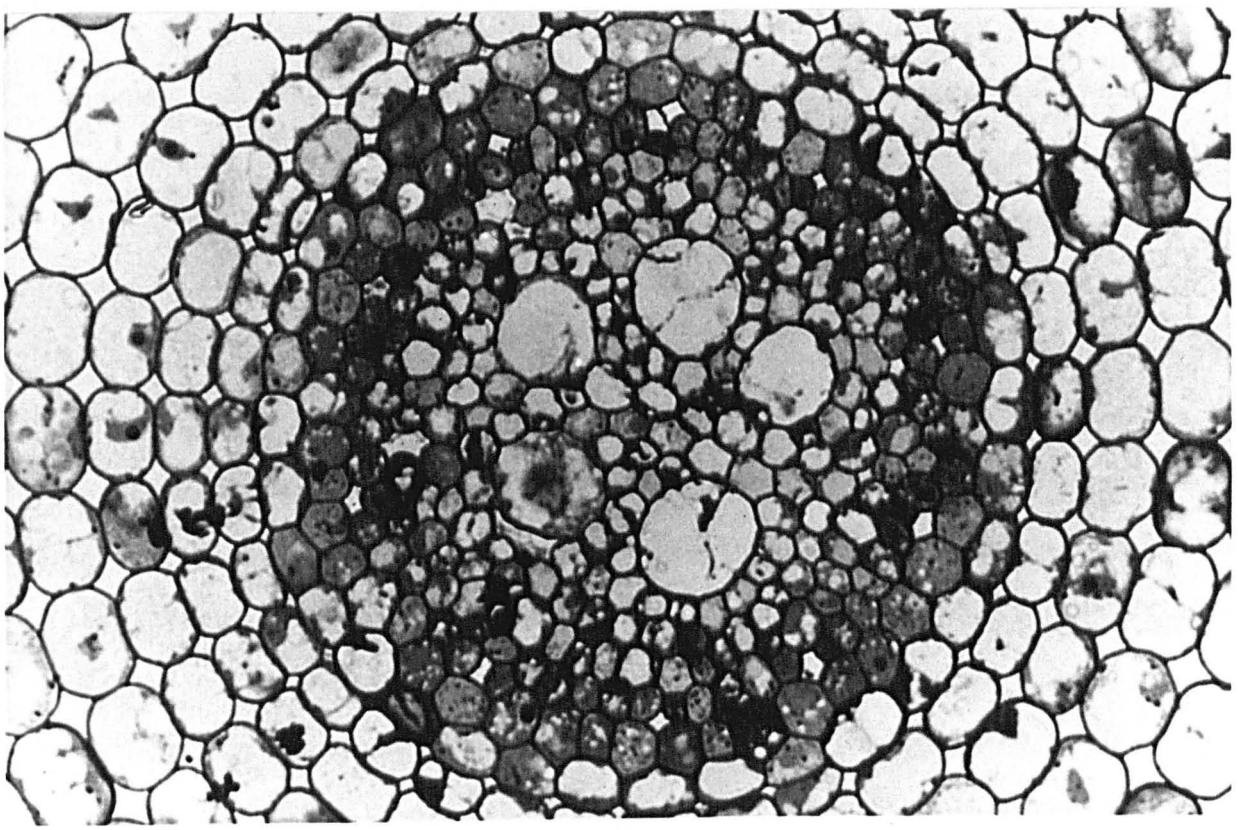

b

and stelar tissues of the root. If this is the case the reduction in respiratory rate at the C.O.P. might be reflected in a lowering of meristematic activity and a consequent reduction in growth rate of the root. The polarographic method for measuring C.O.P. given in the previous section enables the oxygen regime within the root apex to be controlled and monitored. Using this method the effect on root growth of oxygen pressures at and below the C.O.P. was determined and is described below. Eriophorum plants were not available during this part of the study, hence rice was the only test species used.

B. METHOD

The apparatus was that used in the polarographic method for determining C.O.P. The apical radius of the experimental root was measured and the root arranged within an electrode as close as possible to the wall of the containing-vessel to enable a travelling microscope to be focussed on its apex. With air circulating through the leaf chamber and the diffusion current at equilibrium root growth was monitored.

When the root was growing at a constant rate the oxygen concentration within the leaf chamber was lowered, the corresponding concentration within the root apex calculated from the equilibrated diffusion current, and any effect upon root growth observed. If the growth of the root was unaffected by the reduced internal oxygen concentration the oxygen regime in the leaf chamber was reduced still further. This process was repeated until inhibition of root growth was observed. Finally, the gas in the leaf chamber was replaced by air. Root growth in control plants in which air was maintained around the leaves was also monitored.

The aerial parts of the plants received a photosynthetically active radiant flux density of 50μE $m^{-2} s^{-1}$ and experiments were carried out at 23^{o}C.

C. RESULTS

1. Effect of Subjecting Root Apices to Oxygen Concentrations at or below the C.O.P. for Short Periods

The result shown in Fig.4.10 illustrates the manner in which root growth was affected by changes in the internal oxygen regime. Root extension was unchecked at leaf chamber oxygen concentrations above 9.0%; this corresponded to an internal apical concentration of 3.3%. At this oxygen tension, however, root growth was halted and remained so whilst the 9.0% leaf chamber concentration was maintained. Replacing the gas around the leaves with air, so as to bring the apical concentration to 9.7%, resulted in continued growth. In each of six experiments root elongation ceased when the apical oxygen concentration was brought within, or closely approached, the range of C.O.P. values given in the first part of this chapter. No effect was observed in the control experiments.

Root apices were held at the C.O.P. for periods ranging from 2.5 to 5.0h and although retardation of growth was rapid, the time taken for cessation varied from 0.5 to 3.5h. Recommencement of root growth on exposure of the aerial parts to air took from 0.5 to 1.0h.

In four later experiments the oxygen concentration in the leaf chamber was changed from air to 4.9%; this resulted in a low apical concentration of about 0.2% to 0.4%. These conditions were maintained for 4.0 to 7.0h and the aerial parts were then exposed to a sequence of progressively higher oxygen concentrations. A typical result is illustrated in Fig.4.11. Root growth was arrested in 4.9% O_2 and although exposure of the leaves to 7.2% and 9.4% O_2 (1.5% and 2.3% in the root) resulted in renewed growth, this was at only a slow rate and for a short period. However, when the leaf chamber oxygen concentration was raised to 13.65% (4.4% in the root) growth re-commenced at a constant rate similar to its value in air.

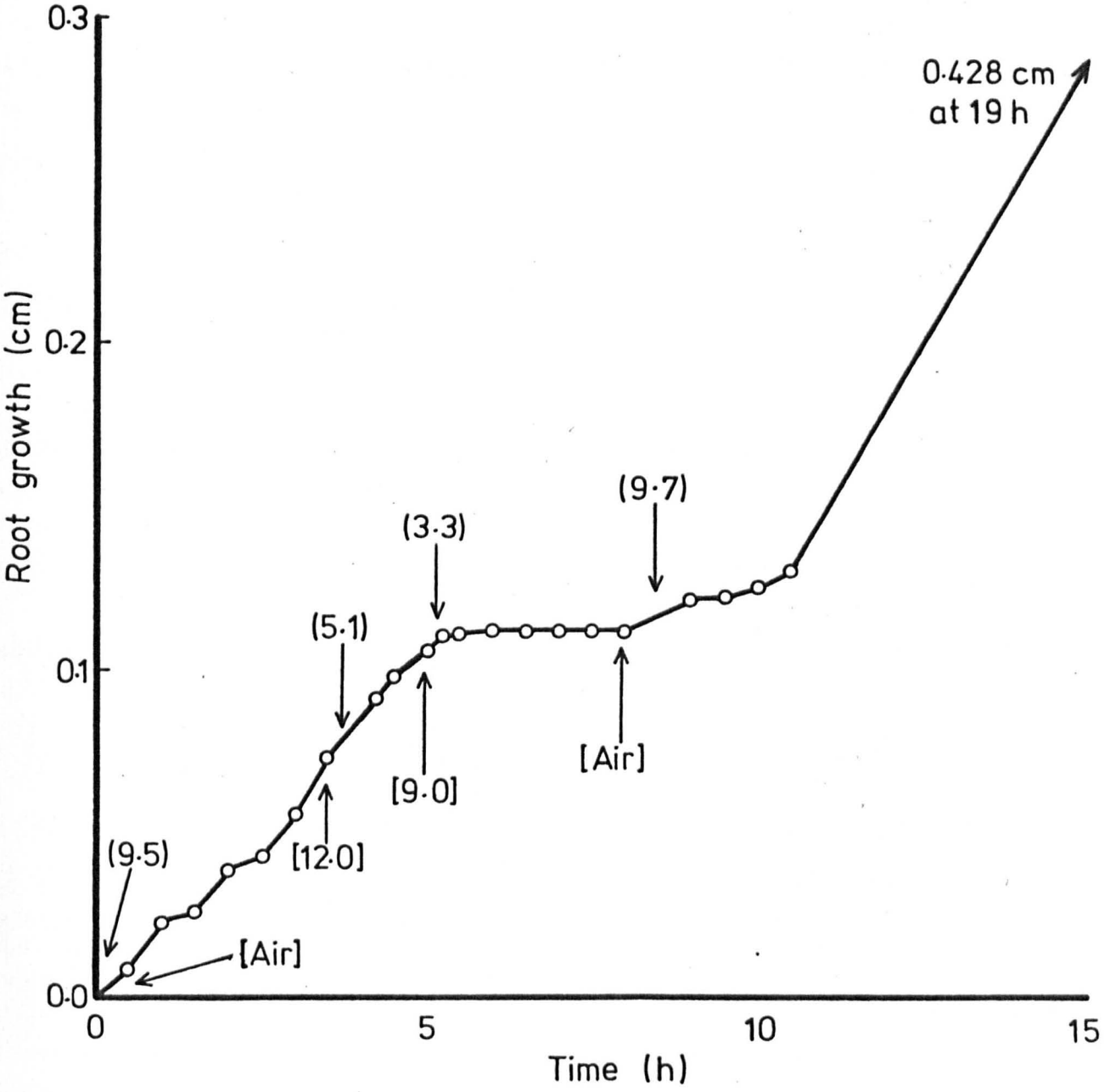

FIG. 4.10 Growth of rice root subjected to various internal oxygen regimes.

Figures in square brackets indicate leaf chamber oxygen concentration (%).
Figures in round brackets indicate equilibrated oxygen concentration in the root apex (%) calculated from flux data.

FIG. 4.11 Growth of rice root subjected to various internal oxygen regimes
Figures in square brackets indicate leaf chamber $[O_2]$ (%)
" " round " " equilibrated " in root apex (%)

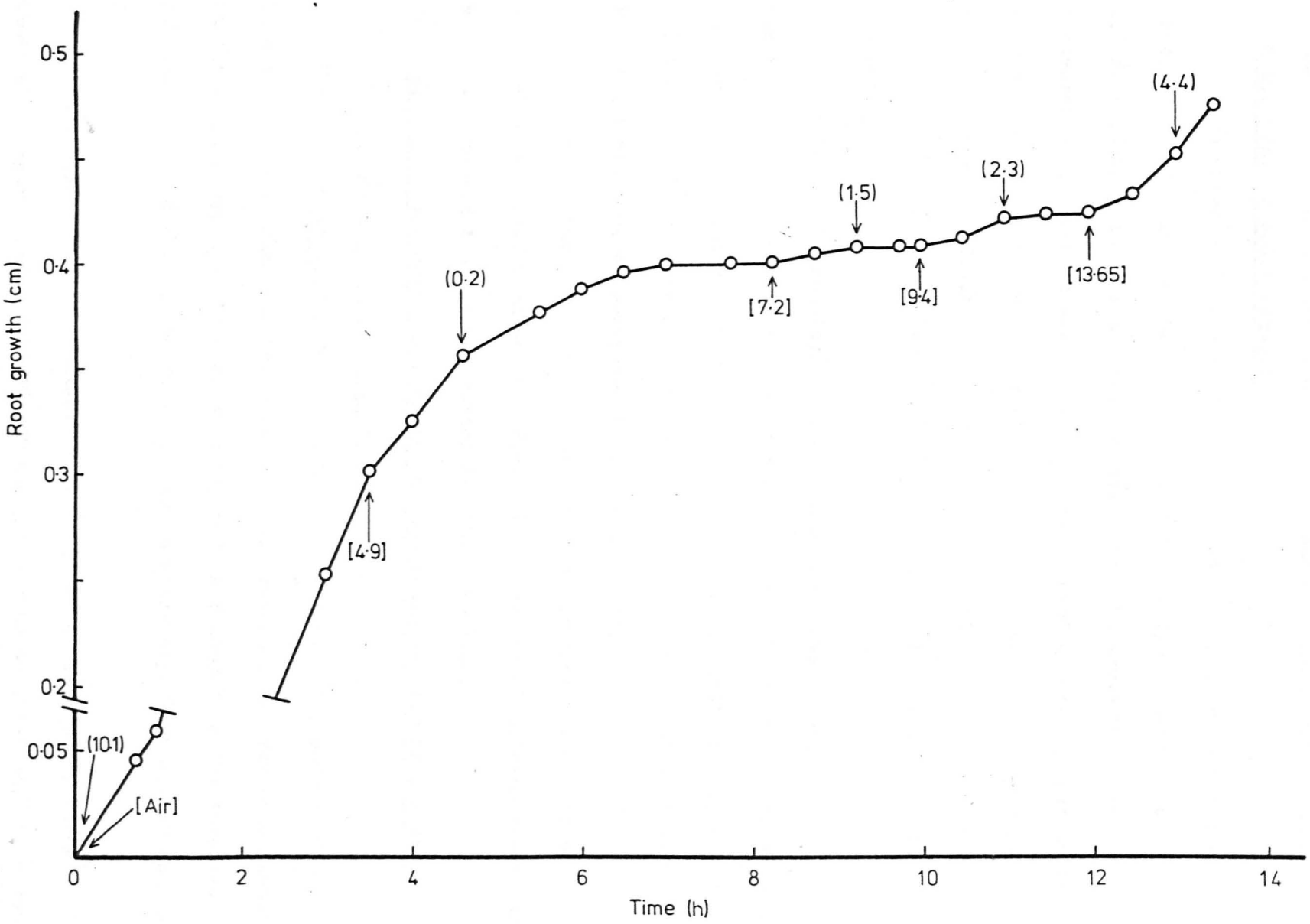
0·5
0·4
0·3
0·2
0·05
Root growth (cm)
(10·1)
[Air]
(0·2)
[4·9]
[7·2]
(1·5)
[9·4]
(2·3)
[13·65]
(4·4)
0
2
4
6
8
10
12
14
Time (h)

2. Effect of Subjecting Root Apices to Oxygen Concentrations below the C.O.P. for Extended Periods

In the experiments described in the previous section root apical oxygen concentration was held at or below values approximating to the C.O.P. (1.6 to 3.3%) for periods not exceeding 7h, after which an increased oxygen regime always resulted in renewed growth. Experiments were carried out also to test whether root apices subjected to oxygen tensions below the C.O.P. for longer periods would suffer such permanent damage as to prevent further growth on re-exposure to normal oxygen concentrations.

The method was identical to that described above except that the gas in the leaf chamber was changed from air to 3.5% oxygen; this resulted in a very low apical concentration of 0.1% to 0.3%. Root growth ceased and the plants were left under these conditions for about 40h, after which the aerial parts were re-exposed to the atmosphere.

In each of four experiments root growth recommenced after air was supplied to the leaf chamber (eg. Fig.4.12). The period between re-exposure to air and renewed root growth varied from 2.5h to 7.0h.

3. Effect of Subjecting Plants to an Atmosphere of Nitrogen, with and without Glucose Supplied to the Roots

Vartapetian et al. (1976, 1977) have shown that mitochondrial damage in excised roots under anaerobiosis could be prevented by providing glucose in the bathing medium. In view of this, and as a sequel to the investigations described above, the following exploratory experiments were carried out.

Plants were arranged as described above, either with their roots immersed in agar medium or in 4% w/v anaerobic glucose solution. When root growth was constant the air in the leaf chamber was replaced by nitrogen for about 17 to 20h, after which air was resupplied.

In each experiment root growth ceased within 2 to 3h exposure to the nitrogen atmosphere. In plants not supplied with glucose (Fig.4.13)

FIG. 4.12 Growth of rice root subjected to an apical [O_2] below the C.O.P. for 40h
Figures in square and round brackets indicate leaf chamber and root apical [O_2] respectively

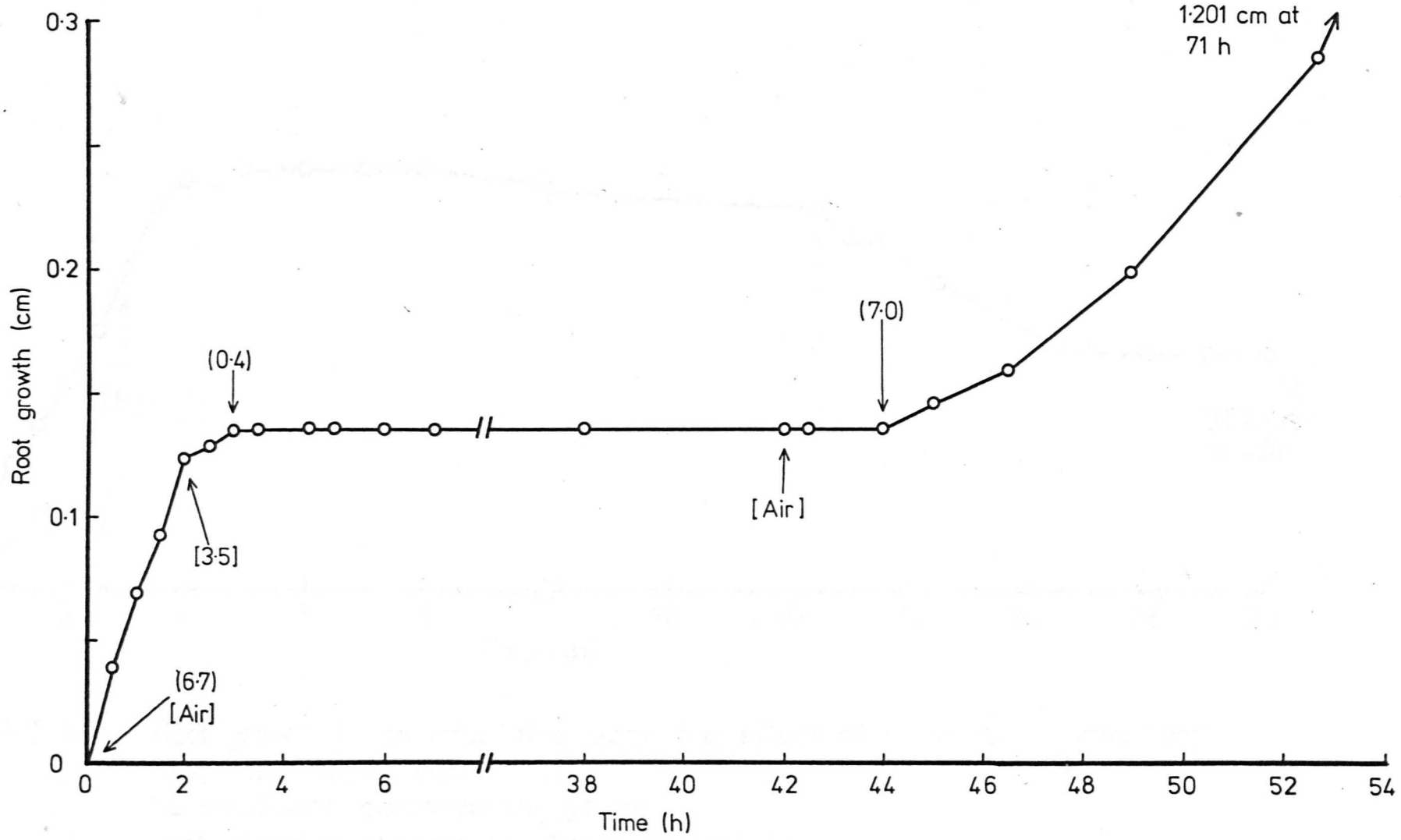
0·3
0·2
0·1
0
Root growth (cm)
1·201 cm at
71 h
(7·0)
(0·4)
[Air]
[3·5]
(6·7)
[Air]
0
2
4
6
38
40
42
44
46
48
50
52
54
Time (h)

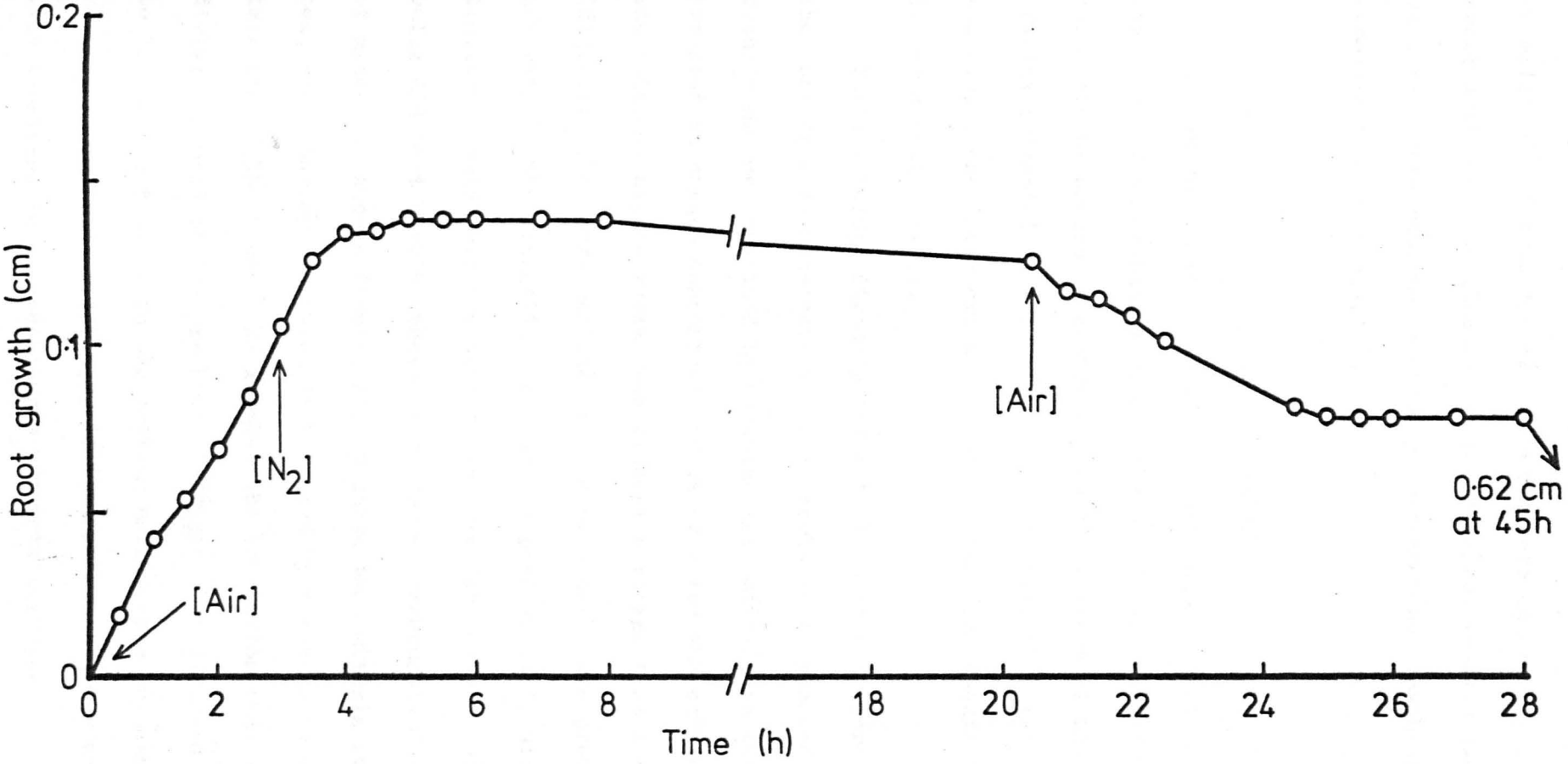

FIG. 4.13 Root growth in an intact rice plant: the effect of a nitrogen atmosphere round the aerial parts
No additional carbohydrate source
Leaf chamber atmosphere shown in brackets

root growth did not recommence on exposure to air; rather, contraction of roots took place. When these plants were removed the roots were waterlogged and both leaves and roots were apparently dead. The visible shoot system of the glucose-fed plants also appeared dead, but in this case the roots remained viable and recommenced growth after only 1h exposure to air (Fig.4.14).

D. DISCUSSION

It was concluded in Part 1 of this chapter that the C.O.P. indicates the onset of anaerobiosis within the plant, and it was suggested that the locus of the anaerobic centre may be the tissues of the meristem. The results presented in this section demonstrate that root growth ceases at the C.O.P. and therefore add to the belief that anoxia has been reached in meristematic cells.

These findings strongly indicate that in rice aerobic respiration in the root apex is necessary if root growth is to proceed unhindered. The results may be explained by assuming that mitosis in the root meristem is arrested at oxygen concentrations at or below the critical value. When the internal oxygen regime was gradually raised from a very low value (Fig.4.11) the short periods of renewed growth were probably due to activity in the elongating zone at the progressively higher oxygen concentrations; only when the oxygen pressure was raised above the critical value did root growth proceed unhindered, presumably due to the resumption of mitosis. Amoore (1961a, b) has shown that mitosis in the root tips of pea, bean, barley and onion is arrested by exposure to an atmosphere of less than 0.5% oxygen. He reached the conclusion that all stages of cell division depend on the presence of oxygen, but stressed that plants adapted to low oxygen tension in the rooting medium were not studied. However, more recently Kordan (1974a,b; 1976) has demonstrated that root growth in rice seedlings is dependent upon adequate aeration.

The renewed root growth in the experiments in which the root apices were

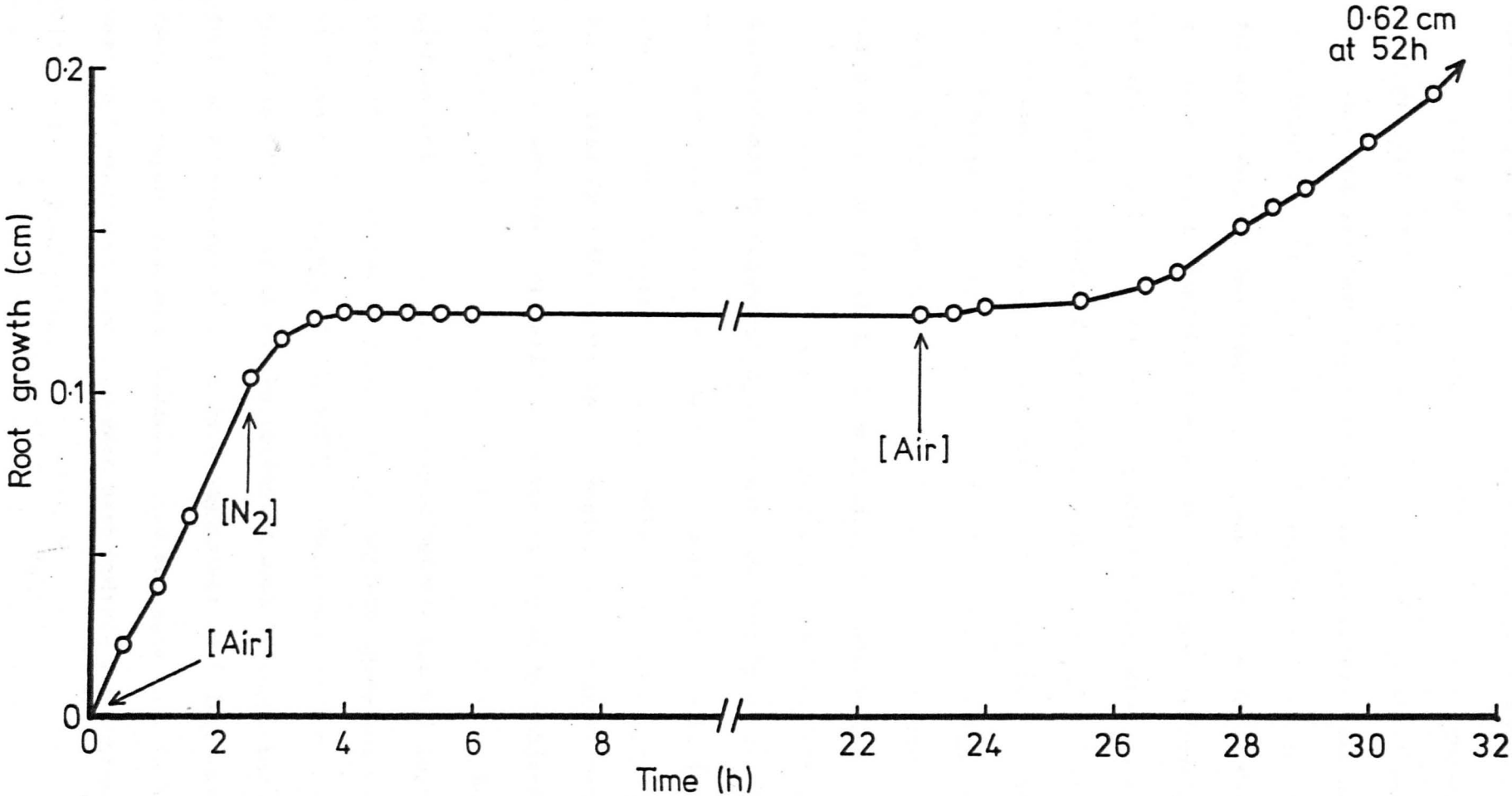

FIG. 4.14 Root growth in an intact rice plant : the effect of a nitrogen atmosphere round the aerial parts
Roots provided with 4% glucose
Leaf chamber atmosphere shown in brackets

subjected to very low oxygen pressures for long periods (Fig.4.12) was particularly interesting. Vartapetian et al (1970) and Vartapetian (1973) have obtained evidence of mitochondrial damage in apical cells of detached rice roots subjected to anoxia. After 4 to 5h nitrogen-bubbling destructive changes were observed in the mitochondria whilst after only 7h mitochondrial structure was irreversibly damaged. In the experiments described here the root meristems were almost certainly subjected to at least partial anoxia for up to 40h yet the renewed root growth was evidence that extensive irreversible mitochondrial damage could not have occurred. Root death was induced only when the entire plant was subjected to anoxia (Fig.4.13); Huck (1970) similarly found that an atmosphere of 100% nitrogen around the roots and shoots of cotton and soybean resulted in tap root death after 3h and 5h respectively. However, in the present study, root viability could be sustained even under total anoxia by providing an exogenous carbohydrate source in the form of dissolved glucose.

These results indicate that rice root survival during periods of anaerobiosis is dependent upon an adequate supply of respiratory substrate. When the aerial parts were maintained above the C.O.P. (3.5%) this presumably was derived from photosynthesis or stored products and was transported from the shoot to the roots. In the experiments in which internal transport of assimilates was prevented by subjecting the plants to total anaerobiosis carbohydrate could be supplied to the roots from a glucose solution. When respiratory substrate was not supplied root death occurred. These observations are in complete agreement with recent results of Vartapetian et al. (1976, 1977). These workers have shown that mitochondrial degeneration can be prevented both by supplying glucose to excised roots under anaerobiosis, or by using intact seedlings (although mitochondria became unusually large). This suggests that in the excised roots used in Vartapetian's earlier work carbohydrate exhaustion contributed to mitochondrial disruption.

For a given quantity of sugar anaerobic respiration yields only about one-tenth of the free energy derived from aerobic metabolism (James, 1971). However, the results of this investigation show that providing carbohydrate supply is not limiting this energy is sufficient to enable rice roots to survive prolonged periods of anoxia. On the other hand, the results show equally conclusively that active growth of the roots demands uninterrupted aerobic respiration and hence an adequate oxygen supply to the root apex; this is a fundamental point for which, as yet, little direct evidence has been obtained.

CHAPTER 5

AERENCHYMA AS AN OXYGEN RESERVOIR

Introduction

It has been suggested that the extensive gas-space system of wetland plants may act as a reservoir for oxygen when normal aeration is prevented (see Williams and Barber, 1961). Surprisingly, however, this aspect of the functional significance of aerenchyma has been the subject of very little experimental work. Laing (1940b) monitored the oxygen concentration within the gas spaces of a portion of Nuphar advenum Ait. rhizome which had been immersed in mercury at room temperature. From the initial value of 19.6% the oxygen concentration fell to 0.07% after 5.6h. Working with intact plants Armstrong (1967b) found that coating the aerial parts of Eriophorum angustifolium with Vaseline did not reduce R.O.L. from the roots to zero even after three hours. He concluded that this was due to oxygen remaining stored in the intercellular spaces of leaf bases and roots, although incomplete stomatal blockage may well have given this result (see Chapter 6). Williams and Barber (1961) suggested that although the lacunae of aerenchymatous plants may incidentally serve as an oxygen store, this is not their primary purpose. The work described in this chapter was designed to test whether aerenchyma actually does serve an important oxygen-reservoir function. The investigation began with some fairly straightforward experimental procedures, but became more involved when it was realised that the electrical analogue was required to aid the interpretation of the results. The study may be divided conveniently into "experimental" and "analogue" investigations.

I. EXPERIMENTAL

A. METHODS

Offshoots of E.angustifolium were prepared as described in Chapter 2. To ensure that the plants would be made entirely dependent upon the oxygen stored in the aerenchymatous structure they were immersed in the dark in

anaerobic medium. The changes in the internal oxygen regime which followed were monitored in two ways:

a) by continuous polarographic measurement of radial oxygen loss from the roots;

b) by extraction and analysis of gas samples from the intercellular spaces of the aerial parts.

All experiments were performed at a laboratory temperature of approximately 23°C.

1. Polarographic method

The direct dependence of the rate of oxygen diffusion from a root apex upon the concentration of oxygen within the root (p. 21) suggested that the cylindrical electrode technique could provide a convenient method of monitoring the changes in the internal oxygen regime following submergence.

a) Procedure

The apparatus was essentially that shown in Fig.2.5, the only modification being that the bung was loose-fitting and a light metal rod was attached to its centre, enabling it to be clamped at any level in the measuring cylinder.

The cylinder was filled with deoxygenated medium, a plant secured in the bung, and the residual current determined with the bung positioned at the cylinder mouth.

A root was then inserted through the electrode and the bung lowered into the cylinder whilst the agar medium was siphoned-off. In this way the electrode and roots remained submerged, so excluding air bubbles from the electrode, whilst stomatal blockage due to wetting of the leaves was prevented. When the plant was entirely contained within the measuring cylinder the metal rod was clamped and any final adjustments made to the position of the electrode. Finally, to prevent photosynthetic oxygen production, light was excluded by wrapping the measuring cylinder in black paper.

When the diffusion current had equilibrated at the plateau potential the cylinder was filled with deoxygenated medium. Care was required to prevent disturbance of the diffusion gradient between root and electrode; by gently introducing the liquid from a large hypodermic syringe fluctuations in the equilibrium current were minimised.

To continuously monitor the fall in internal oxygen concentration the diffusion current was displayed on a chart recorder. It was assumed that a fall to the residual value could be considered indicative of exhaustion of oxygen from the gas space system of the root apex. This assumption was difficult to prove valid by experiment, but later analogue work (p. 88) showed it to be correct.

At the end of each experiment the agar medium was restored to its pre-submergence level. Almost without exception the diffusion current rose to its original value as the moisture dried from the leaf surfaces, indicating that internal blockage of the gas conducting channels had not occurred during the period of submergence.

2. Gas extraction

The method was that described in Chapter 4 and was employed to supplement the more convenient polarographic technique.

3. Determination of leaf area, total volume and gas-space volume

(a) Leaf Area

At the end of each polarographic experiment the plant was surface-dried. Leaf surface area was estimated by approximating leaf shape to a trapezium topped by an apex in the shape of an isosceles triangle. The area of one surface, A_1, is given by:

$$A_1 = \tfrac{1}{2} \left[h_1 (a + b) + a h_2\right] \quad cm^2 \qquad (5.1)$$

where:

h_1 = the perpendicular height of the trapezium (cm)

h_2 = the perpendicular height of the triangle (cm)

a,b are the lengths of the parallel sides of the trapezium (cm)

a = also the length of the base of the triangle (cm)

(b) Total Volume and Gas-Space Volume

Total plant volume was measured by liquid displacement in the apparatus used for gas space volume determination. The latter was estimated by drawing-out the gas under vacuum and injecting the void with a penetrating liquid. Shoots and roots were treated separately. The apparatus consisted of an inverted burette and rubber stopper. Formalin acetic acid (F.A.A.) was used as the penetrant. The plant was cut into short segments which were tied into a loose bundle with thread and held at the stoppered end of the burette by fastening the thread to the stopper. Care was taken to remove air bubbles from the surface of the segments by gently tapping the burette. A vacuum of about 0.6 cm Hg was then applied via the nozzle end of the burette and suction was maintained until gas bubbles ceased to issue from the segments. When atmospheric pressure was restored F.A.A. was forced into the evacuated gas spaces; if any gas could be seen within the lacunae evacuation was repeated.

Since some F.A.A. was lost by evaporation during evacuation it was necessary to apply a correction. This was obtained by noting the decrease in volume of F.A.A. alone after evacuation for a known time.

Gas space volume is given by:

$$V_1 = V_2 - V_3 - V_4 \quad cm^3 \qquad (5.2)$$

where:

V_1 = the gas space volume

V_2 = the volume of F.A.A. + plant before evacuation

V_3 = the volume of F.A.A. + plant after evacuation

V_4 = the volume of F.A.A. lost by evaporation

B. RESULTS

1. Plant volume and gas-space volume

Gas space ("reservoir") volume varied linearly with plant volume as shown in Fig.5.1. The fractional porosity of the plants, ϵ, (i.e. the

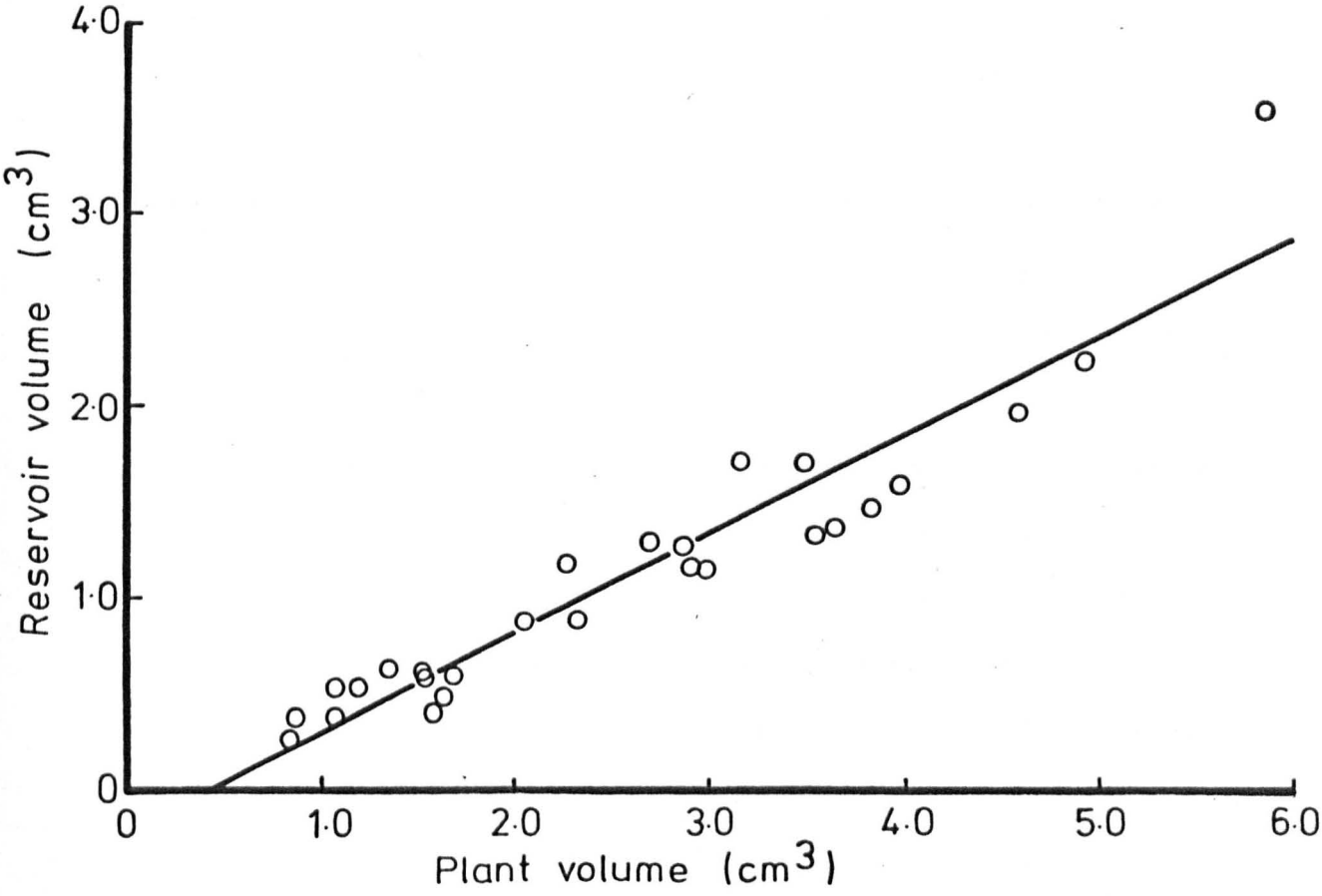

FIG. 5.1 Relationship between reservoir volume and total volume

$$y = 0{\cdot}513x - 0{\cdot}212$$

$$r = 0{\cdot}948$$

proportion of the total volume occupied by gas space), calculated from data on the regression line in Fig.5.1, is plotted against total volume in Fig.5.2. A curvilinear relationship between porosity and plant volume is apparent, ϵ increasing from about 24% in the smallest plants to about 48% in the large, expanded adults.

2. Changes in the internal oxygen regime after submergence

The manner in which the internal oxygen regime of the leaf bases declined after submergence (monitored by gas analysis) has been described on p. 65

The manner in which R.O.L. fell was related to plant size. The commoner relationship between R.O.L. and time after submergence, typical of smaller plants (approximately $4cm^3$ or less), is shown in Fig.5.3a. By substitution of flux values into equation 2.9 and correcting for diffusive resistance in the root wall (see p.149) the oxygen concentration within the cortical gas spaces of the root apex was obtained and values are given in Fig.5.3.

The flux does not fall immediately after submergence; there is first a "lag" period. This is followed by a linear decline, indicative of a constant rate of oxygen depletion, until an internal oxygen concentration of about 1.3% is reached. Linearity is then lost and the curve assumes a "tail" until, after 55 min, R.O.L. is no longer detectable.

Intially it was assumed that the point of inflexion on the R.O.L. curve represented a C.O.P. in the root (Chapter 4); this assumption was validated later using the electrical analogue (p.88). The mean C.O.P. determined by this method was 0.020 atm (S.D. $\pm$ 0.007 atm, 25 plants) and there was a slight but insignificant tendency for C.O.P. to increase with plant size ($P = 0.05$). This C.O.P. is slightly lower than that obtained by the polarographic technique described in Chapter 4. A possible reason for the discrepancy may have been the difficulty in estimating the exact turning point on the R.O.L. traces; any error introduced would tend to produce an underestimate of C.O.P.

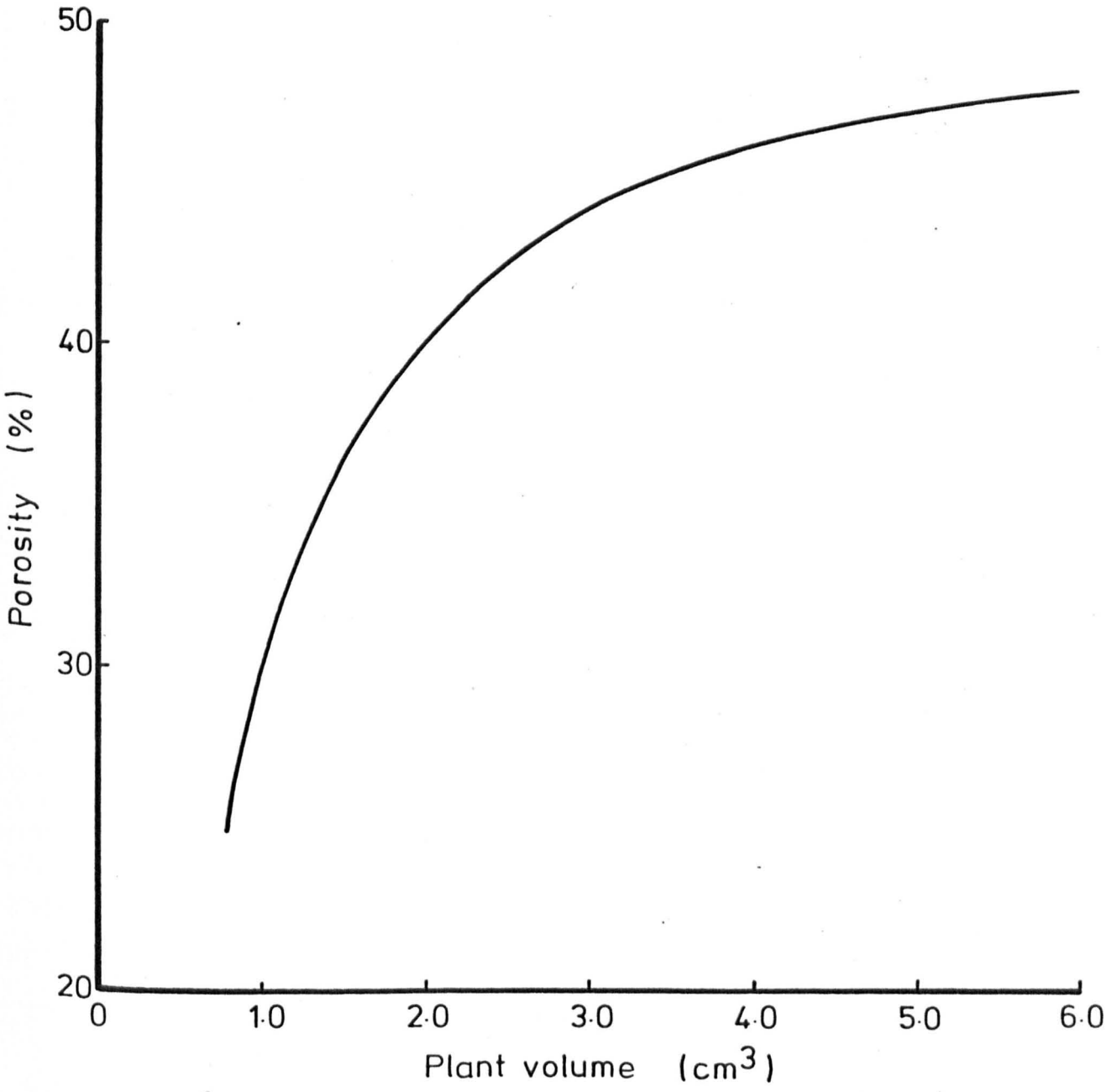

FIG. 5.2 Variation in total porosity with plant volume

FIG. 5.3 Fall in radial oxygen loss and internal apical oxygen concentration following submergence in anaerobic medium at 23° C.

(a) Small plant

(b) Larger plant

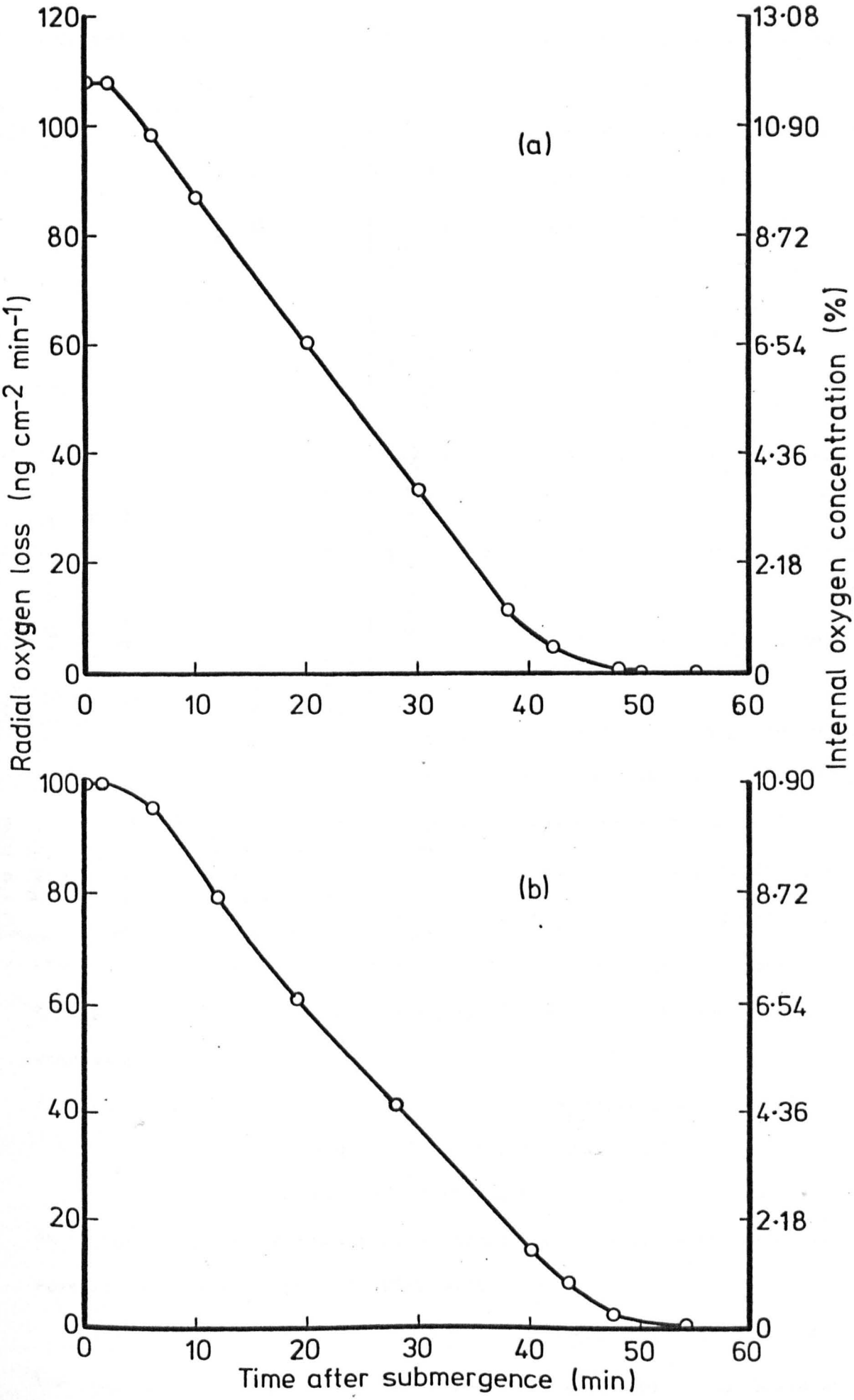
(a)
(b)
Radial oxygen loss (ng cm-2 min-1)
Internal oxygen concentration (%)
Time after submergence (min)
120
100
80
60
40
20
0
13·08
10·90
8·72
6·54
4·36
2·18
0
10
20
30
40
50
60

An interesting feature of the traces was the initial "lag", referred to above. This was invariably present and a possible reason for its occurrence is discussed later (p.92)

The second type of R.O.L. - time relationship, typical of the larger plants, is shown in Fig.5.3b. In this case, after the initial lag, R.O.L. falls for a time with a decreasing slope before the decline becomes linear. The effect is to produce a "shoulder" in the early part of the curve (see p.93). It was thought that this may have been due to concentration-dependent diffusion of oxygen from the aerial parts; such a process would tend to produce an exponential fall in the internal oxygen regime and compared with the decline due to respiration the effect would be more pronounced at higher oxygen concentrations (see Fig.4.5d). The larger plants had a greater ratio of exposed leaf surface to volume (Figs. 5.4 and 5.5), an indication that the significance of the "leaf leakage" effect should have been greater in the larger specimens; this is in agreement with the experimental results.

The "leaf leakage" hypothesis was tested in the following two ways.

1. To determine first of all whether leakage from the leaves could be significant a cylindrical electrode, identical to those used in the measurement of R.O.L. from roots but of the greater radius 0.250cm, was passed over the partly submerged leaves of a plant until situated just above the leaf sheath. When the electrode was polarised a measurable diffusion current indicated that oxygen leakage from the leaves was occurring.

2. R.O.L. from the roots of large plants was monitored after submergence in the presence and absence of leaf leakage.

Large plants were arranged in the usual way and normal submergence experiments carried out using 0.05% agar; the R.O.L. curves produced were similar to that shown in Fig. 5.3b.

The agar was then siphoned off to the pre-submergence level and the leaf surfaces allowed to dry; this was accompanied by an increase

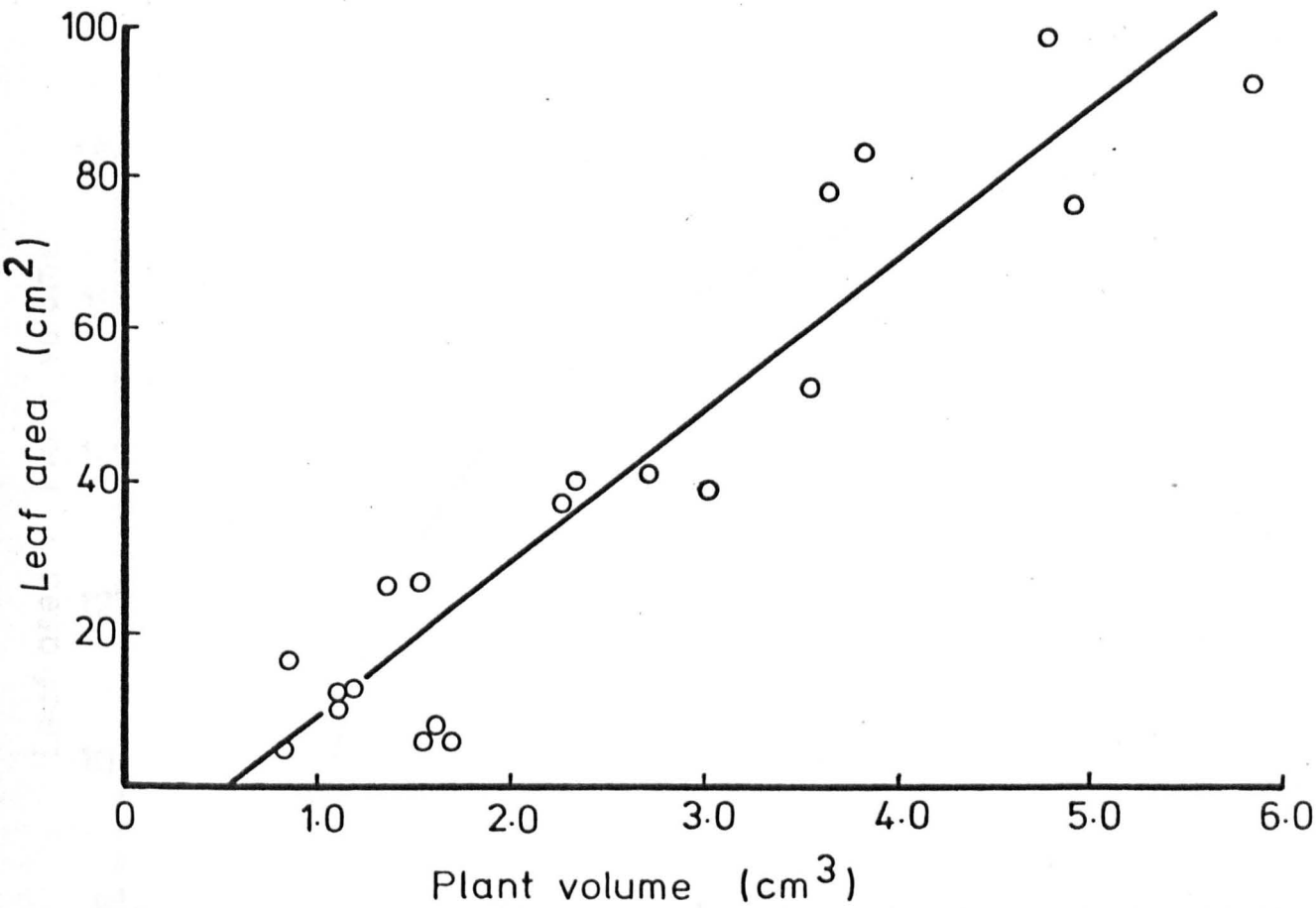

FIG. 5.4 Surface area of exposed leaves as a function of plant volume

$$y = 19{\cdot}7x - 10{\cdot}20$$

$$r = 0{\cdot}935$$

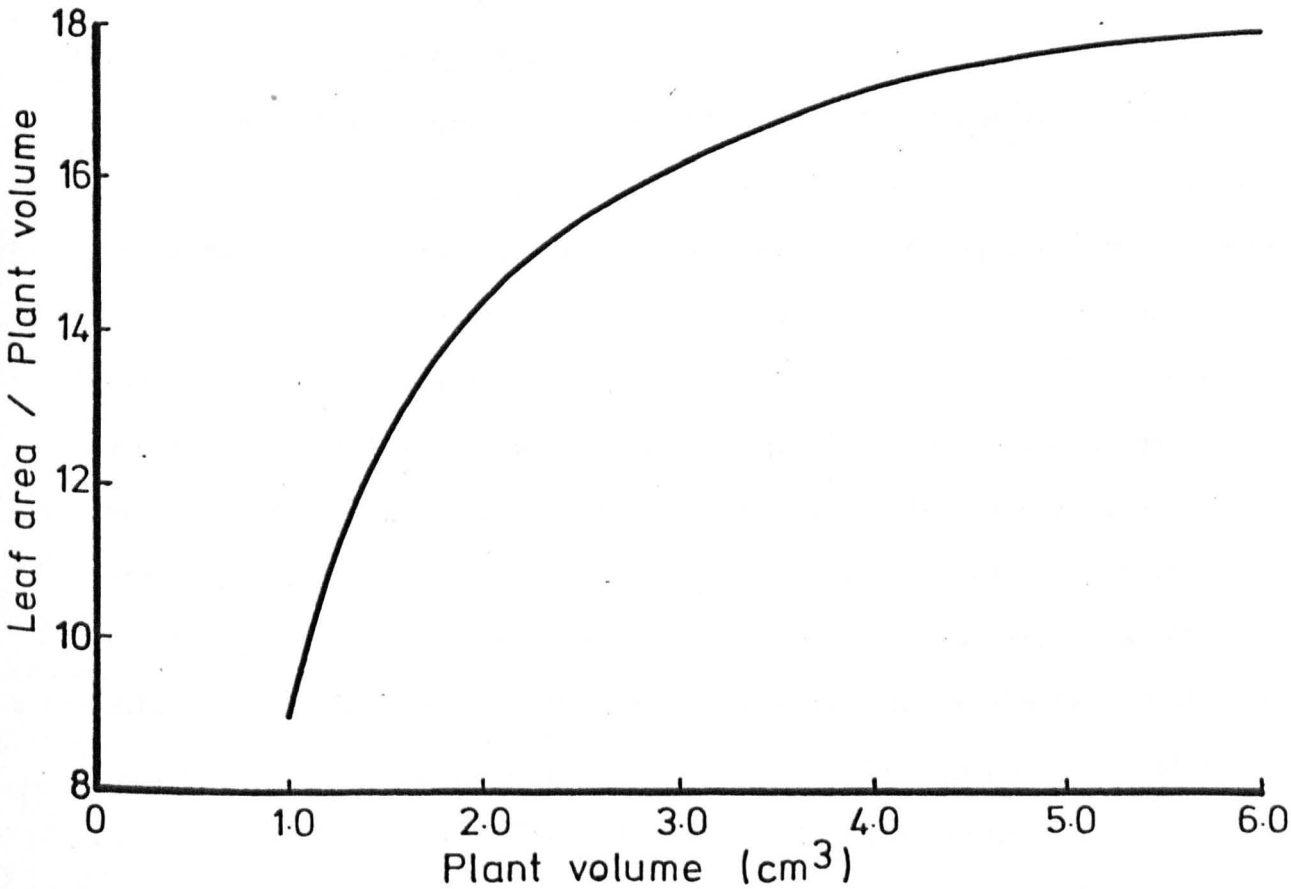

FIG. 5.5 Graph to illustrate the disproportionate increase in leaf area with plant volume

in R.O.L. to the original equilibrium value.

The space between the loose-fitting bung and the measuring cylinder wall was then "sealed" with moist cotton wool, effectively dividing the cylinder into upper leaf, and lower root, chambers. The leaves were then submerged in deoxygenated 0.3% agar; this viscous medium effectively "jacketed" the leaves and reduced oxygen leakage from their surface (see Healy and Armstrong, 1972). The R.O.L. - time curves produced under these conditions were similar to Fig.5.3a, and showed the linear decline typical of the smaller plants.

3. The gas space system as an oxygen reservoir

Due to the very gradual slope in the "tail" portion of the R.O.L. traces it was not easy to estimate the exact point at which the trace intercepted the time axis. Hence, the precise time required for the root apical oxygen concentration to fall to zero was difficult to determine. However, this time was estimated as accurately as possible and is shown as a function of total plant volume in Fig.5.6. There was a slight tendency for the oxygen within the root apices of the larger plants to last longer than that of the smaller ones but this was not significant ($P = 0.05$). The mean time taken to exhaust the apical oxygen was 61 min (S.D. $\pm$ 6 min, 26 plants). The times taken to exhaust the oxygen within the leaf bases fell within the range 55 to 70 min (gas analysis method). The similarity between the two times suggests that exhaustion of oxygen within the aerial parts quickly follows the exhaustion of that within the roots; therefore, zero R.O.L. may be a good indication of oxygen exhaustion throughout the entire plant. Analogue work confirmed this (see p. 91).

The time taken to completely exhaust the plant of oxygen may not be the best criterion in an assessment of the reservoir function of aerenchyma; probably of greater importance is the period for which the internal oxygen concentration can be maintained above the critical value.

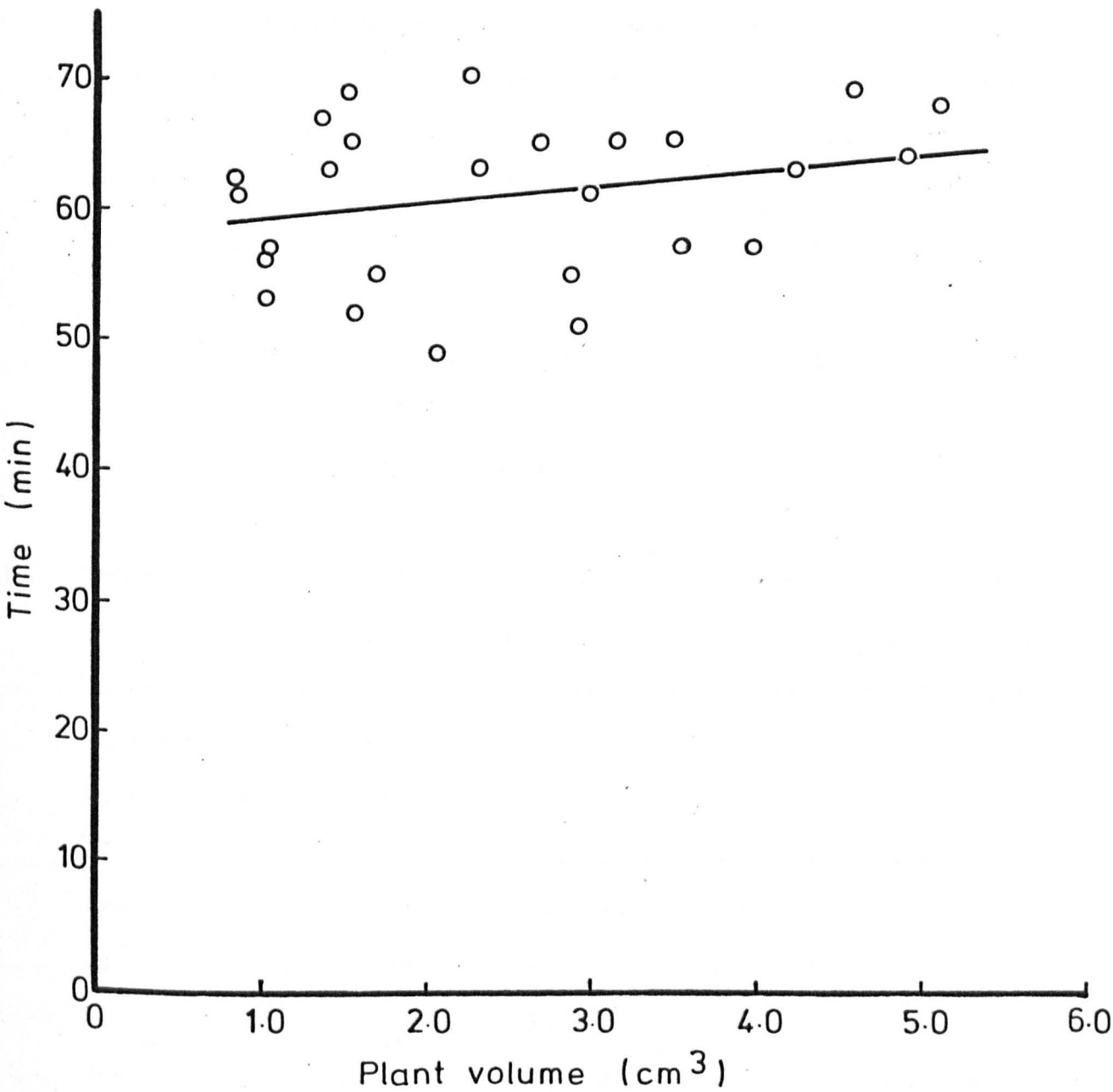

FIG. 5.6 Time taken to exhaust the internal oxygen reservoir as a function of plant volume

$y = 1{\cdot}26x + 57{\cdot}7$

$r = 0{\cdot}271$

This is plotted against plant volume in Fig.5.7. It can be seen that the smaller plants reached the C.O.P. more quickly than the larger ones, and that the maximum time for which the internal oxygen reservoir could sustain aerobic respiration throughout the entire plant was only 44 min. Since there was no tendency towards higher C.O.P.'s in the smaller plants it follows that the slope of the linear portions of the R.O.L. traces must have been steeper for the smaller specimens. This is illustrated in Fig.5.8 where the predicted time required for complete oxygen exhaustion, assuming absence of C.O.P. (found by extrapolation of the linear part of the curves), is plotted against plant volume.

Two factors may have contributed to the faster initial oxygen exhaustion in the smaller plants:

1. Their lower porosity (Fig.5.2)

The total amount of stored oxygen, compared with the volume of respiring tissue, was lower in the smaller plants than in the larger specimens. The corresponding faster exhaustion of this oxygen would produce a steeper gradient to the pre-C.O.P. portion of the R.O.L. curves in the smaller plants.

2. A possible higher respiratory rate in the smaller plants.

This would not be unexpected since the smaller plants, which were presumably younger specimens, would probably contain a greater proportion of actively growing tissue than the larger, older, plants.

The rate of decline in R.O.L. was a function of whole plant, rather than root, respiration (since the oxygen supply to the roots is governed by the oxygen regime of the aerial parts). Unfortunately, because the oxygen concentration gradient between leaves and roots prevented an accurate estimation of the initial volume of stored oxygen, it was not possible to calculate whole plant respiration rate with certainty. However, an approximation could be made, as follows.

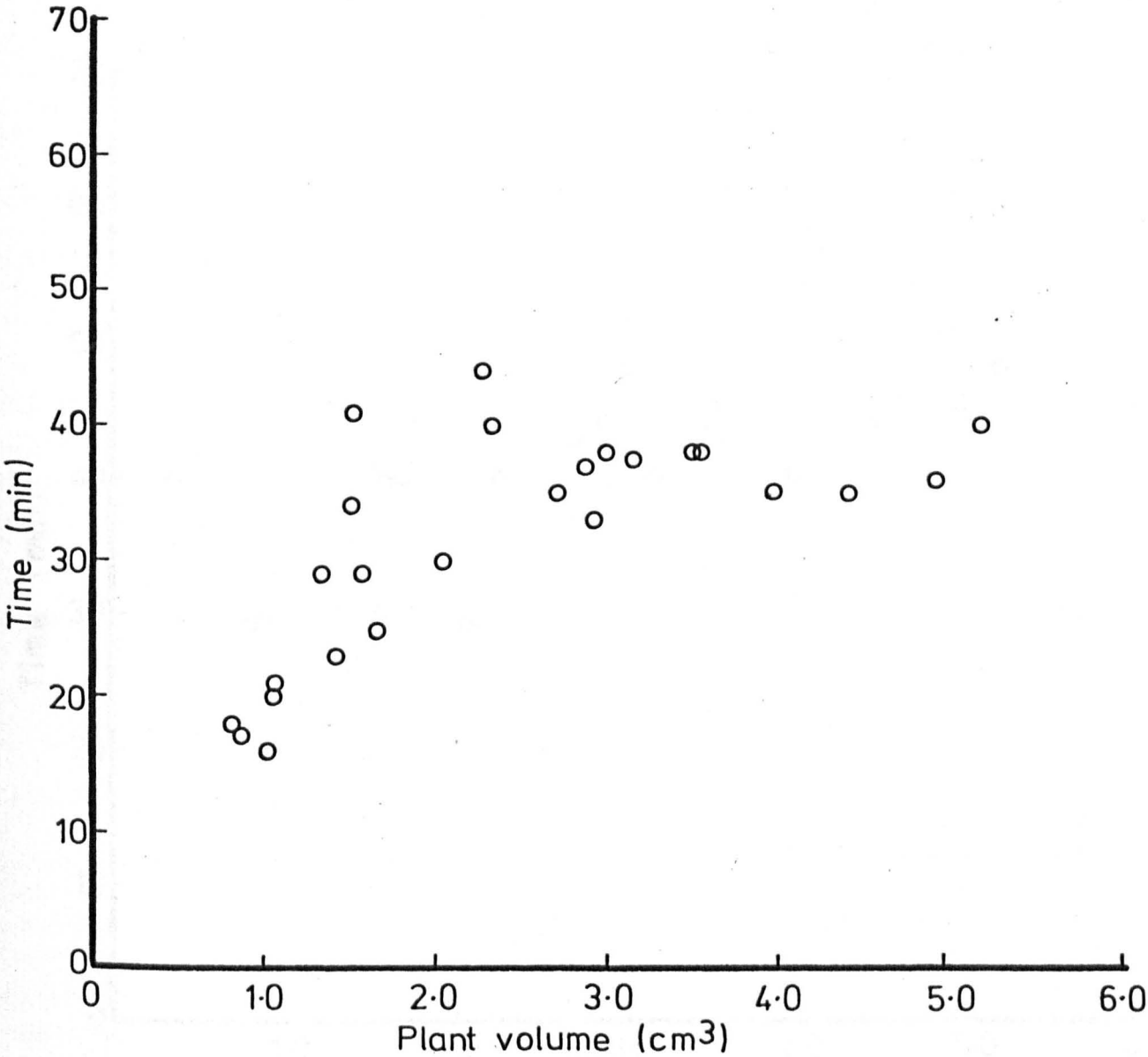

FIG. 5.7 Time taken for the internal oxygen concentration to fall to the critical value as a function of plant volume.

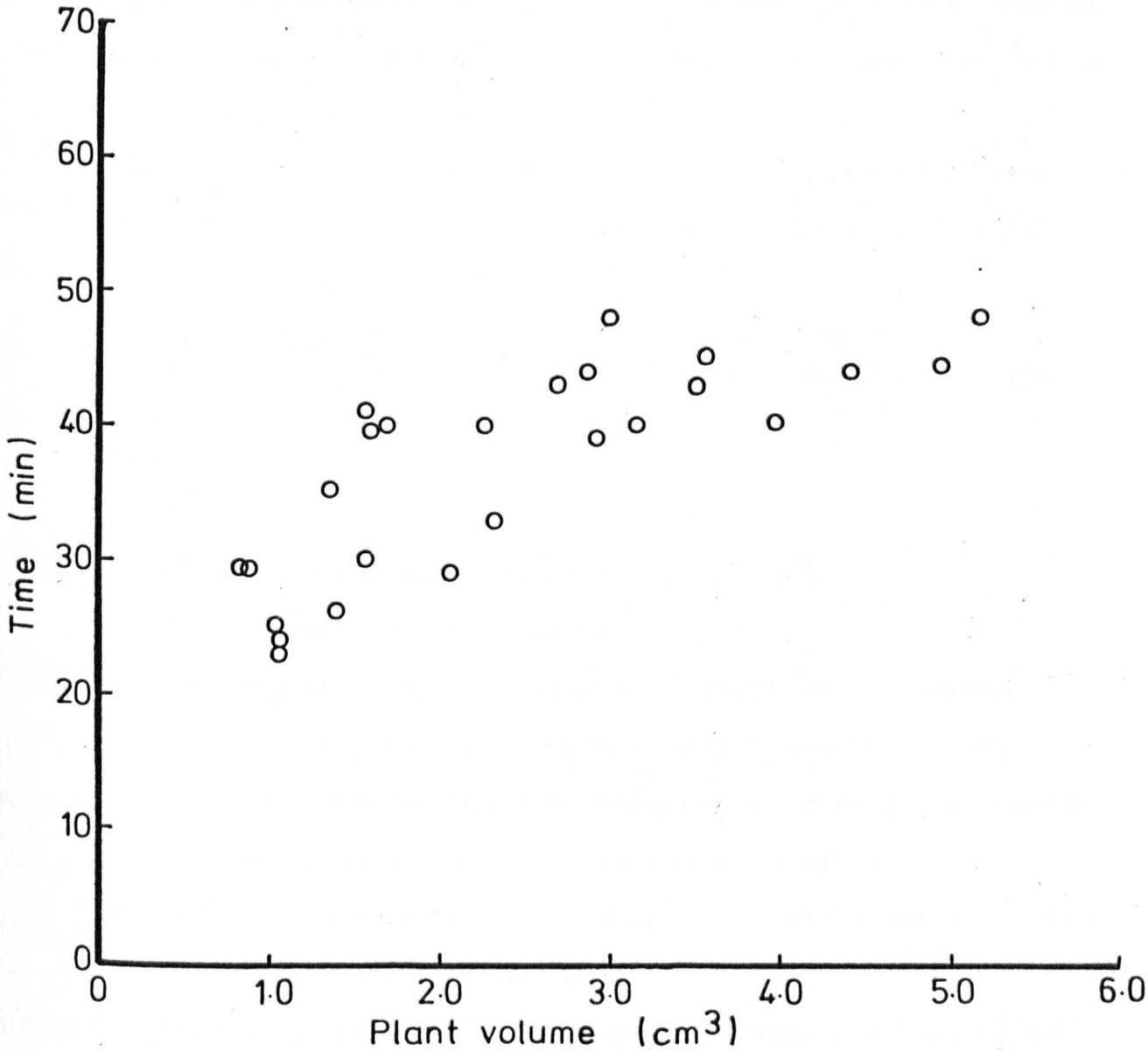

FIG. 5.8 Predicted time to exhaust the internal oxygen reservoir as a function of plant volume. Respiration rate was assumed independent of internal oxygen concentration.

The analysis of gas samples taken from root apices of plants with leaves in air (Chapter 7) gave a mean oxygen concentration of 14.6%. Based on this figure 17% was thought to be a reasonable estimate of the mean oxygen concentration in the root system as a whole. Analyses of gas samples extracted from leaf bases (Chapter 4) indicated that the gas-phase oxygen concentration within leaves in air approaches that of the atmosphere and 20.4% was considered an accurate estimate of leaf oxygen concentration prior to submergence. Knowing the total gas space volume of leaves and roots, the whole plant respiratory rate at 23°C was estimated from the equation:

$$\text{Resp.rate} = \frac{(0.17V_r') + (0.204V_l') \quad 132 \times 10^{-5}}{V_{Pl}t} \; gO_2 \; s^{-1} cm^{-3} \qquad (5.3)$$

where:

V_r' = the gas space volume of the roots (cm^3)

V_l' = the gas space volume of the leaves (cm^3)

V_{Pl} = the total plant volume (cm^3)

t = the time taken to exhaust the internal oxygen reservoir assuming respiration to be totally independent of oxygen concentration (found by extrapolation of the linear portion of the R.O.L. traces to the time axis) (s)

132×10^{-5} = the density of oxygen at 23°C and 1 atm (extrapolated from data of Weast, 1974) ($g \; cm^{-3}$)

Whole plant respiration rate showed considerable variation (mean 51.9 $ngO_2 \; cm^{-3}s^{-1}$, S.D. $\pm$ 15.7ng $cm^{-3}s^{-1}$) but there was no apparent correlation between respiratory rate and plant volume. It therefore seems likely that the alternative explanation, that of porosity differences (Fig.5.2) was probably the main factor contributing to the different initial rates of oxygen exhaustion from the gas spaces of large and small plants.

The faster initial depletion of the internal oxygen store in the smaller plants would suggest that these specimens ought to exhaust their

oxygen reservoirs more quickly than the larger plants. However, it has already been pointed out that there was insignificant correlation between exhaustion time and plant volume (Fig.5.6). A probable explanation is the variation in the proportion of total plant volume occupied by roots. A plot of root volume against total volume (Fig.5.9) shows a significant linear relationship ($P = 0.01$). In Fig.5.10 the ratio root volume to total volume, obtained from the regression line in Fig.5.9, is plotted against total volume. It is clear that in the smaller plants roots comprise a greater proportion of the tissues than they do in the larger plants. Consequently, since the initial internal oxygen concentration of roots is lower than that of leaves, the respiration of a greater part of the tissues of the smaller plants will become limited below the C.O.P. than is the case for the larger specimens. This will result in a reduction in slope and an increase in length of the "tail" portion in the R.O.L. - time curves for the smaller plants. Apparently this longer "post-C.O.P." period balances the shorter "pre-C.O.P." period, producing a total oxygen exhaustion time similar to that of the larger specimens.

II. ANALOGUE INVESTIGATION

A. INTRODUCTION

At this stage several features of the experimental results remained unexplained. In particular the lag, invariably present in the R.O.L. traces, and the "shoulder", a characteristic of the large plant traces, (Fig.5.3b) needed further investigation. In addition it was necessary to confirm the assumptions made earlier that (a) a fall in R.O.L. to zero indicated exhaustion of oxygen in the root apex, and (b) the point of inflexion in the R.O.L. traces mirrored the occurrence of a C.O.P. in the plant. Lastly, the suggestion that zero R.O.L. might also be a good indication of oxygen exhaustion throughout the entire plant (p. 80) required additional proof. Answers to these problems were sought using the electrical analogue.

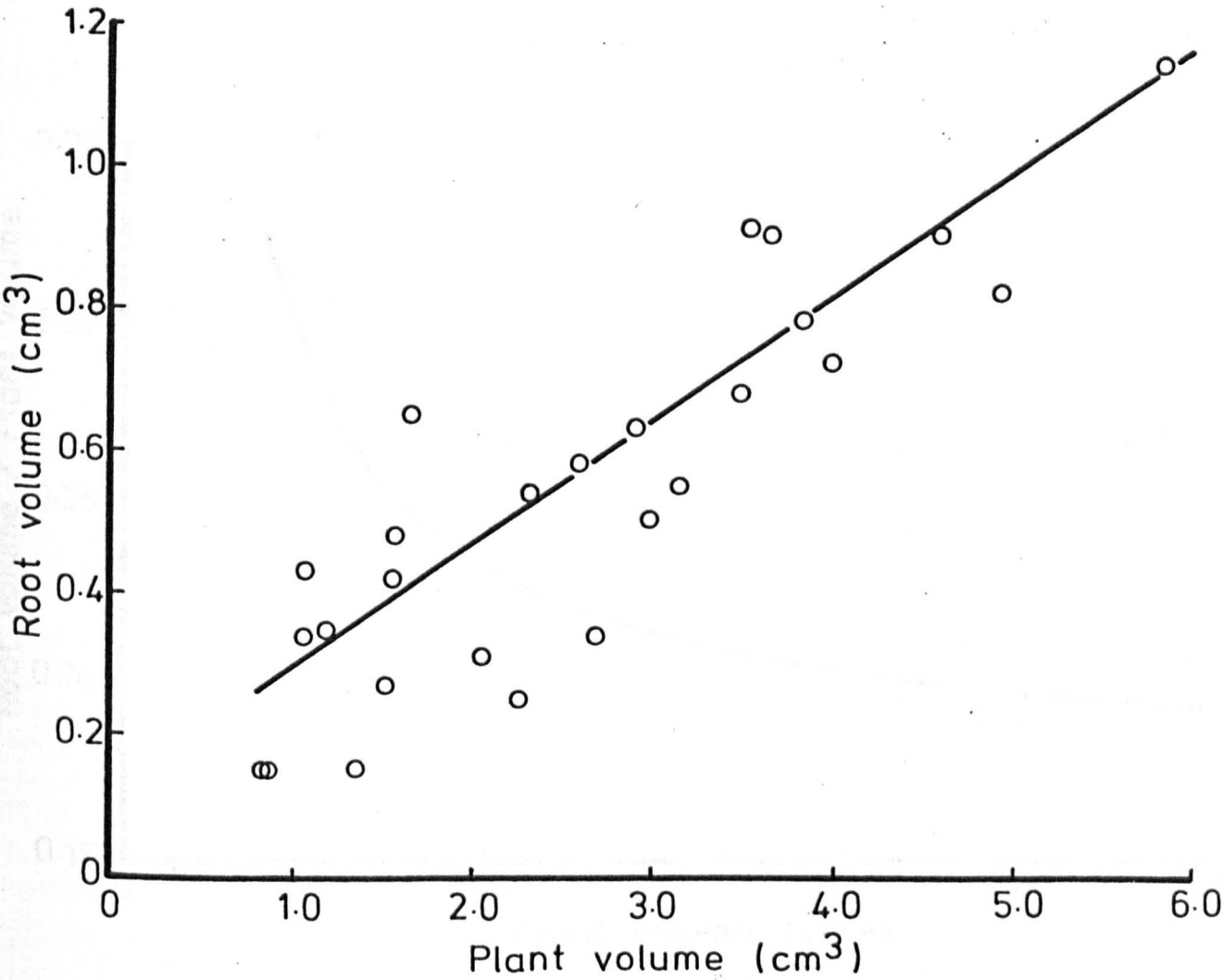

FIG. 5.9 Root volume as a function of plant volume

$y = 0.173x + 0.121$

$r = 0.878$

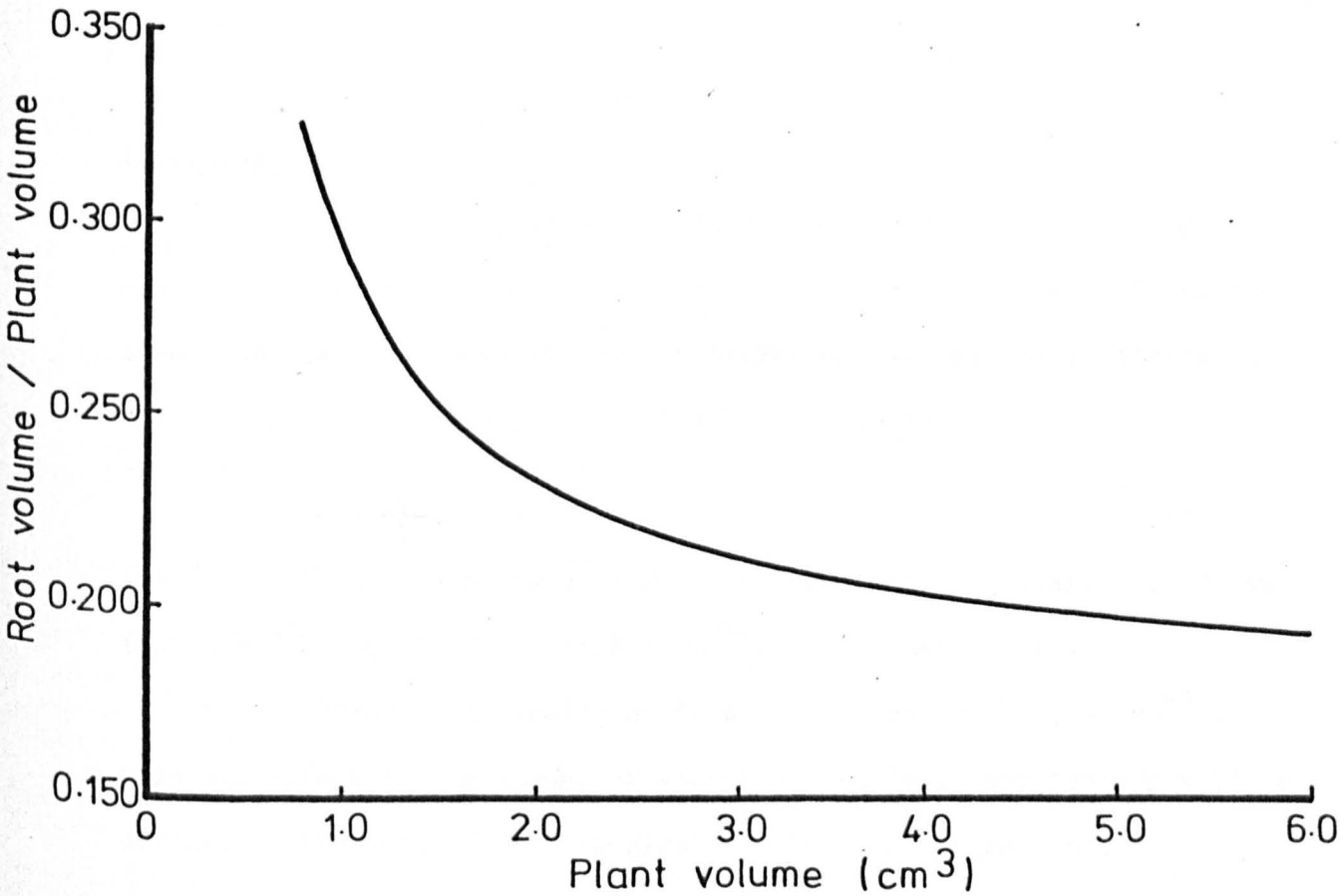

FIG. 5.10 Showing the proportion of the total plant volume occupied by roots

As described in Chapter 2 the analogue in its simplest form simulates the equilibrium oxygen regime of a root situated in an oxygen deficient medium; no provision was made for oxygen storage. The simulation of the submerged plant condition required that the internal oxygen reservoir should be included in the basic circuit. This was done by incorporating electrical capacitors. By using a combination of the approximately correct relative values of capacitance, diffusional resistance and respiration it was possible to model and monitor the internal oxygen regime of a leaf-stem-root system after submergence.

B. CAPACITANCE

1. Analogy

The capacitance, C, of a capacitor is defined as: "the stored charge required to produce a potential difference of 1 volt between the capacitor plates". Capacitance (units:Farads) is related to charge, Q, (coulombs) and potential, V, (volts) by the equation:

$$C = \frac{Q}{V} \qquad (5.4)$$

(The Farad is an excessive unit for most practical purposes, microfarad ($1\mu F = 10^{-6}F$) or picofarad ($1pF = 10^{-12}F$) being more usual).

In the plant: V is analogous to oxygen concentration, (g cm^{-3}); Q is equivalent to the amount of stored oxygen (g); and hence C will be defined as "the space (cm^3) required to make the oxygen concentration 1g cm^{-3}."

2. Capacitance values

Various oxygen-storage regions in the plant-electrode system may be recognised: leaf, stem, root and the liquid shell between root and electrode. The maximum oxygen concentration possible within the darkened plant is that of the atmosphere (20.41% or 268.7 x 10^{-6}g cm^{-3}); since the analogue voltage simulating 20.41% O_2 was 40V, capacitors designed for the working range 0–40V were chosen. Consequently, the maximum

capacitance required in any part of the plant must be such as to produce an oxygen concentration of 268.7 x 10^{-6} g cm^{-3}; this was determined by calculating the space occupied by oxygen at 20.41% concentration.

The discharge of an electrical capacitor is fundamentally a very rapid process (for example a 5μF capacitor charged to a potential of 100V will discharge to earth through a 200Ω resistor in about 0.004s - Scroggie, 1958). For this reason the capacitors required to simulate the changing internal oxygen regime of the submerged plant were necessarily of very large value in order that their discharge characteristics could be monitored with the instruments available. Capacitance values finally used were calculated by direct proportionality from the liquid shell capacitance, which was ascribed a value of 2,500μF (p.86). The capacitances of the various organs are given in Table 5.1 and their arrangement is shown in the abbreviated circuit diagram in Fig.5.11; their calculation is described below.

(a) Liquid Shell

The volume of the liquid shell, V_s, is given by:

$$V_s = L_e (r_e^2 - r_r^2) \quad cm^3 \qquad (5.5)$$

where:

L_e = the length of the electrode (cm)

r_e = the radius of the electrode (cm)

r_r = the radius of the root (cm)

The weight of dissolved oxygen at air saturation, W_o, is given by:

$$W_o = V_s C_{a-w} \quad g \qquad (5.6)$$

where:

C_{a-w} = the oxygen concentration in air-saturated water - i.e. 8.57 x 10^{-6} g cm^{-3} at 23°C.

For a root of radius r_r = 0.05cm enclosed within an electrode of radius r_e = 0.1125cm and length L_e = 1.0cm W_o calculates to 0.273 x 10^{-6} g at 23°C. This is equivalent to a gaseous volume of oxygen of 2.07 x 10^{-4} cm^3 at 23°C and N.P. Cognizance was taken of the relative

oxygen capacitances of the liquid shell and the various plant organs and for convenience the value $2.07 \times 10^{-4} cm^3$ was assigned an electrical capacitance of 2,500μF.

The liquid shell capacitance itself was modelled not as a single 2,500μF capacitor but as five five-hundred μF capacitors connected at 300Ω intervals across the 1.8KΩ shell resistance (Fig.5.11). This was thought to give a truer representation of the stored oxygen by distributing the charge evenly throughout the liquid shell.

(b) Root

The availability of electrical capacitors permitted the simulation of only one centimetre of root.

At atmospheric concentration the volume of oxygen contained within the intercellular spaces of the root is given by:

$$\text{Vol. } O_2 = 0.2041 \, \pi \, r_r^2 \, L_r \, \epsilon_r \quad cm^3 \qquad (5.7)$$

where:

L_r = the length of the root (cm)

ϵ_r = the fractional porosity of the root.

(c) Stem

Stem volumes measured experimentally ranged from 0.08 to 0.20 cm^3; 0.10 cm^3 was chosen for modelling purposes. The volume of oxygen contained within the intercellular spaces of the stem is given by:

$$\text{Vol. } O_2 = 0.2041 \, V_{sm} \, \epsilon_{sm} \quad cm^3 \qquad (5.8)$$

where:

V_{sm} = the stem volume (cm^3)

ϵ_{sm} = the fractional porosity of the stem, taken as 10% (Chapter 3).

However, the volume of leaf tissue which could be represented on the analogue was limited by the availability of capacitors to about one-fifth that of the smaller plants. Therefore, the amount of stem was similarly reduced, and the stem volume finally modelled was 1/5 of 0.10, or 0.02 cm^3.

(d) Leaf

The volume of oxygen contained within a segment of leaf is given by an equation similar to 5.8.

The leaf was modelled as three one-centimetre segments of leaf base plus four two-centimetre segments of mid-leaf (i.e. eleven centimetres of leaf in all - Table 5.1).

C. RESPIRATION AND DIFFUSIVE RESISTANCE

Values of respiration rate and diffusive resistance were based on those obtained experimentally (see Chapters 3 and 7) and are given in Table 5.1. In order to programme the high rate of respiration in the stem two analogue segments were required.

D. GENERAL PROCEDURE

The basic programming details are listed in Table 5.1; any variations are given in the descriptions of the individual "experiments".

Oxygen was considered to enter the system uniformly over the mid-leaf (i.e. stomatal) region, and the stomatal resistance was considered negligible (see Chapter 6). Therefore, at the beginning of each "experiment" the atmospheric voltage (40V) was applied to each mid-leaf segment so that the oxygen concentration within the whole of the mid-leaf was that of the atmosphere - ie., 20.41%.

The system was allowed to equilibrate until the capacitors were fully charged; this was indicated by levelling of recorder traces monitoring R.O.L. and oxygen concentration. Respiration rate and C.O.P. were programmed using the constant current devices (p. 35 and Appendix 3). In all "experiments" C.O.P. in the root was programmed as 1.5% and the proportion of root respiration due to the low-porosity tissues was approximately 44% (see p.59). In some "experiments" C.O.P. was programmed in other organs also.

Submergence of the plant was simulated simply by disconnecting the

TABLE 5.1: ANALOGUE PROGRAMMING DATA USED IN THE SIMULATION OF THE OXYGEN RELATIONS OF SUBMERGED ERIOPHORUM PLANTS

Organ	Capacitance (μF)	Porosity (%)	Pore Space Resistance (Ω)	Respiration (ng $cm^{-2}min^{-1}$)
Mid-leaf (4x2cm segments; ie. 8cm)	33,000 33,000 33,000 33,000	60 60 60 60	100 100 100 100	250 250 250 250
Leaf-base (3x1cm segments; ie. 3cm)	33,000 33,000 33,000	60 60 60	50 50 50	235 235 235
Stem	4,700	-	-	400(2 x 200)
Root-shoot junction	-	see p.144	131	-
Root	4,000	20	31	112
Root wall	-	see p.148	680	-
Shell	2,500	-	1,800	-

NOTES:

a) 2,500μF = 2.07 x 10^{-4} cm^3 oxygen (see p.86).

b) 100Ω electrical resistance = 0.0993 x 10^5 s cm^{-3} diffusive resistance (Armstrong and Wright, 1976b).

c) C.O.P. in the root = 0.015 atm, with the respiration of 44% of the tissue being affected at this limiting value (see p.59).

FIG. 5.11 Analogue simulation of submerged Eriophorum plants: abbreviated circuit diagram to show the arrangement of the capacitors.
Segment boundaries are indicated by arrows and the segments representing the various organs are : 1, root ; 2, stem ; 3-5, leaf base; 6-9, mid-leaf.
Component values are given in Table 5.1

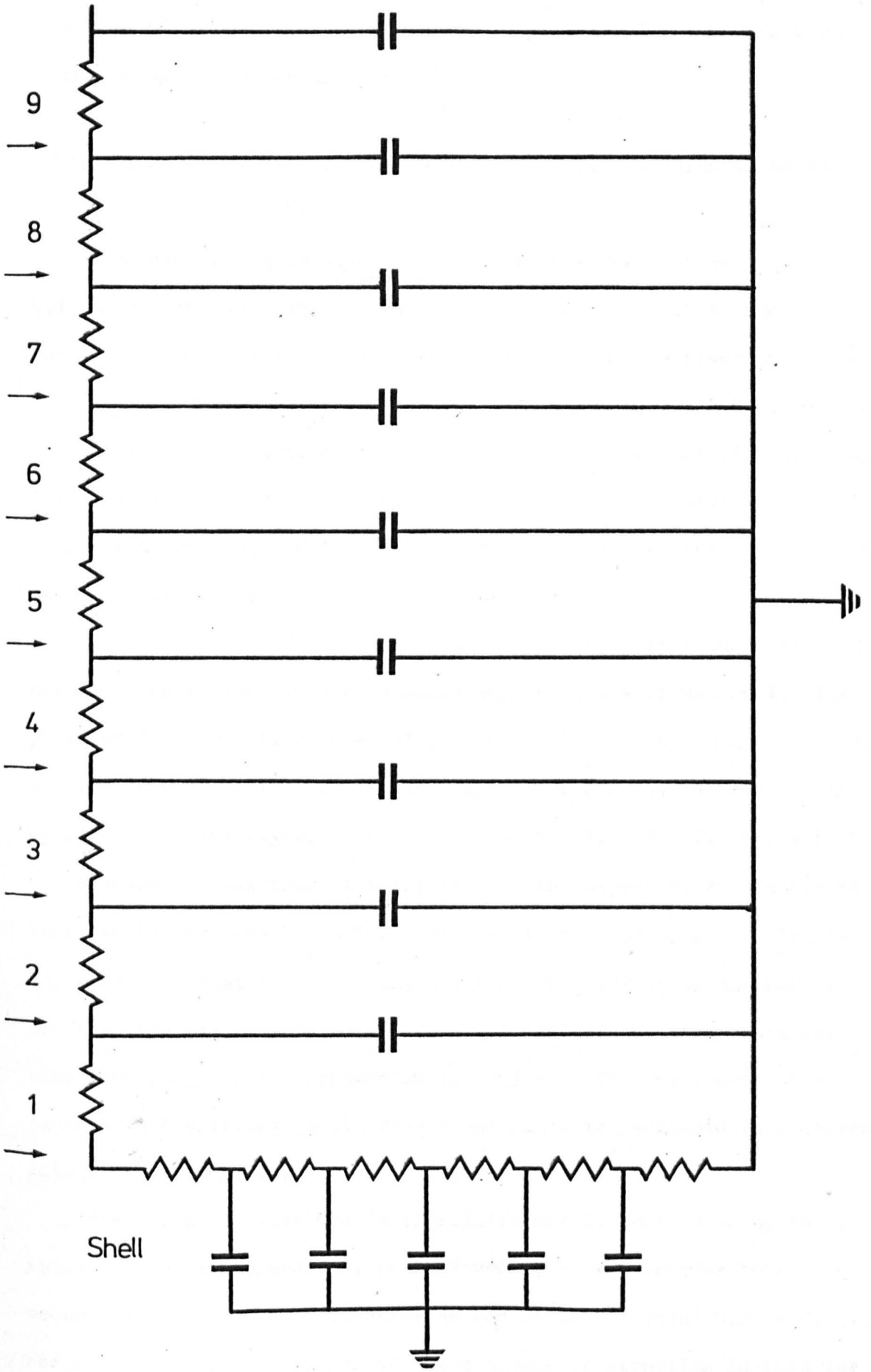
9
8
7
6
5
4
3
2
1
Shell

40V supply; after disconnection the capacitors discharged their "oxygen" to the respiratory devices and through the liquid shell. During this time the R.O.L. and the oxygen concentration at various points were monitored on a twin-channel recorder.

"EXPERIMENT" 1: EFFECT OF SUBMERGENCE ON R.O.L. AND INTERNAL OXYGEN CONCENTRATION

The programming details for this experiment were those given in Table 5.1 and the results, which show the manner in which R.O.L. and internal root oxygen concentration fell after submergence, are given in Fig.5.12.

The similarity between Fig.5.12a and Fig.5.3a, the R.O.L. vs time curve for a real plant, is apparent; both show the initial "lag" phase, followed by a linear fall in R.O.L., indicative of a constant rate of oxygen consumption, and finally the "tail" portion as the rate of oxygen depletion decreases.

A comparison of Figs.5.12(a) and (b) confirms that the fall in R.O.L. mirrors exactly that in the internal oxygen regime of the root. The point of departure from linearity, which marks the beginning of the "tail" portion in each of the two curves (Figs.5.12a and b), coincides with the decline in apical oxygen concentration to the 1.5% C.O.P. Prior to this "experiment" it was thought possible that the oxygen stored within the liquidshell may have had a "buffering action", causing a time lag between the onset of anaerobiosis in the plant and its effect on the R.O.L. trace. However, the result illustrated in Fig.5.12 indicates that this was not the case, and confirms the assumption (p. 78) that the occurrence of anaerobic centres in the living plant after submergence is reflected in a decreased rate of fall in R.O.L.

The onset of curvature in Figs.5.12a and b, corresponding to 1.5% apical oxygen concentration, is followed by a much sharper turn which occurs when the oxygen concentration has fallen to about 0.3 to 0.4%. This second feature is a function of the analogue construction in that the

FIG. 5.12 Analogue simulation of submerged Eriophorum plant

Radial oxygen loss (a) and apical oxygen concentration (b) as functions of time after submergence

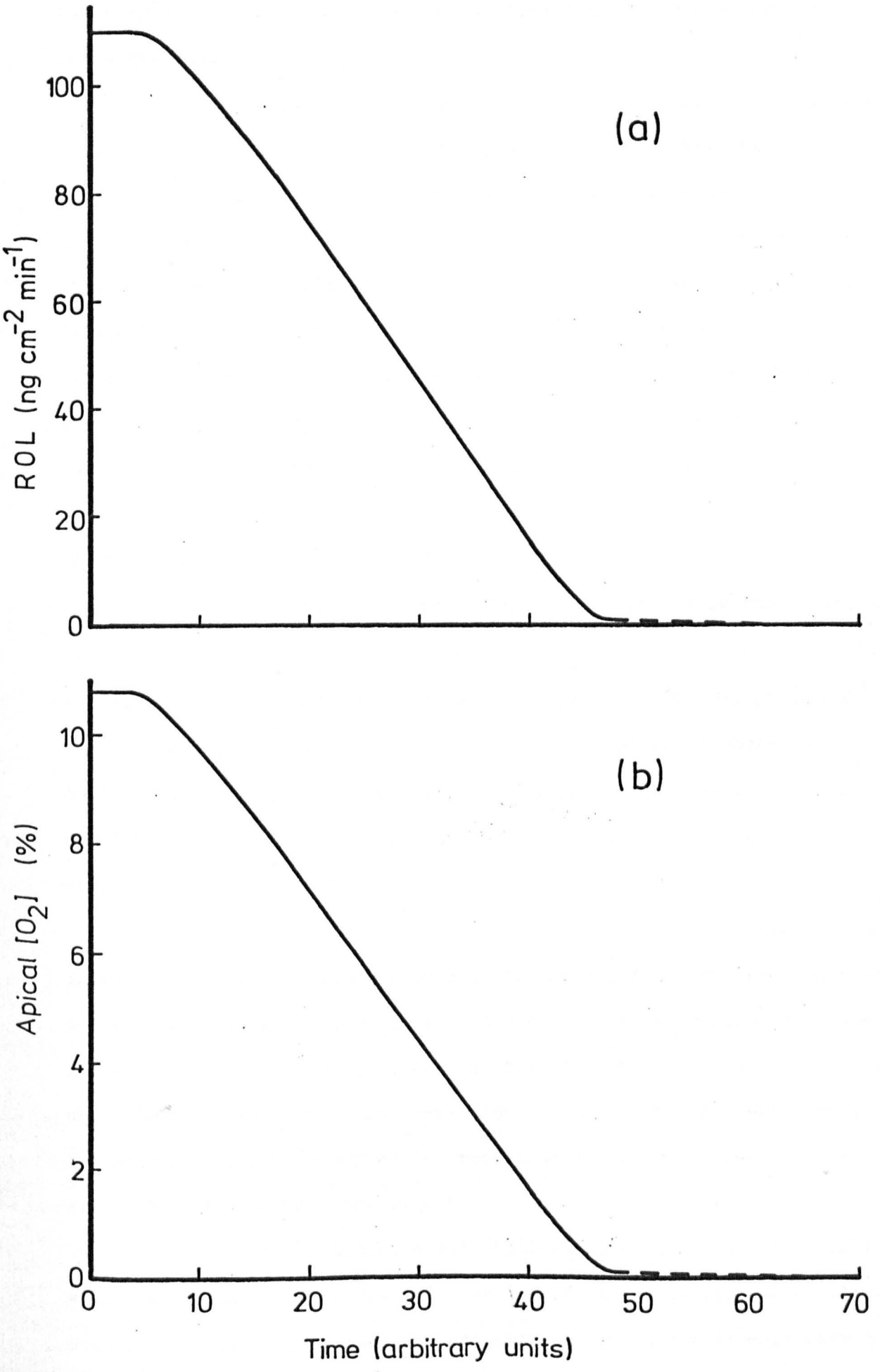
(a)
ROL (ng cm^{-2} min^{-1})
100
80
60
40
20
0
(b)
Apical [O_2] (%)
10
8
6
4
2
0
0
10
20
30
40
50
60
70
Time (arbitrary units)

constant current devices remain functional only above 0.3 to 0.4% O_2; below this value respiration varies in direct proportion to oxygen concentration.

The final portion of the curves in Fig.5.12 is a more or less linear fall to zero. Again, it was thought possible that in the plant the "shell oxygen" may have given rise to an apparent R.O.L. after the internal root oxygen regime had fallen to zero. The analogue result, however, contradicted this hypothesis. As with the living plants the precise time for R.O.L. and internal oxygen concentration to fall to zero was difficult to determine, but as far as could be ascertained from the analogue zero R.O.L. corresponded with zero internal oxygen concentration. This is in agreement with the assumption made in the experiments on living material (p.76)

"EXPERIMENT" 2: THE EFFECT OF CRITICAL OXYGEN PRESSURE IN THE STEM

In the previous "experiment" the fall in R.O.L. below the C.O.P. was more rapid than that associated with the living plant, (compare Figs.5.3a and 5.12a). In "Experiment" 1 critical oxygen pressure was programmed in the root only; it was thought that the rounder curves associated with living material may have resulted from the spread of anaerobiosis brought about by the occurrence of C.O.P.'s in tissues other than those of the root apex. This hypothesis was tested as follows.

The analogue was programmed as in Table 5.1 but C.O.P. was included in the stem also. To take account of the oxygen concentration gradient the stem experienced C.O.P. in two stages: the lower portion when the oxygen concentration in the leaf base fell to 3.0%, and the upper portion when the leaf base oxygen concentration reached 2.3%. In both portions of the stem approximately 60% of the respiring tissue was assumed to be affected by the C.O.P. (see p. 59)

The "tail" of the R.O.L. curve obtained with C.O.P. in the stem is shown in Fig.5.13b; Fig.5.13a is the "tail" of the R.O.L. curve without stem C.O.P. (i.e. Fig.5.12a) for comparison. Fig.5.13b is more akin to

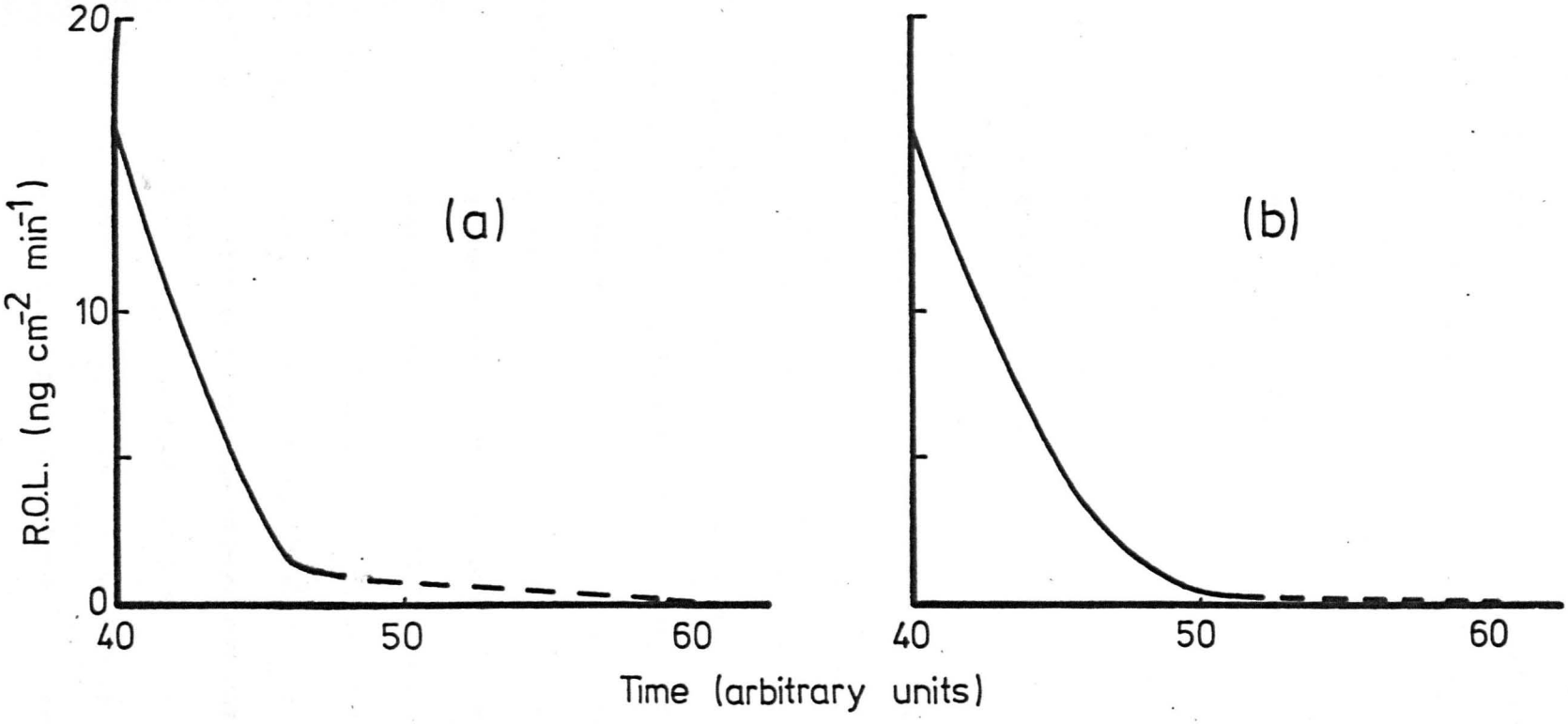

FIG. 5.13 Illustrating the effect of C.O.P. in the stem on the R.O.L. from a submerged Eriophorum plant

(a): Final portion of the R.O.L. curve with C.O.P. in the root only

(b): As (a) but with C.O.P. in the stem also

the R.O.L. curves obtained with living material (Fig.5.3), the sharp fall in R.O.L. being replaced by a less steep decline. This result suggests that in the submerged, intact plant the occurrence of the C.O.P. in the root apex marks the beginning of an upward spread of anaerobiosis throughout the denser tissues.

"EXPERIMENT" 3: THE OXYGEN REGIME WITHIN, AND OXYGEN LEAKAGE FROM, THE LEAF BASE

In Analogue "Experiment" 1 it was shown that the R.O.L. from the root of a submerged plant mirrored the apical oxygen concentration. It has also been suggested (p.80) that a fall in R.O.L. to zero may be indicative of oxygen exhaustion throughout the entire submerged plant. Using a cylindrical electrode passed over the aerial parts (see p.79) attempts to test this suggestion were made but, largely due to the difficulty in preventing the leaves touching the electrode surface, the experiments were not successful. Consequently, use was made of the electrical analogue to simulate this type of experiment, and to determine to what degree zero R.O.L. might indicate the exhaustion of oxygen from the aerial parts.

The analogue was programmed as in Table 5.1 but leakage from the top leaf base segment was included to simulate the electrode sink. A capacitance of 4,500μF (arbitrary value) was incorporated to represent a shell capacitance within the "leaf electrode", and 1.8KΩ to represent a shell resistance. Thus the experiment was similar in type(although not an exact simulation) to that using a living plant. Oxygen flux from the leaf and internal leaf oxygen concentration were monitored and the changes in these quantities after submergence are shown in Figs. 5.14a and b.

As in Fig.5.12 oxygen concentration and flux mirror each other. A comparison of Fig.5.14b with 5.12a shows that, so far as could be judged from the traces, the leaf base oxygen regime fell to zero slightly before

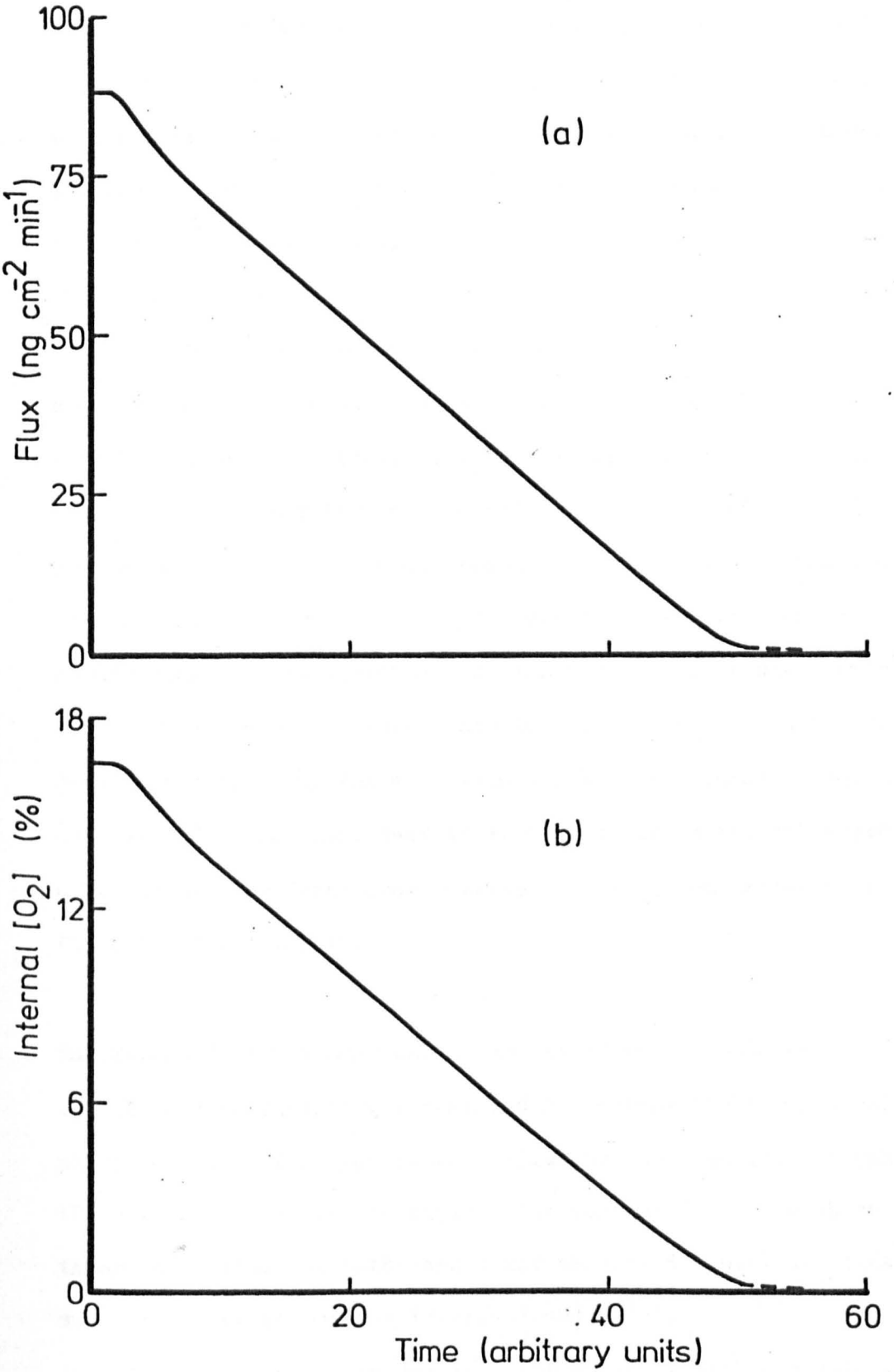

FIG. 5.14 Analogue simulation: oxygen flux from the leaf (a) and internal leaf oxygen concentration (b) following submergence

the R.O.L. from the root; this is the opposite from what might be expected if the oxygen concentration gradient between leaves and roots is taken into consideration. This discrepancy is attributable to the presence of leaf leakage (which was not included in "Experiment" 1), this additional sink contributing to a faster exhaustion time. However, the result indicates that no great time difference is to be expected in the fall to zero of the R.O.L. from the root and the oxygen regime within the aerial parts.

It may be seen from Fig.5.14 that the curves cease to be linear at about forty units on the time axis, coincidental with the turn in the root R.O.L. curve at the C.O.P. (Fig.5.12). Since C.O.P. was not programmed in the leaf it may be concluded that loss of linearity in the leaf curves is a result of the decreased rate of oxygen consumption in the root. In other words, the rate of oxygen depletion in the leaf is not dependent solely upon leaf respiration (and leakage) but also upon activities in other organs, e.g. the root. Similarly, organs such as the root seem to depend upon the leaf for an oxygen supply after submergence. For net movement of oxygen from leaf to root to occur in the submerged plant a concentration gradient must persist; this is demonstrated in the following "experiment".

"EXPERIMENT" 4: THE LEAF OXYGEN REGIME AFTER SUBMERGENCE

This "experiment" was designed to examine the changes which take place in the leaf oxygen regime following submergence. It was hoped that the results might help to explain the curious lag phase which was an important feature of both actual and simulated R.O.L. vs. time after submergence relationships (Figs.5.3 and 5.12).

The analogue was programmed in accordance with the data in Table 5.1. Oxygen concentration was monitored within the leaf base (middle segment), mid-leaf (bottom segment) and mid-leaf (top segment) (see Table 5.1). Since the leaf apex proper was not modelled the top mid-leaf segment has

been referred to as the "apex" for convenience throughout this discussion.

The manner in which the oxygen regime within the leaf fell after submergence at the three monitoring positions is shown in Fig.5.15. Table 5.2, which gives the oxygen concentrations within leaf and root at various times after submergence, clearly shows that the oxygen concentration gradient between leaves and roots persists.

From Fig.5.15 it can be seen that the rate of oxygen depletion varies with position along the leaf. Elsewhere in this thesis it is shown that in the unsubmerged plant the oxygen supply to the roots is probably entirely derived from that entering the leaves via the stomata immediately above the leaf sheath (see Chapter 6). Immediately after submergence the basal mid-leaf segment continues to be the major source of oxygen, as evidenced by the rapid rate of fall in internal oxygen concentration compared with the other regions of the leaf (Fig.5.15). A similar rate of oxygen decline in the leaf apex is prevented by the additional diffusive resistance (due to the increased diffusion path length) between this segment and the root (see p.125). Consequently the initial equality in oxygen concentration within the mid-leaf and apex is disrupted by the establishment of a concentration gradient between the leaf apex and the root (Table 5.2). Hence the apical region, which prior to submergence was insignificant as an oxygen source, now supplies oxygen to the more basal parts of the plant. This in turn is reflected by an increased rate of oxygen depletion in the apex, and a lowered rate in the mid-leaf (Fig.5.15a and b), resulting eventually in a re-equilibration of the leaf oxygen regime (Table 5.2).

It seems likely that the rapid re-adjustment of oxygen within the plant after submergence is the cause of the "lag" feature present in the R.O.L. vs. time relationships. Presumably oxygen consumption in the root by respiration and leakage is not sufficiently rapid to maintain the concentration gradient between leaf and root at its original value. Net flow of oxygen into the root from the aerial parts will prevent a fall in root oxygen concentration for a time after submergence, and R.O.L. will remain

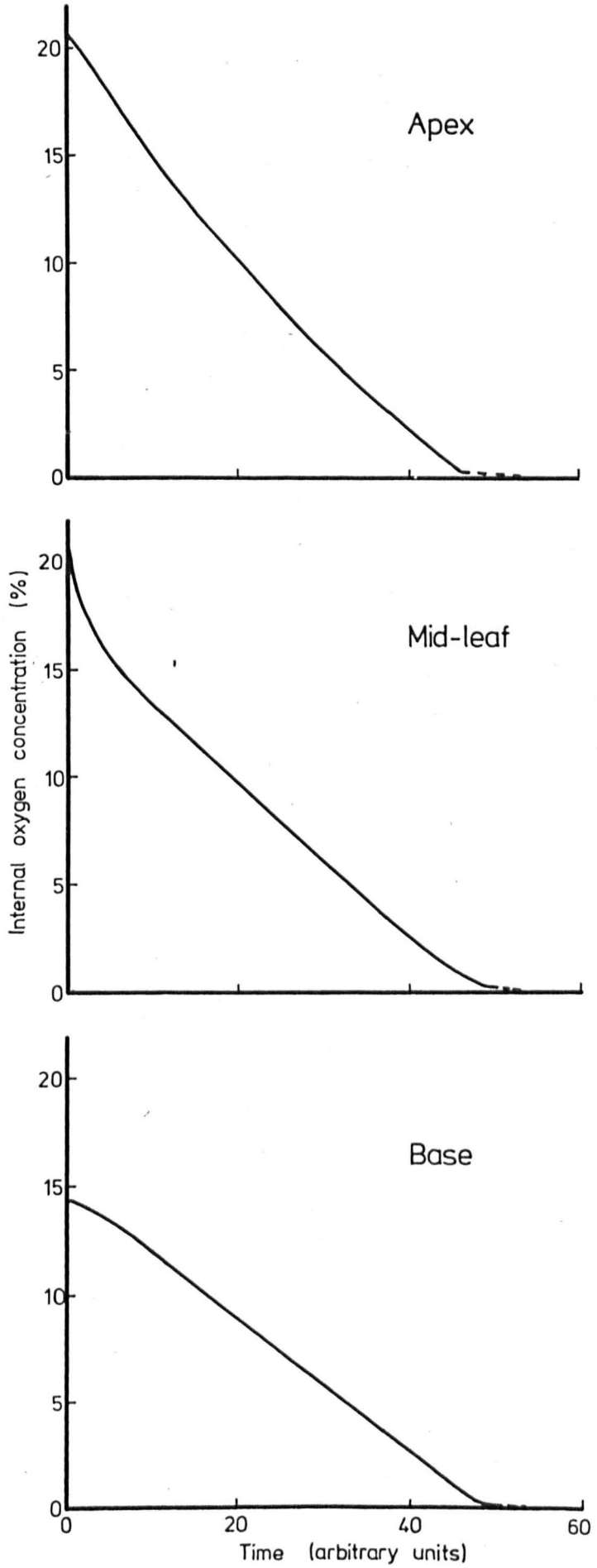

FIG 5 15 Analogue simulation : oxygen concentration within the leaf following plant submergence

TABLE 5.2 : ANALOGUE SIMULATION: INTERNAL OXYGEN CONCENTRATION IN LEAF AND ROOT AT VARIOUS TIMES AFTER SUBMERGENCE

Time (Arbitrary Units)	Internal Oxygen Concentration (%)			
	Root	Leaf Apex	Mid-leaf	Leaf Base
0	10.75	20.41	20.41	14.30
10	9.70	14.90	13.40	12.00
20	7.20	10.10	9.60	8.80
30	4.40	6.00	6.00	5.70
40	1.60	2.30	2.40	2.40

at the pre-submergence value. It is of interest to note that a slight "lag" feature is apparent also in the concentration vs. time relationship for the basal leaf segment (Fig.5.15c).

"EXPERIMENT" 5: THE "SHOULDER"; IMPLICATIONS OF DECREASED RESPIRATION AND INCREASED LEAKAGE FROM THE LEAF.

It was concluded earlier that the "shoulder" present in the R.O.L. curves for large plants (Fig.5.3b) was a result of significant oxygen leakage from the leaves. This conclusion was tested as follows.

The analogue was programmed according to the data in Table 5.1, but leaf leakage from each mid-leaf segment was included, and set initially at 250ng $cm^{-2}min^{-1}$. To enhance the importance of leakage in the depletion of the internal oxygen reservoir, respiration rate was lowered to 150ng $cm^{-2}min^{-1}$ in each leaf segment, and to 250ng $cm^{-2}min^{-1}$ in the stem.

The result is presented in Fig.5.16a, whilst Fig.5.16b is the normal curve (ie. Fig.5.12a) for comparison. A distinct 'shoulder' is present in Fig.5.16a, confirming the original conclusion that concentration-dependent oxygen leakage from the aerial parts was a cause of this feature.

III DISCUSSION

The primary aim of the investigation described in this chapter was to determine whether the gas-space system of E.angustifolium is able to store oxygen in sufficient quantity to satisfy respiratory demand during periods of curtailed external oxygen supply. During the study information was obtained concerning the manner in which the internal oxygen concentration falls after submergence of the plants in anaerobic medium, the dynamic relationship between the oxygen regimes of leaves and roots and the critical oxygen pressure for aerobic respiration in the submerged plant.

The two experimental techniques employed showed that in the dark at $23^{o}C$ the internal oxygen reservoir of Eriophorum falls to zero after only

FIG. 5.16 Analogue simulation: radial oxygen loss from a submerged plant

(a) Showing the "shoulder" produced by increased O_2 leakage from the leaves and reduced respiration in the stem

(b) Normal curve

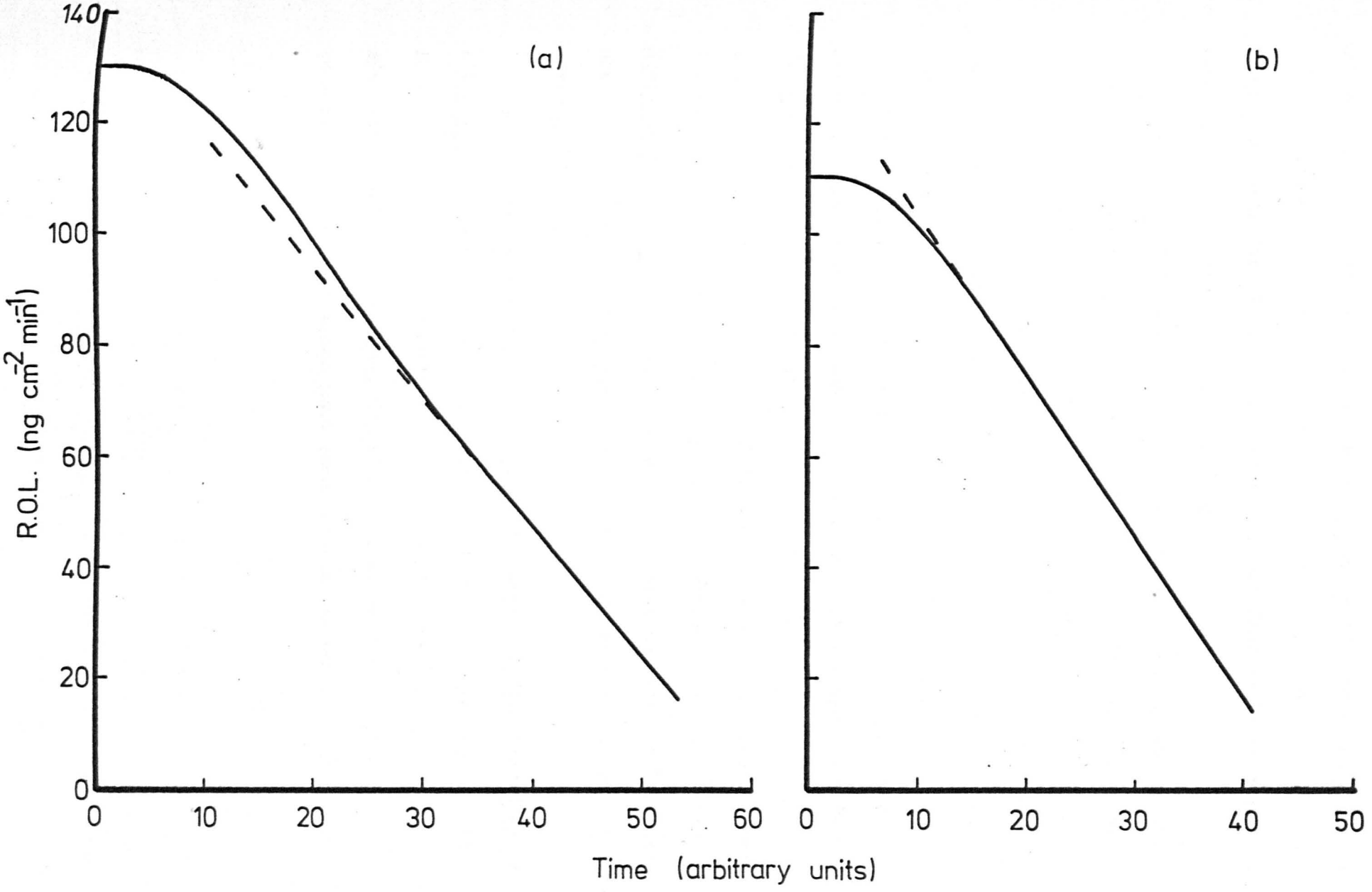
140
120
100
80
60
40
20
0
R.O.L. (ng cm^{-2} min^{-1})
(a)
(b)
0
10
20
30
40
50
60
0
10
20
30
40
50
Time (arbitrary units)

50 to 70 min submergence. The main contributing factor to the exhaustion of oxygen is aerobic respiration, which proceeds at a constant rate until the C.O.P.(about 2.0% in the root apex) is reached. The fall in internal oxygen concentration to the critical value took from 15 to 45 min only, depending on the size of the plants (Fig.5.7).

A second factor contributing to the exhaustion of oxygen was leakage from the leaves, though this was important only in the large plants.

Following submergence there is a complex re-distribution of oxygen within the plant body. A concentration gradient between leaves and roots persists, with the associated diffusive flow of oxygen into the roots from the leaves.

The evidence presented in this chapter is unfavourable to the hypothesis that aerenchyma may serve as a functional oxygen reservoir in E.angustifolium. It was thought that in species subjected to frequent inundation in their natural habitat (eg. saltmarsh plants) the reservoir function of aerenchyma may be of greater importance. Several plants of Spartina x townsendii H. and J.Groves were tested but the results were similar to those for Eriophorum, the internal oxygen store being exhausted after only about 55 min.

It must be concluded that in Eriophorum angustifolium (and Spartina x townsendii) aerenchyma does not serve an important oxygen-reservoir function. In times of inundation (unless conditions are such that photosynthesis boosts the internal oxygen regime - see Chapter 8) aerobic respiration in these species must cease within one hour.

CHAPTER 6

STOMATAL CONTROL OF INTERNAL AERATION

INTRODUCTION

It is generally accepted that stomata provide the most important route for the passage of gases into and out of the leaves of terrestial plants (eg. Thomas et al., 1973). Their variable apertures distinguish stomata from other ventilating pores (eg. lenticels) and many workers have investigated the physiological and environmental factors responsible for stomatal movements.

In addition, the extent to which stomatal movements influence the passage of gases has been extensively studied. However, a survey of the literature reveals that work has been restricted to considerations of water vapour and carbon dioxide fluxes; there is no investigation known to the author in which the control of oxygen entry by stomata has been studied.

In this chapter an account is given of work aimed at determining the extent to which the stomata of Eriophorum angustifolium influence the internal aeration of the plant. For convenience the investigation is described in three sections: firstly, experimental work is discussed; this is followed by a short theoretical treatment, and lastly, several confirmatory experiments are described.

I. EXPERIMENTAL

A. STOMATAL APERTURE

A non-destructive method to determine aperture dimensions was sought and it was found that the technique described by Sampson (1961) was the most convenient,especially since it could be used to examine moist leaf surfaces. In this procedure a primary (negative) impression of the leaf surface was obtained from which a transparent secondary (positive) replica was derived for microscopic examination. The primary impression was cast in silicone rubber monomer ("Silflo Dental Plastic", J. and S. Davis Ltd.,

Torrington Park, London, N.12). The liquid rubber was mixed with its catalyst (the amount of which determined the curing-time) and spotted onto the leaf surface. The minimum quantity of catalyst necessary to effect hardening produced the best results as it allowed sufficient time for the rubber to penetrate the stomata before setting. After hardening the rubber was carefully lifted away from the leaf surface with forceps and washed in detergent solution; it was then thoroughly dried to avoid "misting" of the positive impression. This was done by blotting the rubber and allowing it to stand in a P_2O_5 desiccator for 10 min. Clear nail varnish was then painted onto the impressed surface and dried in the desiccator for 15 min; if left for longer periods the varnish became brittle with a tendency to fracture on removal.

For examination the positive replica was placed, impressed surface uppermost, on a microscope slide and covered loosely with a coverslip attached to the slide by "sellotape". Sandwiching the impression between two slides as suggested by Sampson (1961) distorted the replicas. A replica of the lower surface of an Eriophorum leaf is shown in Plate 6.1.

B. PRELIMINARY OBSERVATIONS

1. Stomatal distribution and frequency

Epidermal impressions were taken at 1cm intervals along the upper and lower surfaces of intact E.angustifolium leaves and the stomata counted under the microscope. Stomata were found only on the abaxial surface and here there was a marked acropetal increase in frequency (Fig.6.1). There were never any stomata lower than 1-2 cm from the leaf base; above this they were relatively infrequent up to the end of the leaf sheath. Above the sheath stomatal frequency increased sharply until at 9 to 10cm from the leaf base it became fairly constant, at 9-10 x 10^3 cm^{-2}. Meidner and Mansfield (1968) reported a similar, though less marked, variation in stomatal frequency along leaves of Zea mays L.

PLATE 6.1: Epidermal impression of the abaxial surface of a leaf of *E.angustifolium* (x 2,090).

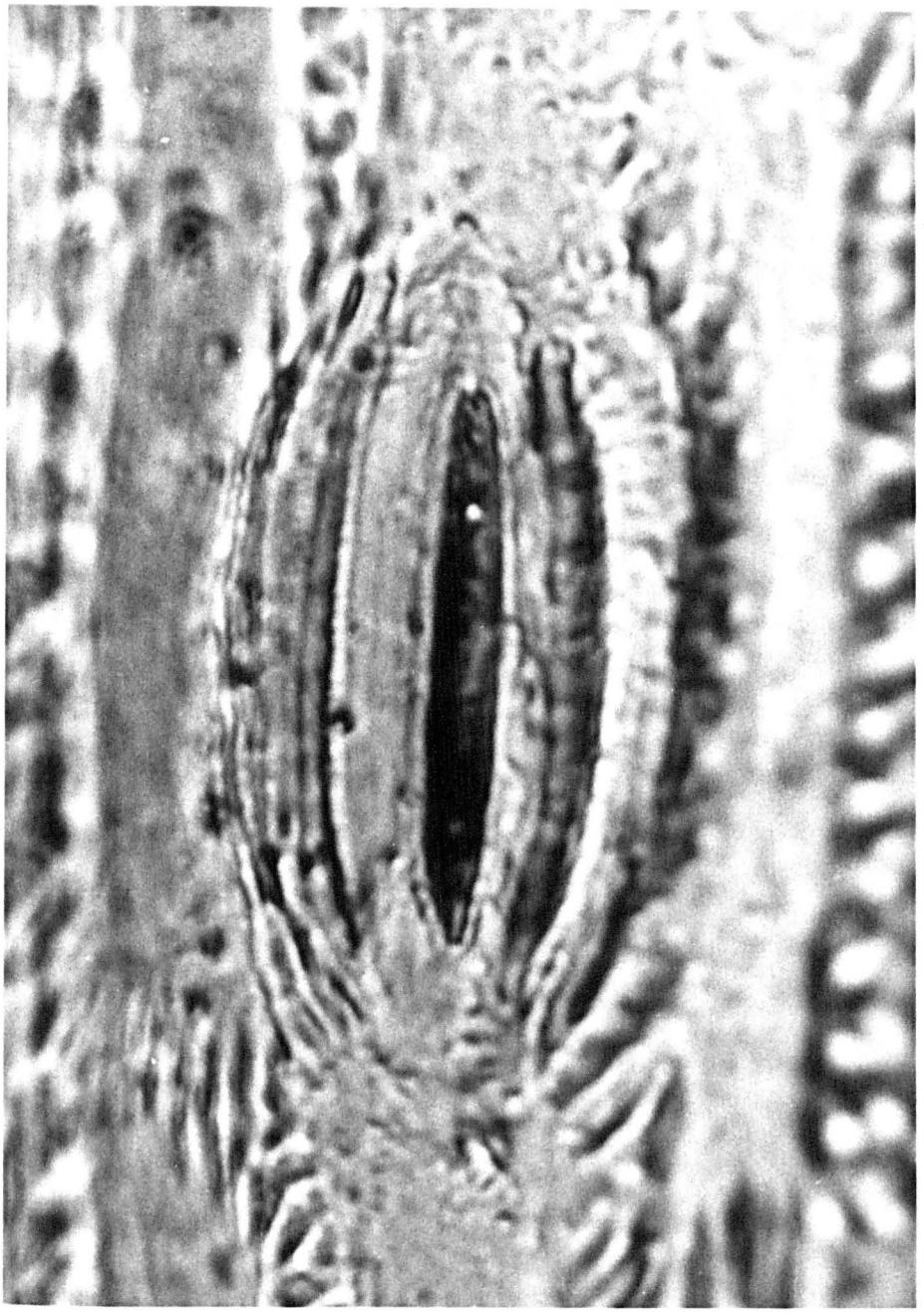

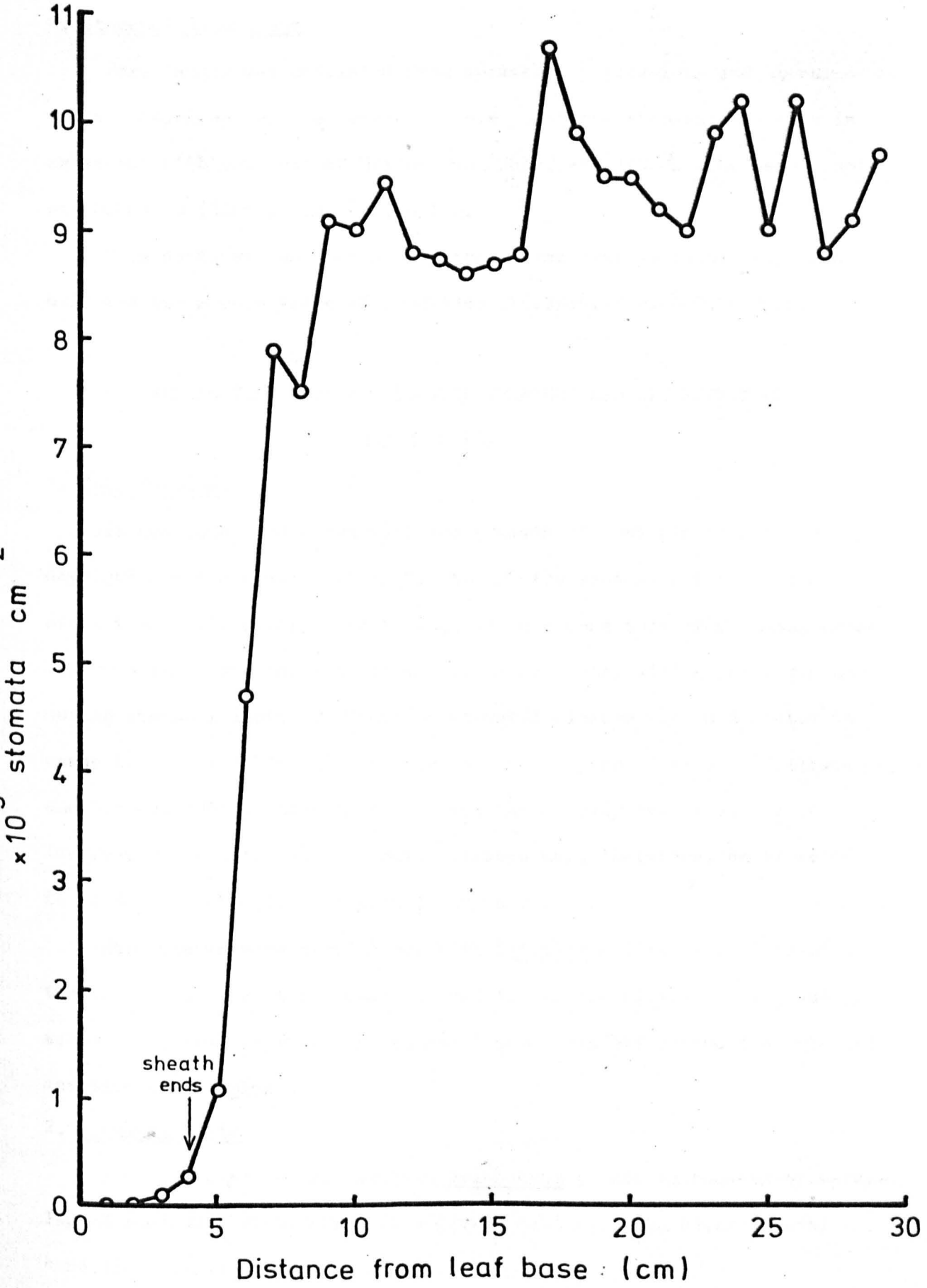

FIG. 6.1 Variation in stomatal frequency along the lower surface of a leaf of E. angustifolium.

2. Stomatal dimensions

Pore length was estimated from epidermal impressions and appeared to be independent of the degree of opening of the stomata; this is in agreement with comments of Meidner and Mansfield (1968). The mean length was 0.0032cm (32μm), S.D. ± 0.0001cm.

Pore depth was estimated from transverse leaf sections (e.g. Plate 6.2) and had a mean value of 0.00163cm (16.3μm), S.D. ± 0.00002cm.

C. DIURNAL VARIATION IN STOMATAL APERTURE AND ITS EFFECT ON OXYGEN ENTRY

1. Introduction

It has long been known that the stomata of most plants open during daylight hours and close at night (though the reasons for this behaviour are not entirely clear). It is logical to assume that if stomatal movements do influence internal aeration, oxygen entry will be at a minimum during stomatal closure. Complete stomatal closure may be a factor to cause the plant to depend upon the internal oxygen reservoir (Williams and Barber, 1961); this oxygen source has already been shown to be ineffective (Chapter 5). Stomatal closure may, therefore, be expected to lead to a sub-optimal internal oxygen regime.

Experiments were carried out with Eriophorum firstly to determine the degree to which the stomata closed during the diurnal cycle, and secondly to test whether such stomatal movements influenced the internal aeration of the plant.

2. Stomatal Cycle

Fourteen days before sampling Eriophorum plants in buckets of water-logged soil were transferred to a growth cabinet. The environmental conditions were:

Day length 16h (04.00 - 20.00)

Photosynthetically active radiant flux density 150μE m^{-2} s^{-1} at soil level.

PLATE 6.2: Transverse section through a stoma of E.angustifolium

(x 1,780)

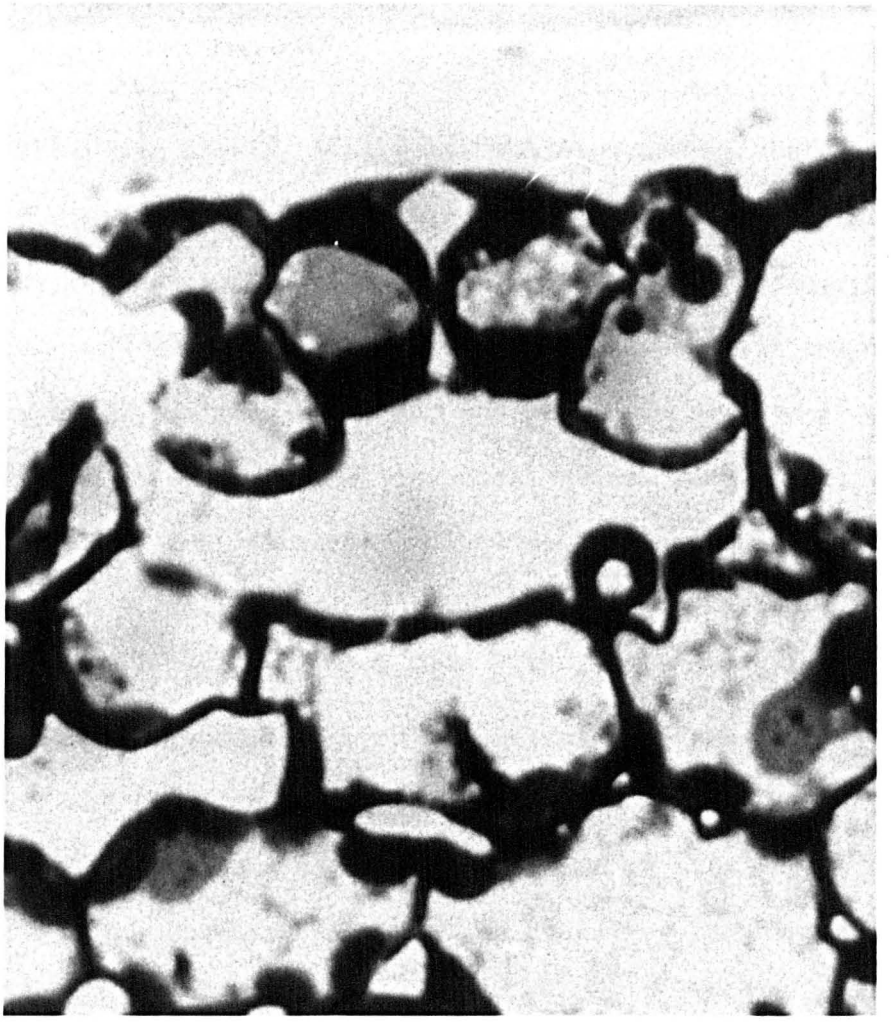

Day temperature $20^{\circ} \pm 1^{\circ}C$

Night temperature $18.5^{\circ} \pm 1^{\circ}C$

Relative humidity 80%

Stomatal aperture was measured over a 24h period by taking impressions of the lower leaf surface at two-hourly intervals. Samples were taken at 2cm above the sheath, 2 cm below the apex and at the mid-point of the leaf. The same leaf was used throughout the investigation and twenty stomata were measured at each point. The data has been expressed as mean pore width and the stomatal cycle at each of the three sampling positions, together with the "mean cycle"for the leaf, is shown in Fig.6.2.

Although there was much variation between pore widths at the three positions a distinct diurnal fluctuation is clear. Apertures ranged from a maximum of 9.2μm (mean 8.0μm) during the light period at 09.30 to a minimum of zero (mean 0.6μm) during darkness at 01.30. It is of interest that although some stomata were not measurably open during darkness at no time were all pores shut simultaneously.

A further point in connection with the stomatal cycle is the rapid rate of opening compared with that of closing, a phenomenon which has been described by other workers (eg. MacDowell, 1963). Mansfield and Heath (1963) have correlated rate of stomatal opening in Xanthium pennsylvanicum L. on exposure to light with the duration of the preceding dark period - longer nights producing faster opening. Stalfelt (1963) attributes this "readiness to open" of stomata to an endogenous increase in guard cell turgor during the dark period.

3. Stomatal cycle and oxygen entry

The following experiment was designed to test whether the marked decrease in stomatal aperture which accompanies darkness lowered the rate of oxygen entry into the Eriophorum plant. Changes in the internal oxygen regime were sought by monitoring R.O.L. from roots.

(a) Procedure

Several Eriophorum plants from the batch used in the previous experiment

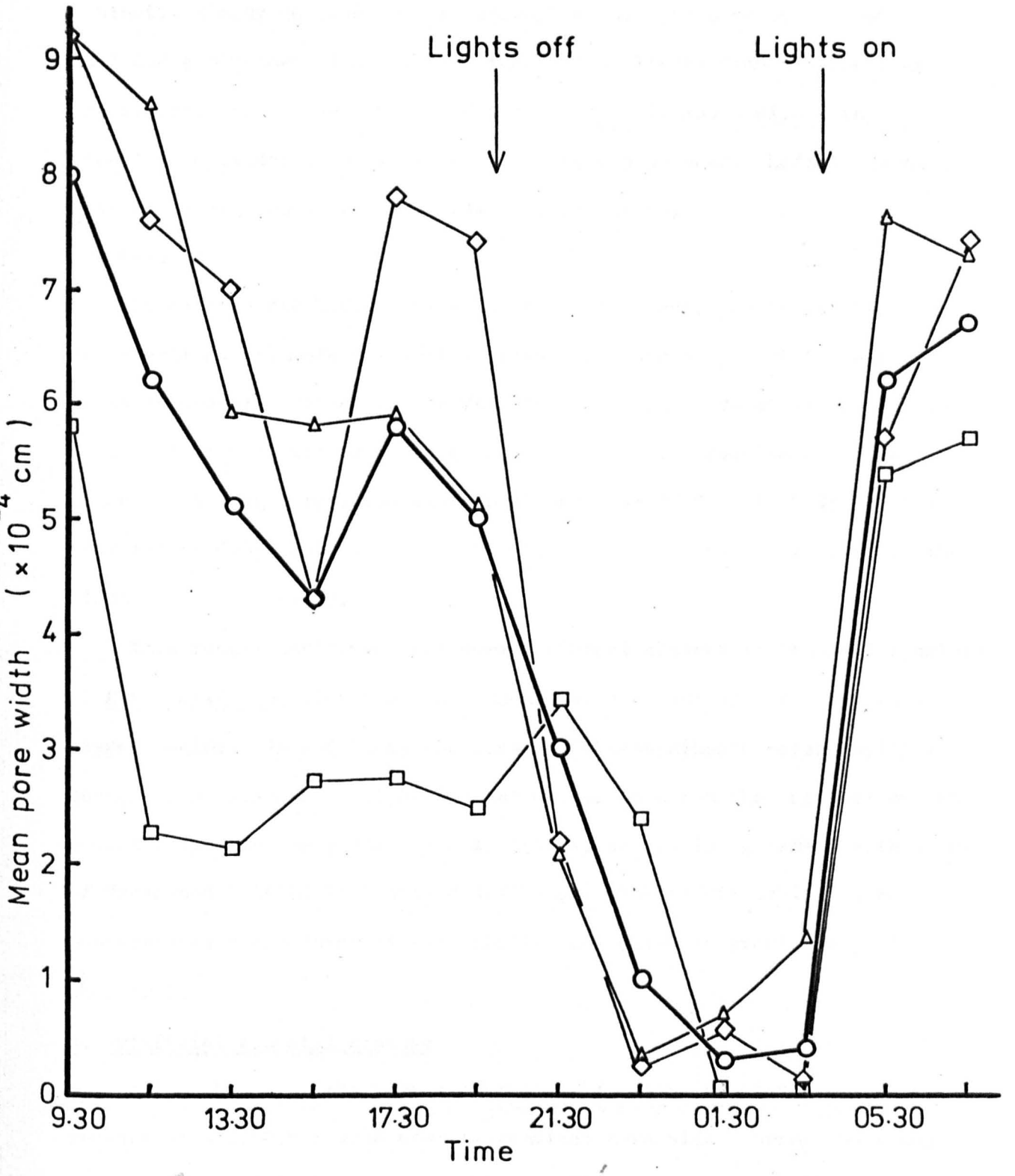

FIG. 6.2 Changes in stomatal aperture during 24hr under growth cabinet conditions.

(□) apex
(△) mid-leaf
(◇) base
(○) mean for leaf as a whole

were arranged for R.O.L. measurement (Chapter 2) inside the growth cabinet. Electrode leads passed through a small hole in the cabinet wall and environmental conditions remained unaltered from the previous experiment. Plants were arranged with only their roots within the measuring cylinders, the walls of which were blackened. Radial oxygen loss was continuously recorded over a 24hr period.

(b) Results.

At no time did R.O.L. decrease during darkness. On the contrary, in several experiments a slight increase corresponding with the onset of darkness occurred followed by a fall to the original value on re-illumination. This was attributed to a reduction in plant respiration rate caused by the day-night temperature change from 20°C to 18.5°C; such a temperature drop would decrease the effective diffusive resistance of the plants (see Chapter 7).

This result indicates that normal diurnal changes in stomatal aperture of E.angustifolium plants had an immeasurable effect upon the internal oxygen regime. In addition, the onset of photosynthesis accompanying the change from darkness to light did not appear to boost the internal oxygen concentration in the roots. These conclusions are in agreement with those of Greenwood (1967b) for mustard seedlings. The relationship between photosynthesis and internal aeration is considered in greater detail in Chapter 7.

4. Artificial stomatal closure

Although during the normal diurnal cycle mean stomatal aperture was reduced to only 0.6μm some stomata remained more widely open; this may have accounted for the observed unrestricted oxygen entry. It was thought that more uniform stomatal closure might be induced artificially. To this end two methods were adopted viz increasing the ambient CO_2 concentration and spraying with an antitranspirant.

(a) Increased CO_2 Concentration

Since Scarth (1932) suggested that light-dark responses of stomata

may be linked to photosynthetic removal, and respiratory production, of carbon dioxide there have been numerous reports that increased ambient CO_2 concentration brings about stomatal closure (eg. Freudenberger, 1940; Heath, 1948, 1950; Health and Milthorpe, 1950). The magnitude of the effect is enhanced at lower light intensities (Heath and Russell, 1954; Gaastra, 1959) and appears greatest at about 0.05 to 0.15% CO_2 (Gaastra, 1959; Pallas, 1965).

To test the effect of increased carbon dioxide plants were arranged for R.O.L. measurement within the growth cabinet. One hour after the dark period had commenced a quantity of solid CO_2 ("cardice") was introduced into the growth cabinet to bring the ambient concentration to about 0.15%. The required weight of "cardice" was calculated by the equation:

$$W_c = \frac{0.15 \rho_c t_1 V}{100\ t_2} \qquad (6.1)$$

where:

W_c = the required weight of solid CO_2 at temp. t_1 (g)

ρ_c = the density of gaseous CO_2 at temp. t_1 ($g\ l^{-1}$)

V = the internal volume of growth cabinet (l)

t_2 = the growth cabinet temperature (^oA)

No fluctuations in growth cabinet temperature were detected on introduction of the "cardice".

As in the previous experiment no decrease in R.O.L. was detected. Although the plants were subjected to apparently optimal conditions for stomatal closure (0.15% CO_2, darkness) any such closure was insufficient to affect oxygen entry into the plants.

(b) Effect of an Antitranspirant

Several compounds have been shown to cause stomatal closure when applied to leaf surfaces (Walker and Zelitch, 1963). Of these phenylmercuric acetate (P.M.A.) is notable in that it is effective at very low concentrations (5×10^{-5}M) (Zelitch, 1965) and that stomata may remain shut for as long as 14 days (Zelitch and Waggoner, 1962). Although P.M.A. is a

poison which inhibits photophosphorylation it is relatively immobile in the plant and does not affect growth significantly (Zelitch and Waggoner, 1962), though Shimshi (1963a) has reported some toxicity in Sunflower and suggests the need for caution when applying the chemical to easily wetted leaves.

The immobility of P.M.A. in the plant necessitates thorough coverage of the foliage to ensure treatment of all stomata. For this reason all but one leaf were removed by severing them approximately 0.5cm above their bases; cut ends were sealed with lanolin. Plants so prepared were arranged for R.O.L. measurement with the cut leaves below the level of the agar medium. They were placed in a fume cupboard and left to equilibrate for 2h in the light.

The P.M.A. solution was made up at 5.0×10^{-5}M in 0.05% v/v Triton X-100 wetting agent. This relatively low concentration of surfactant was used to prevent over-penetration by the P.M.A. and was that used with success by Shimshi (1963b). At zero time the leaves were thoroughly sprayed with the P.M.A. solution and R.O.L. was recorded continuously for several hours. Simultaneously epidermal impressions were taken at the apex, mid-region and base of the leaves to follow changes in stomatal aperture. At a point during the experiment the lights were extinguished to test for any photosynthetic effect.

The manner in which stomatal aperture and R.O.L. (expressed as diffusion current) changed after application of the P.M.A. is shown in Fig.6.3. The narrowness of the initial stomatal width (3.0μm) was probably due to the low intensity of the laboratory illumination (10μE $m^{-2}s^{-1}$).

The P.M.A. application was effective in reducing stomatal aperture to a mean of 0.2μm, and though few stomata appeared closed none had a pore width greater than 0.3μm. This narrow stomatal aperture remained unchanged throughout the experiment. Again, however, there was no detectable change in the internal oxygen regime apart from a slight initial fall in R.O.L. This was undoubtedly due to blockage of the stomata by wetting and

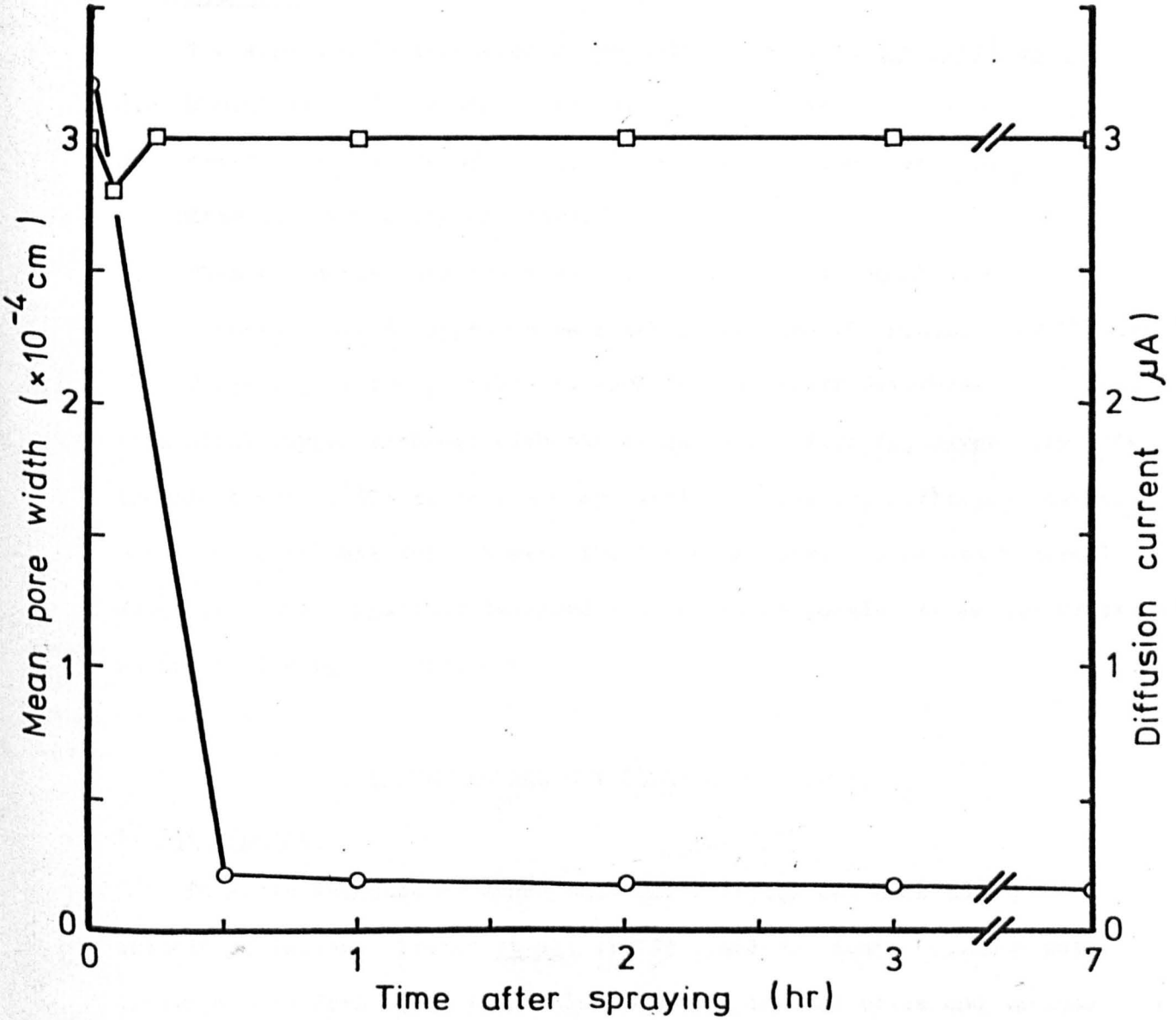

FIG. 6.3 Effect of P.M.A. application on stomatal aperture (o) and diffusion current (□)

the R.O.L. rose to its original value as the liquid dried from the leaf surfaces.

It was thought that at the narrow stomatal widths photosynthetic oxygen may have been retained within the plant, giving rise to elevated R.O.L. Darkening the plants produced no evidence of this, though it should be noted that rate of photosynthesis was likely to have been low under the low intensity illumination.

5. Discussion

The experiments described above indicate that in E.angustifolium:

1. Normal diurnal stomatal movements have no effect on oxygen entry.
2. Artificial closure of stomata to very narrow apertures (0.2μm) does not reduce oxygen entry.
3. Photosynthesis does not appear to enrich the internal atmosphere with sufficient oxygen to measurably increase the R.O.L. (see Chapter 7).

There may be two possible reasons for the ineffectiveness of stomata to control oxygen exchange with the atmosphere. Firstly, oxygen may enter the plant across the cuticle and epidermis. Secondly, sufficient oxygen may be able to pass through even the narrowest pores to maintain normal aeration. Investigations designed to test these possibilities are described in the following sections.

D. EPIDERMAL AND CUTICULAR OXYGEN ENTRY

1. Introduction

There is abundant evidence that water vapour can pass through the cuticle of leaves. Thomas et al. (1973) conclude that, "...some water is evaporated from the outer walls of most epidermal cells and escapes as vapour through the cuticle." However, they also point out that a thick cuticle is very efficient in preventing water loss. Whilst the cuticle may or may not also offer a considerable resistance to oxygen transfer, it is likely that the aqueous phase in the epidermal cells themselves will

offer a substantially greater resistance than the stomatal path (Heath, 1969). Nevertheless, it was considered necessary to establish the significance of epidermal oxygen entry in Eriophorum.

2. Method

As in the P.M.A. experiments plants had all but one leaf removed before R.O.L. assay. When the oxygen diffusion current had equilibrated the entire lower leaf surface was coated with lanolin and changes in R.O.L. monitored. Since the leaves were known to be hypostomatous the R.O.L. after lanolining was assumed to be a function of oxygen entry across the cuticle and epidermis of the adaxial surface. Three methods of lanolin application were used, viz smearing the leaf with the fingers, application of a lanolin-coated paper strip, and painting melted lanolin onto the leaf. Experiments were carried out in the dark.

3. Results

It can be seen from table 6.1 that results varied according to the method of lanolin application. When the lower leaf surface was efficiently coated by painting, R.O.L. fell to zero. From this it may be concluded that if oxygen diffusion across the adaxial epidermis was occurring its magnitude was small and by no means sufficient to maintain adequate internal aeration. The other methods of lanolin application apparently left sufficient numbers of unblocked stomata in communication with the atmosphere to allow considerable oxygen entry. The likelihood that the number of such stomata was small suggests that few stomata are required to permit the entry of an appreciable quantity of oxygen. The next stage in the investigation was designed to obtain further information concerning the number of stomata required for adequate internal aeration.

E. THE NUMBER OF STOMATA REQUIRED FOR ADEQUATE AERATION

By blocking stomata in stages it was hoped to discover the approximate number of functional pores necessary to allow sufficient oxygen entry. Furthermore, it was hoped to demonstrate how the position of these

TABLE 6.1: THE EFFECT OF STOMATAL BLOCKAGE BY LANOLIN APPLICATION ON R.O.L.

Method of Lanolin Application	Diffusion Current (Untreated) (μA)	Diffusion Current (treated) (μA)	% Fall in Current
Smearing	1.60	1.05	34.4
Paper strip	1.58	0.37	76.6
Painting	1.50	0.00	100.0

stomata on the leaf might influence their ventilating efficiency. Two methods were employed.

1. Lanolin application

(a) Procedure

Plants with one leaf only were used and were immersed in agar medium to sheath level. The experiments were similar to those aimed at assessing cuticular oxygen entry, but differed in that the lanolin was painted onto the leaf in stages, beginning at the apex and working towards the base. Each experiment was carried out in the dark.

(b) Results

Diffusion current varied with the extent of lanolin application as shown in Fig.6.4. Progressive stomatal blockage had no effect until relatively few functional stomata remained. Further lanolining reduced R.O.L. and complete coverage caused R.O.L. to fall to zero.

The results of the previous experiments suggested that few stomata were required to maintain normal internal aeration in Eriophorum; it is now possible to make an approximation of the number required. From Fig.6.4 it can be seen that a normal oxygen regime is provided by approximately 1.0cm exposed leaf immediately above the sheath. Since the stomatal frequency in this region is about $500cm^{-2}$ (Fig.6.1) and the width of the experimental leaf was 0.4cm, the required number of stomata is as low as 200.

An approximation may be made also of the minimum number of stomata needed to support maximum respiration in the plant (ie. maintain the root apical oxygen concentration above the critical value). Assuming that the 1.76μA diffusion current from the untreated plant indicates a root apical oxygen concentration of about 15% (ie. the mean oxygen concentration in the root apices when the leaves are in air - Chapter 7), an apical concentration of 2.5% (ie. the C.O.P.) is indicated by a current of 0.3μA. This current occurs when about 0.1cm of leaf (about 20 stomata) remains exposed.

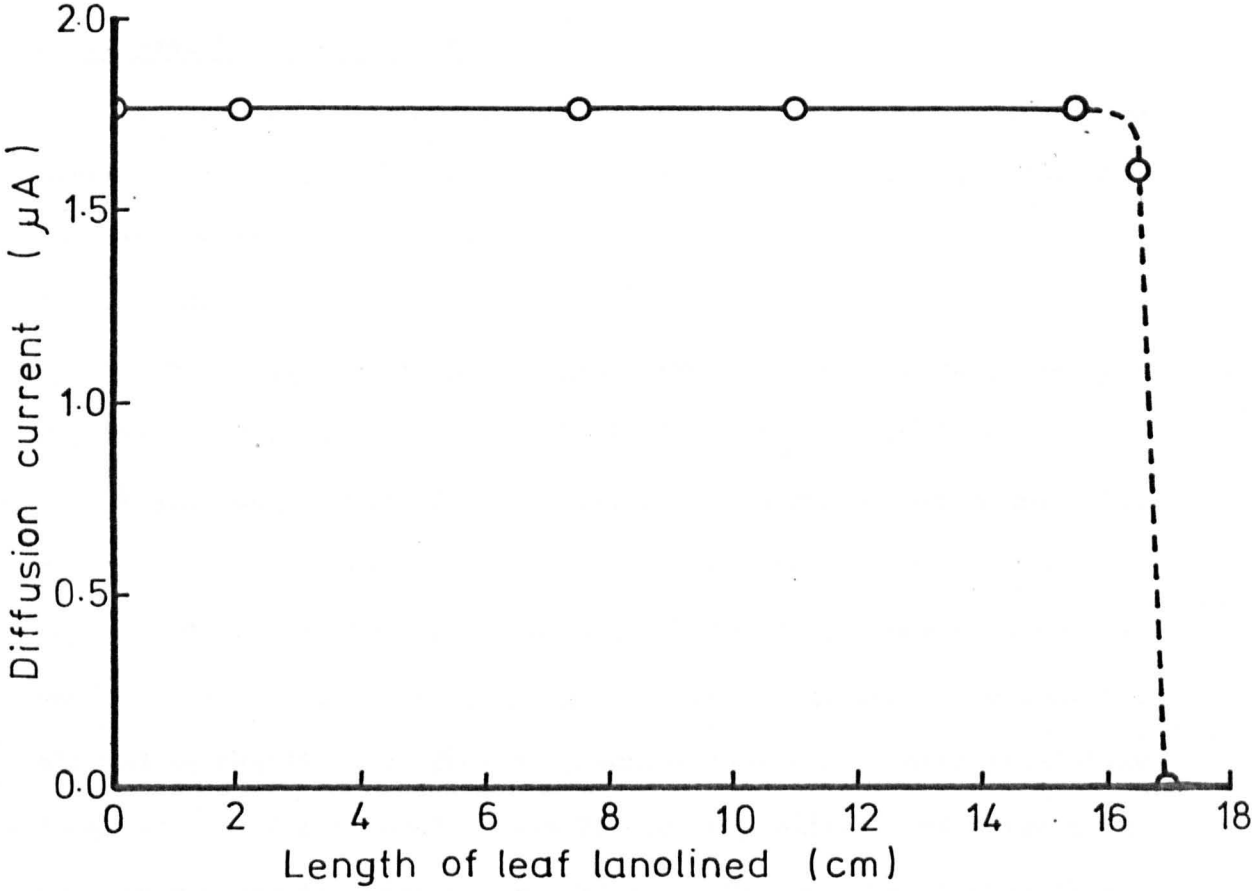

FIG. 6.4 Effect of lanolining on oxygen diffusion current. Single-leaf preparation, lanolined from apex to base. Leaf length 26·5 cm, submerged to sheath level (9·5 cm)

Again it must be stressed that the above estimates are very approximate due largely to the assumptions made concerning initial apical oxygen concentration and stomatal density. In fact, work described later in this chapter showed that the required numbers of stomata are appreciably smaller than the above values.

2. Progressive submergence

In the preceding experiments stomatal blockage was from the apex to base of the leaves. The following experiments tested the effect of progressive stomatal blockage in the opposite direction.

(a) Procedure

Both intact plants and single-leaved preparations were used and experiments were carried out in both light (15μE $m^{-2}s^{-1}$) and darkness.

Plants were arranged for R.O.L. measurements within a measuring cylinder as described in Chapter 5 and the level of the agar medium adjusted to the root-shoot junction. Whilst R.O.L. was continuously monitored the plants were submerged in stages (diffusion current being allowed to equilibrate after each submergence step) until completely immersed. In the case of single-leaved preparations relative stomatal frequency along the leaf was recorded at the end of each experiment.

(b) Results

(i) Single leaves in the dark: see Fig.6.5.

Unlike the result obtained in the previous experiment R.O.L. declined with submergence even though a large number of stomata (about 16cm of leaf) remained exposed; on complete submergence oxygen flux from the root fell to zero. There was a marked correlation between the fall in R.O.L. and the distribution of stomata; submergence of the sheath region, where stomata are infrequent, had little effect; submergence in the regions of high stomatal density markedly reduced R.O.L.

Assuming that an R.O.L. of 93ng $cm^{-2}min^{-1}$ from the untreated plant indicates a root apical oxygen concentration of 15% (p.148), a flux of 15.5ng $cm^{-2}min^{-1}$ indicates an apical C.O.P. of 2.5%. This flux occurs

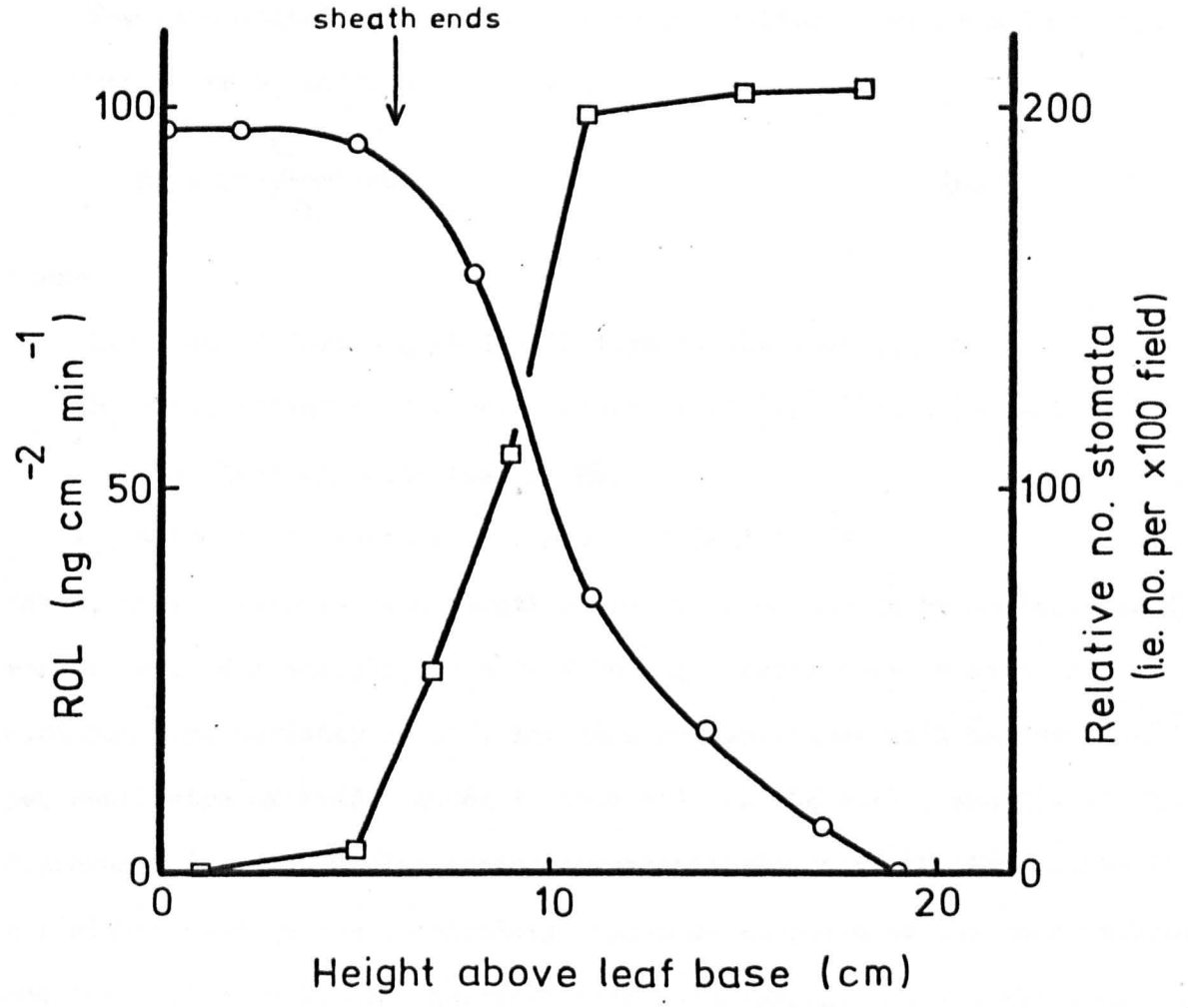

FIG. 6.5 Effect of leaf submergence on ROL in relation to stomatal distribution.

Single leaf, length 19·0 cm.

Experiment carried out in the dark.

(o) ROL

(□) Stomata

when about 4.6cm of leaf apex, and hence very many stomata, remain exposed. This substantial increase in the number of stomata required for maximum plant respiration (c.f. p.104) is undoubtedly due to the increased diffusion path length between the functional stomata and the root apex (see Chapter 7).

The non-metabolic resistance to oxygen diffusion along a leaf, R_l, is given by an equation similar to 2.10.

$$R_l = \frac{L_l}{D_e A_{xl}} \quad scm^{-3} \qquad (6.2)$$

where:

L_l = the diffusion path length through the leaf (cm)

D_e = the effective diffusion coefficient ($cm^2 s^{-1}$), dependent on leaf porosity (see p.126)

A_{xl} = the cross sectional area of the leaf (cm^2)

Hence, an increase in path length should be accompanied by an increase in resistance. For example, in a leaf having a cross section area of $0.0125cm^2$ and porosity of 50%, the lacunar resistance will be 780 s cm^{-3} per centimetre of leaf. Added to this will be the resistance due to the diaphragms (p. 150), whilst acting synergistically with the non-metabolic resistance will be the respiratory oxygen consumption of the leaf (p.124) and this effect will also increase with path length. Hence, although the previous experiments showed that few stomata were necessary to maintain the oxygen pressure in the root apex above the critical value, these stomata were situated at the base of the leaf (i.e. L_l was minimised). By submerging the leaf L_l was increased, with a corresponding increase in R_l. To maintain adequate aeration the rise in R_l had to be balanced by a decrease in stomatal resistance, and this was achieved by an elevation of stomatal number (p. 116).

(ii) Whole plants in the dark: see Fig.6.6.

The submergence of whole plants gave results similar to those for single leaves (see Fig.6.6A). However, the basic pattern was modified in

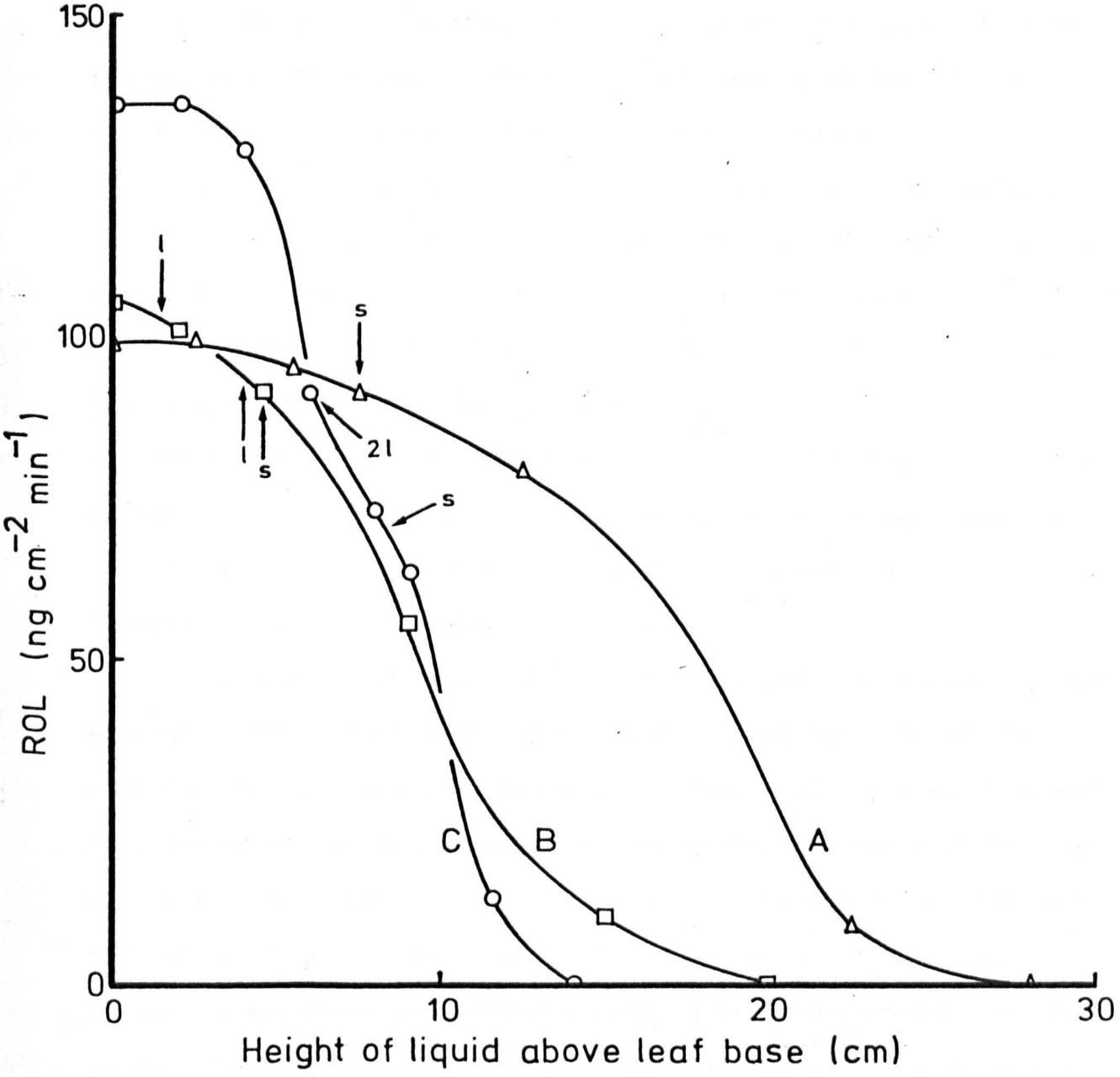

FIG. 6.6 Effect of leaf submergence on ROL from intact plants

Length of longest leaf (A) 28cm (B) 20cm (C) 14cm

Length of 'free' leaves indicated by (l)

End of sheath indicated by (s)

Experiment carried out in the dark

those plants having "free" leaves - ie. short leaves free from the main sheath (Chapter 3). Stomatal distribution along these leaves is similar to that along normal leaves, but their length is less than the ensheathed portion of the plants. In Fig.6.6B free leaves extend to 1.5cm and 4.0cm; submergence of the shorter masks the initial plateau, whilst submergence of the longer probably sustains the relatively steep decline in R.O.L. In Fig.6.6C the initial plateau is present but the simultaneous submergence of two free leaves extending to 6cm is reflected as a sharp fall in R.O.L. Further submergence to 8cm results in a slight decrease in slope, but inundation past the sheath (8.4cm) causes the R.O.L. to fall steeply again.

(iii) Single leaves in the light: see Fig.6.7

Illumination caused a major departure from the flux pattern obtained in darkness; in the latter stages of submergence the decline in R.O.L. was very much reduced and a tendency to plateau formation was apparent. As before R.O.L. ceased at total submergence.

The tendency to plateau formation was tentatively attributed to photosynthesis. It was thought that a "balance" may have been reached when sufficient leaf was submerged to contain photosynthetic oxygen and channel it to the roots (see Chapter 8) but yet the number of exposed stomata was such as to allow adequate carbon dioxide entry. Under these conditions a gradient of CO_2 would exist down the leaf. A similar oxygen gradient would prevent the escape of photosynthetic oxygen into the atmosphere, with the tendency for this gas to remain at a "constant" concentration within the leaf. This effect would naturally be transmitted to the root, where it would give rise to the R.O.L. plateau. Complete submergence of the leaf, so as to curtail the atmospheric CO_2 supply and reduce photosynthesis, would result in depletion of the internal oxygen regime and the fall in R.O.L. to zero.

(iv) Whole plants in the light: see Fig.6.8.

The effect of "free" leaves is apparent as in the corresponding dark experiment, but again a "photosynthesis plateau" occurs, between 18cm and

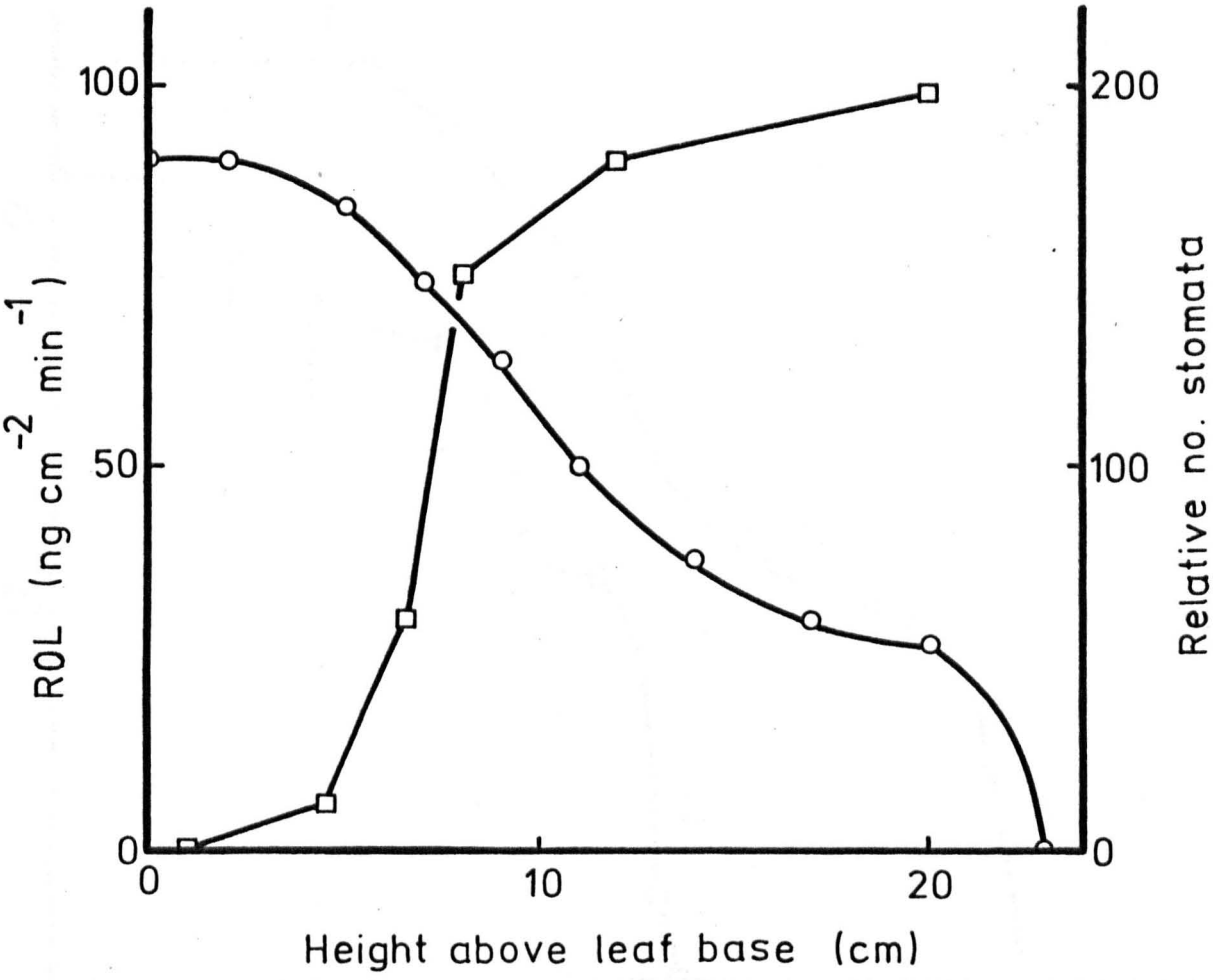

FIG. 6.7 Effect of leaf submergence on ROL in relation to stomatal distribution.

Single leaf, length 23·0 cm.

Experiment carried out in the light.

(o) ROL

(□) Stomata

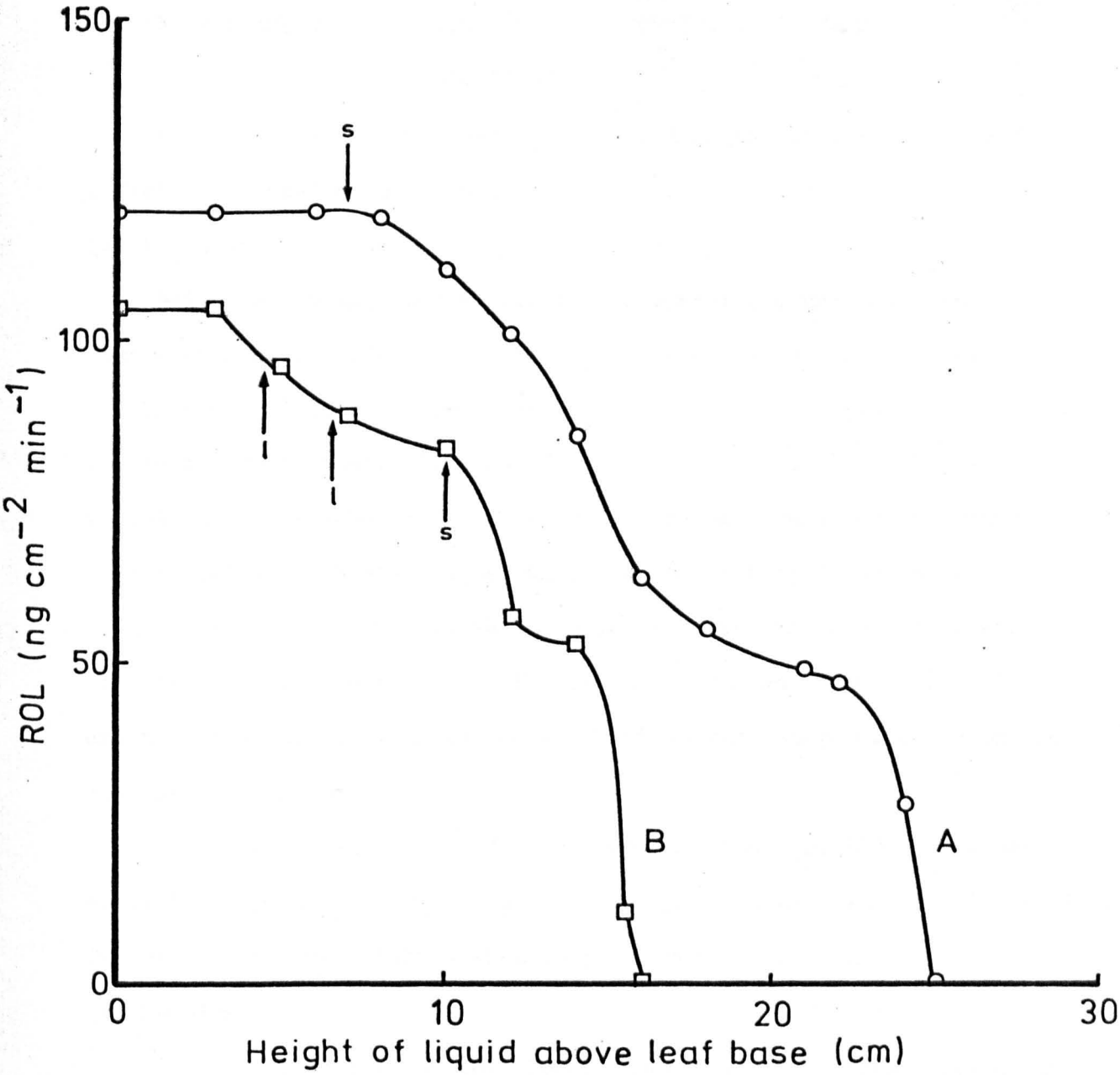

FIG. 6.8 Effect of leaf submergence on ROL from intact plants.

Length of longest leaf (A) 25cm (B) 16cm

Length of 'free' leaves indicated by (l)

End of sheath indicated by (s)

Experiments carried out in the light.

22cm submergence in curve A, and 12cm and 14cm in curve B.

F. THE EFFECT OF REDUCED STOMATAL NUMBER: ADDITIONAL EXPERIMENTS

The experiments described below were designed to test further the effect of reduced stomatal number upon internal aeration.

(a) Procedure

Both whole plants and single-leaf preparations were used and experiments were performed in the dark. In order to monitor R.O.L. a slight modification in procedure was necessary since plants were to be cut to the root bases. Instead of supporting the plants in bungs they were held at the stem region by clamped forceps. Only the experimental root passed through the bung in which it was held by loose cotton wool. In the case of whole plants the main leaves were cut to equal length and free leaves were removed. The cut leaf ends were sealed with lanolin and the level of the agar medium was kept approximately 0.3cm below the root-shoot junction.

The leaves were shortened in stages, and the equilibrium diffusion currents recorded both with the cut ends open and then sealed with lanolin. The experiments were halted when only the roots remained.

(b) Results

The effect of reduced leaf length upon the R.O.L. from a whole plant is illustrated in Fig.6.9. Cutting the leaves from 27cm to 12cm had no influence on R.O.L. with either open or sealed leaf ends. However, further cutting led to a divergence in the "sealed" and "open" curves, the former remaining constant, while the latter rose. The point of divergence is not clearly defined due to the amount of leaf cut, but results of the preceding experiments (eg. p.104) indicate that it might occur at a leaf length approaching that of the sheath rather than at the point indicated in Fig.6.9. In the "unsealed" series of measurements a further increase in R.O.L. took place at the next cut but in the "sealed"

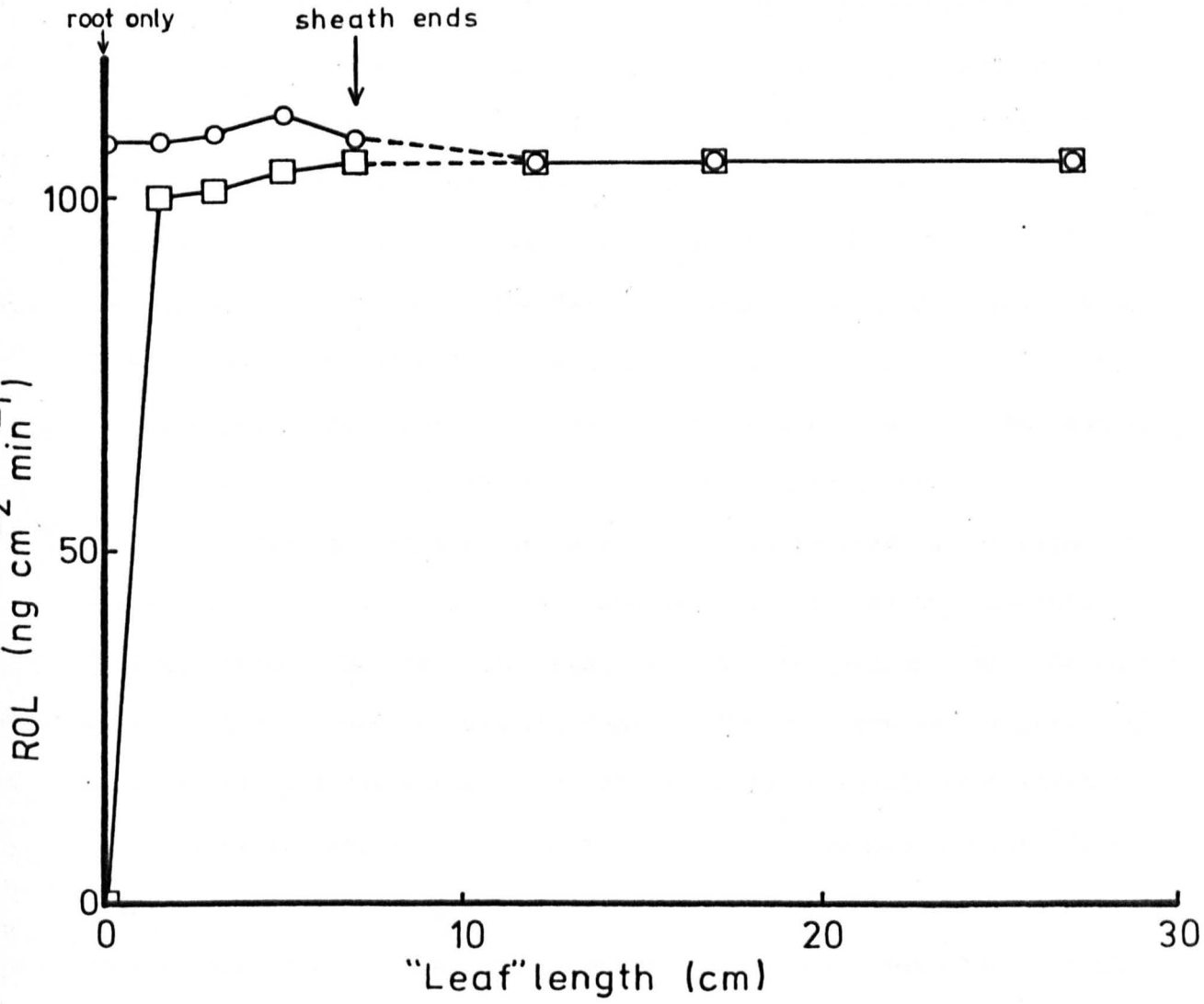

FIG. 6.9 Effect of reducing length of "leaves" on ROL

Intact plant in the dark

(□) Cut ends of leaves sealed

(o) Cut ends of leaves open

series there was a fall. Subsequently there was a slight fall in R.O.L. in the unsealed series. This was unexpected and could be attributed to the partial blockage of the lacunae by liquid which had risen between the leaves by capillarity. Similarly when only the unsealed root remained leakage of sap from damaged cells would seem to have prevented an anticipated rise in R.O.L. It was never possible to prevent the wetting of the cut leaf ends in the whole plants; in the single leaf preparations, however, the capillary effect did not occur and in later experiments, when the cut root base was dried with a gentle air stream, the continued increase in R.O.L. occurred as anticipated (Fig.6.10). In both Fig.6.9 and Fig.6.10 the R.O.L. in the "sealed" series continued to fall as the leaves were shortened and became zero when only the sealed root remained.

The procedure adopted in these experiments enabled stomatal number to be reduced without increasing the diffusion path length between the functional stomata and the root apex. In this respect the experiments are similar to those in which the stomata were blocked by lanolining (p.108), though the comparison must be made with caution since the cutting process also reduced respiratory demand. However, the experiments again demonstrate that few stomata are sufficient for adequate root aeration. In the unsealed series of measurements the open lacunae provided low-resistance access for oxygen when stomatal number was reduced by cutting to the leaf base; R.O.L. increased as the diffusion path length (and hence the internal diffusive resistance) between the cut leaf ends and the root apex was lessened. In the "sealed" series, on the other hand, oxygen entry was exclusively through the stomata, and a drastic reduction in stomatal number, brought about by cutting to the sheath region of the leaves, resulted in a lowering of R.O.L. Even so, the very few stomata present in the basal 1.5cm of the leaves of the whole plant (Fig.6.9, and see also Fig.6.1) were sufficient to maintain the R.O.L. at 95% of its original value. In the single-leaf plant (Fig.6.10) 2.0cm of leaf base maintained the R.O.L. at 76% of the pre-treatment level.

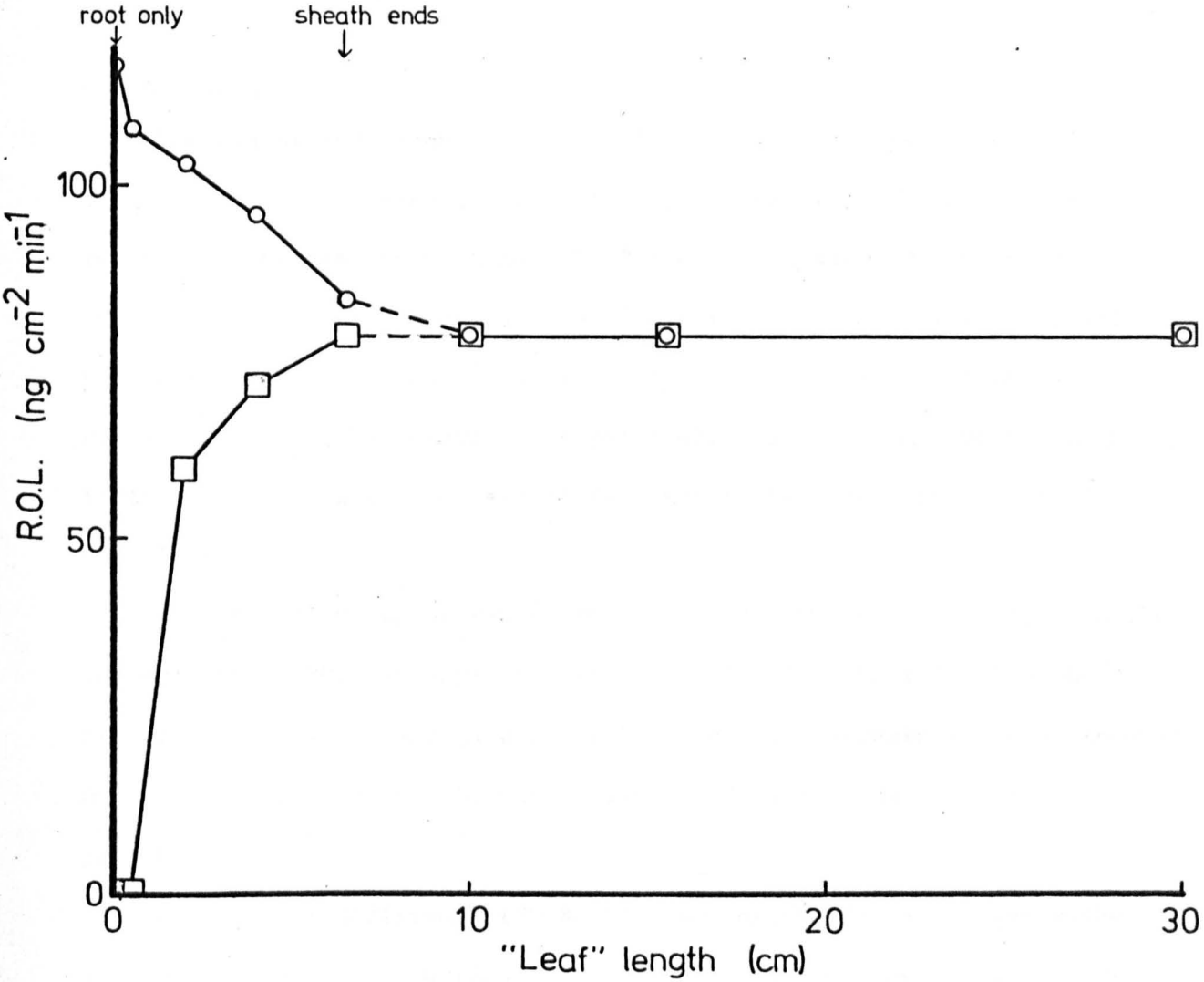

FIG. 6.10 Effect of reducing length of "leaf" on R.O.L.
Single-leaf plant in the dark
(□) Cut ends sealed
(o) Cut ends open

G. A MODEL

1. Introduction

In providing an explanation for the stomatal effects observed in the foregoing experiments it was found helpful to consider a model system. Using this model it was possible to simulate theoretically the cutting-sealing experiments described in the previous section, and to show why, under normal conditions, stomata do not restrict internal aeration.

2. Principle

The electrical circuit shown in Fig.6.11 represents a single 'leaf-with-root' system. Each segment (1 to 11) represents the diffusive resistances present in unit length of leaf (1-8), stem (9) and root (10 and 11). The diffusive resistances in leaf, stem and root are respectively indicated by R'_l, R'_{sm} and R'_r and are connected in series. Stomatal resistances, R'_{st}, are arranged in parallel. Values (ohms) were assigned to these resistances in an effort to express their relative magnitude in the plant.

The overall value of resistors in parallel varies inversely with the number; thus, 20Ω in segment 7 ($R'_{st'}$) represents the reduced number of stomata at the leaf base (see Fig.6.1). In leaf segments 1-6 the stomatal number is assumed constant, whilst segment 8 represents the astomatal leaf base.

A potential difference (20 volts), analogous with an oxygen concentration difference, is applied between the atmosphere and a sink external to the root apex represented by a connection to earth. Current flowing to earth is analogous with a radial loss of oxygen from the root, but is not quantitatively equivalent to loss to an electrode.

It is important to note that neither respiration nor photosynthesis is included in the model.

To simulate cutting in the model consecutive segments are omitted from

FIG. 6.11 Simulation of stomatal effects based on electrical theory.

The circuit represents the resistances present in unit segments of a single leaf-stem-root system.

Resistor values are as follows :-

R'_{st}	2 Ω	Stomatal resistances
$R'_{st}{}'$	20 Ω	
R'_{l}	10 Ω	Resistances within the leaf
R'_{sm}	40 Ω	Stem resistance
R'_{r}	30 Ω	Resistances within the root
$R'_{r}{}'$	50 Ω	

Segment boundaries are indicated by arrows.

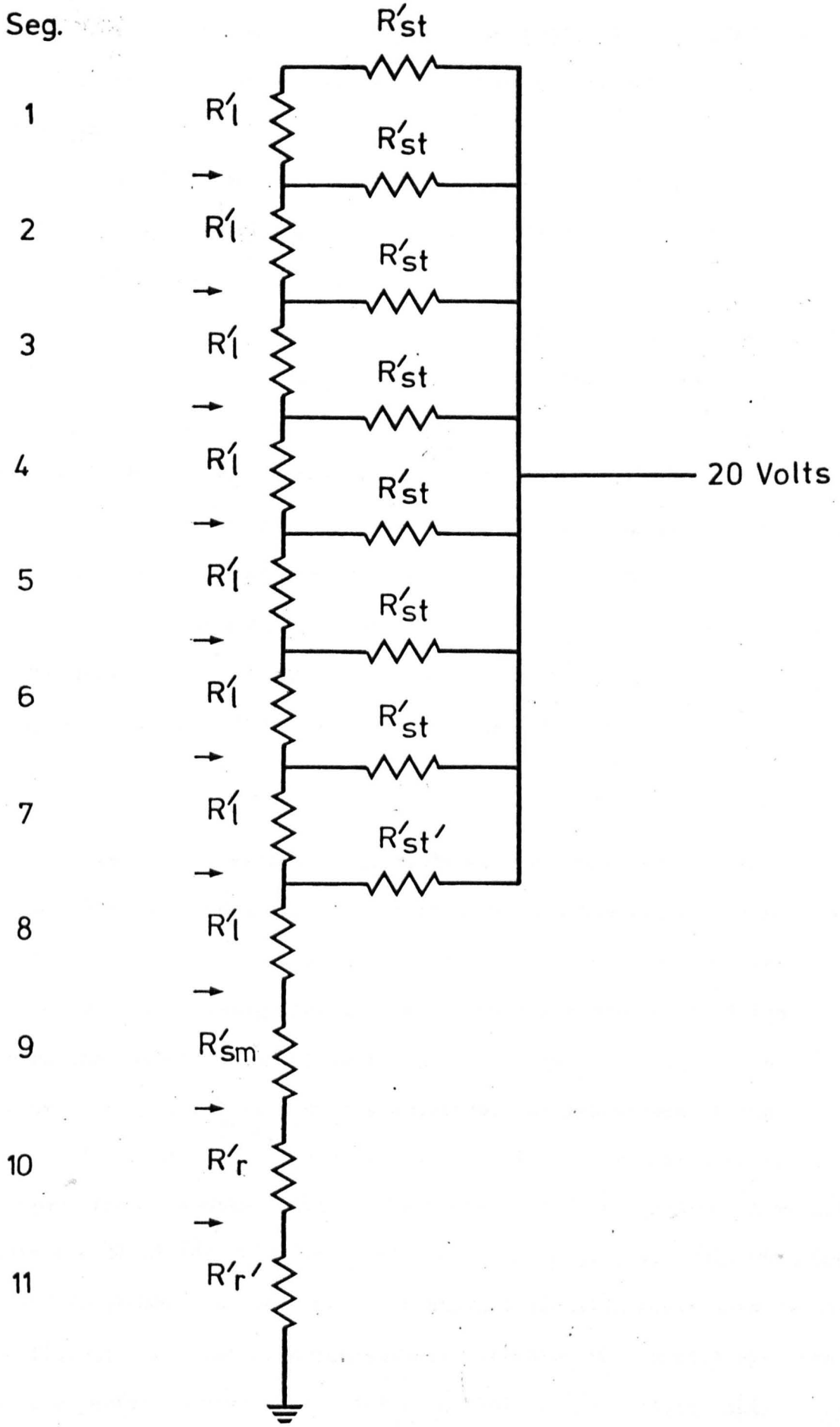
Seg.
1
2
3
4
5
6
7
8
9
10
11
R'st
R'l
R'st
R'l
R'st
R'l
R'st
R'l
R'st
R'l
R'st
R'l
R'st'
R'l
R'sm
R'r
R'r'
20 Volts

the calculations; in the "unsealed" condition the atmospheric potential is applied to the non-stomatal resistor currently at the top of the series, as well as to the stomatal resistors so long as these remained.

3. Results

The data obtained from the model is plotted in Figs. 6.12 and 6.13: "R.O.L." is shown in Fig.6.12 and total diffusive resistance at the various cutting stages in Fig.6.13.

A similarity between Fig.6.12 and the experimental curves, Figs.6.9 and 6.10, is apparent: the "sealed" and "unsealed" currents are coincident until two stomatal segments only remain. An explanation is provided by Fig.6.13. It can be seen that the total resistance of the system also remains unchanged in the "sealed" and "unsealed" conditions until only the two basal stomatal resistances are left.

This effect is a function of the parallel arrangement of the stomatal resistances. The total resistance, R, of a number, n, of stomatal resistances, each of the same value R_{st}, is given by:

$$R = \frac{R_{st}}{n}$$

If n is large R will be negligible and the magnitude of the overall resistance of the model will be little more than the value of the non-stomatal resistance in segments 8 to 11. This situation is directly comparable to the living plant. When stomata are present in large numbers the overall stomatal resistance to oxygen entry will be effectively zero even though, due to a narrow aperture, the resistance of the individual stomata may be considerable. In these circumstances oxygen transport from the atmosphere to the roots will be a function of resistances within the plant (eg. diffusion path length, see p.125). Only when the number of stomata has been much reduced will stomatal resistance become significant; under these circumstances variation in stomatal aperture may be expected to influence internal aeration. The relationship between stomatal number, pore width and internal aeration is considered further in

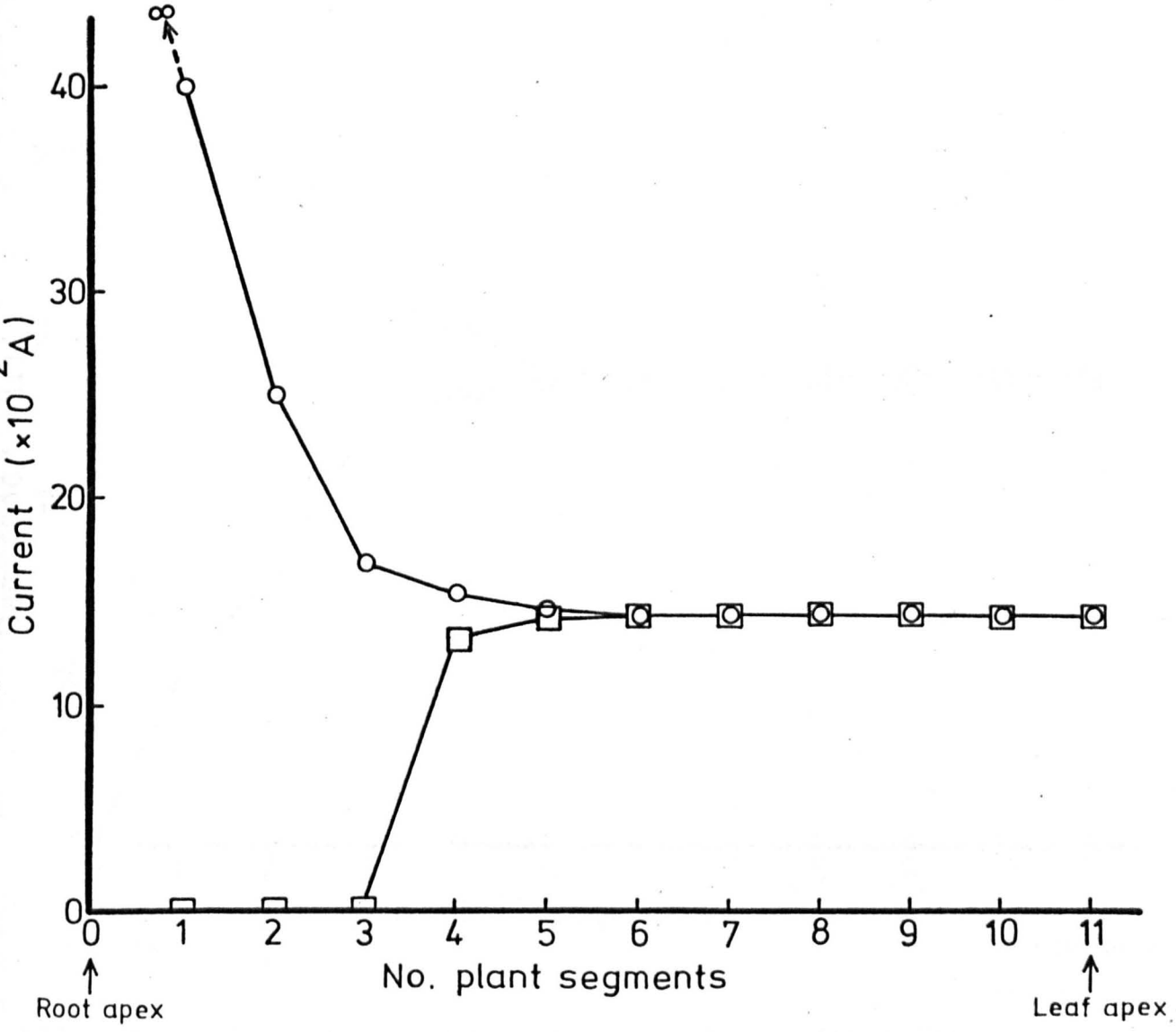

FIG. 6.12 Variation in ROL with plant length

Simulation based on electrical theory and the circuit given in fig.6.11

Single leaf in the dark.

(□) Cut end of leaf sealed

(o) Cut end of leaf open

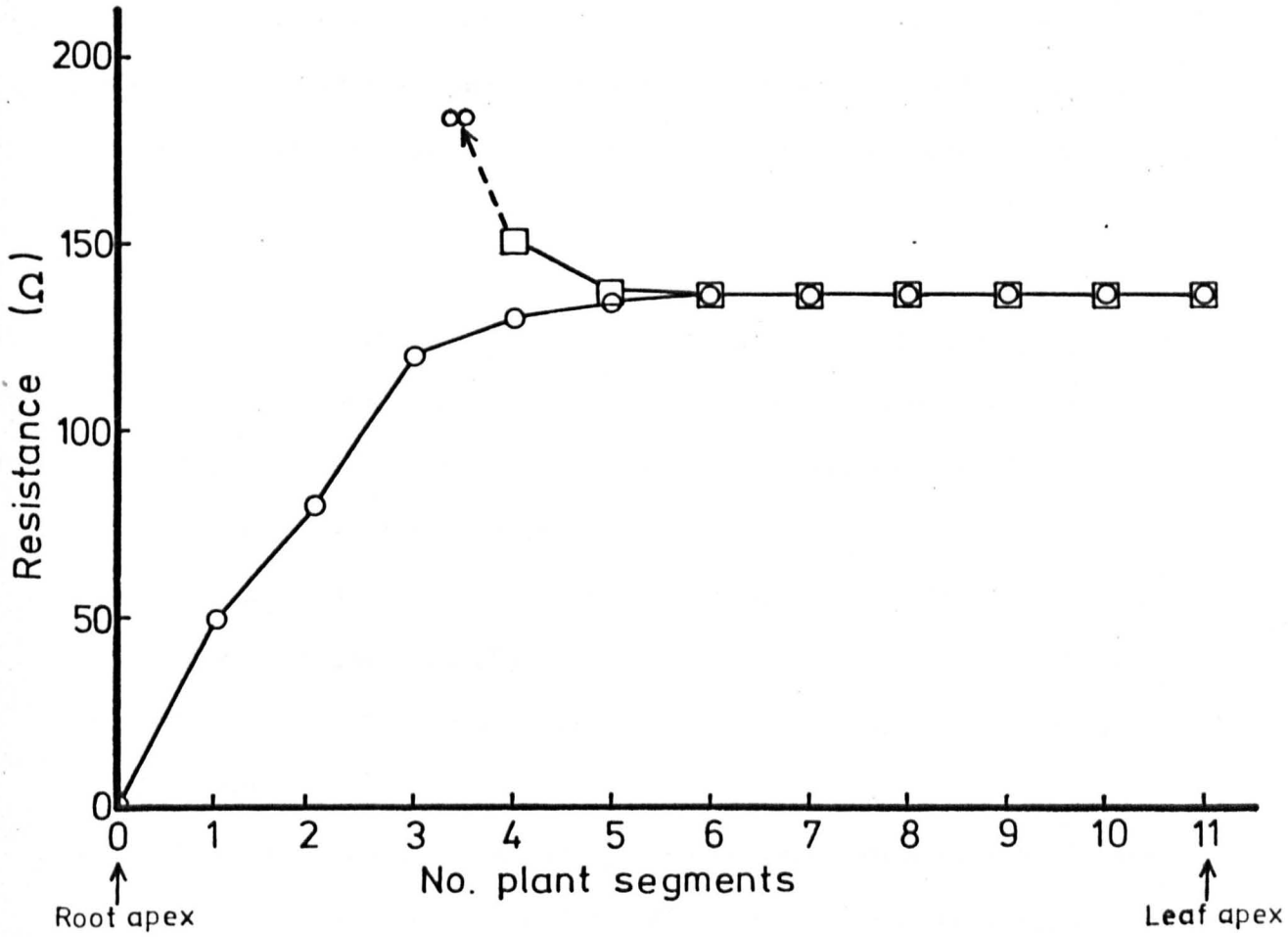

FIG. 6.13 Variation in resistance with plant length.

Simulation based on electrical theory and the circuit given in fig. 6.11

Single leaf in the dark.

(□) Cut end of leaf sealed

(o) Cut end of leaf open

the second and third parts of this chapter.

II THEORETICAL PREDICTIONS CONCERNING STOMATA AND INTERNAL AERATION

In the previous section it was demonstrated experimentally that stomata may influence oxygen entry providing their number has been much reduced. In this section theoretical predictions are made concerning the relationship between stomatal number, aperture and resistance and certain effects which these factors may have upon internal plant aeration are discussed.

A. THE CALCULATION OF STOMATAL RESISTANCE TO OXYGEN DIFFUSION

The resistance to gaseous diffusion through a single stoma is the sum of three components. These are the resistances offered by:

1. The stomatal tube itself
2. The extra diffusion path at the entrance and exit to the tube (the "end correction")
3. The boundary layer of still air at the surface of the leaf.

1. Tube resistance

Consider a tube of length L_{tb} and uniform cross sectional area $A_{x,tb}$. The resistance to oxygen diffusion along the tube, R_{tb}, is given by:

$$R_{tb} = \frac{L_{tb}}{D_o A_{x,tb}} \quad s\ cm^{-3} \qquad (6.3)$$

where:

D_o = the diffusion coefficient of O_2 in air ($cm^2 s^{-1}$)

The stomatal tube in Eriophorum more closely approximates in cross section to an elipse than to a circle (Plate 6.1). The cross sectional area at any point along the tube, therefore, is given by the formula for an elipse, ie:

$$A_{x,ep} = 0.5\ \pi\ x\ y \quad cm^2 \qquad (6.4)$$

where x and y are the lengths of the long and short axes respectively. Therefore, the quantity 0.5 x y is equivalent to r_{ep}^2, where r_{ep} is the radius of a circle of area equal to $A_{x,ep}$.

However, the variation in cross sectional area along a stomatal tube (see Plate 6.2) prevents the use of equation 6.4 per se. Instead some average value must be estimated for the cross sectional area of the tube and this was done using the equation recommended by Penman and Schofield (1951):

$$A_{x,st} = \pi\, r_{th} \sqrt{r_{th}\, r_m} \quad cm^2 \qquad (6.5)$$

where

$A_{x,st}$ = average cross sectional area of the tube (cm^2)

r_{th} = equivalent radius of the stomatal throat (cm)

r_m = equivalent radius of the stomatal mouth (cm)

Therefore, $r_{th} \sqrt{r_{th}\, r_m}$ is equivalent to r_{st}^2, where r_{st} is the radius of a circle of area $A_{x,st}$.

It was found that the throat width in E.angustifolium was always approximately half the mouth width, therefore both r_{th} and r_m could be calculated from measurements of the mouth width (y in equation 6.4); mean pore length (x in equation 6.4) had the constant value of 0.0032cm (p. 97).

2. End correction

When considering diffusion through a narrow tube such as a stoma resistance cannot be based solely upon the geometry of the tube since, due to the fan-like diffusion patterns at the entrance and exit to each pore, the concentrations of diffusing gases are not usually known at the exact ends (Meidner and Mansfield, 1968). Consequently diffusion through the tube must be treated as if occurring through a tube of the same cross sectional area but situated between the regions of known concentration. The extra path length involved is called the "end correction" and the diffusion rate across it may be calculated from Stefan's Law which states

that the diffusion rate, J, through small apertures is proportional to the diameter, d, of the aperture and the concentration difference, C, between the underside of the pore and a point some distance away from it. In the case of a stoma it may be expressed in equation form as:

$$J = 2\, D_o C\, d_{st} \quad g\ s^{-1} \qquad (6.6)$$

where d_{st} is the equivalent diameter of the stomatal pore (see p.113).

The diffusive resistance offered by the end correction, R_{end}, is given by:

$$R_{end} = \frac{C}{2D_o C\, d_{st}} = \frac{1}{2D_o\, d_{st}} \quad s\ cm^{-3} \qquad (6.7)$$

Since end corrections must be made at both ends of the tube the total end correction resistance is:

$$R_{end} = \frac{1}{D_o\, d_{st}} \quad s\ cm^{-3} \qquad (6.8)$$

3. Boundary layer

When an air stream passes over a flat surface such as a leaf a layer of still air - the boundary layer - occurs close to the surface. Gases diffusing across the boundary layer have normal diffusion coefficients, but beyond the boundary layer turbulent air flow occurs and gases are transported much more rapidly. Consequently, the resistance to gaseous diffusion offered by the turbulent air is negligible compared with that offered by the boundary layer, and the ambient oxygen concentration may be regarded as that at the outer surface of the boundary layer.

Several authors give equations defining boundary layer thickness, but since this quantity is difficult to determine - it varies in a complex manner with wind speed - these have been simplified by approximating leaf shape to a circle (e.g. Penman and Schofield, 1951; Heath, 1969; Meidner and Mansfield, 1968). In the case of a cyperaceous leaf, however, an expression involving linear dimensions is required. In the present study the approximation given by Nobel (1974) was used:

$$L_b \simeq 0.4 \sqrt{\frac{L_l}{V_a}} \quad \text{cm} \qquad (6.9)$$

where:

L_b = the thickness of boundary layer (cm)

L_l = the linear dimension of leaf in downwind direction (cm)

V_a = the air velocity (cm s^{-1})

and the factor 0.4 has dimensions $\text{cm s}^{-0.5}$

The dependence of L_b upon wind speed is apparent, and this is illustrated in Fig.6.14 for a leaf of width 0.5cm situated with the long axis normal to the wind direction. In the laboratory environment air currents were likely to have been minimised and subsequent calculations assume "still" air conditions (ie. V_a = 10cm s^{-1} - Powell, 1940; Nobel, 1974).

The diffusive resistance offered by the boundary layer, R_b, is given by:

$$R_b = \frac{L_b}{D_o A_l} \quad \text{s cm}^{-3} \qquad (6.10)$$

where:

A_l = the area of the leaf, or leaf segment (cm^2).

4. Total stomatal resistance

The three components of stomatal resistance described above act in series, hence their combined resistance is obtained by their addition.

The resistance offered by the stomatal tube and end correction is given by:

$$R_{tb} + R_{end} = \frac{L_{tb}}{D_o A_{x,st}} + \frac{1}{D_o d_{st}} \quad \text{s cm}^{-3}$$

and, if $A_{x,st}$ is considered as $\frac{\pi d_{st}^2}{4}$, the equation may be written as:

$$R_{tb} + R_{end} = \frac{1}{D_o A_{x,st}} \left(L_{tb} + \frac{\pi d_{st}}{4}\right) \quad \text{s cm}^{-3} \qquad (6.11)$$

The quantity $\frac{\pi d_{st}}{4}$ is the end correction term for gas entry and exit, and $\left(L_{tb} + \frac{\pi d_{st}}{4}\right)$ is the "effective length" of the stomatal tube.

The total resistance is given by adding the resistance of the boundary layer:

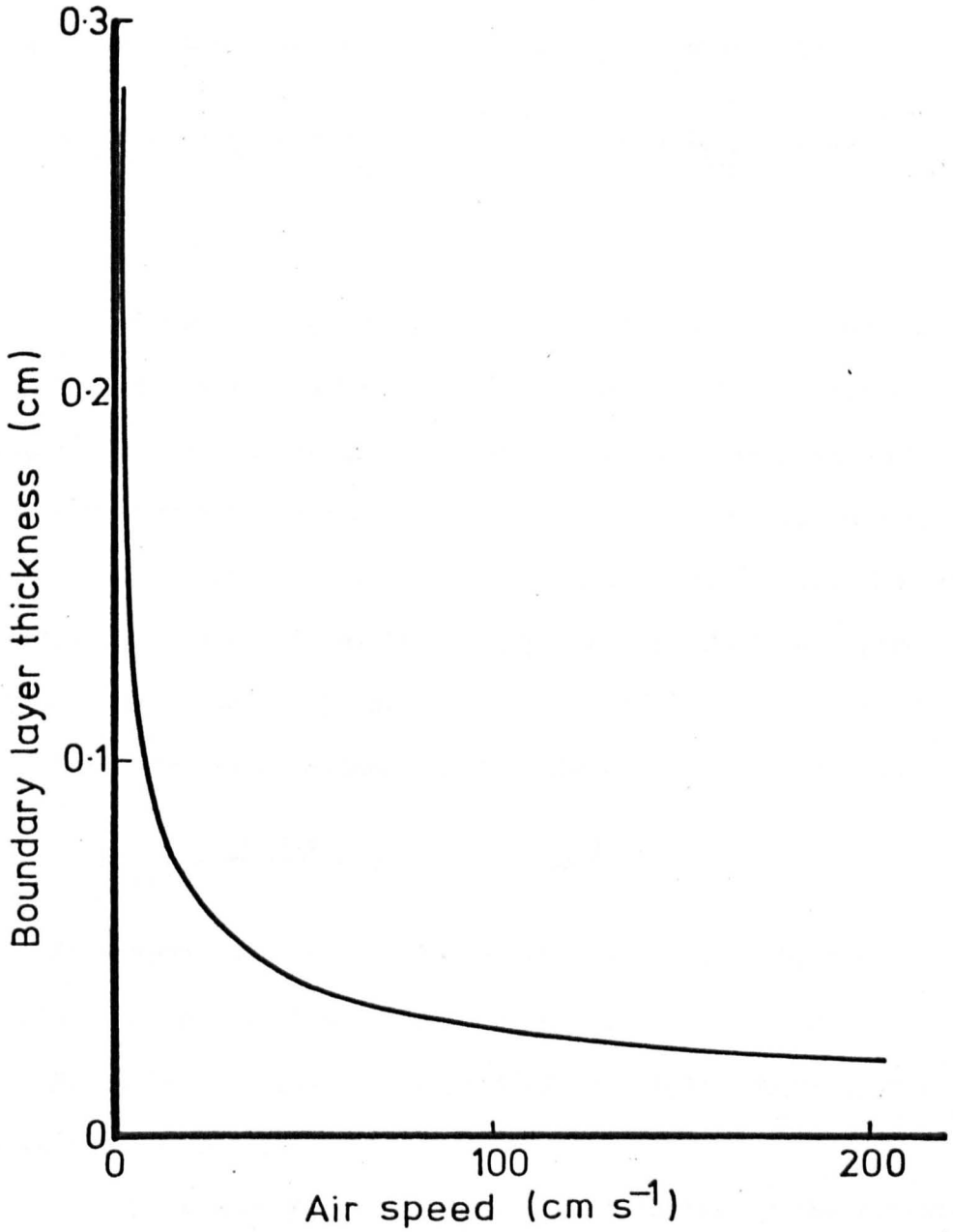

FIG. 6.14 Variation in boundary layer thickness with air speed for a leaf of width 0·5cm.

$$R_{tb} + R_{end} + R_b = \frac{1}{D_o A_{x,st}} \left(L_{tb} + \frac{\pi d_{st}}{4}\right) + \frac{L_b}{D_o A_l}$$

$$= \frac{1}{D_o A_l} \left[\frac{A_l}{A_{x,st}} \left(L_{tb} + \frac{\pi d_{st}}{4}\right) + L_b \right] \text{ s cm}^{-3} \qquad (6.12)$$

Stomatal resistances act in parallel, therefore, if there are n stomata over A_l cm^2, the total resistance, $R_{l,st}$, is given by:

$$R_{l,st} = \frac{1}{D_o A_l} \left[\frac{A_l}{n A_{x,st}} \left(L_{tb} + \frac{\pi d_{st}}{4}\right) + L_b \right] \text{ s cm}^{-3} \qquad (6.13)$$

B. RELATIONSHIP BETWEEN STOMATAL NUMBER AND RESISTANCE

Equation 6.13 has been used to determine the relationship between stomatal number and resistance and in Fig.6.15 stomatal numbers from 100 to 10,000 are plotted against resistance for a 1.0cm long leaf segment of width 0.5cm (i.e. $A_l = 0.5$ cm^2) in 'still' air. The stomata were assumed to have a pore width of 5.0μm (see Fig.6.2) and pore length and depth of 32μm and 16.3μm respectively (p. 97).

The curve is a rectangular hyperbola with the equation:

$$R_{l,st} = \frac{15,644}{n} + 0.868 \text{ s cm}^{-3}$$

ie. the assymptote y = 0 displaced from the x axis by the value of the boundary layer resistance (0.868 s cm^{-3}).

Fig.6.16 is a double log plot of stomatal numbers from 1 to 10,000 against resistance.

It can be seen from the figures that initially the resistance decreases rapidly with increasing stomatal number. It then decreases more slowly until further increase in the number of stomata has little effect and $R_{l,st}$ tends towards the limiting value of the boundary layer resistance.

With 5,000 stomata per 0.5cm^{-2} leaf surface (ie. the stomatal density over most of the Eriophorum leaf - Fig.6.1) the resistance has the very low value of 4 s cm^{-3}. For comparison, a 1.0cm segment of root, of radius

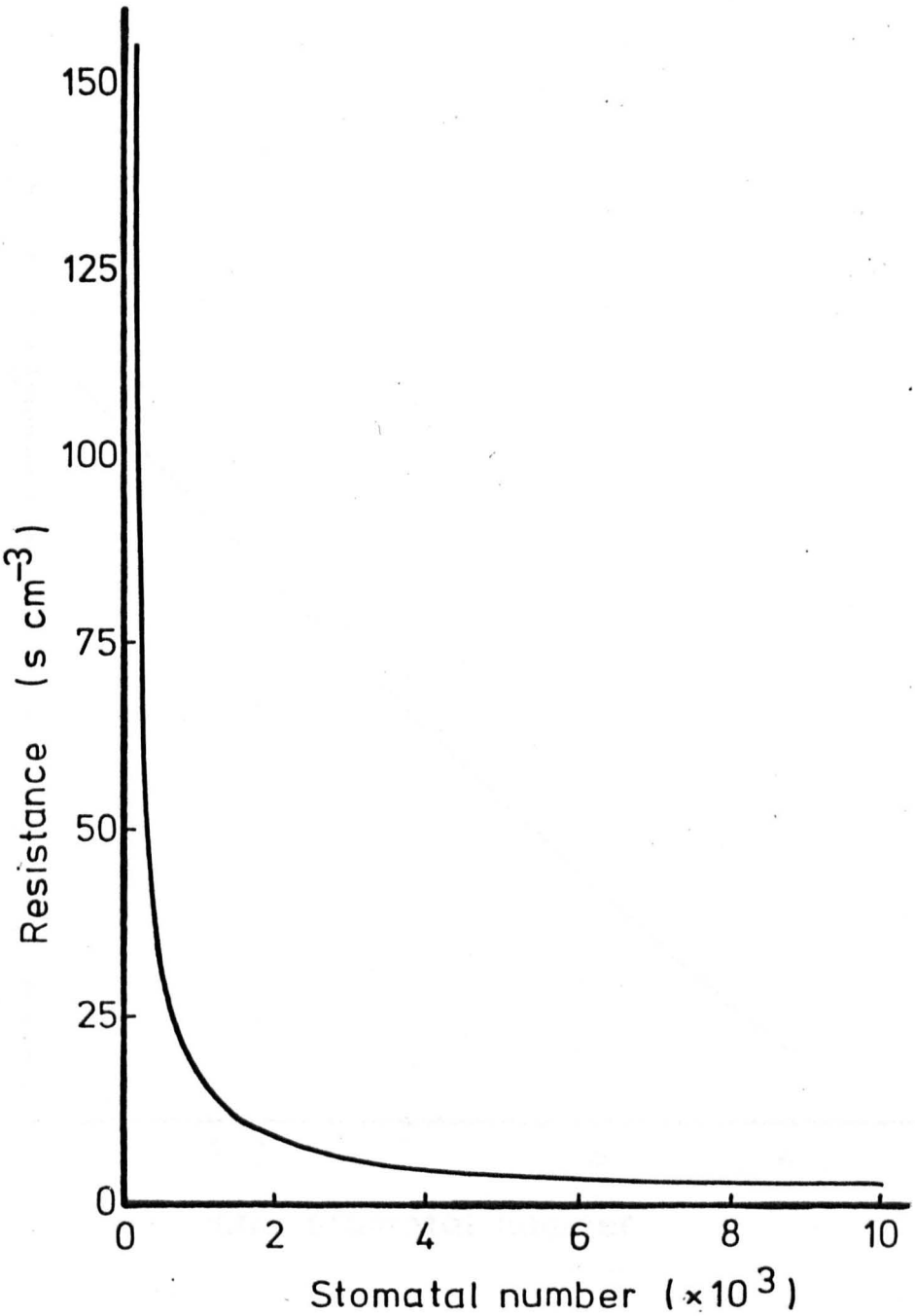

FIG. 6.15 Relationship between stomatal number and effective resistance for a 1·0 cm leaf segment of width 0·5 cm in "still" air (10 cm s^{-1})

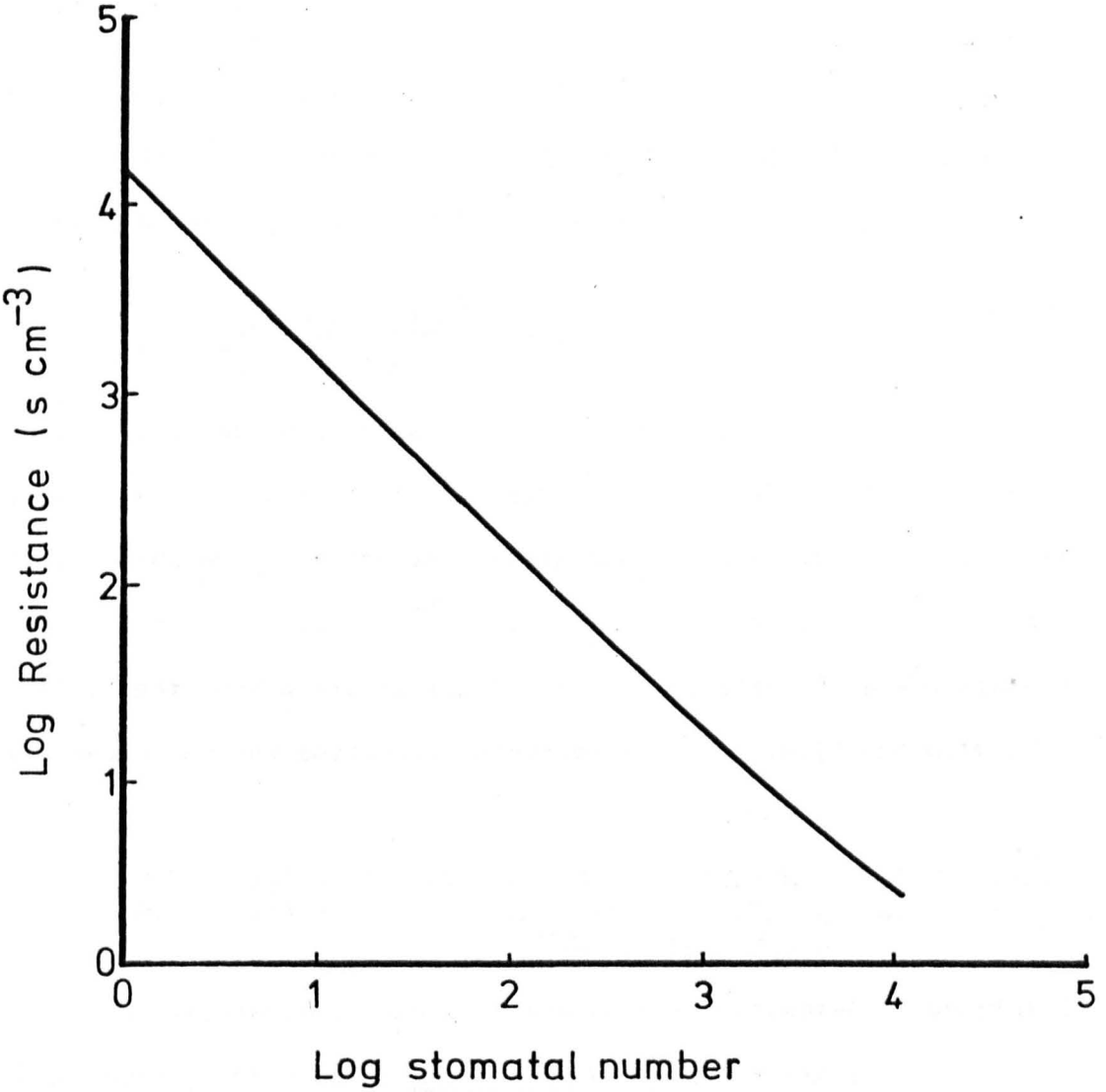

FIG. 6.16 Log_{10} plot of stomatal number against effective resistance for a 1·0 cm leaf segment of width 0·5 cm in "still" air

0.05cm and porosity 20% has a diffusive resistance of 3,105 s cm^{-3} (see p.126); this is the resistance afforded by a reduction in stomatal density to only five per $0.5cm^2$.

C. THE RELATIONSHIP BETWEEN STOMATAL APERTURE AND RESISTANCE

Equation 6.13 was used also to show the way in which stomatal resistance varies with degree of opening for a 1.0 x 0.5cm leaf segment with 5,000 stomata situated in still air; see Fig.6.17. The curve is again hyperbolic, described by the equation:

$$R_{l,st} = \frac{1}{r_{st}} \left(\frac{5.06 \times 10^{-7}}{r_{st}} + 4.878 \times 10^{-4}\right) + 0.868 \quad s\ cm^{-3}$$

where r_{st} is the mean stomatal radius (see p.113).

It can be seen that within the range of stomatal apertures considered (1.0 to 10.0μm), the stomatal resistance in the 1.0cm long leaf segment does not exceed 13.9 s cm^{-3}. The increased stomatal number associated with larger leaf areas will, of course, greatly reduce the stomatal resistance at any particular aperture (see Figs.6.15 and 6.16).

D. THE RELATIONSHIP BETWEEN STOMATAL APERTURE AND THE MINIMUM NUMBER OF STOMATA REQUIRED TO MAINTAIN THE INTERNAL OXYGEN CONCENTRATION ABOVE THE CRITICAL VALUE

With reference to the respiratory data presented in Chapter 3 consider a portion of an Eriophorum plant comprising:

1. 5cm of astomatal leaf base, of width 0.5cm, and total respiratory oxygen consumption of 6.0×10^{-9} g s^{-1}.
2. 1cm of stomatal leaf of width 0.5cm and oxygen consumption of 1.0×10^{-9} g s^{-1}.
3. A spherical stem of volume $0.065cm^3$ and oxygen consumption of 8.0×10^{-9} g s^{-1}.
4. Five roots, each of length 5cm and radius 0.05cm, with a rate of oxygen consumption of 5.0×10^{-9} g s^{-1}.

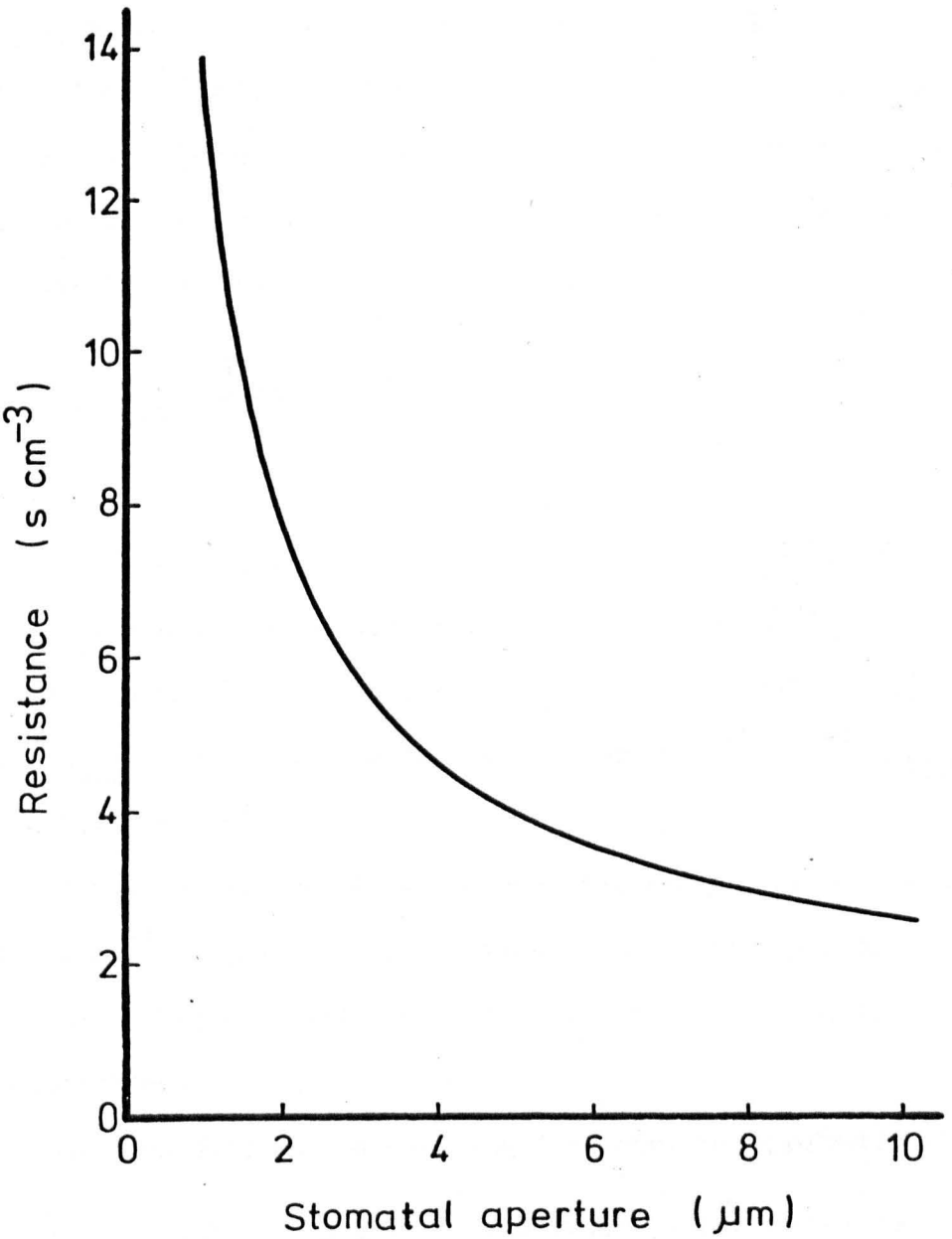

FIG. 6.17 Variation in stomatal resistance with stomatal aperture for a 1·0 cm leaf segment of width 0·5 cm having 5000 stomata ("still" air conditions)

The total rate of oxygen consumption by this system is 40 x 10^{-9} g s^{-1}, and this O_2 must enter the plant by the stomata of the 1cm stomatal leaf segment. The gas analysis data presented in Chapter 4 indicates that the oxygen concentration within the leaves of Eriophorum is similar to that of the atmosphere (Figs.4.7 and 4.8). Assuming, then, that 20.4% O_2 within the leaves results in a concentration of about 15% in the root apices (see p.148), then the C.O.P. of 2.5% in the root would correspond with a leaf oxygen concentration of approximately 3.5%. Therefore, the maximum stomatal resistance which will allow normal respiration (ie. maintain 3.5% O_2 in the leaf) is given by:

$$R_{l,st} = \frac{C_{o,a} - C_{o,l}}{J} \quad s\ cm^{-3} \qquad (6.14)$$

where:

$C_{o,a}$ = the O_2 concentration in the ambient air (g cm^{-3})

$C_{o,l}$ = the O_2 concentration in the leaf (g cm^{-3})

J = the O_2 diffusion rate through the stomata (g s^{-1})

Since $C_{o,a}$ = 20.4%; $C_{o,l}$ = 3.5% and J = 40 x 10^{-9} g s^{-1}, $R_{l,st}$ is found to be 5,133 s cm^{-3}.

Having established that the stomatal resistance must not rise above 5,133 s cm^{-3} for maximum respiration to be maintained, the conditions of stomatal number and aperture which would contribute to this value may now be determined.

Equation 6.13 may be rearranged to give the quadratic:

$$R_{l,st} = \frac{a}{r_{st}^2} + \frac{b}{r_{st}} + c \qquad (=5,133)\ \ s\ cm^{-3} \qquad (6.15)$$

where:

$$a = \frac{L_{tb}}{\pi D_o n}$$

$$b = \frac{1}{2 D_o n}$$

$$c = \frac{L_b}{D_o A_l}$$

and r_{st} = the mean radius of the stomatal pores.

Equation 6.15 was solved for r_{st} by substitution of values of n, and the corresponding pore widths (y) were calculated using equations 6.4 and 6.5.

The relationship between stomatal aperture and the minimum number of stomata required for maximum respiration in the system described above, is shown in Fig.6.18. It must be mentioned that the graph is probably accurate only for stomatal widths of about 1.0μm and above; at narrower apertures the pore width approaches the mean free path of the diffusing oxygen molecules and normal diffusion laws no longer apply (Meidner and Mansfield, 1968). Nevertheless, Fig.6.18 illustrates well that few stomata are required to sustain normal respiration. For example at a pore width of 8.0μm three stomata only are necessary, whilst at a pore width of 1.0μm the number is twenty.

Similar calculations to those described above may be employed to show that 48 stomata at a pore width of 8.0μm and 288 at a width of 1.0μm are sufficient to maintain the internal leaf oxygen concentration at the normal figure of about 20%.

E. THE EFFECT OF STOMATAL BLOCKAGE ON THE INTERNAL OXYGEN REGIME

In an attempt to confirm the pattern of results obtained in the lanolining experiments (p.104 and Fig.6.4) the above theory was used to simulate stomatal blockage in a plant having a total respiratory rate of 50ng $O_2 s^{-1}$, and a single leaf, length 20cm, with the characteristics given in Table 6.2. Stomatal width was assumed to be 5.0μm.

For the plant to respire at its maximum rate the minimum gradient of oxygen concentration between the atmosphere and the inside of the leaf must be such as to allow stomatal oxygen entry at a rate of 50ng s^{-1}. Using equations 6.13 and 6.14, and assuming atmospheric oxygen concentration to be 20.75%, the relationship between the number of functional stomata and

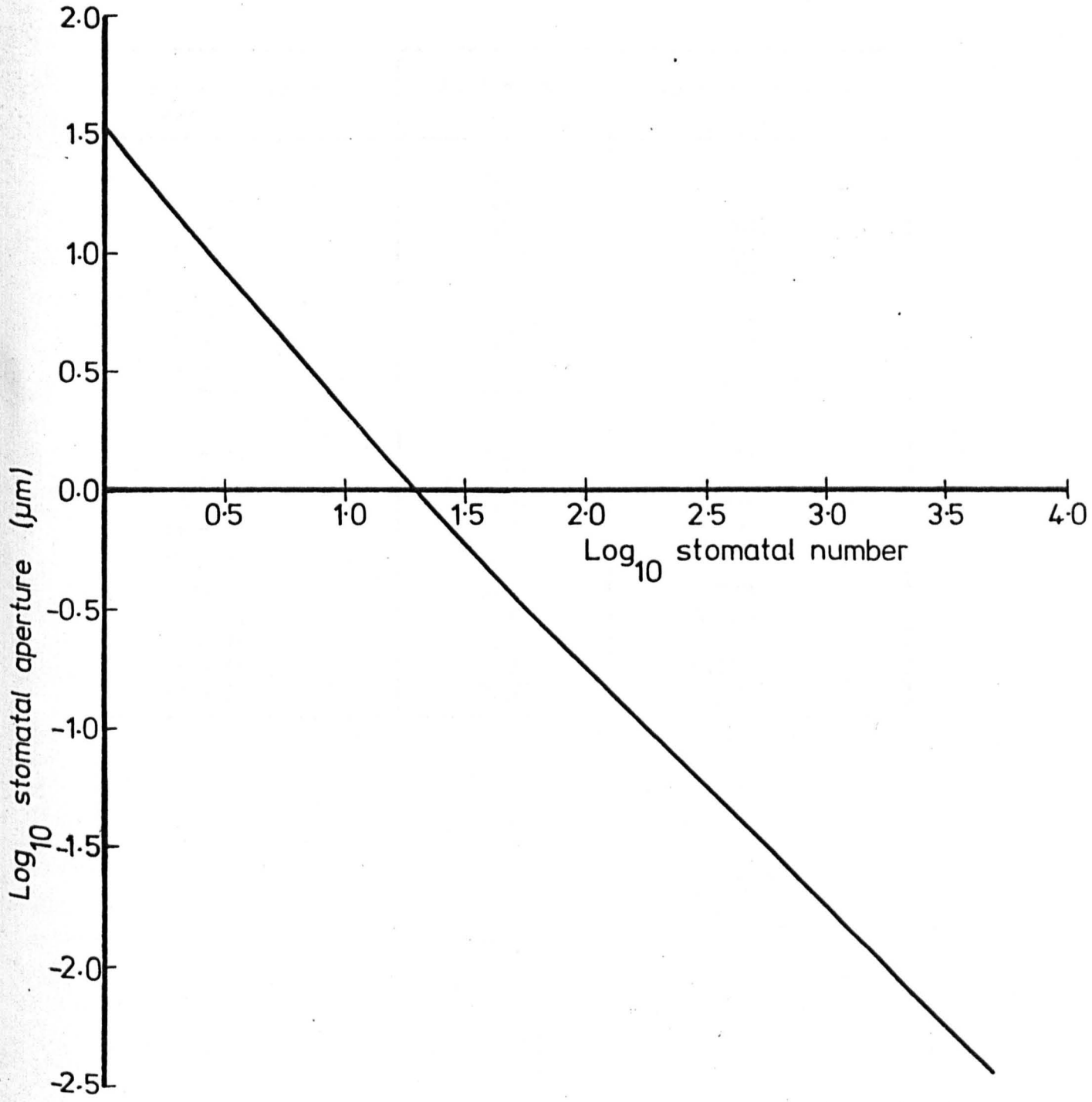

FIG. 6.18 Relationship between stomatal aperture and the number of stomata required to maintain maximum respiration in a plant having a total rate of oxygen consumption of 40 ng s^{-1}.

TABLE 6.2: LEAF CHARACTERISTICS USED TO PREDICT THE RELATIONSHIP BETWEEN STOMATAL BLOCKAGE AND INTERNAL OXYGEN REGIME

(All stomata were assumed to have a pore width of 5.0μm)

Distance from Leaf Base (cm)	Leaf Width (cm)	Stomatal Density (cm^{-2})
0 - 1	0.75	0
1 - 2	0.75	0
2 - 3	0.75	50
3 - 4	0.75	150
4 - 5	0.50	800
5 - 6	0.50	3,000
6 - 7	0.50	6,500
7 - 8	0.50	8,000
8 - 9	0.50	9,000
9 - 10	0.50	9,000
10 - 11	0.50	9,000
11 - 12	0.50	9,000
12 - 13	0.50	9,000
13 - 14	0.50	9,000
14 - 15	0.50	9,000
15 - 16	0.50	9,500
16 - 17	0.50	9,500
17 - 18	0.50	9,500
18 - 19	0.20	9,500
19 - 20	0.20	9,500

the leaf oxygen concentration required to produce this gradient was established. The results, expressed as internal leaf oxygen concentration v. length of leaf "lanolined", are given in Fig.6.19.

The similarity between Figs. 6.19 and 6.4 is apparent, and it may be seen that in the theoretical curve there is little change in leaf oxygen concentration until about 2cm of stomatal leaf remain; this is the equivalent of only 150 functional stomata. Consequently R.O.L. from the roots of the plant should similarly remain unchanged (c.f. Fig.6.4).

It must be mentioned that the theory used to derive Fig.6.19 will apply only whilst the plant is respiring at its maximum rate (ie. at leaf oxygen concentrations of and above 3.5% - see p.118). From Fig.6.19 it can be seen that this critical oxygen concentration will occur when only 0.1cm of leaf, or about 4 stomata, remain functional.

III. CONFIRMATORY EXPERIMENTS AND DISCUSSION

A. CONFIRMATORY EXPERIMENTS

The experimental and theoretical work described in the preceding sections has clearly shown that very few open stomata are required to sustain normal respiration, particularly when these are situated at the leaf base; the precise number, however, was not determined. Also, the relationships between stomatal number, aperture and diffusive resistance indicate that only when stomata are present in small numbers will change in aperture alter resistance sufficiently to influence oxygen entry. The experiments described below were designed:

(a) to determine more precisely the number of stomata required for adequate aeration,

(b) to test experimentally the hypothesis that closure of stomata present in small numbers will influence internal aeration.

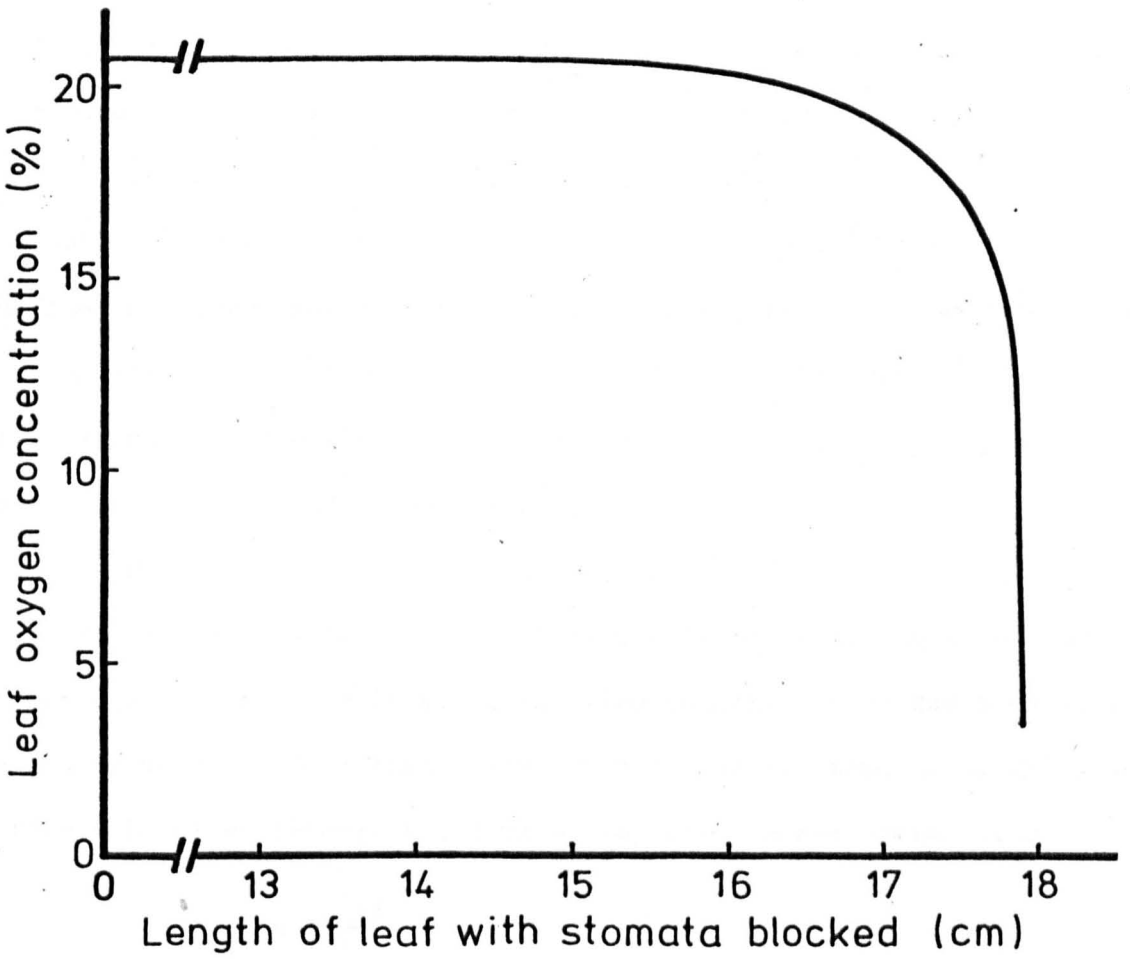

FIG. 6.19 Theoretical influence of stomatal blockage on leaf oxygen concentration.

Single leaf preparation with a rate of oxygen consumption of 50 ng s^{-1}
Stomatal width was assumed to be 5 μm and blockage was from apex to base.

1. The number of stomata required for adequate aeration

(a) Method

A plant, with all but one leaf removed, was arranged for R.O.L. measurement and the leaf cut in the astomatal region below the sheath (see Fig.6.1). When the diffusion current had equilibrated the cut end was sealed with lanolin and the current allowed to fall to the residual value. At this stage the leaf surface was scanned with a travelling microscope to ensure that stomata were absent. With the aid of the microscope and a micro-manipulator a small hole was made through the epidermis into a lacuna using fine wire (radius = 0.0028cm). The diffusion current was then allowed to re-equilibrate in the dark. The new equilibrium value was always indicative of an oxygen pressure in the root which exceeded the C.O.P. (see Table 6.3 and Chapter 4), and the experiment was halted at this stage.

(b) Theory

The resistance to oxygen diffusion offered by the hole, R_h, is given by an equation similar to 6.11, ignoring boundary layer resistance, the value of which is less than unity. The number of stomata, n, which would offer a total resistance equal to R_h may then be calculated from:

$$n = \frac{R_{st}}{R_h}$$

where R_{st} is the resistance of one stoma.

(c) Results

The results of three experiments are summarised in Table 6.3. In each experiment a single hole, the equivalent of only nine stomata of pore width 8.0μm, was sufficient to bring the root apical oxygen concentration to a value approaching that with the unsealed leaf. This was, of course, much in excess of the critical value of 2.5%, and it is apparent that the number of stomata of aperture 8.0μm required to maintain the C.O.P. will be less than nine. In the whole plant the required number of stomata per leaf should be even smaller, theoretically by a factor equal to the

TABLE 6.3.

For Explanation see P. 121

Experiment	Oxygen Entry through Cut Leaf End		Oxygen Entry through Hole	
	R.O.L. ($ng\ cm^{-2} min^{-1}$)	Root apical O_2 (%)	R.O.L. ($ng\ cm^{-2} min^{-1}$)	Root apical O_2 (%)
1	121.9	12.6	104.5	10.8
2	117.1	12.7	98.2	10.7
3	126.7	12.6	117.2	11.6

reciprocal of the leaf number.

2. The effect of induced closure of stomata present in small numbers

(a) Method

These experiments were similar to the P.M.A. work described earlier. However, in this case, when the diffusion current had equilibrated prior to spraying, the leaf was cut in stages (the cut ends being sealed with lanolin) until the current began to fall; this usually occurred when about 0.5cm of leaf remained above the sheath (c.f. the point of divergence in Figs.6.9 and 6.10). The diffusion current was allowed to re-equilibrate in this condition and then the leaf was sprayed with P.M.A. solution.

(b) Results

The result of a typical experiment is given in Table 6.4. It is clear that when the number of stomata was limiting oxygen entry (indicated by the slight fall in diffusion current) a reduction in pore size (to about 0.2μm - see Fig.6.3) had a marked influence on internal aeration.

B. DISCUSSION

The work described in this chapter shows conclusively that under normal conditions stomatal movements are unlikely to affect internal plant aeration. Indeed, induced stomatal closure to very narrow apertures is ineffective in reducing the amount of oxygen entering the E.angustifolium plant. This is attributable to the very low diffusive resistance of stomata when present in large numbers.

Although fewer than nine open (8.0μm) stomata may be sufficient to allow almost maximum aeration of the stem and root system in Eriophorum, the pores must be situated at the leaf base. In more apical regions more stomata are required due to the increased diffusion path between the point of oxygen entry and the root apices, and to the synergistic respiratory oxygen uptake in the leaf. These observations lead to the prediction that partial inundation of plants in the field might cause sub-optimal oxygen

TABLE 6.4: THE EFFECT OF P.M.A. ON STOMATA PRESENT IN SMALL NUMBERS

Condition	Diffusion Current (μA)
Leaf uncut; length above sheath 15.5cm	2.50
Leaf cut and end sealed; length above sheath approximately 0.5cm	2.35
P.M.A. applied:	
after 30 min.	0.80
after 1h	0.75

entry.

The results emphasise the need for caution in referring to stomata as "closed". For example, when assessing the effect of azide on the stomata of tobacco leaf discs, Walker and Zelitch (1963) considered pores of 2μm or less to be closed; so far as oxygen entry is concerned normal aeration could be maintained by very few stomata of this aperture.

Since the diffusivity of water vapour in air is of the same order as that of oxygen (eg. 0.25 and 0.20 $cm^2 s^{-1}$ at 20°C respectively) it seems likely that if concentration gradients are sufficient water vapour fluxes through stomata of narrow apertures could similarly be considerable. If this is the case, the apparent cuticular transpiration observed by various workers in plants with "closed" stomata (eg. Meidner, 1976) could be due, at least in part, to diffusion through stomatal pores of sub-microscopic widths.

Other authors also have stressed the need for caution in this respect. For example Pallas (1965) found that in several crop species rates of transpiration continued to fall after stomata had apparently closed, whilst Hygen and Midgaard (1954) attributed a proportion of the "cuticular transpiration" in Pinus sylvestris needles to diffusion through sub-microscopic stomatal apertures.

CHAPTER 7

INTERNAL RESISTANCE TO OXYGEN TRANSPORT

I. INTRODUCTION

The similarity between the diffusive flow of oxygen within the plant body and the flow of electricity along a conductor has been mentioned several times (e.g. Chapter 2). In much the same way that current flow is impeded by electrical resistance, oxygen transport from the atmosphere to the roots, and from the roots to the surrounding medium, will be limited by internal diffusive resistance of the plant.

Although several authors have made reference to internal resistance as a factor influencing plant aeration (e.g. Coult, 1964; Greenwood, 1967b; Armstrong, 1972; Armstrong and Wright, 1975) very little research has been directed specifically towards its characterisation. Apart from the estimates of root wall permeability in rice and maize made by Luxmoore et al. (1970b) there is only one experimental study known to the author in which internal resistance has been quantified: this was made by Healy (1975) who measured the resistance to oxygen transport in the mesophyte, Pisum sativum L. However, whilst being the first work of its kind, Healy's research was concerned solely with diffusive impedance in the primary root; stem and leaf factors were not considered. The purpose of the research described in this chapter was twofold: to study the internal resistance to oxygen transport in a wetland plant (Eriophorum angustifolium) and to assess the contribution of diffusive impedances in the leaves, stem and root.

Two types of internal plant resistance may be distinguished. These are:

(a) The actual physical resistance to gaseous diffusion offered by the intercellular space system,

(b) A "pseudo-resistance", caused by respiration and lateral leakage of oxygen from the plant.

These two components constitute an "effective" diffusive resistance and before considering resistance in Eriophorum it is necessary to discuss them in greater detail.

A. PHYSICAL RESISTANCE

The magnitude of the diffusive resistance offered by the gas space system (i.e. the pore space resistance, R_p) depends upon the length of the diffusion path, the porosity of the tissues and the tortuosity of the gas-conducting channels (Armstrong and Wright, 1975).

1. Diffusion path length

The simplest analogue of internal oxygen transport is the diffusive flow of oxygen from a source to a sink along a tube of uniform cross-section. If diffusion is in one dimension only (i.e. along the x-axis) and there is no lateral loss or gain of diffusible species, the resistance offered by the tube is given by an equation similar to 2.15:

$$R = \frac{L}{D_o A_x} \qquad s\ cm^{-3} \tag{7.1}$$

where:

L = the length of the tube (cm)

D_o = the diffusion coefficient for oxygen ($cm^2 s^{-1}$)

A_x = the cross-sectional area of the tube (cm^2)

It is apparent from this equation that if A_x is constant R will increase linearly with path length L.

If the oxygen source is situated at one end of the tube, x = 0, and the sink at the other end, x = L, the oxygen diffusion rate along the tube, J, is given by:

$$J = \frac{D_o A_x (C_o - C_1)}{L} \qquad g\ s^{-1} \tag{7.2}$$

where C_o and C_1 are the oxygen concentrations at the source and sink respectively ($g\ cm^{-3}$).

From equation 7.2 it can be seen that the oxygen diffusion rate, J, will decrease hyperbolically with increasing path length. Using artificial silicone rubber "roots" Armstrong (1972) showed this to be the case and, for example, recorded a 60% reduction in R.O.L. from a 3.75% porous root when the diffusion path increased from 0 to 13.2cm. Healy (1975) and Armstrong (1978) have obtained experimental evidence to show that in the absence of respiratory activity the R.O.L. from the primary root apex in pea declines with increasing root length; in this case, however, the hyperbolic relationship was masked by the changes in porosity and root shape which accompanied growth.

In the simple case of a root of constant porosity and with an external oxygen sink operating only at the apex, the homogeneity of diffusive resistance also gives rise to a linear fall in concentration between the source and sink along the x-axis (eg. Armstrong and Wright, 1976b).

2. Gas-filled porosity and tortuosity of the gas spaces

In the plant the diffusion system is much more complex than the simple model considered above, and the basic resistance equation (7.1) must be modified to include fractional porosity (ϵ) and, where appropriate, tortuosity of the gas-conducting channels. These factors increase the diffusive resistance, the former by decreasing the area (A_x) available for diffusion, the latter by increasing the path length, L. However, it is customary to consider the effects of porosity and tortuosity as a reduction in diffusivity; the "effective" diffusion coefficient, D_e, is given by:

$$D_e = D_o \epsilon \tau \qquad cm^2 s^{-1} \qquad (7.3)$$

where:

τ is a tortuosity factor $\leqslant 1$.

The corresponding diffusive resistance is then given by:

$$R_p = \frac{L}{D_e A_x} \qquad s\ cm^{-3} \qquad (7.4)$$

where:

L = the observed diffusion path length (e.g. root length) (cm)

A_x = the total cross-sectional area of the organ under consideration (cm^2)

R_p = the resistance due to the gas space system (i.e. "pore space" or "non-metabolic" resistance)

It must be noted that the calculation of R_p using equation 7.4 may be complicated by the non-uniform distribution of porosity both within the plant and within individual organs (Chapter 3; Armstrong, 1971a). In addition, a change in cross-sectional area can affect resistance (Healy, 1975). However, the roots of wetland plants are commonly of approximately constant radius and complications due to change in root shape did not arise in the present study.

It has been demonstrated, both for wetland and mesophytic species, that the intercellular spaces do form a continuous system for the diffusion of gases within the plant. For example, Evans and Ebert (1960) used ^{15}O to follow the transport of oxygen down the root of Vicia faba L. They concluded that the movement of the gas was by diffusion through continuous gas spaces, and it had the same kinetics as diffusion down a polythene tube of diameter 0.5cm. In order to fit a theoretical curve to their experimental data they found it necessary to assume a path length, L_1, which was somewhat greater than the actual root length, L (e.g. when L = 15cm, L_1 = 21cm). They attributed this discrepancy to the tortuosity of the gas channels.

In a similar piece of work Barber et al. (1962) showed that the diffusion of ^{15}O from leaves to roots of rice and barley was along continuous gas spaces. Again a theoretical path length greater than the actual root length was required for rice. However, they considered that this may not have been a consequence of tortuosity so much as an increase in diffusion path length, caused by entry of the gas along the whole length of the leaves rather than at the root base.

In their study of labelled oxygen diffusion through roots of barley, corn and rice Jensen et al. (1967) used data of Evans and Ebert (1960) and

Barber et al. (1962) to calculate a tortuosity factor (τ) of 0.433, but they point out that τ may vary with porosity. Values of D_e obtained for the three species increased in the order barley < corn < rice, in agreement with a corresponding increase in root porosity.

Unlike the forementioned workers Greenwood (1967b), who measured the increase in oxygen concentration at the root surface of mustard seedlings when the atmosphere around the leaves was changed from N_2 to O_2, concluded that the gas diffused along non-tortuous channels. Examination of longitudinal sections of the roots of Eriophorum (Plate 7.1) and rice (Plate 3.2b) similarly indicate that tortuosity is low. (The apparent discontinuity of the gas channels in the root apices of Eriophorum and rice is simply a consequence of the curvature of the cell columns in this region (see Plate 3.2).

Armstrong and Wright (1976b) and Armstrong (1978) used the electrical analogue (p. 29) to predict the influence of "effective porosity", ϵ_e ($=\epsilon\tau$), upon the internal oxygen regime of roots in anaerobic media. Increased porosity was shown to enhance the internal oxygen status and R.O.L. and it was suggested that roots having the low porosities characteristic of non-wetland species are entirely unsuited to growth in waterlogged soil. Luxmoore et al. (1970a-d) used a mathematical model to study the oxygen relations of rice and maize roots and also predicted that increased internal oxygen levels would accompany increased effective porosity in both species.

B. PSEUDO-RESISTANCE

1. Concept

In much the same way that electrical resistance reduces the current flow between the ends of a linear conductor, lateral loss of oxygen along a linear diffusion path will reduce the diffusive flux between the ends of the path. Respiration and R.O.L. both contribute to the loss of

PLATE 7.1: Eriophorum angustifolium; longitudinal section through a segment of cortex in the region 0.15 to 0.20 cm behind the root tip.

Note the lack of tortuosity in the gas conducting channels. (x 760).

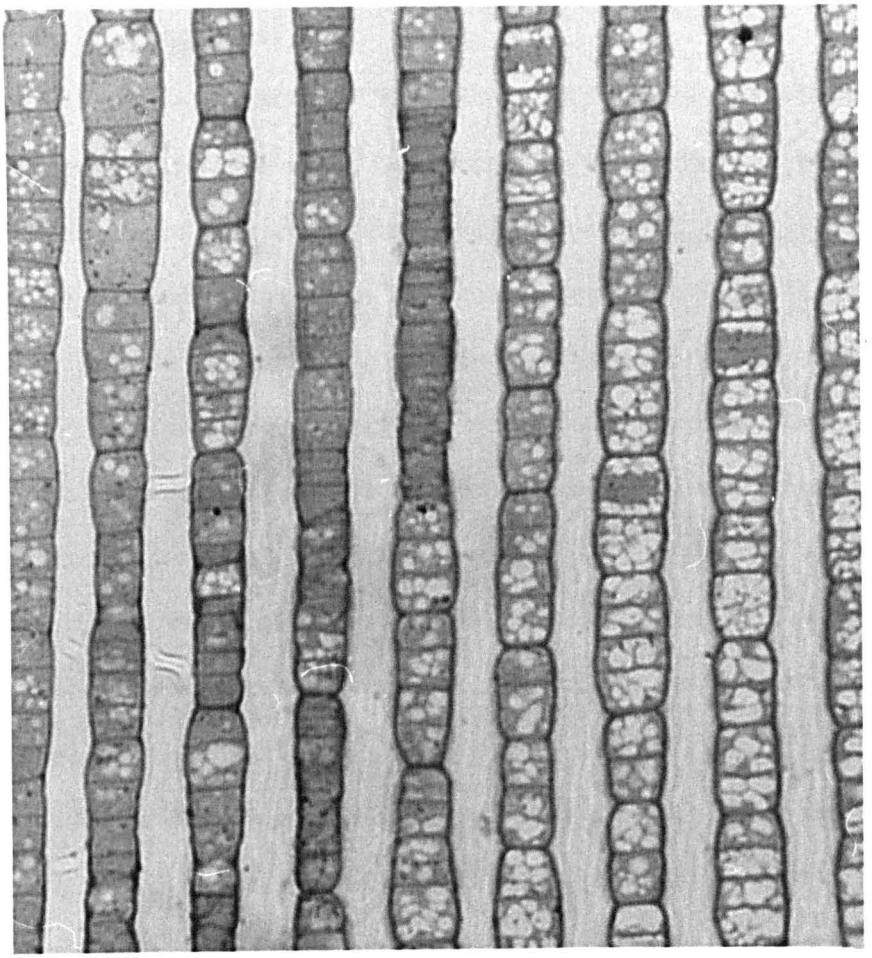

oxygen from the internal atmosphere of the plant and in this respect these processes act as pseudo-resistances, contributing to the effective resistance of the plant.

Considered in this way the idea of effective resistance seems straightforward and the work described in this chapter was begun with a view to characterising effective resistance in E.angustifolium. However, as the work neared completion it became apparent that this simplistic view of effective resistance, implied by Armstrong and Wright, 1975, is deceptive; in fact the concept is much more complex than at first thought, and this will become apparent in the following discussion.

(a) Electrical Analogy

The way in which respiration and radial oxygen leakage from the root can contribute to effective resistance can be conveniently illustrated by a simple electrical analogy.

Consider a simple circuit (Fig.7.1a) in which the two series conductors, A and B, each of value 100 ohms, represent the physical reistance to the longitudinal diffusion of oxygen within the plant (i.e. the pore space resistance). The potential difference of 200 volts between points X and Z is analogous to the oxygen concentration difference between the atmosphere (at X) and a sink external to the root apex (at Z). The current measured at Z, which represents R.O.L. from the apex, is 200 volts ÷ 200 ohms, or 1 ampere. There is a linear fall in potential between X and Z, and at Y the potential is 100 volts.

Now, consider a similar situation in which a third conductor, C, of value 10 ohms, is situated laterally as shown in Fig.7.1b; the current flowing through C represents a lateral loss of oxygen from the system. Conductors B and C are in parallel and their combined resistance is approximately 9.1 ohms. The total resistance in the system is, therefore, 100 ohms + 9.1 ohms, or 109.1 ohms, and the current flowing through conductor A is 200 volts ÷ 109.1 ohms, or 1.833 amperes. The potential

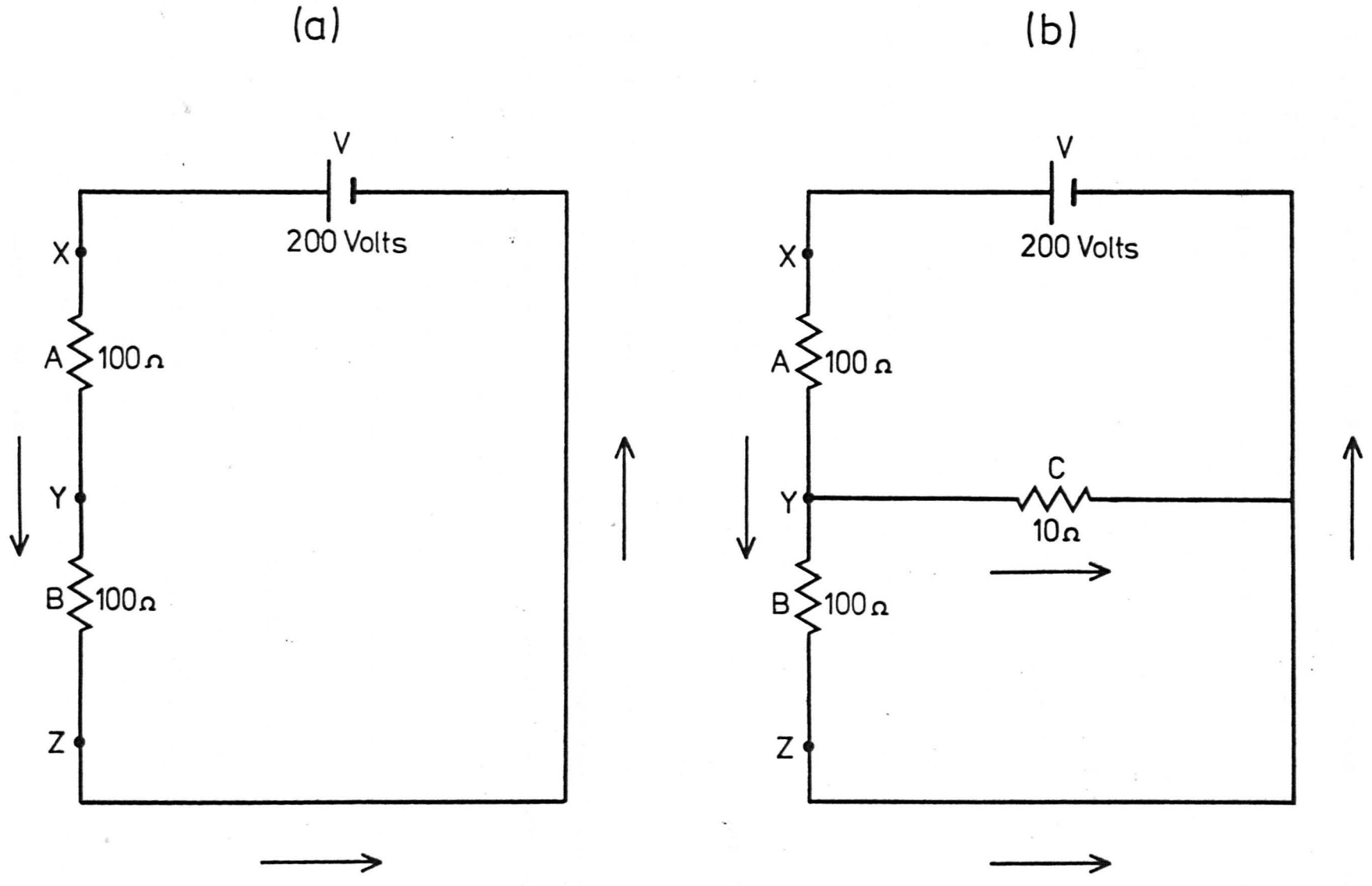

FIG. 7.1 Circuits to illustrate the concept of effective diffusive resistance

drop between X and Y is given by 1.833 amperes x 100 ohms = 183.3 volts, and hence the potential at Y is (200 - 183.3) volts, or 16.7 volts. Therefore, the current measured at point Z is in this case only 16.7 volts ÷ 100 ohms, or 0.167 amperes.

If it was possible only to measure the current at Z and the potential difference between X and Z (cf. the cylindrical platinum electrode technique) the apparent resistance in the first system (Fig.7.1a) would be 200 volts ÷ 1 ampere, or 200 ohms; but in the second system (Fig.7.1b) the resistance would be 200 volts ÷ 0.167 amperes, or 1,250 ohms. In other words the shunting of current through C (crudely equivalent to the removal of oxygen by respiration or leakage) causes an apparent increase in resistance of 1,050 ohms, to give a total effective resistance of 1,250 ohms. In the diffusion system effective resistance may conveniently be expressed in the same units as physical resistance - i.e. s cm^{-3}.

It must be noted that whilst serving to illustrate the concept of effective resistance, the simple analogue described above is by no means an accurate representation of respiratory oxygen uptake or lateral leakage. Respiration is largely independent of oxygen concentration (Chapter 4), whereas current flow through C in Fig.7.1b is entirely dependent upon difference in electrical potential. In this respect the model more closely illustrates the effect of oxygen leakage, the magnitude of which varies with the oxygen concentration difference between the internal atmosphere and the external sink.

(b) Effective Resistance and Oxygen Concentration.

An equation has already been presented which defines apical oxygen flux in terms of total effective root resistance (i.e. physical plus pseudo-resistance) and oxygen concentration (equation 4.4). A similar equation may be written to relate flux to total effective plant resistance, R_t, and ambient oxygen concentration, C_o:

$$f = \frac{C_o}{A_r(R_t + R_s)} \quad g\ cm^{-2}s^{-1} \qquad (7.5)$$

This equation may be rearranged to define R_t as:

$$R_t = \frac{C_o}{f\ A_r} - R_s \qquad s\ cm^{-3} \tag{7.6}$$

If respiration is significant the respiratory component of the pseudo-resistance, and hence R_t calculated using equation 7.6, will not take absolute values but will vary with C_o. This is due to the lack of direct proportionality between flux and oxygen concentration (C_o) and may be illustrated as follows.

Purely hypothetical relationships between ambient oxygen concentration, C_o, and apical flux are shown in Fig. 7.2a, with respiration inactive (i) and active (ii) (c.f. Fig.4.1a and c and Fig.4.2). If A_r is taken as 0.1 and R_s as 1.0, total resistance in the absence of respiration, calculated from Fig.7.2a(i) using equation 7.6, is shown as a function of C_o in Fig.7.2b(i). In this case R_t is clearly independent of ambient oxygen concentration, and is, in fact, equal to the physical resistance, R_p. With respiration active the R_t v. C_o relationship above the C.O.P. is as shown in Fig.7.2b(ii), and it can be seen that the apparent total resistance decreases with increasing oxygen concentration. As C_o becomes larger the effect of respiratory oxygen consumption as a component of R_t becomes less and as C_o tends to infinity, R_t will tend towards the value of the physical resistance. It should be noted that the dependence of R_t upon C_o is a function only of the respiratory component of the pseudo-resistance; leakage, being concentration-dependent, will merely alter the slopes, but not the shapes, of the plots in Fig.7.2a.

Due to the variation of R_t with C_o it is not possible to derive an absolute value for total resistance, and for purposes of comparison it is essential that R_t be determined at a standard ambient oxygen concentration. In this thesis the standard chosen was 20.41%, the oxygen concentration in moist air.

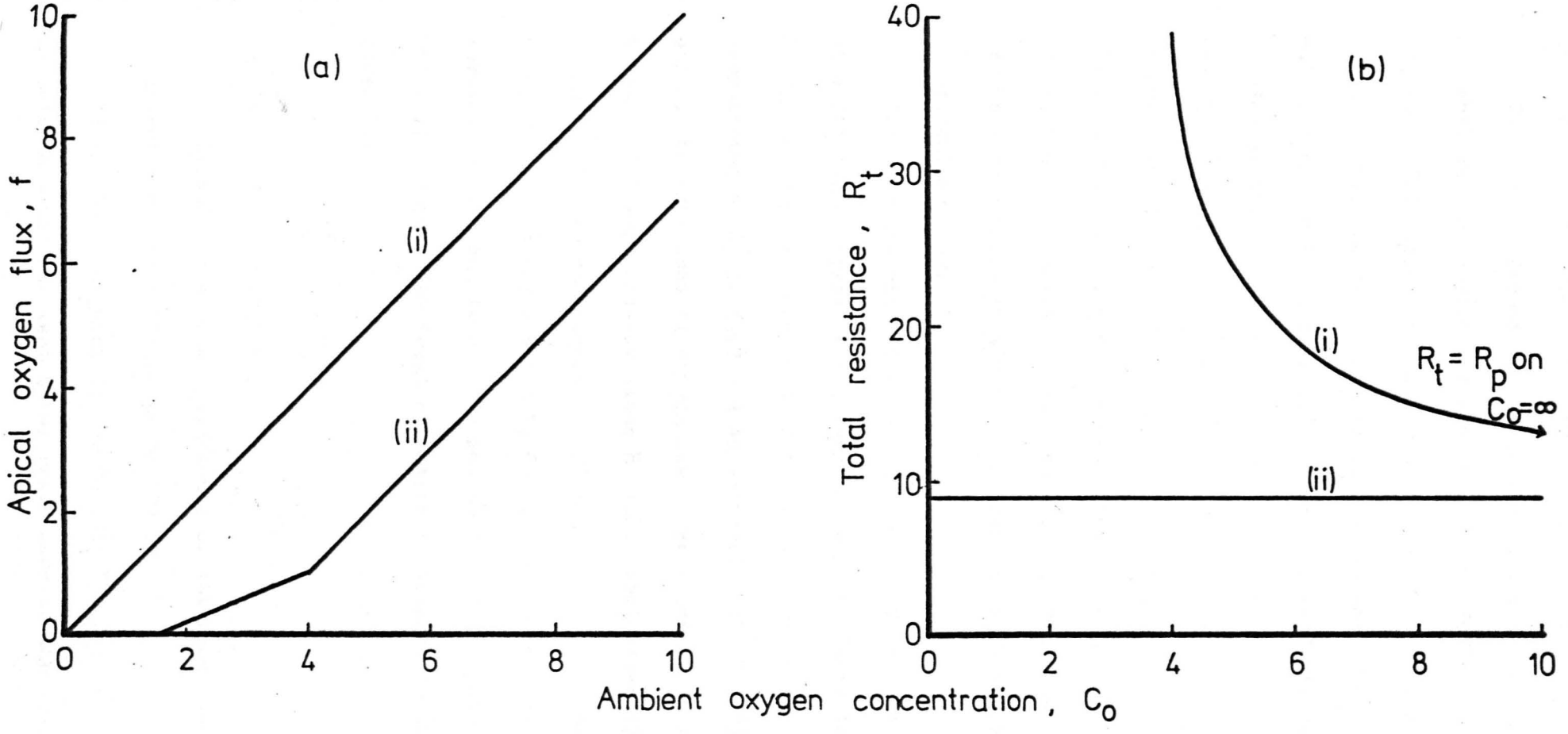

FIG. 7.2 Illustrating the variation with ambient oxygen concentration of total resistance in the respiring plant

(a) Hypothetical relationships between ambient $[O_2]$ and apical flux with respiration inactive (i) and active (ii)

(b) Total plant resistance v. ambient $[O_2]$ - calculated from (a) using equation 7.6

(Figures in arbitrary units)

(c) The Total Resistance of Organs Excised and In Situ

In order to deduce the total resistance of the various plant organs a technique was adopted whereby total plant resistance was measured (equation 7.6) before and after excision of a portion of tissue. It was expected that the difference in the two values of R_t would give an estimate of the total resistance of the excised tissue segment. However, in view of the relationship between oxygen concentration and total resistance discussed above, and because the internal oxygen concentration in any part of a plant depends upon activities in all other parts of the plant, a fundamental question was raised: is the apparent total resistance of an excised tissue segment identical to the total resistance of the same segment in situ? An answer was again sought using a simple electrical analogy.

Consider the circuit shown in Fig.7.3. Resistors R_1' and R_2', each of value 10Ω , represent the physical resistance to longitudinal oxygen diffusion along two segments of root. A liquid shell resistance is represented by R_s' (= 5Ω) and an external sink (C = 0) by a connection to earth. Lateral loss of oxygen due to respiration is represented by tapping a constant 2 Amps mid-way along R_1' (the basal segment) and 3 Amps mid-way along R_2' (the apical segment). If the oxygen concentration at the root base, $C = C_o$, is represented by 500V, the current loss to earth, I, (crudely equivalent to R.O.L.) may be calculated (see p.153) and has the value 17.8 Amps. The total effective resistance in the system, R_t, is then given by:

$$R_t' = \frac{V}{I} - R_s'$$

and is found to be 23.089 Ω

Similiarly, the total resistance of the basal segment in situ may be calculated, and is found to be 10.48Ω.

If the basal segment is now "excised" - i.e. C_o = 500V is applied at point X - the apparent total resistance of the system remaining may

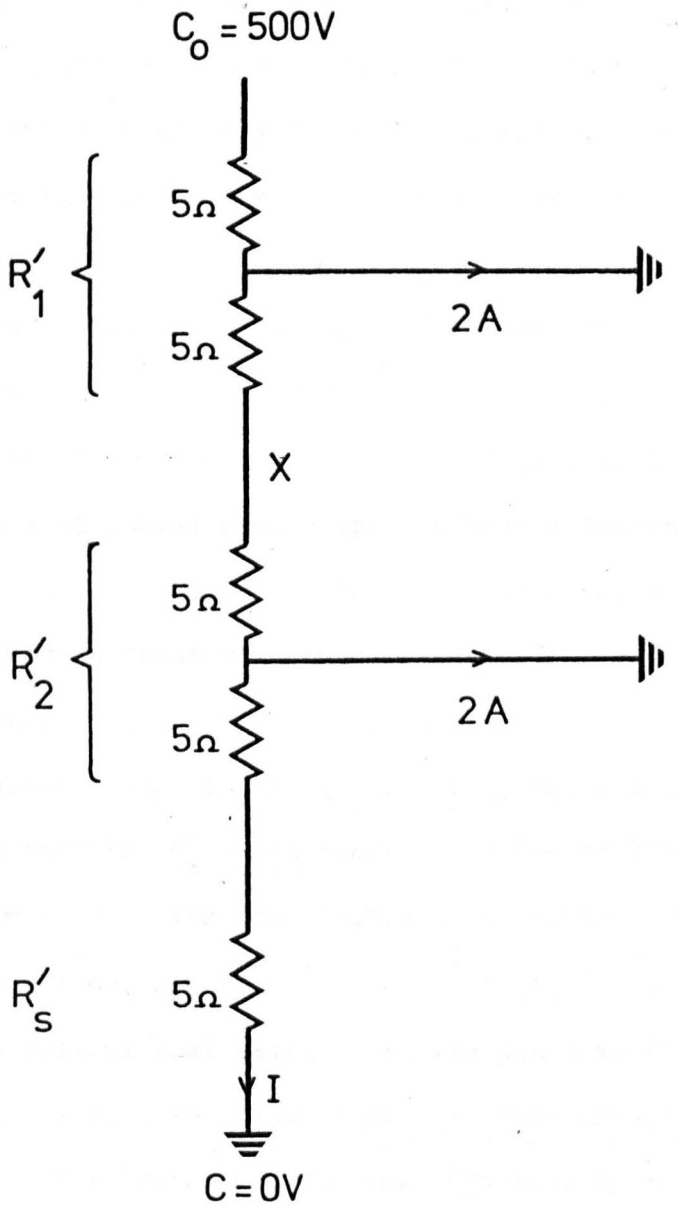

FIG. 7.3 Circuit to illustrate the effective resistance of a plant segment excised and <u>in situ</u>

be recalculated, and has the value 10.465Ω. The apparent resistance of the excised basal segment is then given by the difference in the two values of R_t', i.e. 23.089Ω - 10.465Ω = 12.624Ω. Clearly, this apparent resistance is in excess of the 10.48Ω which the basal segment offered when *in situ*.

It is apparent, therefore, that it is not possible to deduce the total resistance of organs by excising them from the plant and noting the fall in total plant resistance. Data obtained in this way, however, are still meaningful in that they indicate the extent to which the various organs contributed to the overall resistance of the intact plant when *in situ*.

(d) Total Effective Resistance and Liquid Shell Resistance

The concentration-dependent oxygen flux from a root to an ensheathing electrode will vary with the magnitude of the liquid shell resistance, R_s. The occurrence of radial oxygen loss decreases internal oxygen concentration and this, in turn, will alter effective resistance as described above. Thus, effective plant resistance is dependent upon the value of the shell resistance.

Again this concept may be illustrated using the circuit shown in Fig.7.3. If, for example, R_s' is increased from 5Ω to 20Ω the total effective resistance is raised from 23.089Ω to 24.94Ω, whilst a shell resistance of 200Ω increases the value of R_t' to 47.5Ω.

From this it follows that total effective plant resistance deduced using the cylindrical electrode technique will vary with liquid shell thickness, and therefore with root radius. However, in the present study, it is unlikely that this effect of root radius would have been significant since for the range of root radii encountered (about 0.035 - 0.045cm) R_s varied from 5.139×10^5 to 4.033×10^5 s cm^{-3} only. Electrical analogue data indicated that this variation in R_s would influence R_t by a maximum of only 0.1×10^5 s cm^{-3}.

From reasoning identical to that above it may be deduced that just

as liquid shell resistance influences the total effective plant resistance, so too will root wall resistance, since this factor also controls R.O.L. This topic is considered further on p. 149.

The logical conclusion from the above discussion is that it is impossible to measure an absolute total plant resistance using the cylindrical platinum electrode, or other concentration-dependent sensor. An absolute value of total resistance could in theory be obtained only if it was possible to ascertain the internal oxygen concentration at some sub-apical point in the root, together with the oxygen diffusion rate into the root apex. However, although total resistance obtained using the cylindrical platinum electrode must be kept in perspective, being in part a function of the "sensing system", it is a useful concept for comparative illustration of diffusive impedence, as the work described in this chapter will illustrate.

2. The Components of Pseudo-Resistance

(a) Leakage

(i) Leakage from the root

If the internal oxygen concentration of a root situated in anaerobic soil is greater than zero, and providing the root wall is to some degree permeable to oxygen, a gradient of oxygen concentration will arise between the root and the soil. Oxygen will diffuse out of the root along the concentration gradient and the internal oxygen regime will be reduced. The experimental literature dealing with this radial oxygen loss has been reviewed in Chapter 1.

The quantity of oxygen lost by leakage will be influenced in part by the degree and extent of the wall permeability. There is much evidence to suggest that R.O.L. from the roots of wetland plants is restricted to the apical region. Goto and Tai (1957) showed the apical region of rice roots to be highest in oxidising activity and by use of a redox indicator dye Armstrong (1967c) obtained a similar result for Menyanthes trifoliata and Molinia coerulea. Use of the cylindrical Pt electrode has shown that

oxygen leakage is also confined to this region (Fig.2.7 and Armstrong, 1964, 1967b), although Armstrong (1971a) obtained evidence that the basal regions of longer rice roots can regain permeability and suggested that this may be associated with pre-emergent laterals. This observation may explain results of van Raalte (1941) which indicated that the walls of the basal regions of rice roots allow oxygen entry.

Luxmoore et al. (1970b) estimated the root wall permeability of rice roots to O_2 from respiratory data obtained from root segments of known surface area in a solution of 4.4% oxygen. Although the dubious assumption was made that the centres of the root segments were anaerobic, the results indicate a decrease in permeability from 11 x 10^{-4} cm s^{-1} at 0.5cm behind the apex to less than 1 x 10^{-4} cm s^{-1} at 6cm.

In contrast to the situation in wetland plants the root walls of mesophytes appear to be permeable to oxygen along the whole of their length. Healy and Armstrong (1972) have shown that the roots of pea seedlings are permeable to oxygen along their length and Luxmoore et al. (1970b) found that the permeability of maize roots 10cm behind the apex was 50% of the apical value.

The low permeability over the greater length of the wetland root will reduce the total oxygen leakage to a low value and in comparison with respiratory oxygen losses its effect upon the internal oxygen regime is likely to be negligible. In non-wetland plants, on the other hand, leakage may considerably influence the oxygen regime at the apex. Healy and Armstrong (1972) showed that R.O.L. from the apex of a pea root was 25ng $cm^{-2}min^{-1}$ when leakage from the basal parts was prevented by "jacketing" with agar gel, but only 7.5ng $cm^{-2}min^{-1}$ when the jacket was removed.

Since the sub-apical root-leakage component of effective resistance was likely to have been negligible in E.angustifolium (see Fig.2.7) no account of this factor was taken in the present study. The importance of leakage in roots having non-wetland characteristics is discussed further

in Chapter 9.

(ii) Leakage from the aerial parts

In the present study diffusive resistance in the aerial parts of Eriophorum was investigated. It is necessary, therefore, to consider the extent to which leakage of oxygen from the submerged leaves might contribute to this resistance.

Results presented in Chapter 6 have shown that when the aerial parts are unsubmerged an adequate supply of oxygen for root aeration enters the plant through the stomata immediately above the sheath. Consequently, as regards resistance in the aerial parts of unsubmerged plants, diffusion in the sheath region only need by considered. On the other hand partial submergence increases the diffusion path length in the leaves since oxygen must pass to the roots through the submerged parts. In this case leakage from the submerged stomatal leaf surface could influence the passage of oxygen to the roots and contribute to the effective resistance. However, results presented in Chapters 4 and 5 indicated that in all but very large plants the influence of leakage from even totally submerged leaves is negligible compared with respiratory effects. Therefore, it is doubtful whether leakage from the aerial parts will exert an important influence on the internal oxygen regime, and its contribution to effective resistance has not been investigated in the present study.

(b) Respiration

A survey of the literature reveals that respiration is likely to reduce the internal oxygen regime of roots, and so add to the effective resistance. This applies to both wetland and non-wetland species, though the effect in the latter will be greater.

Healy and Armstrong (1972) showed that the R.O.L. from the apex of a pea root increased from 7.5 to 98ng $cm^{-2}min^{-1}$ when respiration was minimised by cooling the root from 23° to 3°C. Working with rice Armstrong (1971a) estimated that for roots of 7-9cm in length respiration reduced oxygen flux from the apex by 50% when the plants had been grown in non-waterlogged conditions, and by 20-30% when grown in waterlogged soil.

The difference was undoubtedly due to the greater porosity of the water-logged roots. Yu et al. (1969) showed that roots of barley, despite a low mean porosity of 2.4%, could attain lengths of 12-13cm in flooded soil; they attributed this to a low respiratory rate.

In contrast to the above workers, Evans and Ebert (1960) concluded that little oxygen is lost from the gas spaces as it passes down the root of Vicia faba. They attributed this to impermeability of the walls of the cells lining the gas spaces. It is difficult to accommodate these results in view of those outlined above and the data presented later in this chapter.

Respiratory oxygen demand is not evenly distributed in the root but is closely associated with the distribution of porosity and tends to decrease with distance from the apex. This is particularly evident in the roots of wetland species (Figs.3.2 and 3.3), and consequently the apex will offer a greater effective resistance than an equal length of root base.

II. RESISTANCES IN ERIOPHORUM ANGUSTIFOLIUM

Several experimental techniques were employed to quantify physical (pore space) resistance, R_p, and total resistance, R_t, in intact plants and various organs (leaf, root, root wall, root shoot junction).

A. RESISTANCE IN THE INTACT PLANT

1. Methods

(a) Pore Space Resistance

(i) Theory

Providing the internal oxygen pressure is above the critical value the flux, f, from a root apex to an ensheathing Pt electrode can be expressed by the equation:

$$f = \frac{C_o}{(R_p + R_s)A_r} - \text{Resp.} \quad g\ cm^{-2}\ s^{-1} \qquad (7.7)$$

where:

C_o = the O_2 concentration at the point of entry into the plant (g cm^{-3})

R_p = the physical resistance within the plant, including any resistance in the apical root wall (s cm^{-3})

Resp.= a quantity determined by the respiratory activity in the plant (g $cm^{-2}s^{-1}$) - see p.52

If the external oxygen concentration is increased to a value C_o' g cm^{-3}, the new flux, f', is given by:

$$f' = \frac{C_o'}{(R_p+R_s)A_r} - \text{Resp.} \quad \text{g cm}^{-2}\text{s}^{-1} \qquad (7.8)$$

These two equations can be combined with respect to Resp., which remains constant above the C.O.P., to give:

$$R_p = \frac{C_o' - C_o}{(f' - f)A_r} - R_s \qquad \text{s cm}^{-3} \qquad (7.9)$$

(ii) Procedure

The procedure was identical to that employed for the gas-mixtures method of measuring critical oxygen pressure (Chapter 4). The oxygen concentrations used were 13.64% and 20.41% (Air).

(b) Total Resistance

The total resistance of the plants used in the experiments described above was determined by substitution of the flux when C_o = 20.41% into equation 7.6.

2. Results

Non-metabolic resistance (eight experiments) ranged from 1.556×10^5 to 2.390×10^5 s cm^{-3}, with a mean of 2.056×10^5 s cm^{-3}. Values of total resistance fell in the range 3.102×10^5 to 4.715×10^5 s cm^{-3}, mean 3.782×10^5 s cm^{-3}. Although respiration certainly increases the overall diffusive resistance its contribution cannot be regarded as excessive. This is a likely consequence of the aerenchymatous structure, oxygen consumption being minimised in the highly porous tissues which constitute the bulk of the plant body.

B. THE INFLUENCE OF DIFFUSION PATH LENGTH : RESISTANCE IN LEAVES AND ROOTS

In the experiments described above the contribution to plant resistance made by the unsheathed portion of the aerial parts would be negligible, since the oxygen source to the roots was effectively applied via the stomata immediately above the sheath. (see Chapter 6). In order to investigate resistance in the aerial parts it was necessary to apply the oxygen source some distance along the leaves, whilst by altering the point of application the effect upon resistance of diffusion path length could be studied.

1. Method

The modifications made to the basic experimental assembly for measuring R.O.L. (Fig.2.5) are shown in Fig.7.4. The arrangement of the two bungs on the supporting rod allowed progressive excision of the aerial parts whilst the root was left supported in the lower bung. The electrode fitted into a recess in the lower bung, enabling the root to be cut until the apical 1.5cm only remained. The experimental procedure was as follows.

A plant with all but one leaf removed, or a whole plant with the leaves cut to equal length, was arranged as shown in Fig.7.4 and lowered into the blackened cylinder until completely submerged. The diffusion current was allowed to fall to zero and the plant left for several minutes to exhaust the internal atmosphere of oxygen. The plant was then raised slightly to expose about 0.2cm of leaf. The leaf ends were then cut with a razor blade and, if necessary, dried with an air stream. The diffusion current was allowed to re-equilibrate.

The diffusion path length between the atmosphere and electrode was then shortened by raising the plant and excising a measured length of leaf, the effect on oxygen flux being monitored as a change in diffusion current. This process was repeated down the plant. The stem was excised as a whole, leaving the root severed at the base, and this in turn was cut

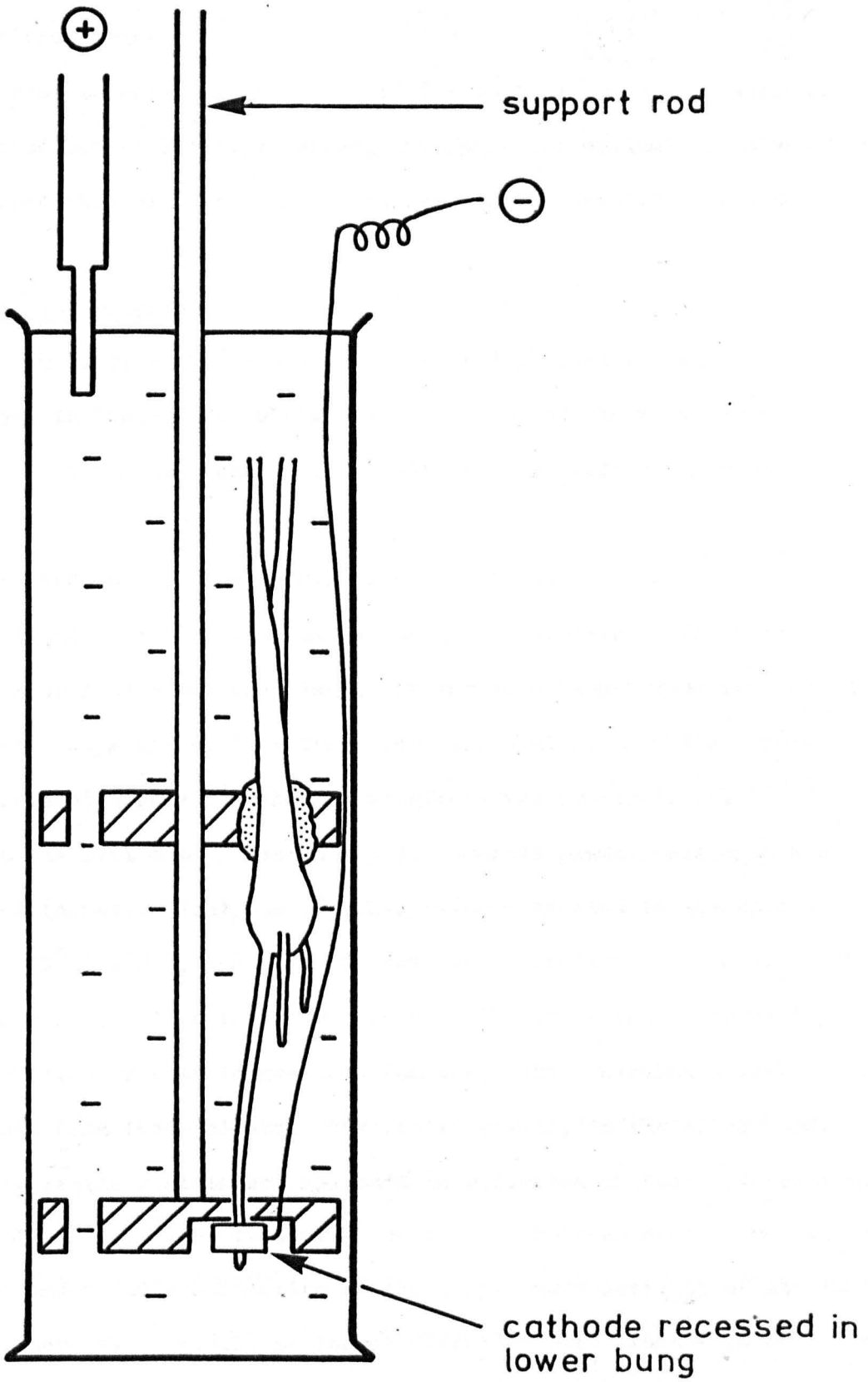

FIG. 7.4 Apparatus used in diffusional resistance experiments.

to finally leave 1.5cm of root apex. At each current equilibrium the plateau voltage was checked and any necessary adjustments made before recording the current.

In order to determine the effect of respiration, some experiments were carried out at 3°C by immersing the measuring cylinder in ice-water; it was hoped that at this temperature respiratory activity would be minimised.

2. Results and Discussion

The R.O.L. from the root apex is plotted against apparent diffusion path length in Fig.7.5 for whole and single-leaved plants at 23°C and 3°C. The position and length of the stem is indicated on each curve by arrows.

There was an increase in R.O.L. with decreasing path length in all plants but the variation in flux was much less pronounced in those plants in which respiration was minimised. At any path length flux from the 3° plants was always higher than that from plants at 23°C, whilst whole plants produced higher fluxes than single-leaved preparations.

From the flux data given in Fig.7.5 overall plant resistance was calculated (equation 7.6), the 3° values being converted to equivalent values at 23° (p.55), and this is shown as a function of apparent path length in Fig.7.6. The resistance is markedly increased in respiring plants, particularly at longer path lengths; this correlates with the lower flux values from these plants. The cooled plants, on the other hand, offer relatively little resistance, and this is reflected in their higher flux values. This difference in overall resistance between cooled and uncooled plants is undoubtedly a function of the respiratory activity of the latter.

The decrease in R.O.L. at longer diffusion path lengths is a result of the increased diffusive resistance associated with lengthening of the diffusion path. However, the shape of the resistance v. path length curves (Fig.7.6) requires further comment. If the plants had uniform cross-section area and zero respiration, and if D_e was constant along the whole

FIG. 7.5 Apical oxygen flux as a function of apparent diffusion path length.

◇ Whole plant, 3°C } Data converted to
Δ Single leaf, 3°C } values at 23°C
o Whole plant, 23°C
□ Single leaf, 23°C

The position and length of the stem is indicated on each curve by arrows.

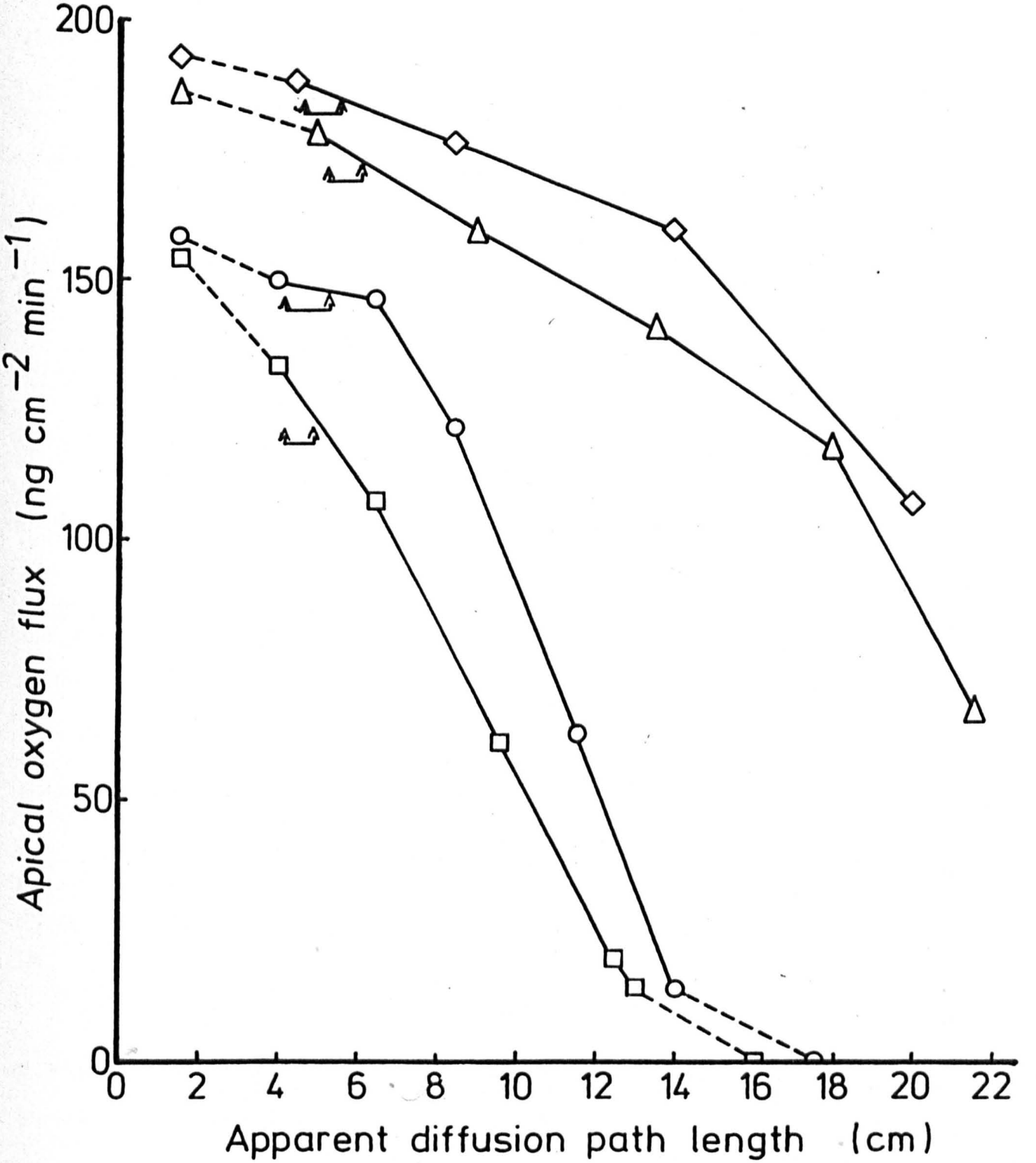
200
150
100
50
0
0
2
4
6
8
10
12
14
16
18
20
22
Apical oxygen flux (ng cm^{-2} min^{-1})
Apparent diffusion path length (cm)

FIG. 7.6 Effective diffusional resistance as a function of apparent path length.

◇ Whole plant, 3°C
Δ Single leaf, 3°C
} Data converted to values at 23°C

o Whole plant, 23°C

□ Single leaf, 23°C

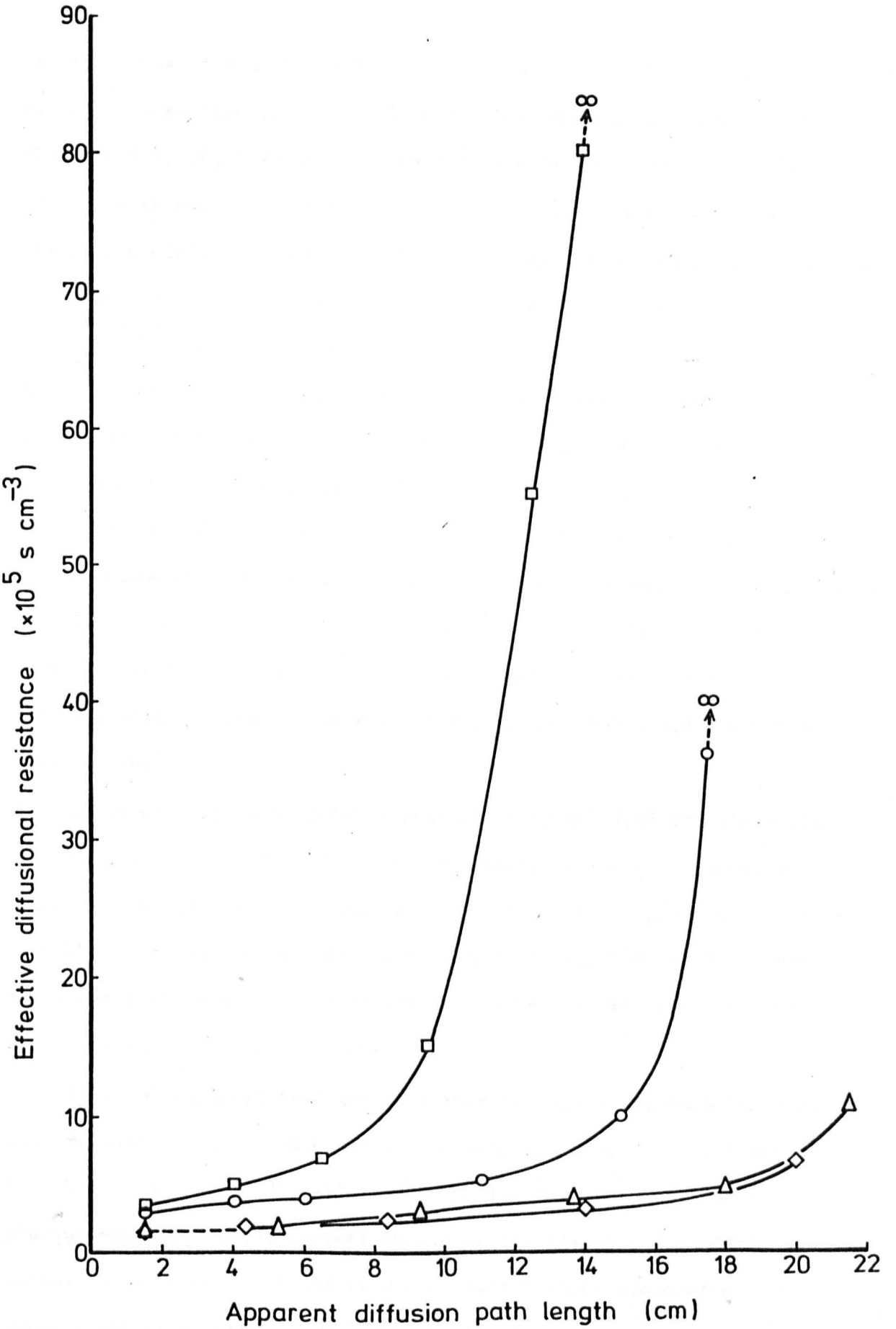
Effective diffusional resistance (×10^5 s cm^-3)
Apparent diffusion path length (cm)
0
10
20
30
40
50
60
70
80
90
0
2
4
6
8
10
12
14
16
18
20
22
∞
∞

length of the plant, then reference to equation 7.4 shows that resistance would increase linearly with diffusion path length. All the experimental plots in Fig.7.6, however, show some degree of curvature, this being much more pronounced for the respiring plants. In the case of the cooled plants the plots are approximately linear for about 15cm path length and then curve slightly over the remaining increase in diffusion path. The linear portion of the curves may be attributed to the high porosity and fairly constant cross-sectional area of the leaves for much of their length, whilst the decreased porosity and cross-sectional area at the leaf apex accounts for the disproportionate increase in resistance at longer path lengths; residual respiration may have added to the effect. The enhanced curvature in the respiring plants is undoubtedly due to the accumulation of respiratory activity associated with lengthening of the diffusion path, superimposed upon the diffusive factors discussed above; the acropetal increase in leaf respiration rate (Table 3.1) may have added to the curvature.

In general lower resistance patterns were obtained for the whole plants, both at 3° and $23^{\circ}C$. The most likely explanation seemed to be that in these plants the leaves act as resistances in parallel, so that the overall resistance of the shoot system is less than that offered by the individual leaves. This effect is comparable with the parallel arrangement of stomata discussed in Chapter 6.

It is of interest that the stem does not appear to contribute any more resistance to the plant than, for example, a comparable length of leaf base. Conway (1937) attributed the resistance in the stock of Cladium mariscus to the compact nature of its tissues, for although the cortex had a porosity of 35% it formed only a small proportion of the whole stock, the porosity of the stele of which was as low as 6%. In addition Conway suggested that the diffusion path through the cortex would be tortuous. The stem of E.angustifolium, with its comparatively high respiratory rate and overall porosity of about 10%, might also be

expected to offer a high resistance to the flux of oxygen. However, a detailed examination indicated that the cortex may occupy up to 60% of the total volume. No attempt was made to measure experimentally the porosity of the cortex alone, which may therefore be appreciably higher than the 10% overall porosity; Plate 7.3 tends to confirm this. Also, the diffusion path between leaf and root in the Eriophorum stem may be much shorter than the overall length of the stem, since leaf and root bases lie in close proximity (Plate 7.2). Resistance in the stem is discussed in more detail in the following section.

It must be pointed out that great care must be taken when the cooling method is used to determine non-metabolic resistance. Residual respiration, blockage of the exposed lacunae by liquid creep, and possibly even condensation within the finer intercellular spaces could all contribute to elevated R_p values. For example, in the experiments described above the apparent pore-space resistance per cm of mid-leaf ranged from 0.085 to 0.20×10^5 s cm^{-3}. When resistance in the lacunar diaphragms is taken into account (p.150), the effective lacunar porosities calculated from these two values of R_p are 25% and 2.5% respectively. The former value is in good agreement with the mid-leaf porosity determined earlier (Fig.3.1), whereas the latter is extremely low. Clearly, residual respiration and/or blockage of the gas spaces had elevated the apparent R_p of 0.20×10^5 s cm^{-3} above the true value.

The cooling method must be regarded, therefore, as less reliable than the gas-mixtures method (p.138) for the estimation of non-metabolic resistance. However, since R_p in the root and leaf is easily calculated by substitution of porosity data (Chapter 3) into equation 7.4, its further experimental investigation was not pursued. For the determination of non-metabolic resistance in the stem and lacunar diaphragms, where the necessary porosity data is not easily obtained, the gas-mixtures method proved a convenient technique.

PLATE 7.2: Eriophorum angustifolium; thick hand section (ca. 0.05cm) through the stem showing the short diffusion path between the bases of the root and outer leaves (x 8).

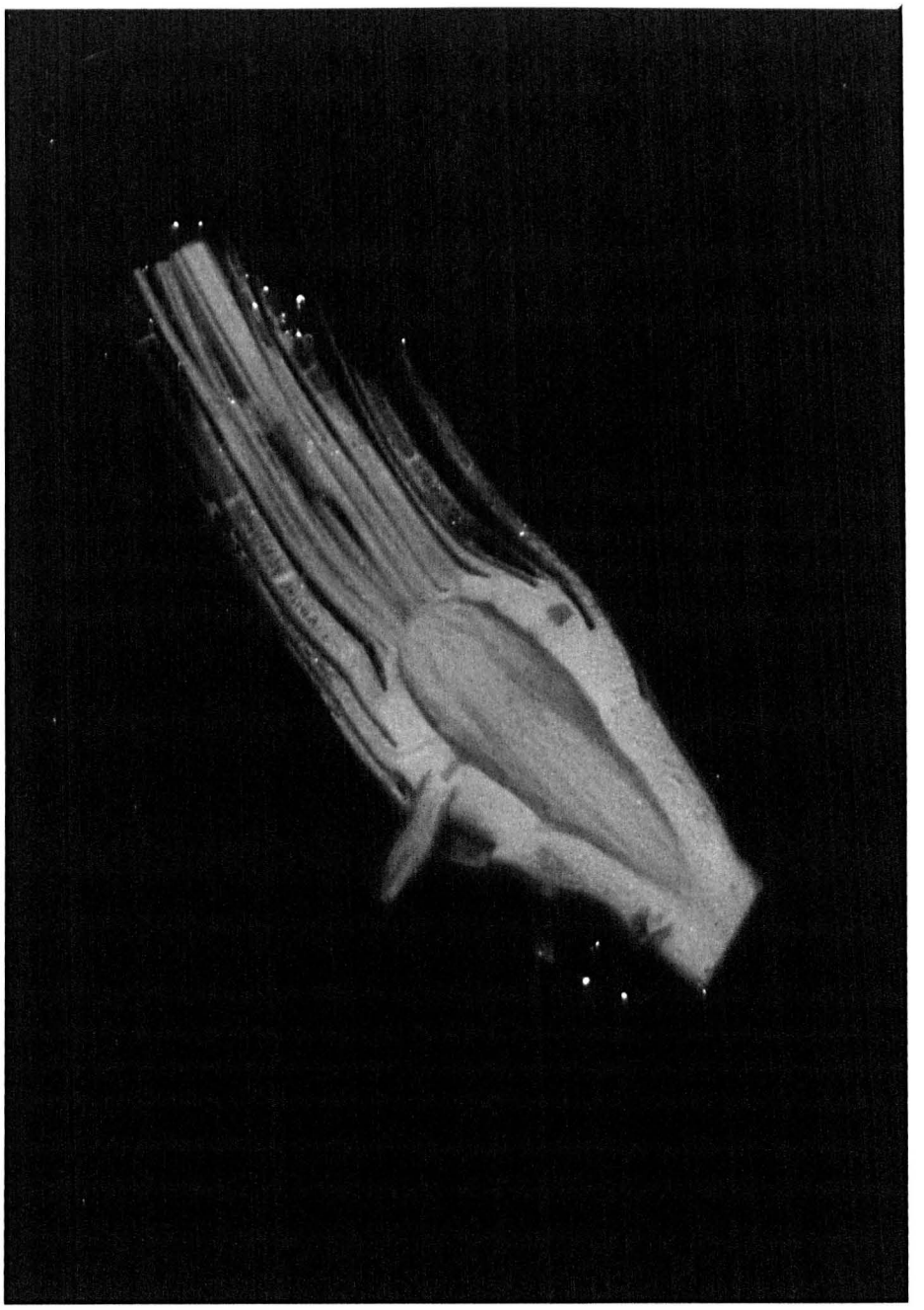

C. RESISTANCE IN THE STEM/ROOT-SHOOT JUNCTION

There is very little literature dealing with the resistance to oxygen transport offered by the junction of the root and shoot. Laing (1940b) stated that gases are unable to pass readily into a very young root due to a compact mass of undifferentiated tissue at the root base; as the root grows the compact region narrows and gas movement into the root becomes easier. Coult (1964) considered that in Menyanthes trifoliata diffusion of oxygen across the compact cortical tissues at the root base would be in the liquid phase and would contribute little to the oxygen supply to the root. Conway (1937) found that the stock of Cladium mariscus, taken as a whole, offered appreciable resistance to the passage of air, but the actual junction of the root and stock did not.

In the present study two methods were employed to evaluate the resistance to oxygen diffusion offered by the root-shoot junction of E.angustifolium.

1. Methods

(a) Gas Mixtures

The theory of this method is that given for the determination of the pore space resistance of intact plants (p.138). The procedure was as follows.

A plant was arranged for R.O.L. measurement in the double bung system shown in Fig.7.4 with the liquid just covering the base of the experimental root. Prior to application of the gases the leaves were excised with a razor blade as close as possible to the stem and the cut ends dried with an air stream. The available gas mixtures were air and 40.4% O_2. These were applied to the cut leaves as described in Chapter 4, but in this case a small glass tube replaced the measuring cylinder as a leaf chamber.

When equilibrium currents had been obtained for both gases the plant was raised in the measuring cylinder and the root cut immediately below the stem. The cut root end was dried with an air stream and the gases again

applied in sequence to obtain the diffusion currents after stem excision.

The difference in R_p before and after excision of the stem gives a value for the non-metabolic resistance in the stem/root-shoot junction, R_{pj}.

The total resistance contributed to the plant by the junction, R_{tj}, was given by the difference in R_t before and after stem excision by substitution of the flux in air into equation 7.6.

(b) Excision of the Stem

This method made use of the 23° and 3°C resistance data obtained by the "excision procedure" described in the previous section (p.139). Although not designed solely for the estimation of root-shoot junction resistance (i.e. portions of leaf and root base were excised with the stem), it enabled estimates to be made of R_{pj} and R_{tj}.

2. Results

Using the gas mixtures method non-metabolic resistance in the root-shoot junction ranged from 0.057×10^5 to 0.130×10^5 s cm^{-3}. Total resistance in the junction when in situ had contributed 0.084×10^5 to 0.202×10^5 s cm^{-3} to the total resistance of the plant. Considering the relatively high respiratory rate of the stem tissues (Chapter 3) the respiratory component did not markedly increase the resistance values. It is possible that this was due to the short diffusion path between the leaf and root bases referred to earlier (p.142).

Values of R_{pj} obtained by the second method ranged from 0.10×10^5 to 0.28×10^5 s cm^{-3}, whilst the total resistance contributed from 0.235×10^5 to 0.586×10^5 s cm^{-3} to the plant resistance. Since this second method was not intended specifically for the estimation of root-shoot junction resistance, relatively long lengths of leaf and root base were excised with the stem, and this is a likely explanation of the higher values of R_{pj} and R_{tj}. Hence, the results obtained by the gas mixtures method must be considered the more reliable.

An important point to emerge from the above results is that the low

resistance in the root-shoot junction provides strong evidence for the continuity of the gas space system between leaves and roots. This was confirmed by anatomical investigation, and in Plate 7.3, which shows a transverse section through the root base in the region of the root-shoot junction, the uninterrupted intercellular space system between the root and stem cortices may be clearly seen.

D. RESISTANCE IN THE ROOT WALL

1. Introduction

There is evidence that in a number of species the diffusive resistance offered by the apical root wall at normal temperatures is very low or negligible. Armstrong (1967b) found that if root wall resistance was assumed to be zero the theoretical flux values based on the measured internal oxygen concentrations of several wetland species (not including E.angustifolium) corresponded closely to values measured by the cylindrical electrode method. Working with mustard seedlings Greenwood (1967b) estimated the maximum root wall resistance to be equivalent of only 12 μm of water path (i.e. one cell layer); for a root segment of length 0.5cm and radius 0.05cm the corresponding wall resistance is only 0.098×10^5 s cm^{-3} (see equation 4.8). Luxmoore et al. (1970b) obtained root wall permeabilities for rice and maize of 11×10^{-4} and 8×10^{-4} cm s^{-1} respectively; corresponding wall resistances for root segments of length 0.5cm and radius 0.05cm are 0.058×10^5 and 0.080×10^5 s cm^{-3} (i.e. about 10 to 12 μm of water path). The actual liquid diffusion path offered by the apical rice root wall (i.e. the cell layers beyond the observable cortical gas spaces) is 50 to 60 μm. Armstrong and Wright (1975) have suggested that the discrepancy between observed and effective wall thickness may be partly accounted for by cytoplasmic streaming.

During the present study it became apparent that the apical root wall resistance in Eriophorum was not negligible. If wall resistance was ignored, and the electrical analogue programmed using other resistances

PLATE 7.3: Section through the root-shoot junction of E.angustifolium, showing the continuity of the gas spaces in the cortices of root and stem (x 270).

Note: Satisfactory penetration of the stem tissues could be obtained only by use of an ultra-low viscosity resin (Taab Laboratories, 52 Kidmore Road, Emmer Green, Reading, England).

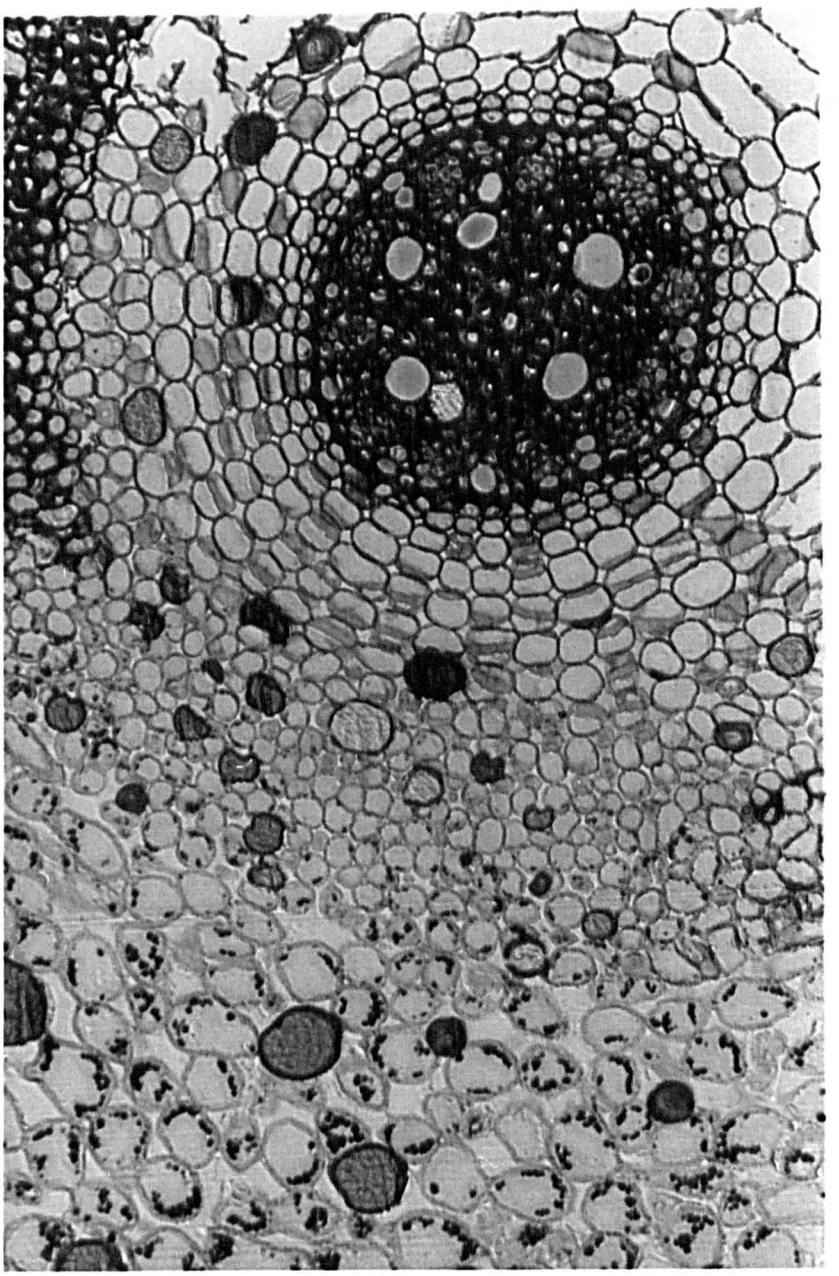

quantified in this chapter, predicted flux values were substantially higher than those measured experimentally. Experimental and analogue data could be brought into agreement simply by programming for wall resistance. In view of this, and because a knowledge of wall resistance is of great importance to the prediction of internal oxygen concentrations using the cylindrical electrode technique (see p.53) the apical root wall resistance in Eriophorum at 23°C was measured experimentally.

2. Method

Plants were arranged for R.O.L. assay as described in Chapter 2, the apical radius of the experimental root having in each case been previously measured. When the diffusion current had equilibrated the plant was removed and the root system immersed in a bath of acid citrate (see Chapter 4). The portion of the root previously contained within the electrode was excised and using spade-ended forceps was gently squeezed beneath the cup of a gas analyser (Chapter 4) to extract the gas from the intercellular spaces. The whole procedure was carried out as rapidly as possible to minimise changes in the oxygen content of the gas to be extracted. The oxygen concentratinn in the gas sample was then determined as described on p.63.

3. Theory

The total diffusive resistance offered by the apical root wall, $R_{t,wl}$, is given by:

$$R_{t,wl} = \frac{60Cr}{f\ A_r} - R_s \quad s\ cm^{-3} \qquad (7.10)$$

where:

C_r = the gas phase oxygen concentration in the root (measured by gas analysis) ($g\ cm^{-3}$)

f = the experimental flux ($g\ cm^{-2} min^{-1}$)

However, just as total plant resistance varies with oxygen concentration (p.130), so will respiration in the root wall cause $R_{t,wl}$,

(obtained using equation 7.10), to vary with C_r. Consequently, for each experiment, R_{wl} at the standard oxygen concentration (20.41%) was estimated using the following procedure.

The oxygen concentration within the root, C_r, may be related to the concentration at the root surface, C_{wl}, and to the oxygen flux from the root, f, by an equation which embraces the oxygen consumption and diffusivity in the wall layers:

$$C_r - C_{wl} = \frac{Mr_o^2}{4D_e}\left(\frac{r_i^2}{r_o^2} + 2\log\left(\frac{r_o}{r_i}\right) - 1\right) + r_o \log\left(\frac{r_o}{r_i}\right)\frac{f}{D_e} \quad g\ cm^{-3} \qquad (7.11)$$

(for derivation see Appendix 4)

where:

M = the rate of oxygen consumption by the root wall, assumed uniform in the radial direction ($g\ cm^{-3}s^{-1}$)

r_o = the root radius (cm)

r_i = r_o minus the thickness of the root wall, the mean value of which was 65μm, S.D.$\pm$ 2μm (cm)

D_e = the effective diffusion coefficient in the root wall (cm^2s^{-1}), assumed uniform in the radial direction.

Using a value for M of $75ngO_2\ cm^{-3}s^{-1}$, the mean respiratory rate of the Eriophorum root apex (Fig.3.3) and experimental values for C_r, C_{wl}, f, r_o and r_i, D_e may be calculated. This value may then be substituted back into equation 7.11, and the flux predicted when C_r is ascribed a value of 268.7×10^{-6} g cm^{-3} (i.e. 20.41%). Finally the flux so obtained may be substituted into equation 7.10 to obtain the total wall resistance at the standard oxygen concentration. The values of $R_{t,wl}$ so obtained are necessarily approximate because of the possible error introduced in assuming a wall respiratory rate of $75ng\ cm^{-3}s^{-1}$. However, such an error is likely to be minimal, since variation in root wall respiratory rate, even by a relatively large amount, has little effect on $R_{t,wl}$. For example, equation 7.11 may be used to show that in a root of radius 0.05cm, with a

wall of thickness 65μm, total wall resistance (at 20.41% oxygen concentration) is 1.26×10^{5} s cm^{-3} when respiratory rate is 50ng $cm^{-3} s^{-1}$ and 1.29×10^{-5} s cm^{-3} when M is 100ng $cm^{-3} s^{-1}$.

Non-metabolic resistance in the root wall, $R_{p,wl}$, may be estimated by substitution of the values of D_e, obtained from equation 7.11 as described above, into equation 4.8.

The permeability of the apical root wall to oxygen, $Perm._{wl}$, may be derived from $R_{t,wl}$ and $R_{p,wl}$, by the relationship:

$$Perm._{wl} = \frac{1}{R_{wl} A_r} \quad cm\ s^{-1} \qquad (7.12)$$

4. Results

The results are summarised in Table 7.1. The gas samples from the roots showed that the oxygen concentration within the apices, C_r, had a mean value of 14.6%, S.D. ± 1.17%. This figure is higher than those obtained by various workers for other wetland plants: e.g. Menyanthes trifoliata, 11.2% (Coult and Vallance, 1958); rice, 8.4% (van Raalte, 1944); Spartina alterniflora, 3.5 - 5.0% (Teal and Kanwisher, 1966); Schoenus nigricans, 12.5 - 13.5% (Armstrong, 1967b).

In all the Eriophorum plants studied a wall resistance was evident. Uncorrected total resistance had a mean value of 1.75×10^{5} s cm^{-3}, S.D. ± 0.95×10^{5} s cm^{-3}; the corresponding mean wall permeability was 6.97×10^{-5} cm s^{-1}, S.D. ± 4.86×10^{-5} s cm^{-3}. This permeability is a factor of ten less than the values obtained for rice and maize by Luxmoore et al. (1970b) (p.145), reflecting the greater resistance in the Eriophorum apical root wall. Total wall resistances at the standard (20.41%) oxygen concentration differed only slightly from the uncorrected resistances, the mean value being 1.68×10^{5} s cm^{-3}, S.D. ± 0.93×10^{5} s cm^{-3}. Calculations based on equation 7.11 show, however, that the apparent wall resistance becomes increasingly significant at low internal oxygen concentrations (C_r), since the oxygen consumed by the root wall is then no longer negligible compared with that lost by leakage.

TABLE 7.1: INTERNAL APICAL OXYGEN CONCENTRATION, AND RESISTANCE AND EFFECTIVE DIFFUSION COEFFICIENT IN THE APICAL ROOT WALL OF *E.ANGUSTIFOLIUM*

Root Radius	Internal oxygen conc.		Wall resistance			Water path equivalent to $R_{p,wl}$	Effective diff.coeff.	Wall.Perm. (from $R_{p,wl}$)
	From analysis C_r	From flux $C_{r,ex}$	Total uncorrected $R_{t,wl}$	Total corrected $R_{t,wl}$	Non-metabolic $R_{p,wl}$			
(cm)	(%)	(%)	($x10^5$ s cm^{-3})	($x10^5$ s cm^{-3})	($x10^5$ s cm^{-3})	(μm)	($x10^{-5}$ cm^2 s^{-1})	($x10^{-5}$ cm s^{-1})
0.0435	12.9	8.0	2.38	2.28	2.30	177	0.70	3.18
0.034	15.4	14.0	0.55	0.47	0.51	47	4.14	18.35
0.0415	15.7	8.9	3.09	3.00	3.00	204	0.57	2.55
0.0345	15.1	12.2	1.16	1.12	1.14	79	1.82	8.09
0.037	15.7	9.1	3.23	3.14	3.15	189	0.61	2.37
0.036	13.9	10.8	1.34	1.29	1.32	93	1.51	6.70
0.0415	12.7	9.8	1.19	1.15	1.17	97	1.41	6.87
0.0375	15.3	9.9	2.41	2.36	2.38	156	0.80	3.57
0.0335	13.8	11.7	0.88	0.85	0.88	61	2.45	10.80
0.038	15.5	12.1	1.24	1.19	1.23	93	1.52	6.81

NOTE: Apical root wall thickness taken as 65μm

In Fig.7.7 uncorrected total wall resistance is shown as a function of total plant resistance (obtained using equation 7.6); it can be seen that the relationship is significantly linear (P. = 0.01). The broken line is the regression line for the "standardised" wall resistance. The graph indicates that at values of total plant resistance greater than about 1.6×10^5 s cm^{-3}, total wall resistance is an important component of total plant resistance. At plant resistances less than 1.6×10^5 s cm^{-3} wall resistance is probably negligible. However, the contribution of total wall resistance to total plant resistance is not merely additive; it has already been pointed out (p.134) that the presence of a wall resistance, by virtue of its effect on R.O.L., will increase the apparent total resistance in the rest of the plant.

Non-metabolic resistance in the root wall (mean 1.71×10^5 s cm^{-3}, S.D. $\pm$ 0.92×10^5 s cm^{-3}) was little different from the total resistance. This implies that the respiratory component contributes only a small amount to the root wall resistance.

In all but two experiments the water path equivalent to the non-metabolic wall resistance was substantially greater than the measured thickness of the root wall (i.e 65μm - p.147). This is in marked contrast to the situation in rice and maize (p.145), for which Armstrong and Wright (1975) have suggested that cytoplasmic streaming may increase diffusivity in the wall layers (see p.145). The low effective diffusivity in the Eriophorum root wall is probably explained by suberisation; in the two plants where wall resistance was low suberisation may have been minimal. The effective diffusion coefficients in these two root walls were higher than that in water; again it is tempting to invoke cytoplasmic streaming as an explanation of this observation.

An important effect of root wall resistance is to cause the internal oxygen concentration deduced from flux data to be less than the true value. Thus, if equation 2.9 is to be used for estimating internal oxygen concentration a correction must be applied to take account of resistance in the

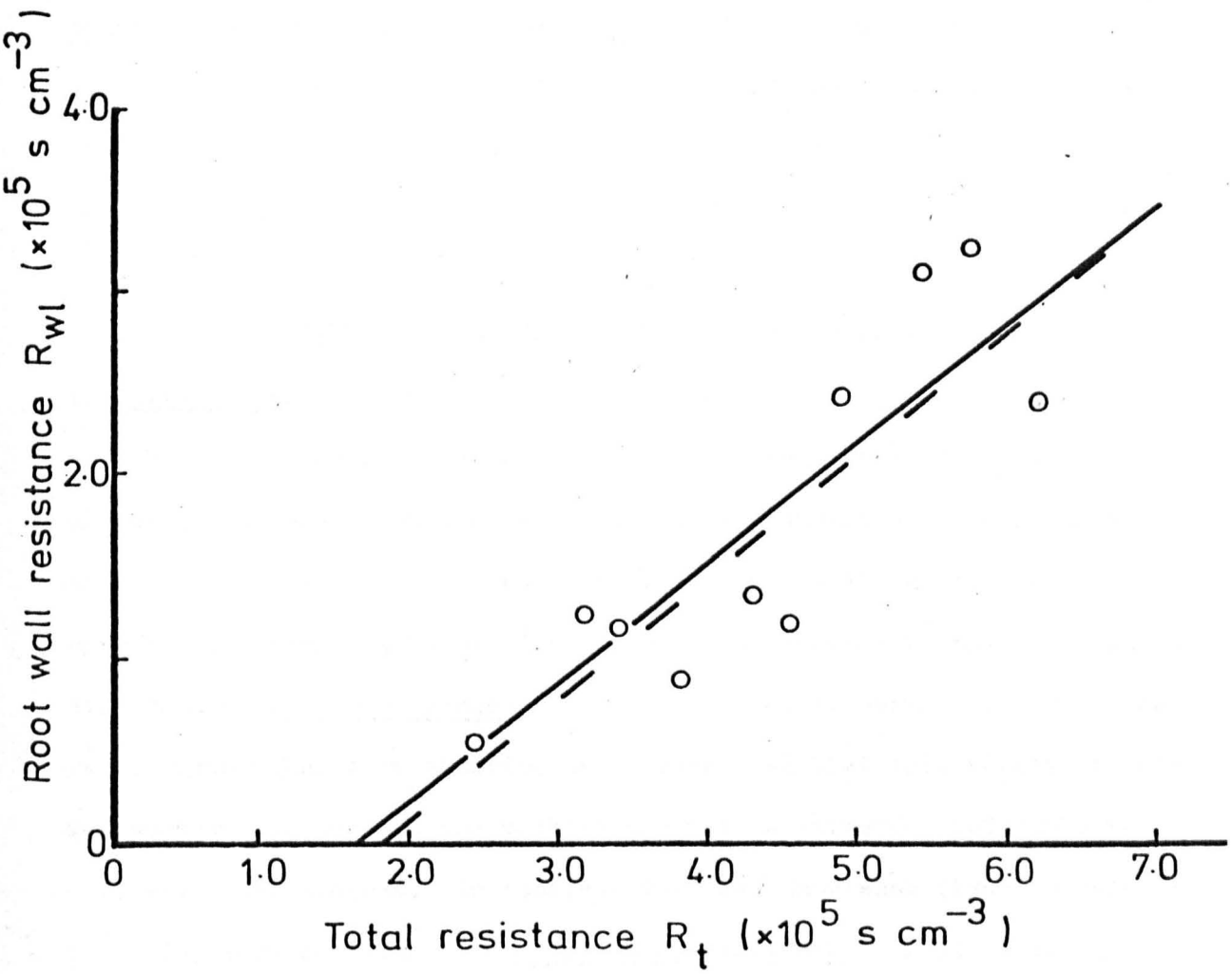

FIG. 7.7 Apical root wall resistance as a function of total plant resistance at 23°C

$$y = 0.6487x - 1.089$$

$$r = 0.830$$

root wall. If the internal concentration calculated from flux data is $C_{r,ex}$, and the actual concentration (found by gas analysis) is C_r, a plot of the ratio $C_{r,ex} : C_r$ against total plant resistance, R_t, is significantly linear (Fig.7.8). If the total resistance of any experimental plant is known, $C_{r,ex}$ may be corrected for wall resistance by dividing by the appropriate value of $C_{r,ex} : C_r$ obtained from Fig.7.7. If total plant resistance is not known a less accurate correction would be division by the mean value of $C_{r,ex} : C_r$.

E. RESISTANCE IN THE DIAPHRAGMS OF THE LEAF.

1. Introduction

Reference has already been made to the occurrence of porous diaphragms in the lacunae of wetland plants (Chapter 3). Opinions differ as to the extent to which these structures impede the diffusive flow of oxygen. For example, Barber (1956, 1961) has shown that the pores in the diaphrams of Equisetum limosum become occluded at certain times of the year; using mass flow experiments he concluded that this results in high resistance. However, these results may not be directly applicable to diffusive flow systems. In contrast Teal and Kanwisher (1966) concluded that diaphragm resistance in Spartina alterniflora is negligible.

Non-metabolic resistance offered by a diaphragm, R_{pd}, will be a function of effective porosity and diaphragm thickness. Although the latter is easily measured, the former is difficult to determine by direct observation due to the surface appearance of the tissue and possible tortuosity of the pores (see Plate3.6a). Little information is available in the literature, the only porosity value known to the author being 0.58% estimated by Coult (1964) for diaphragms (lamellae) in the rhizome of Menyanthes trifoliata.

In the present study two methods were used to estimate the effective porosity and non-metabolic resistance in the diaphrams of Eriophorum.

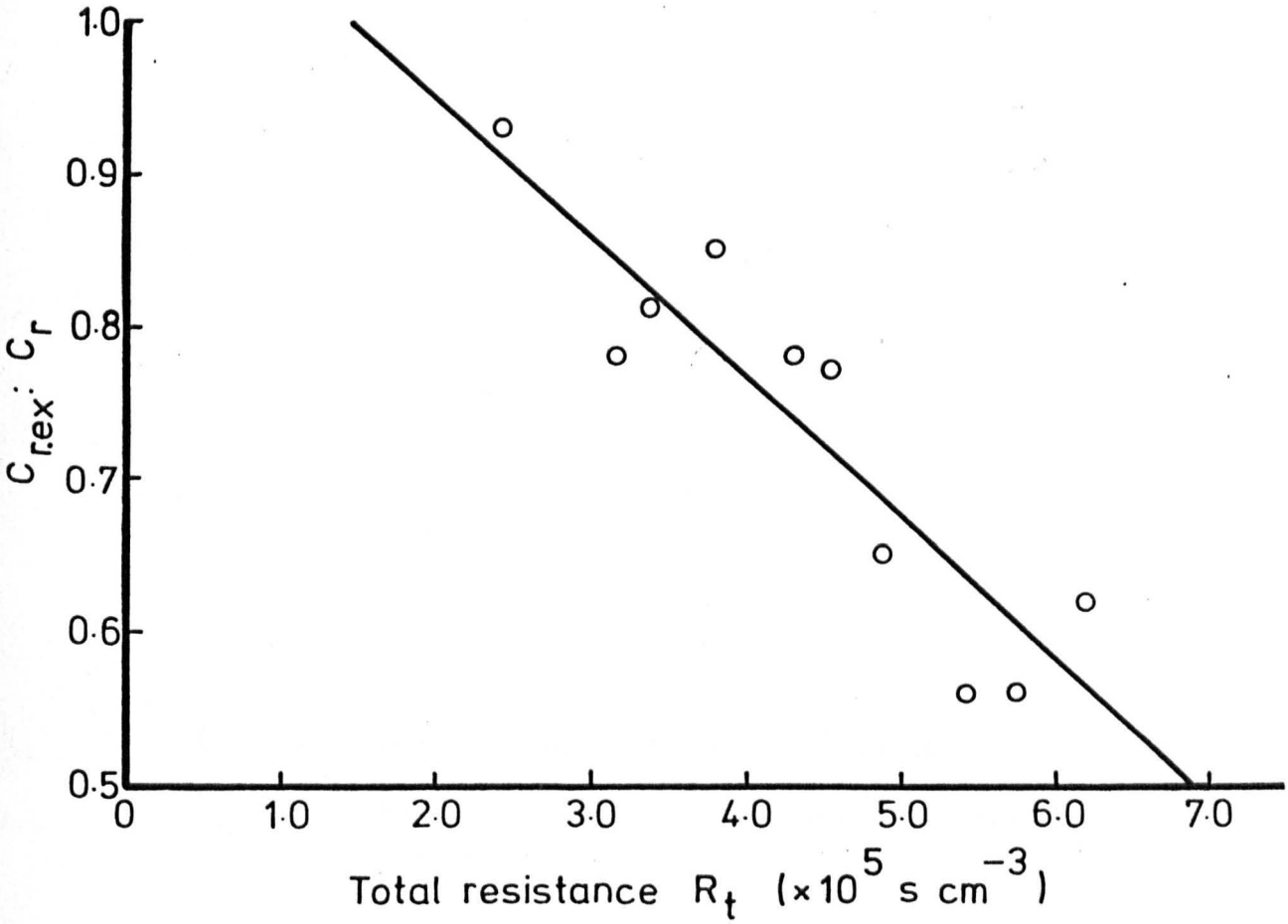

FIG. 7.8 The ratio $C_{r.ex}$: C_r as a function of the total effective diffusional resistance of the plant (R_t)

$C_{r.ex}$ Oxygen concentration within the root apex, calculated from the radial oxygen loss (p.149) and assuming zero wall resistance

C_r Oxygen concentration in gas samples extracted from the root apex.

$$y = -0.091x + 1.13$$

$$r = -0.839$$

2. Methods

(a) Excision of Leaf Segments

This method made use of resistance data obtained from single-leaved plants at 3°C as described on p. 139. Measurements were confined to the mid-leaf segments to take advantage of the uniform cross-sectional area of the leaf in this region.

The length of the excised mid-leaf segments, L_l, was measured using a travelling microscope. The number of diaphragms, n, in each air channel was recorded, as was the mean diaphragm thickness, L_d. Cross-sectional area of the leaf segments A_{xl}, was determined by weighing scale drawings of transverse sections.

The non-metabolic diffusive resistance due to the diaphragms in the segment, R_{pdl}, is given by:

$$R_{pdl} = R_{pl} - \frac{L_l}{D_o A_{xl} \epsilon_l} \quad s\ cm^{-3} \qquad (7.13)$$

where:

ϵ_l = the lacunar porosity of the leaf segment

R_{pl} = the overall non-metabolic resistance of the leaf segment ($s\ cm^{-3}$)

The validity of this equation depends upon the assumption that oxygen was unable to by-pass the diaphragms by diffusing between adjacent lacunae; clearly, this would effectively reduce the apparent diaphragm resistance. Although gas spaces were present within the tissues of the inter-lacunar walls as seein T.S., the lateral surfaces of the walls (i.e. those adjacent to the lacunae) seemed devoid of pores.

Equal numbers of diaphragms occur along air channels of equal length; therefore, R_{pdl} may be considered due to n diaphragms, each of area equal to that of the total lacunar space of the leaf segment, $A_{x,lac}$, acting in series. The resistance of one such diaphragm, R_{pd}, is given by:

$$R_{pd} = \frac{R_{pdl}}{n} \quad s\ cm^{-3} \qquad (7.14)$$

The effective porosity of the diaphragm tissue, ϵ_{ed}, may be

estimated from R_{pd} by:

$$\epsilon_{ed} = \frac{L_d}{D_o A_{xl} R_{pd}} \qquad (7.15)$$

(b) Gas Mixtures

The theory and procedure for this method were identical to those for the gas mixtures method for estimating resistance in the root-shoot junction (p.143). A single-leaved plant, with the leaf cut in the mid-region, was arranged with 0.2cm of leaf exposed to the two gas mixtures. Equilibrium currents were obtained for each mixture before and after excision of a leaf segment. R_{pl} was given by the difference in the two values of R_p, and diaphragm porosity was derived as outlined in method (a) above.

3. Results

Effective diaphragm porosities estimated by method (a) fell in the range 0.13 to 0.30%, with a mean of 0.20% (4 experiments). Using method (b) the range was 0.15 to 0.38%, mean 0.26% (three experiments). The two procedures, therefore, gave results which were in good agreement.

The mean effective porosity for the two methods, 0.23%, is somewhat less than the value of 0.58% given by Coult (1964) for the lamellae in the Menyanthes rhizome. Coult's estimate was based on direct measurement of pore size and did not take account of any tortuosity of the pores, though in the diaphragms of Menyanthes, which are only one cell (40μm) thick, this is likely to be low. The porosity of the Eriophorum diaphragms given above will be inclusive of a tortuosity factor, which may be significant since the diaphragms are 2-3 cells (58μm) in thickness.

Diaphragm resistance may be derived from porosity as follows. Consider a diaphragm of thickness 58μm situated across a lacuna of cross-sectional area 3.57×10^{-4} cm^2. The non-metabolic resistance offered by this diaphragm (ϵ_{ed} = 0.23%) is 0.34×10^5 s cm^{-3} (equation 7.4). However, fourteen air channels are normally present within the Eriophorum leaf, therefore, the overall resistance offered by the occlusion of each of the

fourteen channels by one diaphragm is $0.34 \times 10^{-5} \div 14$, or 0.024×10^{5} s cm^{-3}. Diaphragms occur at a frequency of about 3 per cm in the mid-leaf, hence the resistance due to the diaphragms in 1 cm of leaf will be $3 \times 0.024 \times 10^{5}$, or 0.072×10^{5} s cm^{-3}. For comparison 1 cm of root of radius 0.05cm and effective porosity 10% has a non-metabolic resistance of 0.062×10^{5} s cm^{-3}.

Assuming that the diaphragms in the sheath region of the leaf also have an effective porosity of 0.23%, their resistance in 1cm of leaf, of cross-sectional area 0.036 cm^{2} and porosity 60%, is only 0.017×10^{5} s cm^{-3} if they occur at a frequency of 3 per cm, or 0.0114×10^{5} s cm^{-3} at 2 diaphragms per cm. Even a 1cm long block of diaphragm tissue, of cross-sectional area equal to that of the diaphragms in the leaf base, would offer a resistance of only 0.98×10^{5} s cm^{-3}.

It is clear from the above results that despite their low effective porosity diaphragms do not offer non-metabolic resistance which is excessive in comparison with that offered by other parts of the plant.

III MODELLING

The resistance data obtained in this chapter are suitable for programming the electrical analogue; indeed they were obtained with this in mind and have been so employed in the analogue investigations described in this thesis. However, some knowledge of diffusion mathematics also enables a mathematical model of the plant-electrode system to be derived; this, when used in conjunction with experimental resistance and respiratory data, may be used to compute internal root oxygen concentration and R.O.L. The following illustrates how this may be done.

A. PRINCIPLE

Consider the electrical circuit shown in Fig.7.3. The current, I, to earth can be calculated by summing the voltage drops across the three resistors. With refer ence to the section referring to current tappings

mid-way along the resistors (p.34) the procedure is as follows.

$$\text{Drop across } R_1' = \tfrac{1}{2}R_1'(2) + R_1'(3 + I) \qquad (7.16)$$

$$= 10 + 30 + 10I, \text{ or } 40 + 10I \text{ volts}$$

$$\text{Drop across } R_2' = \tfrac{1}{2}R_2'(3) + R_2'(I) \qquad (7.17)$$

$$= 15 + 10I.$$

$$\text{Drop across } R_s' = R_s' I, \text{ or } 5I \qquad (7.18)$$

The sum of these voltage drops gives the total voltage drop, $C_o - C$, which equals 500V since $C = 0$.

$$C_o - C = 500 = 44 + 25I \qquad (7.19)$$

from which $I = 17.8$ Amps.

This value of I may be used to determine the voltage drops across R_1' and R_2' from equations 7.16 and 7.17, and these are respectively 218 and 193 volts. By subtracting the sum of these two voltage drops from C_o, the potential at the upper end of R_s' (i.e. the "root surface") may be obtained, and is 89 volts.

This simple procedure may now be applied to the plant.

B. THE MODEL

Consider the wetland plant shown schematically in Fig.7.9. For modelling purposes the plant is divided into segments, which are designated by subscripts as follows:

Leaf base : l

Stem/root-shoot junction : j

Root base : b

Sub apical segment : sa

Apex : a

Root wall : wl

Liquid shell : s

The diffusive resistance (non-metabolic) in each segment is given as R_l, R_j etc.

If the oxygen concentration drop across each segment is given the

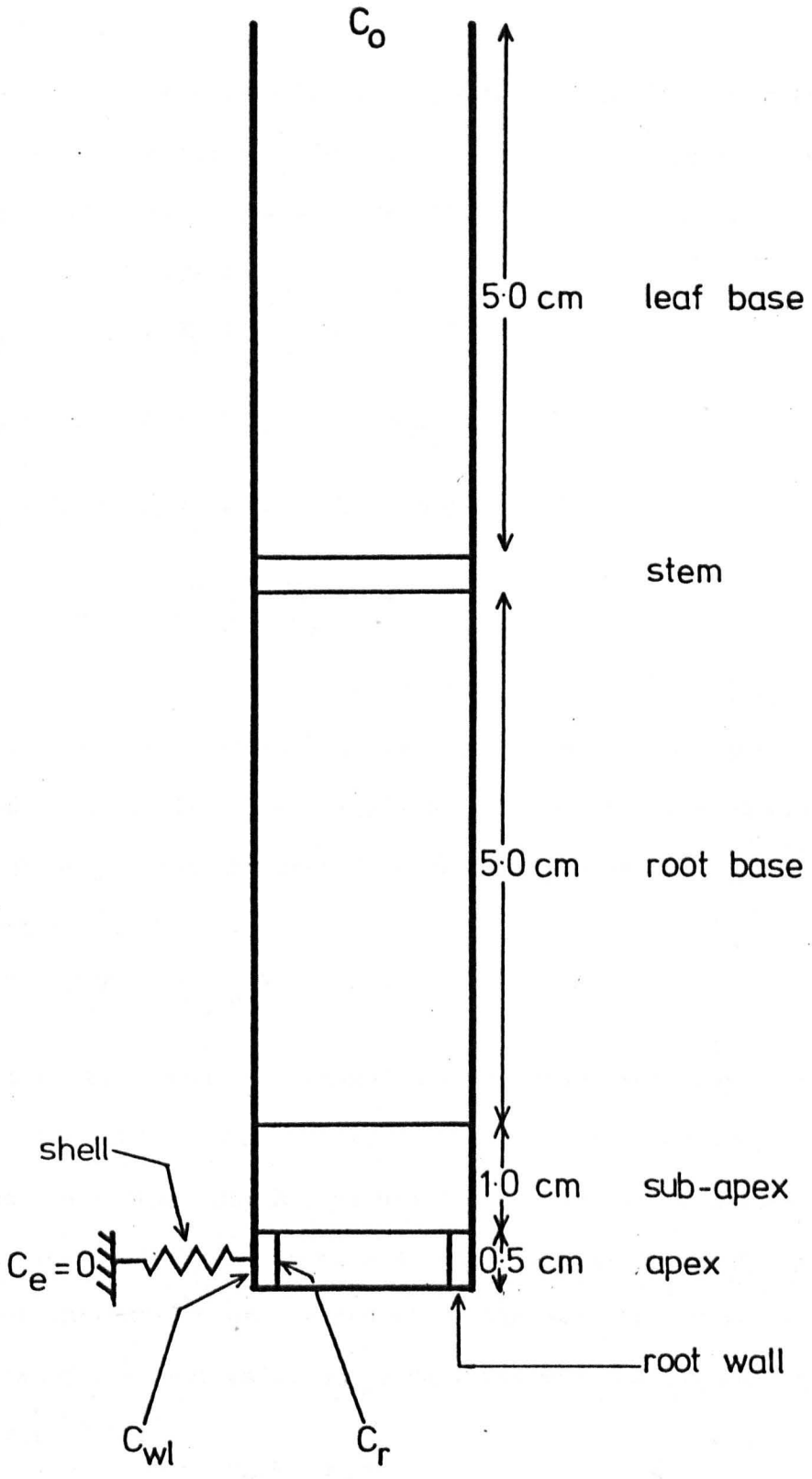

FIG. 7.9 Diagram of a plant used to illustrate the mathematical model described on p. 154

symbol Δ, we have:

$$C_o - C_e = \Delta_l + \Delta_j + \Delta_b + \Delta_{sa} + \Delta_a + \Delta_{wl} + \Delta_s \quad g\ cm^{-3} \qquad (7.20)$$

where $C_e = 0$.

If respiratory rate has the symbol M ($g\ cm^{-3} s^{-1}$) and the volume of the various segments V (cm^3), and if f ($g\ s^{-1}$) is the diffusion rate of oxygen from root to electrode, then the individual concentration drops are given as follows:

$$\Delta_l = R_l \left(\tfrac{1}{2} M_l V_l + \sum_j^{wl} MV\right) + R_l f \qquad (7.21)$$

$$\Delta_j = R_j \left(\tfrac{1}{2} M_j V_j + \sum_b^{wl} MV\right) + R_j f \qquad (7.22)$$

$$\Delta_b = R_b \left(\tfrac{1}{2} M_b V_b + \sum_{sa}^{wl} MV\right) + R_b f \qquad (7.23)$$

$$\Delta_{sa} = R_{sa} \left(\tfrac{1}{2} M_{sa} V_{sa} + \sum_a^{wl} MV\right) + R_{sa} f \qquad (7.24)$$

Δ_a poses certain problems: tapping the respiration at $\frac{1}{2} R_a$ gives the concentration drop between the top and bottom of the apical segment (see p.34). It is more realistic to consider the concentration drop to mid-way along the apex (i.e. corresponding with the centre of the electrode). Thus:

$$\Delta_a = \tfrac{1}{4} R_a \left(M_a V_a + M_{wl} V_{wl}\right) + \tfrac{1}{4} R_a f \qquad (7.25)$$

It is not possible to model the concentration drop across the root wall in the manner common to the above concentration drops. This is because the point along R_{wl} at which the respiration must be tapped may not be mid-way (cf. the other diffusive resistances) but varies with the ratio of the radii from the centre of the root to the inner and outer surfaces of the root wall. Δ_{wl} may, however, be obtained using an equation similar to 7.11:

$$\Delta_{wl} = C_r - C_{wl} = \frac{M_{wl} b^2}{4 D_e} \left[\frac{a^2}{b^2} + 2 \log\left(\frac{b}{a}\right) - 1\right] + R_{wl} f \ g\ cm^{-3} \qquad (7.26)$$

where:

b = the root radius

a = b minus the wall thickness

C_r and C_{wl} are the oxygen concentrations at the inner and outer surfaces of the root wall respectively.

Lastly:

$$\Delta_s = R_s f$$

The delta equations may then be combined to give:

$$C_o - C_e = \left[\sum_{1}^{wl} (\Delta - Rf) \right] + f(R_l + R_j + R_b + R_{sa} + \tfrac{1}{4}R_a + R_{wl} + R_s) \qquad (7.27)$$

The flux, f, may be calculated from equation 7.27. This may then be substituted into equations 7.21 - 7.25 to compute the individual oxygen concentration drops which, when added, and subtracted from C_o, give the oxygen concentration within the root apex.

The model was tested by considering a plant comprising:

(i) A 5cm length of leaf base of cross-section area 0.044cm^2, lacunar porosity of 60%, and diaphragm resistance 0.017 x 10^5 s cm^{-3} per cm (p.153).

(ii) A stem/root-shoot junction of volume 0.1 cm^3, but modelled as only one-fifth of this volume to take account of the single leaf base (i.e. the whole plant was assumed to possess five leaves - see p.86).

(iii) A 5cm length of root base, of radius 0.04cm and porosity 53%.

(iv) A 1cm sub-apical segment, of radius 0.04cm and porosity 25%.

(v) A 0.5cm apical segment, of radius 0.04cm and porosity 20%.

(vi) A root wall of thickness 65μm.

If the root apex lies within a cylindrical electrode of radius 0.1125cm, and mean values of experimental resistance and respiratory data substituted into the equations, the oxygen concentration at the inner surface of the root wall calculates to 12.9% and the flux to 129.5ng cm^{-2}min^{-1}. Clearly, these values lie within the range of experimental values encountered during the present study, indicating that the model is valid. However, although such models may provide fairly accurate data, the mathematics involved is very tedious. Under these circumstances working models may be employed to advantage.

IV. FINAL COMMENTS

The effectiveness of internal aeration is dependent upon the diffusive resistance, both physical and effective, offered by the plant. Internal oxygen transport has reached maximum development in wetland species; therefore, it is a logical assumption that under normal circumstances diffusive resistance in these plants will be correspondingly low. The work described in this chapter provides evidence to validate this assumption, and this is probably best illustrated by comparing *Eriophorum angustifolium* with the mesophyte *Pisum sativum*, the only other plant for which resistance data has been obtained.

Healy (1975) studied diffusive resistance in the primary root of pea under a variety of conditions. He showed that with the intact root system immersed in anaerobic medium, total effective resistance at 23°C in the primary root rose from about 20×10^5 s cm^{-3} at a length of 4cm to infinity at lengths in excess of about 9.5cm. With the roots cooled to 3°C to minimise respiration non-metabolic resistances at the same root lengths were 9×10^5 and 11×10^5 s cm^{-3}. In *Eriophorum* total resistance at a root length of 4cm was about 4×10^5 s cm^{-3} whilst non-metabolic resistance at this root length was about 1.5×10^5 s cm^{-3} (Fig.7.6); it is possible that resistance in the root wall may account for the greater part of these values (Table 7.1). Indeed, total resistances at 23°C for whole *Eriophorum* plants with aerial parts in air did not exceed 6.1×10^5 s cm^{-3} (Fig.7.7). These large differences in diffusive resistance between the wetland and non-wetland plant are reflected in the difference in apical oxygen flux. For example, R.O.L. from the *Eriophorum* root at normal temperatures is frequently as high as 120ng cm^{-2}min^{-1}; in pea flux is seldom in excess of 60ng cm^{-2}min^{-1} even from roots as short as 3cm.

The low diffusive resistance in *Eriophorum* compared to that in pea is undoubtedly a consequence of the high porosity and the associated reduction in respiring tissue, although Healy (1975) has shown that leakage from the pea root can also add to the effective resistance. In this

context it is of interest to recall that many non-wetland plants respond to flooding by producing fresh roots of increased porosity (eg. Yu *et al*, 1969).

Despite the high porosity, internal resistance in *Eriophorum* increases considerably with increased diffusion path length (Fig.7.6). This causes a drastic reduction in internal oxygen transport (Fig.7.5) and it is possible that partial inundation of plants in the field could cause sub-optimal oxygen pressures in the roots.

An important result to emerge from the present study is that non-metabolic resistance in the root-shoot junction of *Eriophorum* is low (R_{pj}: 0.057×10^5 to 0.130×10^5 s cm^{-3}); total resistance in the junction also contributes little to overall plant resistance (R_{tj} : 0.084×10^5 to 0.202×10^5 s cm^{-3}). Coult (1964) concluded that in *Menyanthes trifoliata* the cortical gas space systems of root and shoot became discontinuous at the junction; the results presented here, however, suggest that in *Eriophorum* the opposite is the case. This was confirmed by microscopic observation, and in the section of the root-shoot junction shown in Plate 7.3 the continuity of the gas space systems in the cortices of shoot and root is abundantly clear. (Recent preliminary work on *Menyanthes* does, in fact, indicate a similar gas space continuity).

The effective porosity of the diaphragms of the leaf (0.13% to 0.38%) is lower than the porosity of 0.6% for *Menyanthes* obtained by direct observation (Coult 1964). However, despite the low porosity, diaphragm resistance in *Eriophorum* is small, being only 0.0114×10^5 to 0.017×10^5 s cm^{-3} per centimetre of leaf base; this could well be due to a parallel resistance effect of the diaphragm pores (c.f. stomatal resistance, Chapter 6). Therefore, whilst providing effective barriers against flooding of the gas space system diaphragms are unlikely to offer an important resistance to oxygen transport.

Probably the most surprising result has been the detection of

significant resistance in the apical root wall of Eriophorum since other wetland species for which data are available do not seem to exhibit this feature. It is possible that this degree of root wall impermeability, by reducing R.O.L. to a certain extent, may be the cause of the higher apical oxygen concentrations in Eriophorum than in other species (p.148). Despite this, oxygen flux from the Eriophorum root is considerable and rhizosphere oxygenation is unlikely to be reduced by a significant degree.

CHAPTER 8

PHOTOSYNTHESIS AND INTERNAL AERATION

A. INTRODUCTION

Various investigators have studied the relationship between photosynthesis and internal oxygen levels, though the importance of photosynthesis to root aeration has been less extensively studied. Most research has been carried out using submerged or semi-submerged aquatics. It is widely known that in these plants exposure to bright light produces elevated gas pressure within the intercellular spaces (eg. Barthelemy, 1874). Roodenburg (1927) (cited by van Raalte, 1941) measured increased pressures in the gas channels of Nymphaea L. in sunlight and ascribed this to the production of oxygen by photosynthesis. As early as 1866 Van Tieghem had measured oxygen concentrations as high as 90% in gas bubbles evolved by photosynthesising Elodea Michx.

Laing (1940b) performed detailed analyses of the internal atmospheres of various water plants and showed that the oxygen levels within several semi-submerged species were boosted during photosynthesis. For example, the oxygen concentration within the rhizome of Nuphar advenum Ait. growing in the laboratory rose from 2.2% in the dark to 13.7% in the light; oxygen levels within the roots of a plant under field conditions rose from 1.6% to 7.9%. Laing also demonstrated an accumulation of CO_2 in the leaves during darkness, whilst during illumination the level of this gas fell, presumably due to its being utilised in photosynthesis.

Hartman and Brown (1967) demonstrated a cyclic variation of oxygen concentration in the internal atmosphere of Elodea canadensis. The lowest oxygen concentration, 8%, occurred during darkness at 11 p.m. whilst the highest value, 28%, was reached during daylight at 11 a.m. Variation in CO_2 concentration was much less pronounced but was clearly half a cycle out of phase with that of the O_2 concentration, a result similar to that

obtained by Laing.

Rhizosphere oxygenation by oxygen apparently derived from photosynthesis has been demonstrated by Wium-Andersen and Andersen (1972b). These workers measured the redox potential in the sediment of a Danish lake and found that oxidation to a depth of 20cm was closely correlated with the distribution of roots of Isoetes L.

In contrast to the situation in submerged aquatics there is little evidence that photosynthesis can boost the internal oxygen regime of plants with their aerial parts exposed to the atmosphere. Van Raalte (1941) analysed gas extracted from the roots of rice plants which had been kept in light and darkness but found no difference in oxygen content. In a later paper (van Raalte, 1944) he concluded that photosynthesis did not influence rhizosphere oxygenation by rice roots. Armstrong (1967b) arrived at a similar conclusion: using Eriophorum angustifolium he removed most of the photosynthetic tissue by excising the leaves and found that this did not alter the oxygen diffusion rate from the roots.

However, there are some reports in the literature which provide indirect evidence that photosynthesis may aid internal aeration in plants with exposed aerial parts. Cannon (1932) measured the uptake of oxygen from distilled water by the roots of willow and sunflower plants. In 32 of the 53 experiments performed there was a lower rate of oxygen uptake in the light than in darkness, and Cannon attributed this to photosynthetic oxygen being utilised in root respiration. Vámos and Köves (1972) compared weather data for a period of longer than twenty years with the occurrence of hydrogen sulphide damage in rice crops ("browning disease"). They found that in those years when the disease had occurred there had been very little sunshine whilst in sunny years the disease was almost absent. Experimental studies confirmed the protective role of sunlight in the prevention of damage by H_2S. However, Vámos and Köves invoked a rather complicated explanation for these results. They suggested that in the leaf H_2S is oxidised by free OH^- radicals formed during photosynthesis

($H_2S + 2OH^- \longrightarrow 2H_2O + S$). In the root oxygen evolved from peracids, synthesised from acids and free OH^- radicals, was the main oxidising agent. Little importance was attributed to the role of free dissolved oxygen.

The discrepancy between the magnitude of the photosynthetic effect in submerged and exposed plants would seem to be a consequence of the low diffusivity of oxygen in water (see Chapter 1). Apparently, in submerged plants, oxygen is evolved faster than the rate at which it can leak away to the surrounding medium and elevated internal concentrations result. In plants with exposed leaves, however, photosynthetic oxygen is likely to escape to the atmosphere as rapidly as it is produced and its level in the internal atmosphere will not increase (Stiles, 1960; Greenwood, 1969).

In this chapter experiments are described which were designed to determine the relationship between submergence and the photosynthetic enhancement of the internal oxygen regime. The manner in which the photosynthetic effect could be modified by the CO_2 supply to the submerged parts was also investigated. Eriophorum angustifolium was used as the test species.

B. THE EFFECT OF PHOTOSYNTHESIS ON THE INTERNAL OXYGEN REGIME OF E.ANGUSTIFOLIUM

In view of the relationship between internal oxygen regime, photosynthesis and submergence outlined above, the photosynthetic effect was investigated in Eriophorum plants with the aerial parts submerged to various degrees.

1. Method

Whole plants were arranged for R.O.L. measurement within measuring cylinders as described on p.75 .

The light source was a single 500W incandescent lamp (Phillips

"Argaphoto"). Illumination was unilateral, the half-circumference of the measuring cylinder more distant from the light source being blackened. Experiments were carried out in a darkroom.

Incident radiation was measured using a quantum sensor in conjunction with an LI-185 Quantum/Radiometer/Photometer (Lambda Instruments Corp., Lincoln, Nebraska). This instrument measures photon flux density in the photosynthetically active spectral region (ie. wavelength 400-700nm) in units of micro-Einsteins (μE) $m^{-2}s^{-1}$. (An Einstein is the number of quanta required to activate 1 mole of a photochemically reactive substance - ie. Avogadro's number, or 6.02×10^{23} quanta). The incident radiation was monitored at the surface of the measuring cylinder and was varied simply by altering the position of the light source. To obtain the lower intensities of radiation sheets of tissue paper were placed in the light path. At all times a cold water heat shield was kept between the lamp and plant to absorb infra-red radiation, whilst the ambient temperature was kept constant by using fans to circulate the air. The temperature within the measuring cylinder was noted frequently and fluctuations were minimal.

Radial oxygen loss was monitored whilst the intensity of the incident radiation was varied from zero to 200μE $m^{-2}s^{-1}$ (the maximum value obtainable with the available light source). Plants were subjected to five degrees of submergence (above the root-shoot junction) in 0.05% deoxygenated agar medium (viz. 0, $\frac{1}{4}$, $\frac{1}{2}$, $\frac{3}{4}$ and full), measurements being based on the length of the longest leaf. The agar medium had a pH of about 6 and received no additional CO_2.

The first measured value in each experiment was the R.O.L. from the unsubmerged plant at zero incident radiation. This was used as a reference and ascribed a value of 100%; the data subsequently obtained were expressed relative to this value.

2. Results and Discussion

The relationship between R.O.L. and intensity of radiation for each of the five degrees of submergence is shown in Fig.8.1. At each submerg-

FIG. 8.1 Diffusion current as a function of incident radiant flux

No added CO_2

(◇) Plant unsubmerged

(▽) " 1/4 submerged

(□) " 1/2 "

(△) " 3/4 "

(○) " fully "

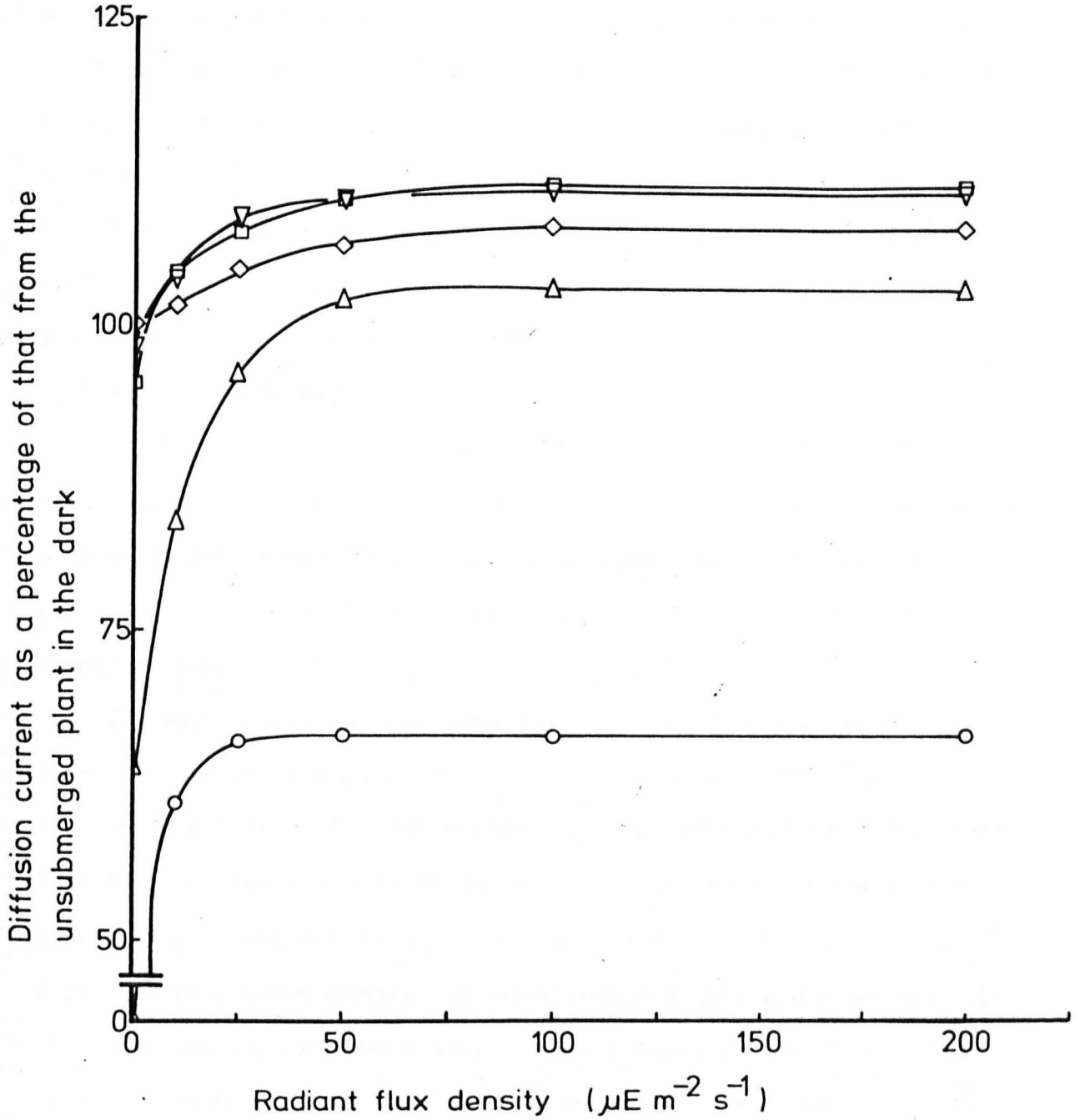
125
100
75
50
0
0
50
100
150
200
Diffusion current as a percentage of that from the unsubmerged plant in the dark
Radiant flux density (μE m⁻² s⁻¹)

ence level R.O.L. increased hyperbolically with increasing incident radiation to about 100 $\mu E\ m^{-2} s^{-1}$, reflecting a similar increase in the internal oxygen regime. The shape of the curves is similar to that presented by various authors to express the relationship between photosynthetic rate and light intensity (eg. Heath, 1969; Bickford and Dunn, 1972). It is likely, therefore, that in the present case the observed variation in R.O.L. indicates a similar variation in photosynthetic activity.

The magnitude of the R.O.L. at any light intensity was strongly influenced by the degree of submergence. In general, R.O.L. under the five degrees of submergence was:

$$\tfrac{1}{2} \geqslant \tfrac{1}{4} > 0 > \tfrac{3}{4} > 1$$

The "jacketing effect" of submergence was demonstrated further by blackening the submerged portion of the aerial parts. When this was done increased light intensity had no effect on R.O.L., indicating that it was photosynthesis in the submerged parts only which enhanced the internal oxygen regime.

In order to explain the above observations it is necessary to consider that under the experimental conditions oxygen leaking from roots can be derived from two sources, viz the atmosphere and photosynthesis. Results presented in Chapter 6 suggest that the effectiveness of the atmospheric source will be at a maximum at zero submergence (ie. when the diffusive resistance between the atmosphere and root apices is minimised). So far as the photosynthetic source is concerned, this will on the one hand be enhanced by increased submergence, since the escape of oxygen from the submerged leaves will be reduced. On the other hand, CO_2 supply from the atmosphere might be reduced by submergence (and with it photosynthetic O_2 production), due to increased diffusive resistance between the atmosphere and the submerged leaf bases. The resulting R.O.L. is due, therefore, to the interaction of these factors, and maximum R.O.L. will occur when the degree of submergence is such that the balance between

"jacketing" and CO_2 entry is optimal.

Any increase in R.O.L. above the 100% value (ascribed to the unsubmerged plant in the dark) must have been due to an elevation in internal oxygen regime caused by photosynthesis. In all but the fully submerged plant photosynthetic oxygen production was sufficient to bring the R.O.L. above this value. Maximum R.O.L. (111%) occurred in the half-submerged plant, but it is of interest that even in the unsubmerged plant the R.O.L. was boosted to the 108% value. This could be attributed to photosynthesis in the astomatal leaf bases; when the basal regions of the leaves were blackened illumination did not affect R.O.L. In the fully submerged plant the R.O.L. was raised from a dark value of zero to only 66% of the darkened, unsubmerged condition. In this case the atmospheric CO_2 source was absent and photosynthesis must have been dependent upon CO_2 derived from respiration, though it is possible that a small amount of the gas may have been present in the agar medium.

C. THE EFFECT OF CARBON DIOXIDE SUPPLY

It was suggested above that under the experimental conditions photosynthesis would be limited by CO_2 availability. The next stage in the investigation was to test whether increased CO_2 supply would elevate the rate of photosynthesis and lead to further boosting of the internal oxygen regime. In terrestial plants the main source of carbon for photosynthesis is atmospheric CO_2. Providing other factors are not limiting the rate of photosynthesis increases hyperbolically with CO_2 concentration (eg.Gaastra, 1959).

Algae and certain aquatic angiosperms are able to assimilate bicarbonate (Steeman-Nielsen, 1960; Raven, 1970). It is believed that HCO_3^- enters the cells by active transport, is dehydrated to CO_2 by the action of carbonic anhydrase, and is fixed by carboxydismutase (Raven, 1970, 1972). All plants able to assimilate HCO_3^- can also utilise free CO_2 (Raven, 1972). Wium-Andersen (1971) investigated photosynthetic carbon

uptake in Lobelia dortmanna L. and concluded that this species is probably unable to utilise HCO_3^- and uses only free CO_2. In addition he showed that the rate of photosynthesis increased three to five times more when CO_2 was added to water around the roots than when added to water around the leaves. He suggested that since the free CO_2 content of the Lobelia lakes is very limited the plant must obtain its CO_2 supply from the sediment. Analysis of the CO_2 content of the interstitial water in the sediment gave concentrations of 1-5mM l^{-1}, sufficient for optimum photosynthesis (Wium-Andersen and Andersen, 1972a). In contrast, Yoshida et al. (1974) concluded that the absorption of CO_2 by rice roots for use in photosynthesis was almost negligible, the main carbon source being atmospheric CO_2.

In the present study, before the effect of increased CO_2 concentration was investigated, preliminary experiments were carried out to determine whether E.angustifolium could:

(a) utilise bicarbonate in photosynthesis

(b) absorb CO_2 by the roots for use in photosynthesis.

1. General Method

The basic method was to monitor R.O.L. from plants under various degrees of submergence whilst the concentration of HCO_3^- or free CO_2 in the bathing medium was altered; the plants were illuminated at a constant flux density of 100μE $m^{-2}s^{-1}$.

In the experiments using free CO_2 the pH of the agar medium was adjusted to 4.0 with hydrochloric acid; at this pH free CO_2 only is present. Carbon dioxide-saturated agar medium was prepared by adjusting the pH of the liquid to 4.0 and bubbling overnight with CO_2 gas. The desired concentration of CO_2 in the bathing medium was obtained by adding the appropriate volume of this saturated solution.

When bicarbonate was used the pH of the medium was adjusted to 8.3 with KOH solution. At this pH the concentration of HCO_3^- is a hundred times that of free CO_2 (Wium-Andersen, 1971). A stock solution of

100mM l^{-1} HCO_3^- (as $KHCO_3$) in agar medium was freshly prepared before each experiment and was added to the bathing medium to obtain the required concentration of HCO_3^-. Since the dissolution of $KHCO_3$ is an endothermic process, care was taken to allow the stock solution to come to laboratory temperature before addition to the bathing medium in order to prevent convection.

To test whether a pH change from 4.0 to 8.3 could alter R.O.L. per se the oxygen flux was monitored from a plant 3/4 submerged in medium at pH 4.0 and illuminated at 100μE $m^{-2}s^{-1}$. The pH was then raised to 8.3 by addition of KOH solution. The R.O.L. after equilibration was identical to that at pH 4.0, indicating that the pH change did not affect photosynthetic rate. Wium-Andersen (1971) obtained a similar result with Lobelia.

2. Utilisation of Bicarbonate

(a) Procedure

Intact plants were 3/4 submerged in agar medium at pH 8.3 and illuminated with 100μE $m^{-2}s^{-1}$. When the diffusion current had equilibrated, stock bicarbonate solution was added to bring the concentration in the bathing medium to 1mM l^{-1} and the diffusion current allowed to re-equilibrate. This was repeated for HCO_3^- concentrations of 2,5 and 20mM l^{-1}.

At the end of the experiment 5cm^3 N HCl were added to the bathing medium.

(b) Results

Regardless of the concentration of HCO_3^- in the bathing medium the oxygen diffusion current never varied from its original value. However, addition of the HCl always produced an almost immediate rapid rise in current.

These results indicate that Eriophorum is unable to utilise bicarbonate in photosynthesis. The waxy cuticle probably prevents the uptake of HCO_3^- through the leaf surface, whilst any bicarbonate absorbed by the roots does not seem to be available for photosynthesis. However, the

rapid increase in R.O.L. on addition of HCl, which would have liberated CO_2 *in situ*, was strong evidence that free CO_2 entered the plant from the bathing medium and caused an elevation in oxygen pressure by increasing the photosynthetic rate.

3. Uptake of Carbon Dioxide by Roots

(a) Procedure

Intact plants were arranged as in the previous experiments but the agar medium was at pH 4.0. The space between the bung and measuring cylinder wall was "sealed" with cotton wool, effectively dividing the cylinder into an upper leaf and lower root chamber.

When the diffusion current had equilibrated stock CO_2 solution was pipetted into the root chamber through a hole in the bung which was immediately sealed with a cotton wool plug. The diffusion current was monitored as the CO_2 concentration was raised to 2.0mM l^{-1}.

(b) Results

Wium-Andersen (1971) found that CO_2 supplied to the roots of *Lobelia* illuminated with 13mW cm^{-2} was limiting only up to about 1mM l^{-1}. In the present experiments the CO_2 concentration was raised to double this value but at no time did an increase in diffusion current occur. This indicates that any CO_2 absorbed by the roots of *Eriophorum* is not utilised to any measurable degree in photosynthesis, a result in agreement with that of Yoshida *et al.* (1974) for rice.

4. Increased Free Carbon Dioxide Supply to the Leaves

(a) Procedure

Intact plants were arranged as in the previous experiments at $\frac{1}{2}$, $\frac{3}{4}$ and full submergence in agar medium at pH 4.0. Incident radiation was maintained at 100μE $m^{-2}s^{-1}$ whilst the concentration of free CO_2 in the bathing medium was increased from zero to 1.0mM l^{-1}.

(b) Results

Radial oxygen loss, expressed as a percentage of that from the unsubmerged plant in the dark, is shown as a function of CO_2 concentration in Fig.8.2. In general R.O.L. increased with CO_2 concentration, though

FIG. 8.2 Diffusion current as a function of dissolved carbon dioxide concentration.
Radiant flux density $100\,\mu E\ m^{-2}\ s^{-1}$

(□) Plant 1/2 submerged

(Δ) " 3/4 "

(o) " fully "

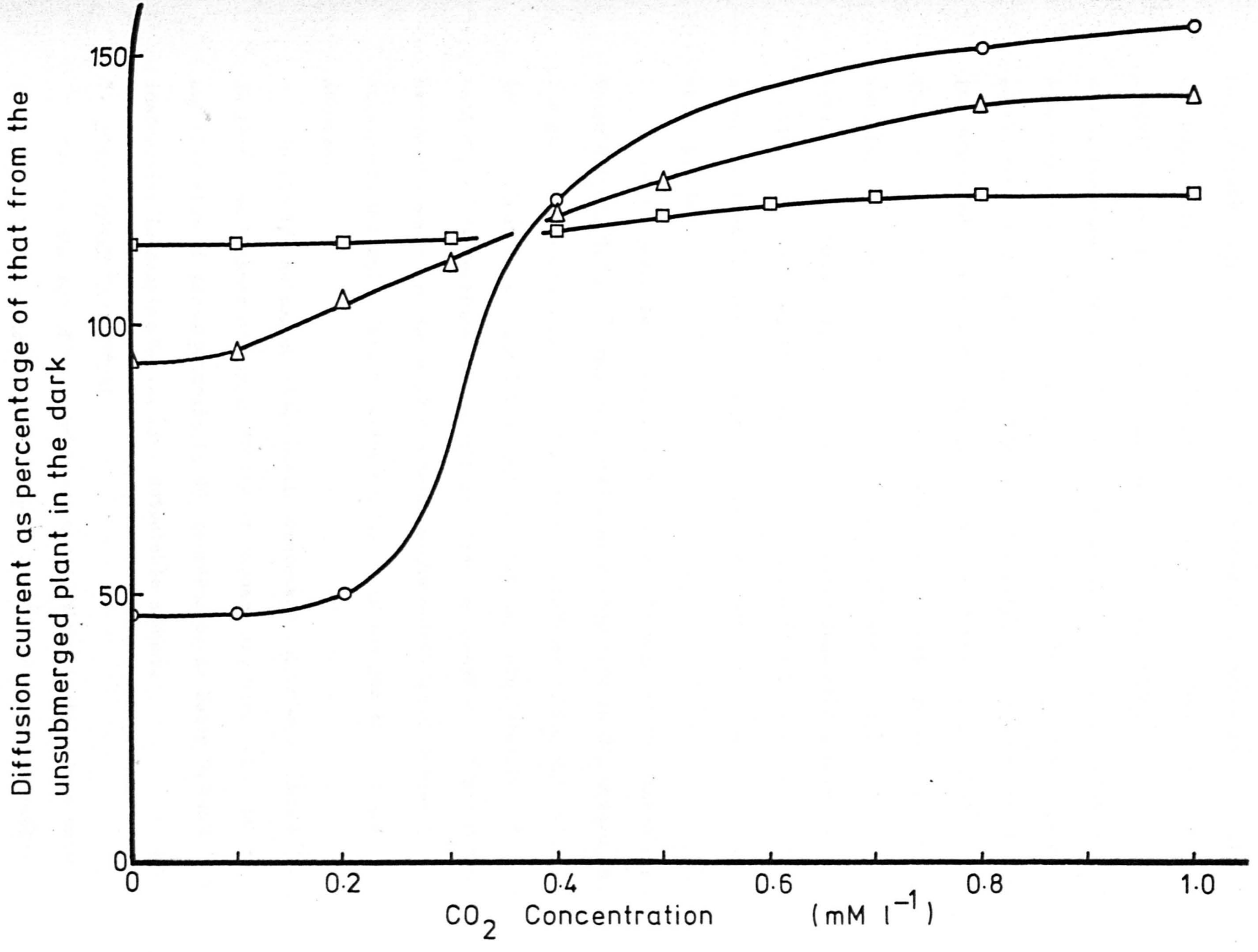
Diffusion current as percentage of that from the unsubmerged plant in the dark
150
100
50
0
0
0·2
0·4
0·6
0·8
1·0
CO_2 Concentration ($mM\ l^{-1}$)

the manner in which it did so requires comment.

In the totally submerged plant there was little effect of increased CO_2 concentration below 0.2mM l^{-1}; above this value increase in R.O.L. was hyperbolic, CO_2 saturation probably occurring at about 1.1-1.2mM l^{-1}. A similar result was obtained for the 3/4 submerged plant; in this case R.O.L. increased hyperbolically above about 0.1mM l^{-1} CO_2. Solution concentrations of 0.1 and 0.2mM l^{-1} CO_2 are equivalent to gas phase concentrations of about 0.25 and 0.50% respectively. It is possible that in the submerged aerial parts respiratory CO_2 could have accumulated to these levels prior to the addition of CO_2 to the bathing medium. Hence, solution concentrations below 0.1 and 0.2mM l^{-1} would not elevate the internal CO_2 concentration in the 3/4 and fully submerged plants and photosynthetic rate would be unaffected. Laing (1940b) measured CO_2 concentrations in excess of 0.5% in the submerged aerial parts of several water plants.

A second possible reason for the ineffectiveness of CO_2 concentrations below 0.1 and 0.2mM l^{-1} may have been a synergism between CO_2 uptake in the guard cells and a high boundary layer resistance to CO_2 diffusion into the plant in the unstirred medium. This may have necessitated threshold CO_2 concentrations in the bulk solution in excess of 0.1 and 0.2mM l^{-1} before the concentration gradient between the solution and internal atmosphere was sufficient to allow diffusion of the gas through the stomata.

In the 1/2 submerged plant R.O.L. increased only above 0.3mM l^{-1} CO_2. In this case leakage of oxygen to the atmosphere may have been such that any elevation of photosynthesis by CO_2 concentrations below 0.3mM l^{-1} was ineffective in raising R.O.L. by a detectable amount.

5. Supplementary Experiments

Towards the end of the work described in this thesis a lamp became available ("Kingston Reflector Spotlight" - 150W) which could provide a radiant flux density of 500μE $m^{-2}s^{-1}$. Using this light intensity the

experiments described in the previous section were repeated with 1/2 and fully submerged plants. Results are presented in Fig.8.3.

It can be seen that the relationships between R.O.L. and CO_2 concentration follow the same pattern as shown in Fig.8.2. However, at CO_2 concentrations above the "threshold values" R.O.L. is substantially higher under the higher level of illumination. The data in Figs.8.2 and 8.3 illustrate fairly typically the influence upon photosynthesis of the interaction of the factors light intensity and CO_2 concentration (see, for example, Heath, 1969).

D. DISCUSSION

The results presented in this chapter show that under certain circumstances photosynthesis can boost the internal oxygen regime of E.angustifolium and can increase radial oxygen loss from the roots. The magnitude of the effect at a particular light intensity depends upon the degree of submergence of the plant and upon the availability of free carbon dioxide in the bathing medium.

With no additional CO_2 in the bathing medium photosynthesis must rely upon the atmosphere and respiration as sources of the gas. Under these circumstances the magnitude of the R.O.L. depends upon the "balance" between the jacketing effect of submergence and the entry of atmospheric CO_2 through the unsubmerged portion of the aerial parts. This balance appears "optimal" at 1/2 submergence when, at a light intensity of 100μE $m^{-2}s^{-1}$, the R.O.L. may rise to 111-115% of its value from the unsubmerged plant in the dark (Figs. 8.1. and 8.2).

With CO_2 added to the bathing medium the photosynthetic effect varies directly with the degree of submergence. Thus, in the fully submerged plant at 100μE $m^{-2}s^{-1}$ and 1.0mM l^{-1} CO_2, R.O.L. is 156% of the value from the unsubmerged plant in the dark. At this CO_2 concentration an incident radiation of 500μE $m^{-2}s^{-1}$ elevates R.O.L. to 274%, whilst at 2.0mM l^{-1} CO_2

FIG. 8.3 Diffusion current as a function of dissolved carbon dioxide concentration
Radiant flux density 500 $\mu E\ m^{-2}\ s^{-1}$
(□) plant 1/2 submerged
(○) " fully "

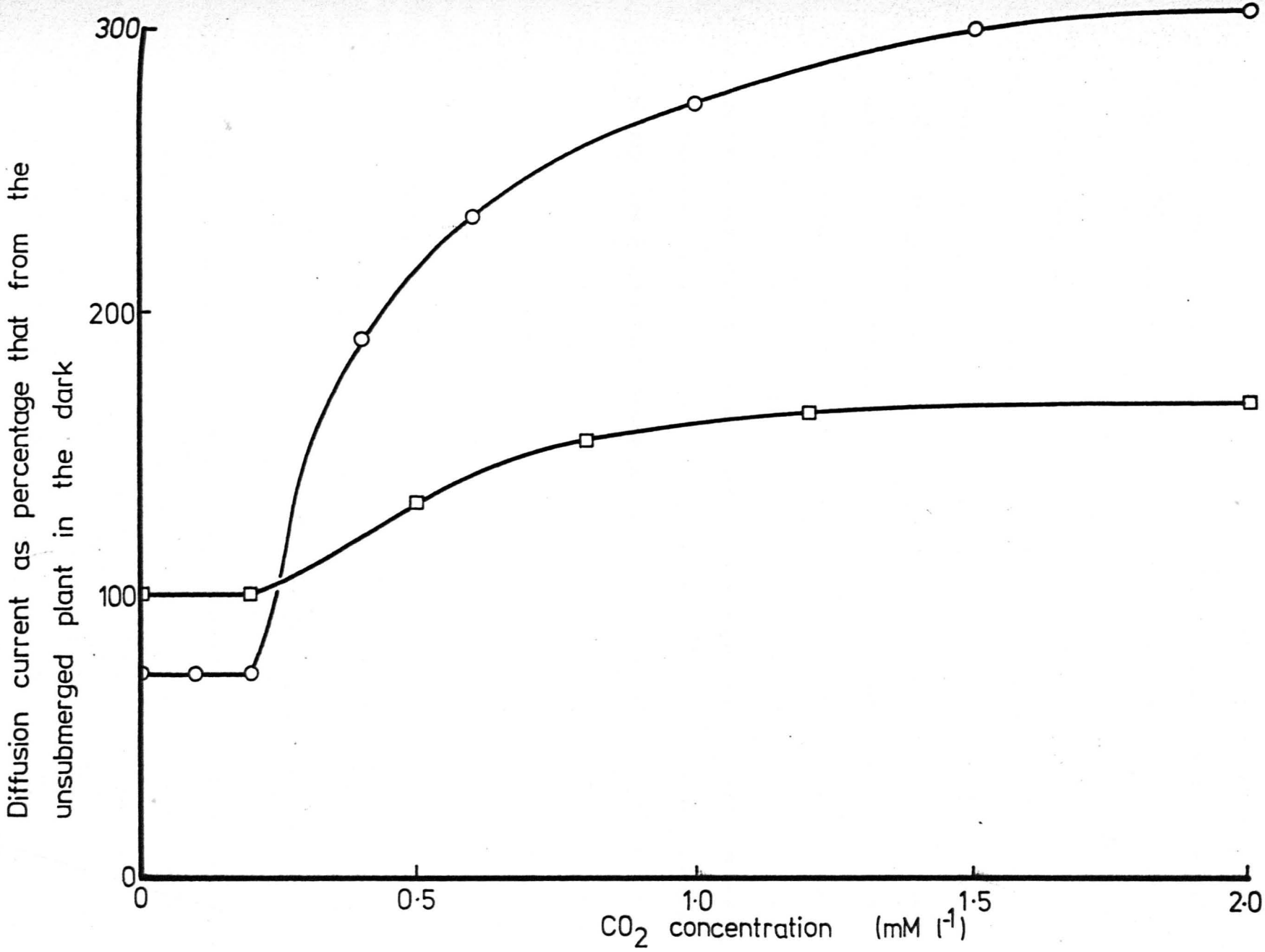
300
200
100
0
0
0·5
1·0
1·5
2·0
Diffusion current as percentage that from the unsubmerged plant in the dark
CO_2 concentration (mM l^{-1})

and 500μE $m^{-2}s^{-1}$ the value is 308% (Fig.8.3).

It is of interest to note that even in the unsubmerged condition photosynthesis can satisfy the oxygen demands of the plant. Although leakage of photosynthetic oxygen from the leaves may prevent elevation of the internal oxygen regime, the fact that such leakage must occur along a concentration gradient means that entry of atmospheric O_2 will be prevented. Hence the oxygen within the plant will be entirely that derived from photosynthesis.

In order to extrapolate the above findings to field conditions measurements were made of solar radiation and of CO_2 concentrations in pools where E.angustifolium was abundant. On an apparently fairly dull day solar radiant flux density was 800μE $m^{-2}s^{-1}$. Using the titration method of Mackereth (1963) it was found that free CO_2 concentrations in the pool water may approach 0.8mM l^{-1}. Therefore, it could well be that in the field, when the aerial parts of the plants are partially submerged, photosynthesis will enhance internal aeration and in so doing increase rhizosphere oxygenation appreciably.

CHAPTER 9

THE SOIL AS AN OXYGEN SINK

Introduction

Facultative aerobes and reduced soil components constitute a latent sink for oxygen in waterlogged (anaerobic) soil (Chapter 1). Plant roots situated in such soil necessarily depend upon internal aeration for their source of respiratory oxygen and should the root wall be gas-permeable some of this oxygen will diffuse into the surrounding soil (p.12). It has been usual to consider this radial oxygen loss from the point of view of its beneficial effects - ie. the formation of an oxidised rhizosphere (Chapter 1); however, R.O.L. must also cause a decrease in the internal oxygen regime and if the quantity of oxygen lost to the soil is great the internal concentration may be lowered below the critical value. For example, Armstrong (1970) has shown that the oxidised rhizospheres due to narrow roots can be much larger, in relation to root radius, than those formed around thick roots. This would seem to be advantageous, but the greater surface area to volume ratio, and the associated higher oxygen flux to the soil, may cause a drastic fall in oxygen concentration along the narrow root.

In this chapter an electrical analogue study is described which was designed to investigate the influence of the soil upon internal root aeration and to assess to what extent root radius might modify this influence.

The analogue as described in Chapter 2 and by Armstrong and Wright (1976b) embodied two major deficiencies. Firstly, the root model was designed to simulate only one radius, r_r = 0.05cm. Secondly, the simulation of specified rates of soil oxygen consumption was not attempted. Instead, soil sink activity was modelled using a method similar to that employed by Luxmoore *et al.* (1970a) in their mathematical model of root aeration. Each centimetre segment of root was considered to lie centrally within a cylindrical shell of water of fixed radius, the outer surface of which

was maintained at zero oxygen concentration (cf. the sink developed by the cylindrical platinum electrodes used in the experimental work). Consequently, soil oxygen consumption varied linearly with internal oxygen concentration. However, it is more realistic to assume that soil respiration rate will remain constant unless the oxygen concentration falls to a very low value (Greenwood, 1963), and this uniformity of soil oxygen demand will cause the relationship between soil oxygen consumption and internal oxygen concentration to be curvilinear (Fig.9.2). Therefore, a necessary prerequisite for the following study was to devise a method whereby (a) soil oxygen demand could be more realistically simulated and, (b) roots of any radius could be modelled. Having carried out these amendments to the analogue the influence of soil oxygen demand on the internal oxygen regime of roots of different radii was investigated.

I. AMENDMENTS TO THE ANALOGUE

A. THE ELECTRICAL SIMULATION OF SOIL SINK ACTIVITY

1. Rhizosphere oxygen consumption

Consider a root segment of length Lcm and radius r_r cm, lying centrally within a cylindrical root-oxygenated rhizosphere, also of length Lcm, and radius r_o cm, such that at a distance $r_o - r_r$ from the root surface the oxygen concentration in the soil becomes zero.

The volume of the oxygenated rhizosphere, V_{rh}, is given by:

$$V_{rh} = \pi L(r_o^2 - r_r^2) \text{ cm}^3 \qquad (9.1)$$

The value of r_o for any particular soil oxygen demand is a non-linear function of root wall oxygen concentration and may be determined from the equation:

$$Z(\log Z - 1) = \frac{2}{A} - 1 \qquad \text{(Armstrong, 1970)} \qquad (9.2)$$

where:

$$Z = \frac{r_o^2}{r_r^2}$$

and A is the dimensionless group $\frac{Mr_r^2}{2D^t_{soil}C^t_{wl}}$

in which:

M = the soil oxygen demand ($gO_2\ cm^{-3}s^{-1}$)

C^t_{wl} = the dissolved oxygen concentration at the root wall at temperature t ($g\ cm^{-3}$)

D^t_{soil} = the diffusion coefficient for oxygen in wet soil at temperature t (taken as $1.0 \times 10^{-5}\ cm^2\ s^{-1}$, Greenwood and Goodman, 1967).

Assuming that soil respiration proceeds at a constant rate even at very low oxygen concentrations (Greenwood, 1963) the rate of oxygen consumption by the soil of the rhizosphere will be

$$V_{rh}M \quad g\ s^{-1}$$

In an equilibrated system this must equal the oxygen diffusion rate from the root surface.

If root wall resistance is negligible, Fig.9.1 shows how the radial oxygen loss (expressed as both flux and diffusion rate) from 1.0cm root segments of radii 0.01 and 0.10 cm, with an internal oxygen concentration of 10%, varies with soil oxygen consumption. It is of interest to note that under the same conditions of soil oxygen demand the flux from the narrower root is substantially higher than that from the root of larger radius. This agrees with the theoretical data obtained by Armstrong (1970) (see p.172), whilst Luxmoore et al. (1970b) concluded that in rice thin roots lost a greater proportion of oxygen to the soil, measured relative to that entering the root base, than did roots of greater radii.

In Fig.9.2 oxygen diffusion rate is plotted against internal oxygen concentration for 1.0 cm long root segments with zero wall resistance, of radii 0.01 cm and 0.10 cm, situated in soil having an oxygen demand of $4.0 \times 10^{-5}\ cm^3\ cm^{-3}\ s^{-1}$. The data illustrated in this figure confirm the curvilinear variation in soil oxygen consumption with internal root oxygen

FIG. 9.1 Radial oxygen loss from 1·0 cm root segments as a function of soil oxygen consumption.

Internal oxygen concentration 10%

Flux :

(□) root radius 0·10 cm

(○) " " 0·01 cm

Diffusion rate :

(◇) root radius 0·10 cm

(△) " " 0·01 cm

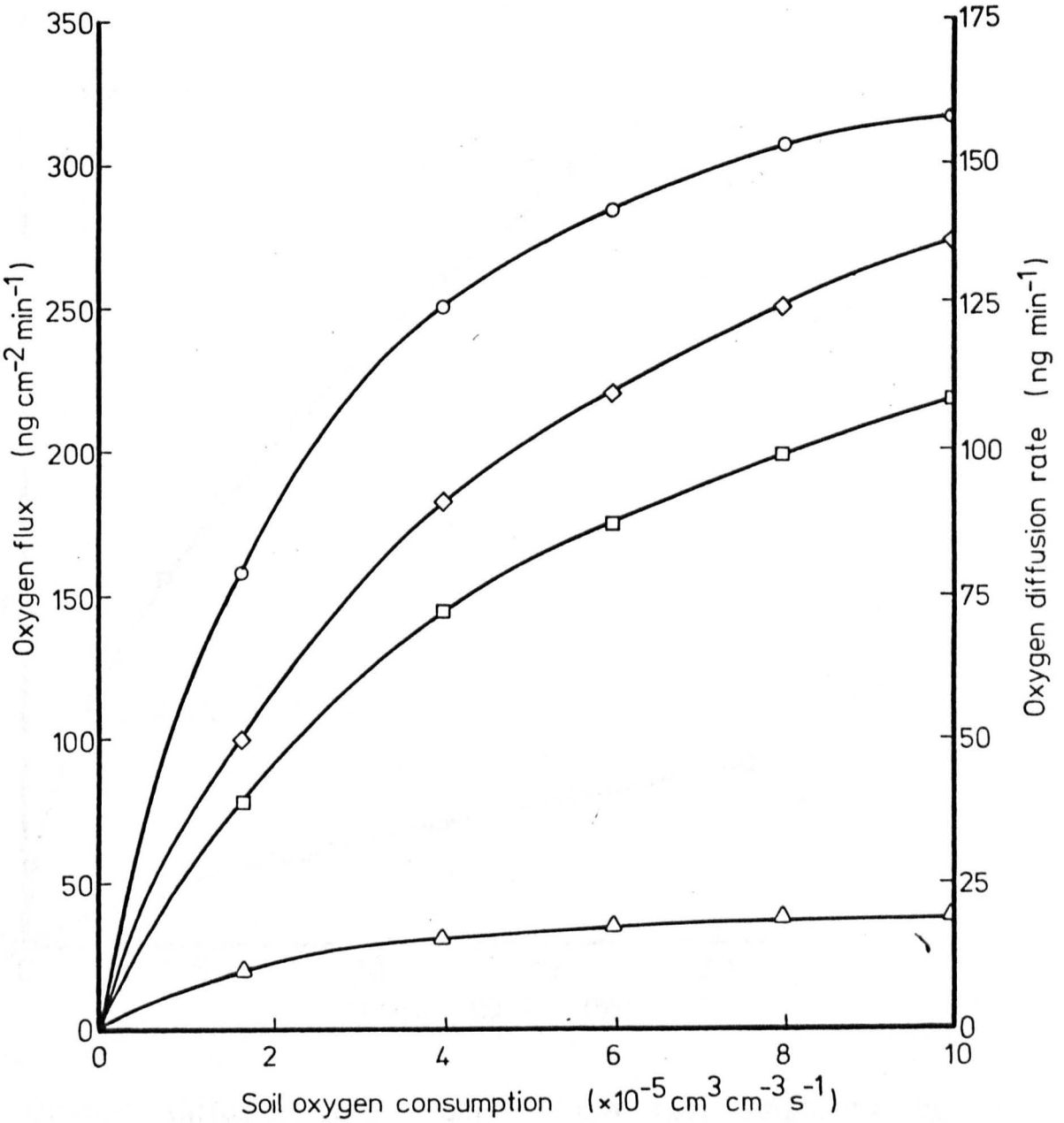
350
300
250
200
150
100
50
0
Oxygen flux (ng cm^{-2} min^{-1})
175
150
125
100
75
50
25
0
Oxygen diffusion rate (ng min^{-1})
0
2
4
6
8
10
Soil oxygen consumption (×10^{-5} cm^3 cm^{-3} s^{-1})

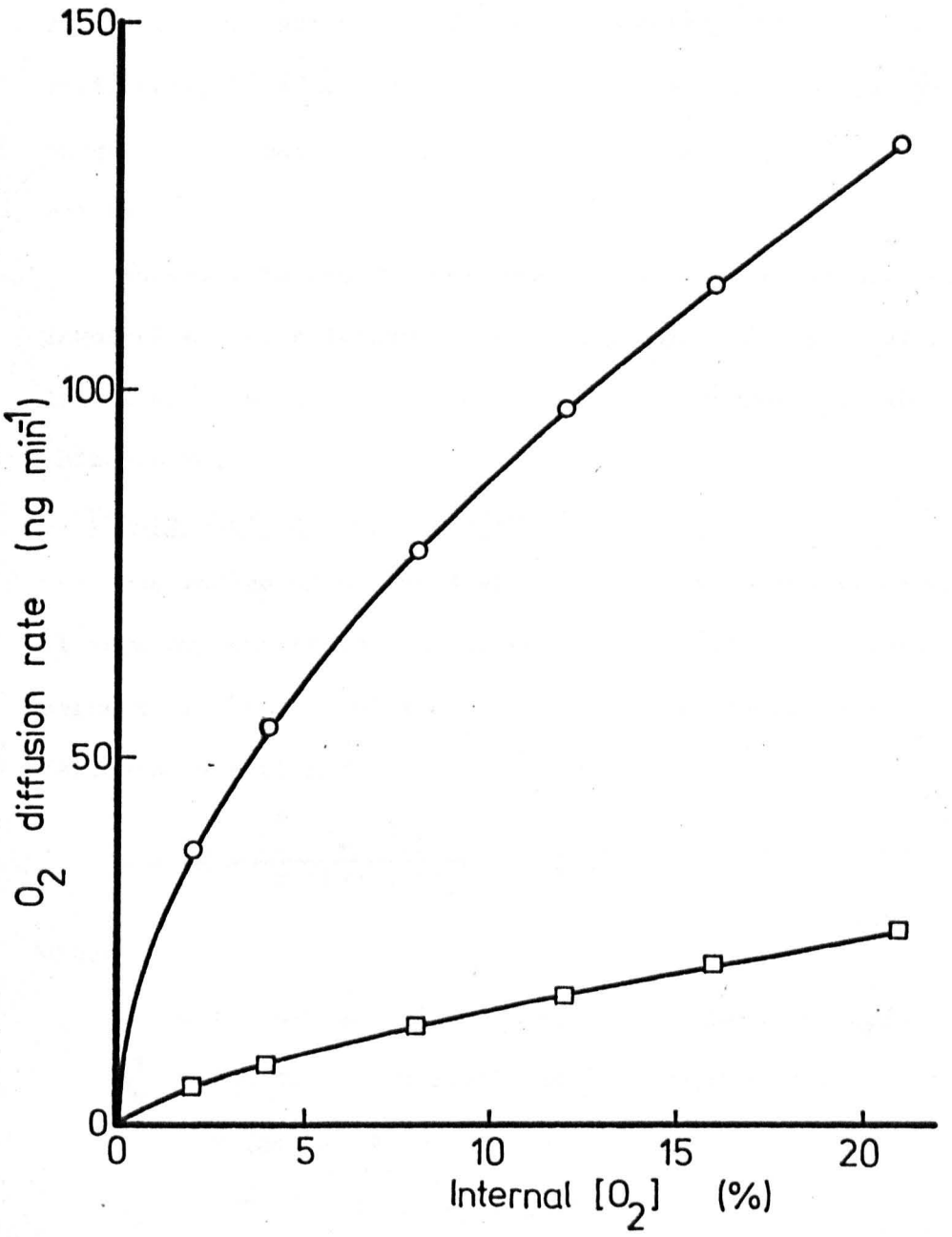

FIG. 9.2 Oxygen diffusion rate from 1·0 cm root segments as a function of internal oxygen concentration.
Soil oxygen consumption 4×10^{-5} cm^3 cm^{-3} s^{-1}
(o) root radius 0·10 cm
(□) " " 0·01 cm

concentration (p.173). This type of relationship also provides one method of programming the analogue for specified rates of soil oxygen consumption: using a graph similar to Fig.9.2 for the root radius under consideration, and with a variable resistor replacing the fixed shell resistance, R'_s (Chapter 2), the oxygen lost to the soil at any internal oxygen concentration could be programmed by adjustment of the variable resistor.

However, in the present study, a second method was adopted, which involved the calculation of the radius and diffusive resistance of a liquid shell which would provide the same oxygen sink as the soil of the rhizosphere.

2. Liquid shell radius and diffusive resistance

The radius of a liquid shell, the outer boundary of which is maintained at zero oxygen concentration, which would impose the same sink on the root segment as the soil of the rhizosphere, may be determined by solving the following equation for r_s.

$$J = VM = \frac{D_w^t \; A_r \; C_{wl}^t}{r_r (\log r_s / r_r)} \qquad g\ s^{-1} \qquad (9.3)$$

where:

J = the oxygen diffusion rate from the root surface ($g\ s^{-1}$)

D_w^t = the diffusion coefficient of oxygen in water at temperature t ($cm^2\ s^{-1}$)

r_s = the radius of the liquid shell (cm)

A_r = the surface area of the root segment (cm^2)

The thickness of the liquid shell is then equal to

$$(r_s - r_r) \quad cm$$

Fig.9.3 shows how the liquid shell thickness varies with internal root oxygen concentration for two values of root radius and five levels of soil sink activity (root wall resistance assumed negligible).

The resistance to oxygen diffusion, R_s^t, offered by the radial path

FIG. 9.3 The variation in liquid shell thickness with internal root oxygen concentration for two values of root radius and five levels of soil sink activity.

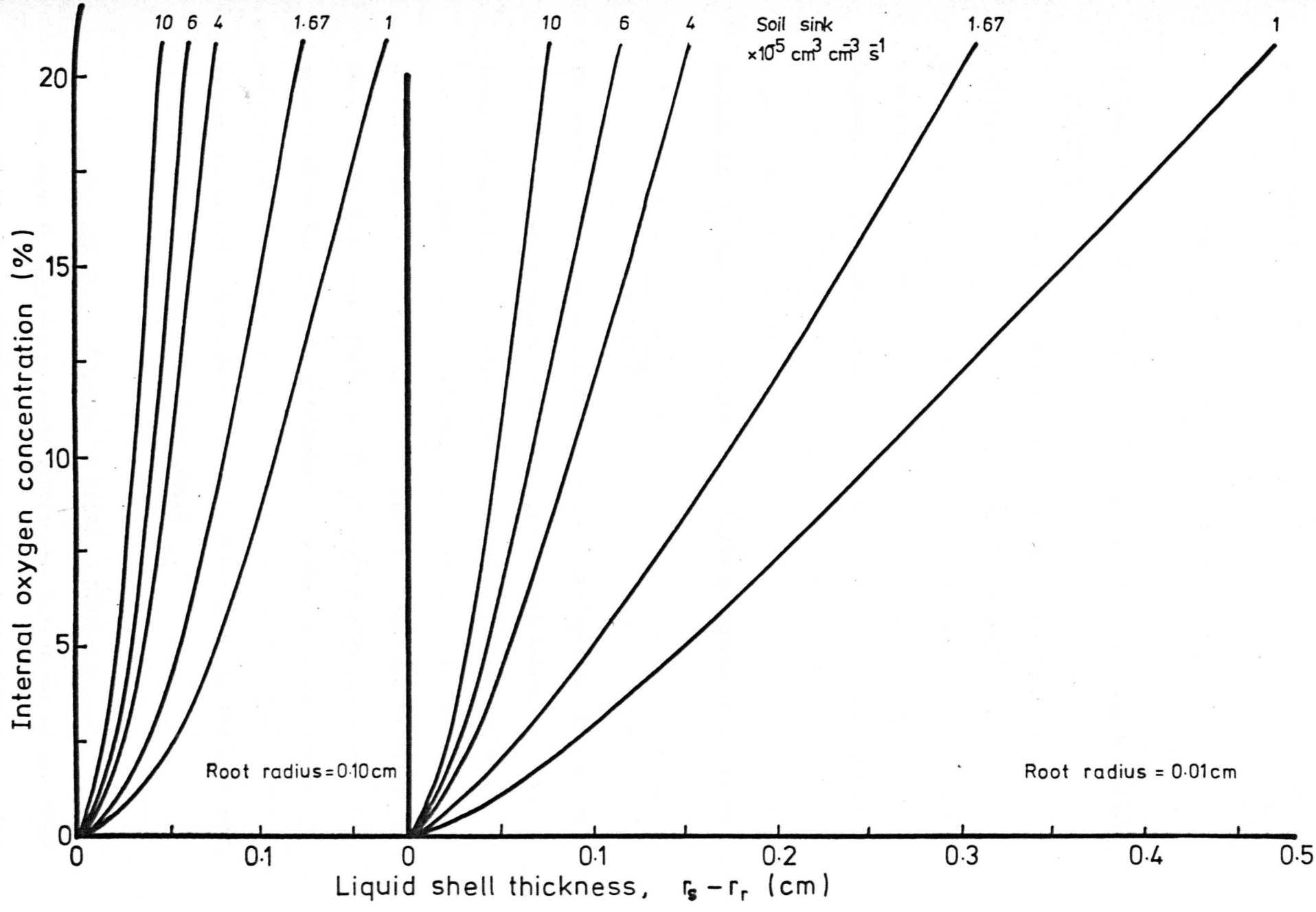
10
6
4
1·67
1
10
6
4
Soil sink
×10⁵ cm³ cm⁻³ s⁻¹
1·67
1
Internal oxygen concentration (%)
20
15
10
5
0
Root radius=0·10cm
Root radius = 0·01cm
0
0·1
0
0·1
0·2
0·3
0·4
0·5
Liquid shell thickness, $r_s - r_r$ (cm)

between the root surface and the outer boundary of the liquid shell is given by equation 4.7, ie.

$$R_s^t = \frac{r_r(\log r_s/r_r)}{A_r D_w^t} \times \frac{C_a^t}{C_{a-w}^t} \qquad s\ cm^{-3}$$

3. Conversion of liquid shell diffusive resistance (s cm^{-3}) to analogue resistance (ohms)

In the case of a root segment of length 1.0cm and 0.05cm radius, within a liquid shell of 0.1125cm radius, $R_s^{23^o}$ calculates to 1.7855×10^5 s cm^{-3}. The analogue construction is such that this resistance is equivalent to 1.8 KΩ. With this resistor value the R.O.L. from the root segment is 78.5ng min^{-1} or 250ng $cm^{-2}min^{-1}$ at an internal oxygen concentration of 18.01% and root wall resistance of zero (Armstrong and Wright, 1976b). Where the liquid shell radius is other than 0.1125cm its electrical resistance, R_s', may be calculated on a simple proportionality basis:

$$R_s' = \frac{1.8\ R_s}{1.7855 \times 10^5} \quad K\Omega \qquad (9.4)$$

The relationship between analogue resistance and internal oxygen concentration is shown in Fig.9.4 for two values of root radius and five levels of soil sink activity. The relationships between analogue resistance, root radius and internal oxygen concentration at two levels of soil sink activity are plotted in Fig.9.5. Using graphs of the type shown in Fig.9.4 a specified rate of soil oxygen consumption may be programmed in the analogue by adjusting the shell resistance to the value indicated either by the internal oxygen concentration (if root wall resistance is not programmed) or by the concentration at the root wall, C_{wl}, (if a wall resistance has been included).

B. THE ANALOGUE SIMULATION OF ROOTS OF DIFFERENT RADII

In order to make use of shell resistances calculated as described above, and to simulate roots of various radii, it was necessary to display

FIG. 9.4 The relationships between analogue resistance and internal oxygen concentration for two values of root radius and five levels of soil sink activity.

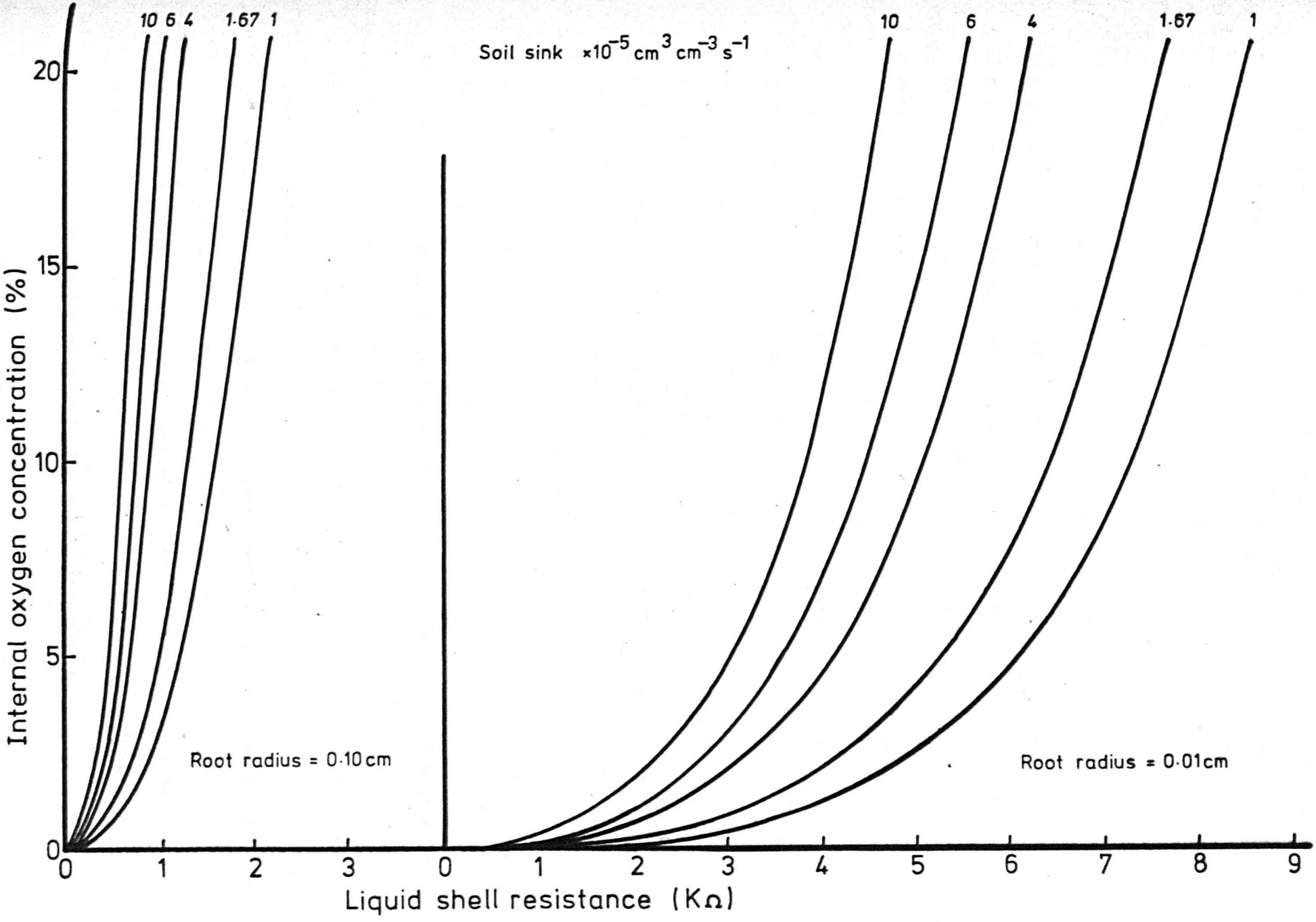
Soil sink ×10⁻⁵ cm³ cm⁻³ s⁻¹
10 6 4 1·67 1
10 6 4 1·67 1
Root radius = 0·10 cm
Root radius = 0·01 cm
Internal oxygen concentration (%)
Liquid shell resistance (KΩ)
0
5
10
15
20
0 1 2 3 0 1 2 3 4 5 6 7 8 9

R.O.L. and respiration as diffusion rate (ng min^{-1}) rather than as flux (ng $cm^{-2}min^{-1}$). Flux, if required, could be derived simply by dividing diffusion rate by the surface area of the root segment in question. Some simple modifications to the analogue circuitry were needed to achieve this.

Because of a scale graduation of fifty divisions a convenient full-scale deflection (f.s.d.) on the respiratory and R.O.L. meters was 125ng min^{-1}. This was sufficient to accommodate diffusion rates from thinner root segments and from thicker segments with lower internal oxygen concentrations. To monitor higher diffusion rates and respiratory activity the f.s.d. could be doubled or trebled by means of meter shunts.

The conversion of the meters from f.s.d. 250ng $cm^{-2}min^{-1}$ to f.s.d. 125ng min^{-1} was a simple modification. For a meter to give an f.s.d. of 125ng min^{-1} the current previously required to cause an f.s.d. of 250ng $cm^{-2}min^{-1}$ must now give a reading of only 78.5ng min^{-1} (since for the same root segment of r_r = 0.05cm the flux of 250ng $cm^{-2}min^{-1}$ and diffusion rate of 78.5ng min^{-1} are equivalent). It is apparent, therefore, that the meter reading must be reduced from f.s.d. to 78.5ng min^{-1} without causing an overall change of current in the circuit. This was achieved by reducing the value of the 10Ω meter-shunt to 6.28Ω (ie. 10 x 78.5/125), the new resistor value being attained by using resistance wire cut to the appropriate length. Since the new resistor had the effect of very slightly increasing the total current the original value was restored by connecting the difference in shunt resistance, 3.72Ω, in series with the liquid shell resistance.

When root wall resistance was programmed it was necessary to use the oxygen concentration at the root wall (rather than the internal concentration) in setting the shell resistance for a particular soil sink value (p.176). The wall concentration was measured simply by connecting voltmeters between the resistors R'_{wl} and R'_s (Fig.2.8).

FIG. 9.5 The relationships between analogue resistance, root radius and internal oxygen concentration at two levels of soil sink activity.

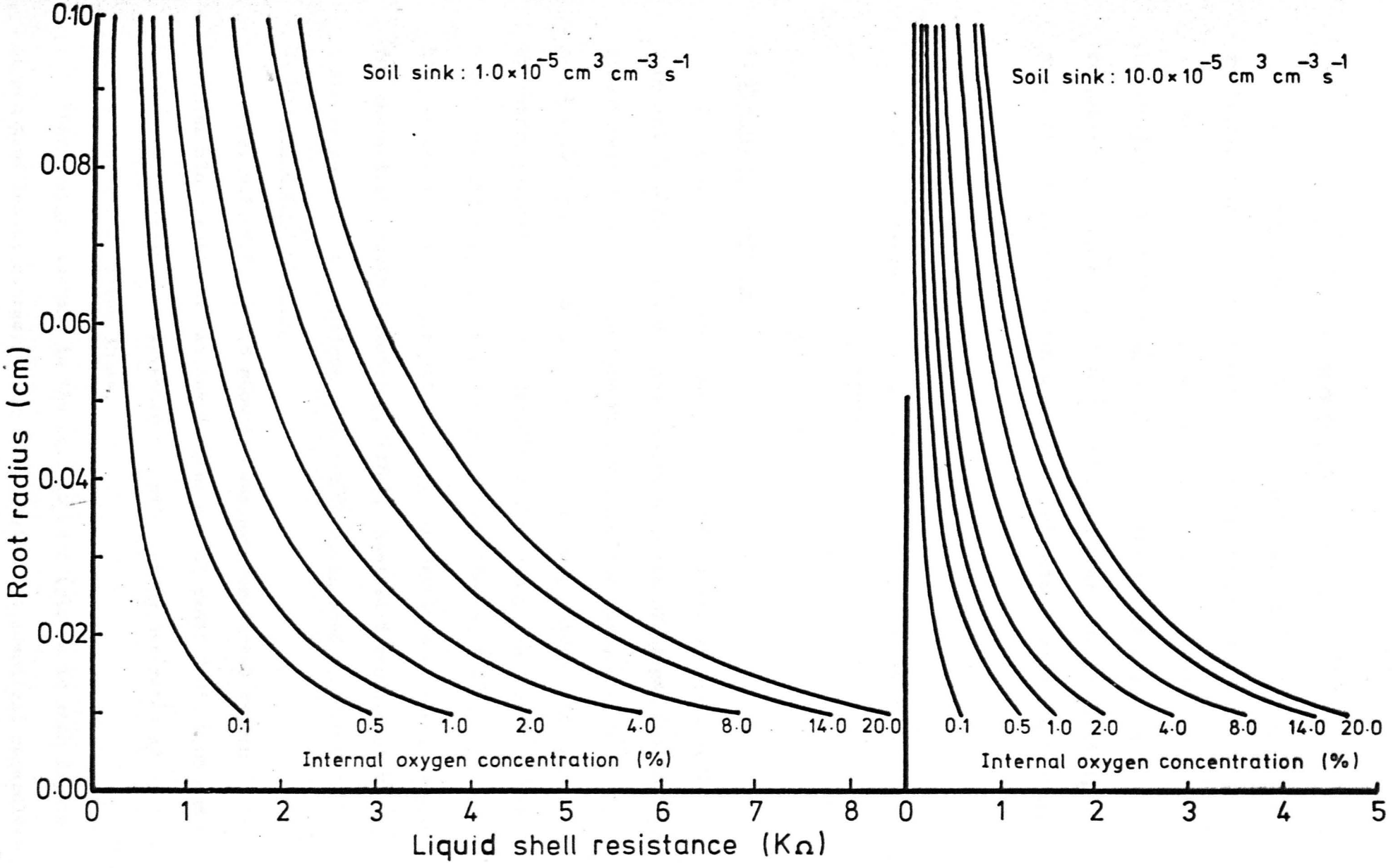
Soil sink : 1·0×10⁻⁵ cm³ cm⁻³ s⁻¹
Soil sink : 10·0×10⁻⁵ cm³ cm⁻³ s⁻¹
Root radius (cm)
0·10
0·08
0·06
0·04
0·02
0·00
0·1
0·5
1·0
2·0
4·0
8·0
14·0
20·0
Internal oxygen concentration (%)
0 1 2 3 4 5 6 7 8
0 1 2 3 4 5
Liquid shell resistance (KΩ)

C. PROGRAMMING

Programming each segment of the analogue for the liquid shell resistance was carried out using three decade resistance switches connected in series between the root wall and the liquid shell boundary. Each of the nine divisions of the switches connected respectively a 1,000Ω , 100Ω and 10Ω resistor into the series, enabling the shell resistance to be varied between zero and 9,990Ω.

II. SOIL OXYGEN DEMAND, ROOT RADIUS AND INTERNAL OXYGEN REGIME

INVESTIGATION 1

1. Programming details

The analogue was programmed to simulate roots of radii 0.01, 0.05 and 0.10 cm situated within soils of rates of oxygen consumption effectively zero (ie. the root wall was impermeable), 4×10^{-6} and 4×10^{-5} cm^3 cm^{-3} s^{-1}. For simplicity respiratory rate and effective porosity were considered constant along the length of the roots; respiratory rate was programmed as 120ng cm^{-3} s^{-1}, a fairly high value, whilst the porosity of 7.5% represents a mid-range value for non-wetland roots (Armstrong, 1978). Root wall resistance was taken as zero and the maximum root length considered was 8.0cm.

2. Results and discussion

Figs. 9.6, 9.7 and 9.8 show the analogue-preducted oxygen profiles along roots of various lengths and of radii 0.01, 0.05 and 0.10cm respectively when situated in soils having the rates of oxygen consumption given above.

Where oxygen leakage to the soil is zero (plot A in each figure) oxygen profiles at corresponding root lengths are identical regardless

FIG. 9.6 Illustrating the effect of soil sink activity on the internal oxygen regime of roots of different length but of uniform porosity ($\epsilon = 7{\cdot}5\%$) and respiratory activity (120 ng cm^{-3} s^{-1})

Root radius $r = 0{\cdot}01$ cm

A Root wall resistance infinite, hence no oxygen leakage to soil.

B & C Root wall resistance negligible.

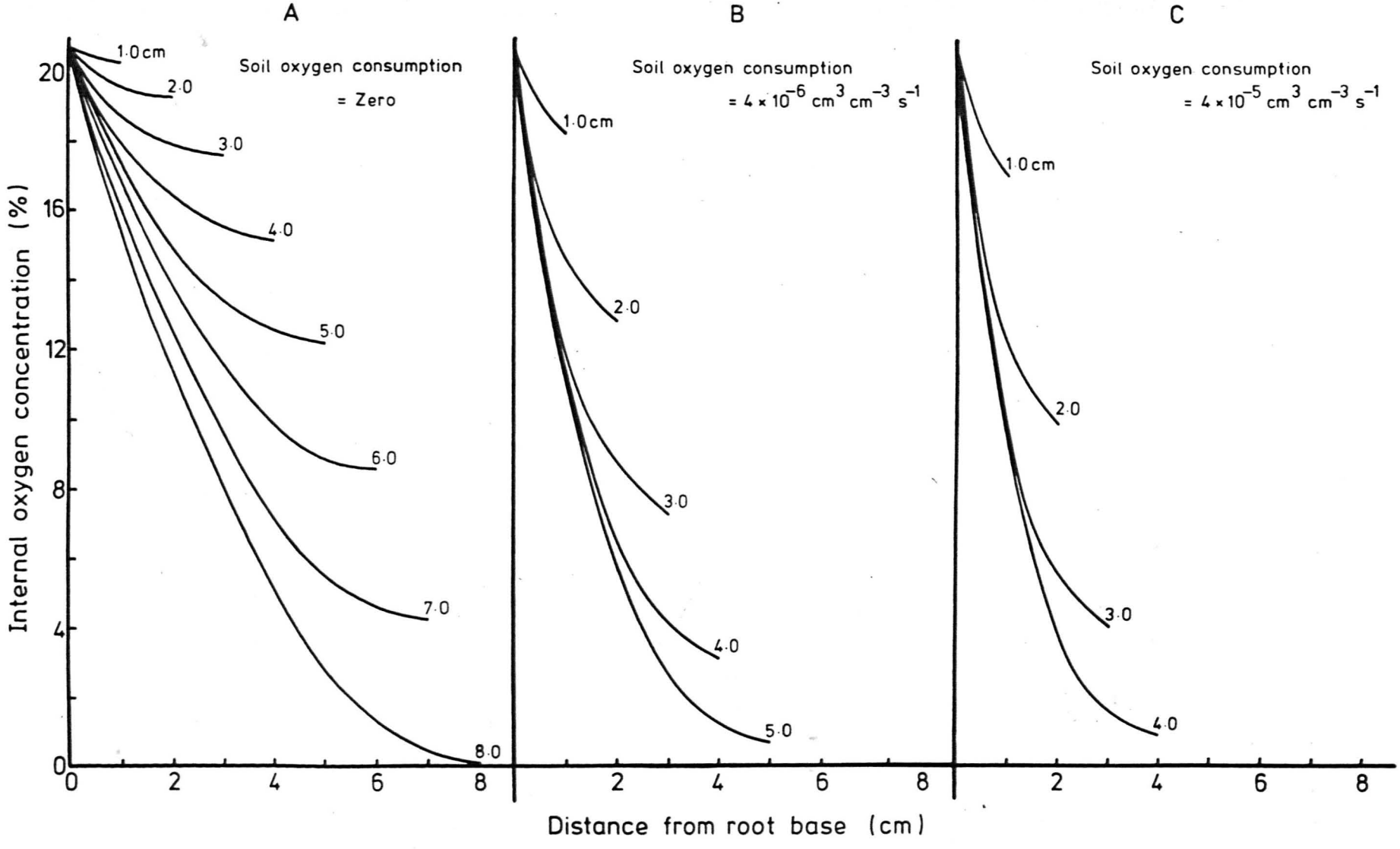
A
B
C
Soil oxygen consumption
= Zero
Soil oxygen consumption
= 4 × 10⁻⁶ cm³ cm⁻³ s⁻¹
Soil oxygen consumption
= 4 × 10⁻⁵ cm³ cm⁻³ s⁻¹
1·0cm
2·0
3·0
4·0
5·0
6·0
7·0
8·0
Internal oxygen concentration (%)
Distance from root base (cm)
0
4
8
12
16
20
2
4
6
8

FIG. 9.7 Legend as for Fig. 9.6 but root radius = 0·05cm

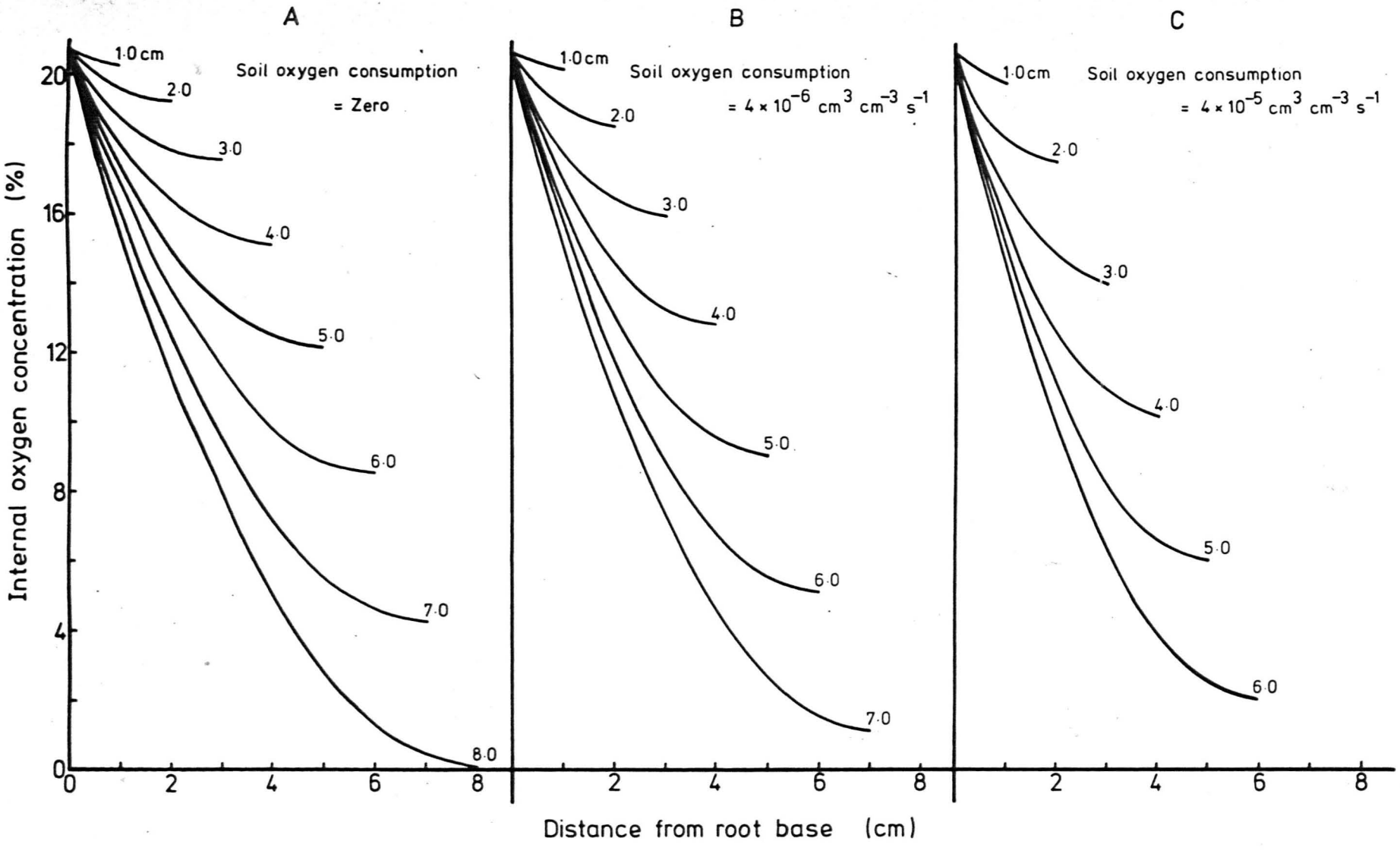
A
B
C
1·0cm
2·0
3·0
4·0
5·0
6·0
7·0
8·0
Soil oxygen consumption
= Zero
Soil oxygen consumption
= 4 × 10⁻⁶ cm³ cm⁻³ s⁻¹
Soil oxygen consumption
= 4 × 10⁻⁵ cm³ cm⁻³ s⁻¹
Internal oxygen concentration (%)
Distance from root base (cm)
0
4
8
12
16
20
2
4
6
8

FIG. 9.8 Legend as for Fig. 9.6 but root radius = 0·10cm

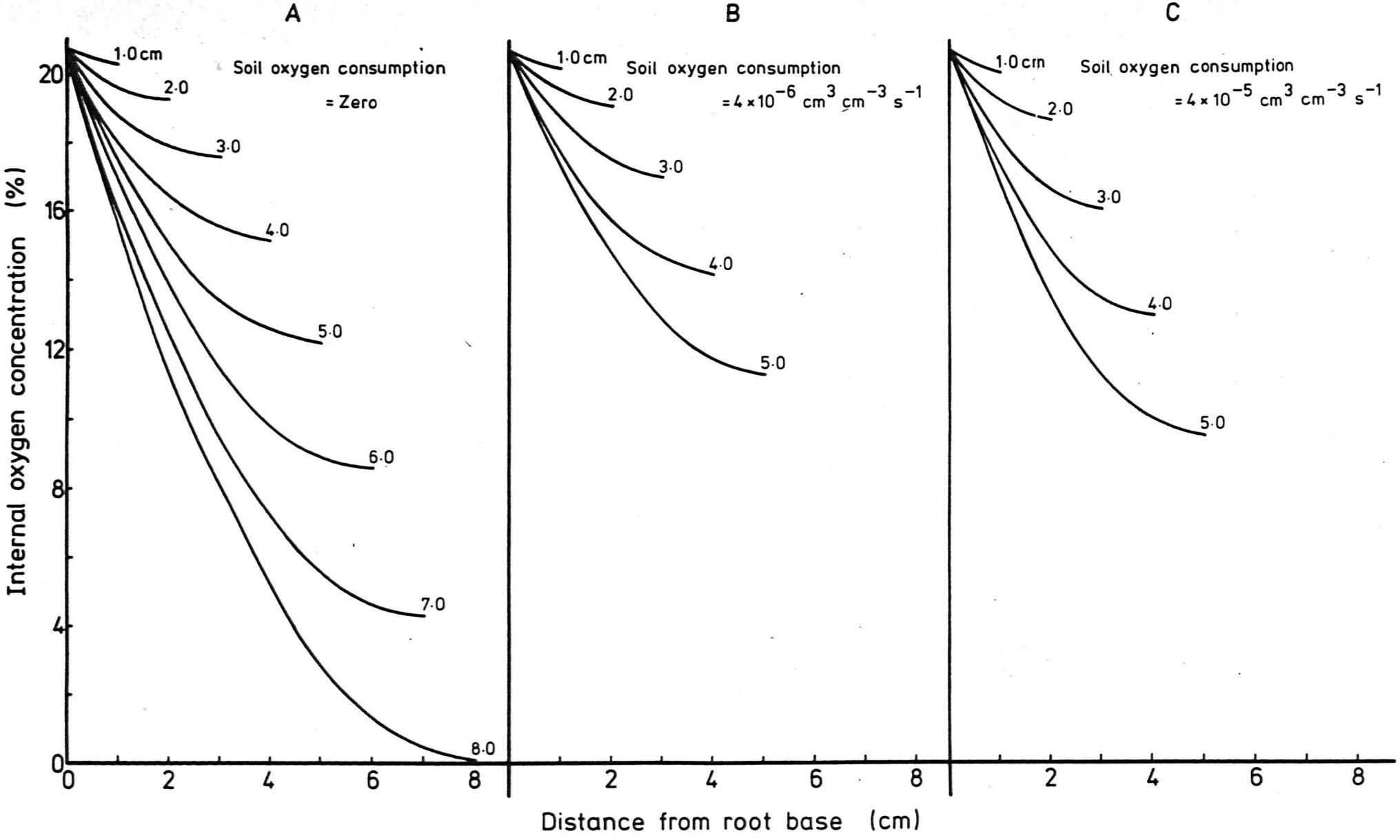
A
B
C
1·0 cm
2·0
3·0
4·0
5·0
6·0
7·0
8·0
Soil oxygen consumption
= Zero
Soil oxygen consumption
= 4 × 10⁻⁶ cm³ cm⁻³ s⁻¹
Soil oxygen consumption
= 4 × 10⁻⁵ cm³ cm⁻³ s⁻¹
Internal oxygen concentration (%)
0
4
8
12
16
20
0
2
4
6
8
Distance from root base (cm)

of the root radius. This is due to the fact that the increase in respiratory oxygen consumption accompanying an increase in root radius is exactly balanced by the corresponding decrease in diffusive resistance (since these quantities are proportional to r_r^2 and $1/r_r^2$ respectively). Consequently the product of diffusive resistance and respiratory consumption for any particular segment is constant.

It may be seen from Figs. 9.6 - 9.8 that soil oxygen demand can exert a considerable influence upon the oxygen regime within the root. At each root length an increase in the rate of soil oxygen consumption produces a decrease in internal oxygen concentration. The effect of the soil sink is more severe in the narrow roots. This agrees with computer predictions made by Luxmoore et al. (1970b) and is undoubtedly due to the synergism between soil oxygen consumption and the increased diffusive resistance

associated with decreased root radius.

If root growth ceases at an apical oxygen concentration of about 2% (Chapter 5) the maximum root lengths attainable in each of the three soils may be deduced from the figures. Greatest depth of penetration occurs when there is no oxygen leakage to the soil (eg. due to an impermeable root wall) and is between 7 and 8cm regardless of root radius. Penetration depth in soils having a finite oxygen demand then becomes dependent upon radius. Thus the narrowest root in the soil of greatest sink activity ($4 \times 10^{-5} cm^3 cm^{-3} s^{-1}$) would grow to a length of only 3-4cm (Fig.9.6C). The high rate of oxygen consumption per cm in the 0.10cm radius root enabled a maximum length of only 5cm to be modelled (Fig. 9.8B,C). However, the results suggest that this root would grow to lengths exceeding those attained by narrower roots in the same soil. It is known that roots growing in waterlogged soil are in general of greater radius than those in soil which is well aerated (Kramer, 1966; Yu et al., 1969).

INVESTIGATION 2

1. Programming details

In this investigation the analogue was programmed to examine the relationship between apical oxygen concentration, root length, effective porosity, respiration and soil oxygen demand. Again, porosity and root respiration were assumed constant along the length of the roots, but wall permeability fell from 100% at the apex to a minimum of 60% at 6cm and beyond. Programming details are summarised in Table 9.1, which refers also to the results illustrated in Fig.9.9.

2. Results and discussion (See Table 9.1 and Fig.9.9)

As in the previous investigation the effectiveness of the soil sink in reducing the internal oxygen regime is greatest in the narrow roots (D,H). On the other hand the influence of respiratory activity is higher in the thicker roots: for example, if the C.O.P. is 2% the maximum length

TABLE 9.1: SUMMARY OF THE ANALOGUE INPUT DATA USED TO PRODUCE FIG.9.9.

Figure	Root Radius (cm)	Root Respiration ($ngO_2\ cm^{-3}\ s^{-1}$)	Soil Oxygen Consumption ($cm^3O_2\ cm^{-3}\ s^{-1}$)
A	Any	120	0
B	0.05	120	4×10^{-6}
C	0.05	120	4×10^{-5}
D	0.01	120	4×10^{-5}
E	Any	30	0
F	0.05	30	4×10^{-6}
G	0.05	30	4×10^{-5}
H	0.01	30	4×10^{-5}

Other conditions:

1) Effective porosity (left to right in each figure) (%): 1.5, 3, 7, 15.

2) Root wall permeability declines from 100% at the apex to 60% at 6cm and beyond.

3) Root growth ceases at 2.0% internal apical oxygen concentration.

FIG. 9.9 Internal apical oxygen concentrations in roots as a function of root length, root respiration, effective porosity, radius and soil oxygen consumption.

(See Table 9.1)

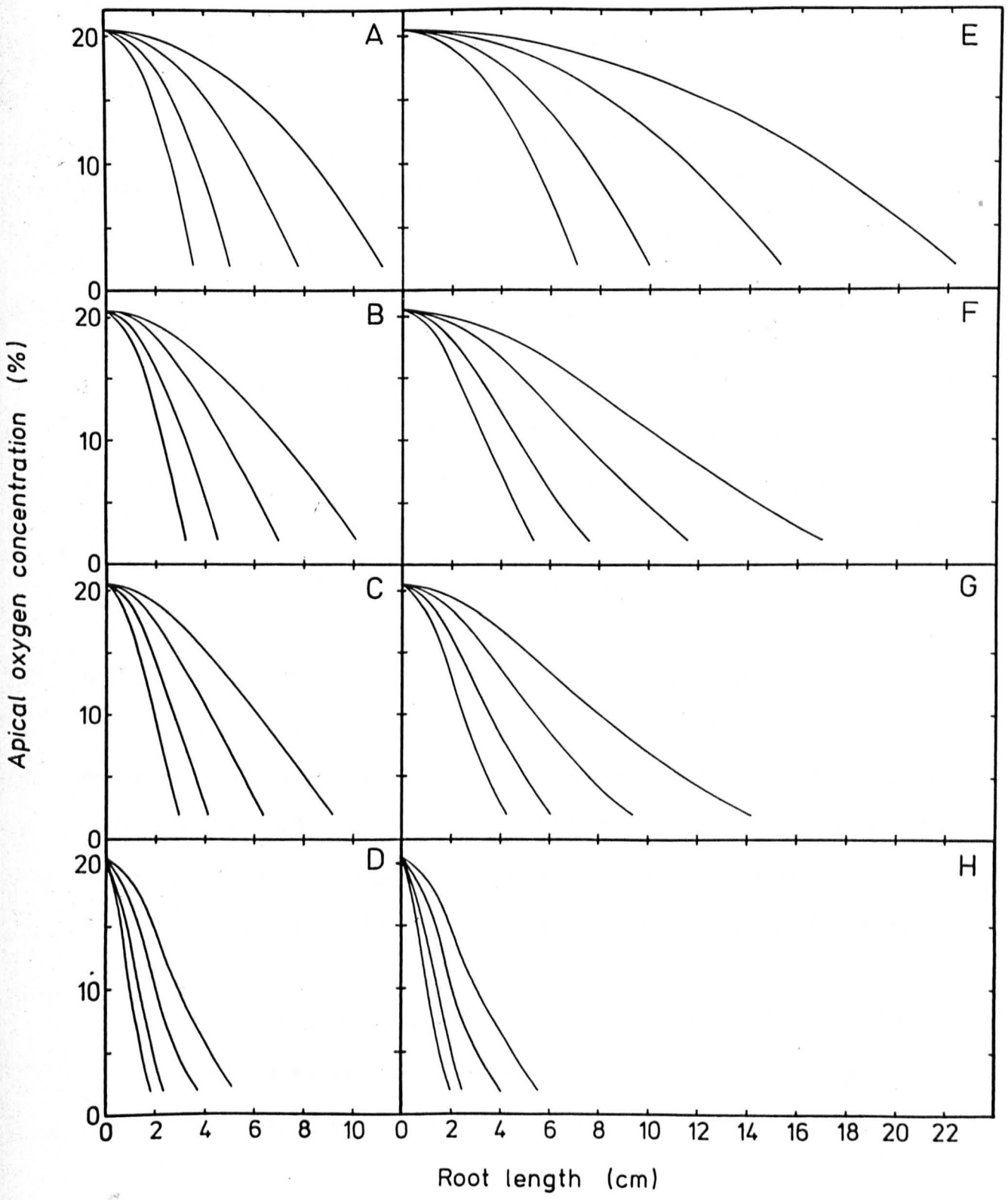
A
B
C
D
E
F
G
H
20
10
0
0 2 4 6 8 10
0 2 4 6 8 10 12 14 16 18 20 22
Apical oxygen concentration (%)
Root length (cm)

predicted for the narrow root (r = 0.01cm) is 5.5cm when respiratory rate is 30ng $cm^{-3}s^{-1}$ (H), but only 0.3cm shorter at a respiratory rate of 120ng $cm^{-3}s^{-1}$ (D). Where leakage to the soil is zero (A,E) the internal oxygen regime is independent of root radius (see Investigation 1) and is a function of porosity and respiratory rate only. In all cases the apical oxygen concentration increases with increasing effective porosity (ie. decreasing internal diffusive resistance).

It is of interest that an increase in the effectiveness of the soil sink is associated with increased concavity of the apical concentration vs. root length curve (compare, for example E and H). Presumably, this is a result of the curvilinear relationship between internal oxygen concentration and soil oxygen consumption (p.174) being superimposed on the otherwise convex concentration vs. root length plots.

Assuming that root growth ceases at apical oxygen concentrations below a critical value (in this case 2%) rooting depth under these circumstances varies directly with root radius and effective porosity and indirectly with soil sink activity and root respiration rate. Thus, a root of radius 0.01cm, effective porosity 1.5% and respiratory rate 120ng $cm^{-3}s^{-1}$, in a soil of oxygen consumption 4×10^{-5} $cm^3cm^{-3}s^{-1}$, would grow to a length of only 1.9cm (D). On the other hand, a root of radius 0.05cm, effective porosity 15% and respiratory rate 30ng $cm^{-3}s^{-1}$ could grow to a length of 17cm in a soil consuming oxygen at the rate of 4×10^{-6} $cm^3cm^{-3}s^{-1}$ (F); if there is no leakage of oxygen to the soil a root having similar porosity and respiratory rate could penetrate to a depth of 22cm irrespective of root radius (E).

It must be noted, however, that the predictions concerning maximum attainable root length given in Fig.9.9 are likely to be in excess of the true values if the importance of rhizosphere oxygenation is taken into account. As the apical oxygen concentration declines with root length R.O.L. will decrease until its magnitude may be insufficient to provide adequate protection against invasion by soil phytotoxins. In addition,

few roots grow devoid of laterals and the sink due to these organs will lower the internal oxygen regime and limit rooting depth still further (Healy, 1975).

CONCLUSIONS

Armstrong (1978) suggests that in the non-wetland root 15% may represent an upper limit for effective porosity, and this only if the tortuosity factor approaches unity. Indeed, the available experimental data indicate that porosities significantly less than this are usual; for example Yu et al. (1969) showed that in a number of non-wetland species growing in drained soil root porosities ranged from 3.5% in barley to 11.5% in corn. The results presented in this chapter indicate that such roots are ill-adapted to growth in waterlogged soil, even though respiratory rate be as low as 30ng $cm^{-3}s^{-1}$ and soil oxygen demand no more than the moderate value of $4 \times 10^{-6} cm^3 cm^{-3} s^{-1}$ (Fig.9.9). This agrees with the results of Yu et al., which showed that the roots were able to penetrate only a short distance below the water table when the soil was "half flooded".

When subjected to soil waterlogging non-wetland species can show some degree of adaptation by producing fresh roots of higher porosity. Even so, the enhanced internal ventilation, whilst possibly enabling the plants to survive in flooded environments, seems insufficient to allow the successful exploitation of permanently waterlogged soil. The new roots produced by corn under conditions of "full flooding" (Yu et al., 1969) had porosities up to 18%, whilst in sunflower the porosity rose from 6% to 11%; these roots penetrated the wet soil up to 17cm and 12cm respectively. The data of Yu et al., agree fairly well with the predictions presented in this chapter in that even "adapted" non-wetland roots may penetrate waterlogged soil only to depths of about 17cm (Fig.9.9 F). On the other hand, the wetland root, with its normally greater radius, higher porosity and

associated lower respiratory rate, and with leakage of oxygen to the soil restricted to the apical region, may be expected to attain substantially greater depths. By means of the mathematical model described in Chapter 7 it was predicted that E.angustifolium could root to a depth of 40cm in a soil having an oxygen demand of 4×10^{-6} cm^3 O_2 cm^{-3} s^{-1}.

CHAPTER 10

FINAL DISCUSSION

The differential sensitivity to conditions of soil anoxia exhibited by wetland and non-wetland plants is undoubtedly due largely, if not entirely, to the presence in the former of an efficient system for the internal transport of oxygen. By gaseous diffusion through large intercellular spaces wetland plants are able to transport oxygen from the aerial parts to the roots in sufficient quantity to maintain normal aerobic respiration; in addition, oxygen may leak from the root into the soil to form a protective oxygenated rhizosphere. Internal oxygen transport in non-wetland species, although probably always occurring to some extent, is less effective (Healy and Armstrong, 1972; Healy, 1975). The high effective diffusive resistance due to low gas-filled porosity and the associated elevation of respiratory demand prevents the transport of oxygen in non-wetland plants in the quantities associated with wetland species. Consequently, if non-wetland plants are subjected to low oxygen concentration in the rooting medium, adequate aeration will be restricted to short roots and to the basal regions of longer roots.

Nevertheless, despite their highly efficient oxygen transport systems, wetland plants must offer some resistance to the internal diffusion of the gas; part of the research described in this thesis sought to identify and quantify the internal resistances to oxygen transport in Eriophorum angustifolium. If photosynthesis is prevented, the atmosphere is the only oxygen source for a plant rooting in anaerobic soil and in Eriophorum the gas was found to enter the plant exclusively via the stomata; oxygen diffusion across the cuticle and epidermis was undetectable. It was shown that under normal circumstances stomatal movements did not restrict internal aeration, and indeed relatively few stomata situated at the leaf base are required for the normal ventilation of the root system. If effective stomata are restricted to more apical regions, for example by partial submergence, the number necessary for adequate root aeration rises due to the

increased diffusive resistance caused by the lengthening of the diffusion path. Artificial stomatal "closure", induced by the antitranspirant phenylmercuric acetate and by increased ambient CO_2 concentration, was ineffective in reducing R.O.L. from the roots unless effective stomata were reduced to small numbers (for example by excising most of the leaf and sealing the cut end). Theoretical considerations led to the conclusion that the presence of stomata in large numbers (e.g. 10,000 cm^{-2} lower leaf surface in Eriophorum) accounts for their negligible diffusive resistance; the only measurable impedance to oxygen entry under normal circumstances seems to be that due to the boundary layer of still air at the leaf surface, and even this is small. Calculations based on these findings indicate that normal respiration could be maintained in small Eriophorum plants having a rate of oxygen consumption of 40ng s^{-1} by four stomata with a pore width of 8μm, or 25 stomata with a pore width of 1μm. Clearly, it is unlikely that darkness will be detrimental to the wetland plant by its effect on stomatal aperture.

The results also illustrate the need for caution when referring to stomata as "closed". For example, Walker and Zelitch (1963) implied that stomata of width less than 2μm were closed, whereas under normal circumstances stomata of this aperture will not impede the diffusive flux of oxygen. It seems necessary, therefore, to qualify statements in which stomata are described as shut. Pores which allow the passage of considerable quantities of oxygen may not, for example, admit a measurable amount of CO_2 because of differences in concentration gradients, and the different demand for the gases by the plant tissues.

Oxygen diffusing from leaves to roots, and from roots into the surrounding medium, encounters a number of discrete impedances. Diffusive resistance was quantified in whole plants and in single-leaf preparations of E.angustifolium at 23°C (respiration normal) and 3°C (respiration reduced) with various degrees of submergence (diffusion path length). Effective

diffusive resistance (i.e. physical or non-metabolic resistance plus the pseudo-resistance due to respiration and leakage) between the atmosphere and the outer surface of the root apex was less in the cooled plants; the difference increased with diffusion path length. For example, effective resistances for uncooled and cooled plants were respectively 35×10^5 and 4×10^5 s cm^{-3} at 17.5 cm path length, and 4×10^5 and 2×10^5 s cm^{-3} at 4cm path length (Fig.7.6). The higher resistance in the uncooled plants was undoubtedly due to respiration, which appears to be the major contributing factor to effective resistance. Healy (1975) similarly found that respiration in the roots of pea seedlings markedly increased effective resistance, but in this species physical resistance due to low porosity and tortuosity of the gas spaces was also important. Tortuosity of the gas conducting channels in the Eriophorum root was found to be very low, and this in conjunction with the high porosity, greatly reduces physical resistance.

Effective resistance was always less in whole plants than in single-leaf preparations. This is a consequence of the parallel arrangement of the leaf resistances, the overall resistance of the leaves being inversely proportional to their number. Clearly, a high leaf number, relative to the volume of the stem and below-ground organs, would be a distinct advantage to the plant.

Unexpectedly, resistance in the stem/root-shoot junction was low, and probably contributed no more to the total plant resistance than a portion of leaf base of length similar to that of the stem. Non-metabolic resistance ranged from 0.057×10^5 to 0.13×10^5 s cm^{-3}, whilst the effective resistance contributed from 0.084×10^5 to 0.202×10^5 s cm^{-3} to the total resistance of the plant. The low values are likely consequences of the short diffusion path between the leaf and root bases, and the continuity of the gas conducting system at the root-shoot junction. Coult (1964) considered that in Menyanthes trifoliata a compact tissue zone at the root base would drastically limit the diffusion of oxygen into the root from

the cortex of the rhizome. This is clearly not the case in Eriophorum, and in fact a brief anatomical study of Menyanthes did show the gas spaces of the root and rhizome cortices to be continuous; however, further work is required on Menyanthes before any firm conclusions can be drawn.

Resistance to oxygen diffusion offered by lacunar diaphragms has been the subject of speculation, but very little research. In this study non-metabolic resistance due to the diaphragms in the Eriophorum leaf was investigated. The mean resistance per diaphragm in the mid-leaf region was 0.34×10^5 s cm^{-3}, corresponding to an effective porosity of 0.23%; however, the diaphragm resistance per cm length of mid-leaf is only 0.072×10^5 s cm^{-3}. Oxygen diffusing from the atmosphere to the roots must always pass along the astomatal leaf bases and it is in this region, therefore, that diaphragm resistance will be of greatest significance under normal circumstances. Calculations showed that in each cm of leaf base resistance due to the diaphragms may be as low as 0.0114×10^5 s cm^{-3}. These results are in agreement with the conclusions of Teal and Kanwisher (1966) and Armstrong (1972) that cellular partitions across the gas conducting channels are unlikely to impose a substantial restraint on oxygen transport.

Unlike the situation in several other wetland species (Armstrong, 1967b) the apical root wall of Eriophorum offers appreciable resistance to the diffusion of oxygen. Wall resistance and total plant resistance are linearly related, the former being an important component of the latter at values of total resistance above about 1.6×10^5 s cm^{-3}. It is important to take account of wall resistance if the cylindrical electrode technique is to be used to predict internal root oxygen concentrations.

If the assumptions were made that the apical root wall had an effective thickness identical to the observed thickness (65μm), and that respiration rate in the wall was that of the root apex as a whole (75ng $cm^{-3}s^{-1}$), the effective diffusion coefficient for oxygen in the wall layers, calculated from physical resistance data, varied between 0.57×10^{-5} and 4.14×10^{-5}

$cm^2 s^{-1}$. This variation was reflected in the range of wall resistance values and was probably a consequence of different degrees of wall suberisation. Where wall diffusivity was high suberisation was presumably at a minimum and in two experiments the diffusion coefficients were greater than the diffusivity of oxygen in water; it is very tempting to offer cytoplasmic streaming as an explanation of these enhanced diffusion coefficients.

At normal internal root apical oxygen concentrations (mean about 15%) respiration in the root wall contributed little to effective wall resistance measured by the cylindrical electrode technique. This is because respiratory oxygen consumption by the wall is insignificant compared with the oxygen flux from the root. At lower internal oxygen concentrations (ca. 2% or less), when flux is much reduced, respiration may add considerably to effective wall resistance. One can, therefore, envisage a situation in which resistance in the wall could reduce the oxygen flux from the root to an immeasurable amount whilst the internal oxygen concentration might still be significant.

In contrast to the situation in wetland plants, in which the root wall is permeable to oxygen only in the apical region, oxygen leakage apparently occurs along the entire length of the roots of mesophytes. Healy (1975) found that in pea seedlings loss of oxygen from roots in an anaerobic medium constituted a significant part of the effective plant resistance. In E.angustifolium loss of oxygen from the root apex is negligible compared with that consumed in respiration. Also, leakage of oxygen from the leaves of semi-inundated plants did not appear to add to the total resistance under the experimental conditions. However, oxygen does leak from the leaves and it is interesting to recall that oxidised iron deposits frequently coat the leaves of buried, emerging plantlets, which rely upon gas diffusion from the parent plants for their oxygen supply. It is possible, therefore, that under these conditions leakage of oxygen from the leaves may influence

the internal oxygen regime of young plants.

An important point, which emerged towards the end of the work on plant resistance, was that effective resistance is a concept of much greater complexity than was previously thought (Armstrong and Wright, 1975). Whereas the physical (non-metabolic) resistance component is independent of oxygen concentration (in much the same way that electrical resistance is independent of electrical potential), the respiratory component is very much dependent upon oxygen pressure. It was shown theoretically that because of this the effective resistance measured by the cylindrical electrode technique is inversely proportional to the ambient oxygen concentration. Consequently it was necessary to choose a standard oxygen concentration in order to compare effective resistances. It was also found that the apparent effective resistance of an excised plant segment is not identical to the resistance of the same segment in situ.

Total effective plant resistance was also shown to vary with the resistance of the liquid shell between root and electrode, whilst in a similar manner root wall resistance influences the effective resistance in the remainder of the plant. All these effects are consequences of the concentration-dependence of the respiratory component of effective resistance. It was concluded, therefore, that by using the cylindrical platinum electrode (or, apparently, any other concentration-dependent sensor) it is not possible to obtain absolute values of effective resistance.

In spite of the low resistance to oxygen diffusion offered by the wetland plant under normal circumstances, situations could arise, for example during partial inundation, when the diffusive resistance is effectively increased (by lengthening of the diffusion path). In such conditions internal aeration may become restricted and the oxygen concentration in remote parts of the plant may become insufficient to support aerobic respiration. Prior to the present study the minimum internal oxygen pressure required for uninterrupted aerobic metabolism (the C.O.P.)

had never been determined for intact plants.

If conditions are such as to reduce the internal oxygen status towards a C.O.P., then since there is always a gradient of oxygen concentration between leaves and roots (Chapter 5), it would be expected that the C.O.P. will first occur in the root apex; this was found to be the case. Ambient oxygen concentrations of about 10-11% round the leaves produced concentrations of about 2.5% within the cortical intercellular spaces of the root apices of rice and Eriophorum. At this concentration respiration in the low-porosity tissues of the meristem and developing stele became limited by oxygen deficiency.The experimental situation was modelled and it was concluded that due to the proximity of the gas spaces and the cortical cells, respiration in the tissues of the cortex was uninhibited above gas phase oxygen concentrations of 0.1% or less. These C.O.P.'s are appreciably lower than those obtained by other workers using in vitro methods. There is abundant evidence that under normal conditions the oxygen concentration within the root apices of wetland plants is much in excess of the critical value of about 2.5%.

Should oxygen pressures of 0.025 atm or less occur in the root apex the onset of anaerobiosis in parts of the meristem and stele may be expected to result in retarded root growth, and possibly even in death of the apex due to irreversible ultrastructural damage (Vartapetian, 1973; Vartapetian et al., 1970). In the present work roots of intact rice plants ceased to elongate when the oxygen concentration in the apex was brought within the range of C.O.P. values previously determined. However, providing the aerial parts had been maintained at a higher concentration, the roots recommenced growth at approximately normal rate on re-aeration; this was the case even when the apical concentration had been kept as low as 0.1 to 0.3% for 40h. Subjecting the plants to an atmosphere of oxygen-free nitrogen around the aerial parts for about 20h resulted in the death both of leaves and roots. Under these circumstances roots remained viable, and recommenced growth on

re-aeration, if provided with a respiratory substrate in the form of dissolved glucose. These results indicate that root growth depends upon unrestricted aerobic respiration in the meristem, and hence upon adequate aeration. They also suggest that anaerobic respiration in the plant is unable to support active root growth, but can be sufficient to maintain viability providing a supply of respiratory substrate is available (see Vartapetian et al., 1976, 1977).

There has been speculation concerning the possibility that the gas space system of wetland plants may function as an oxygen reservoir. It has been suggested that oxygen stored within the extensive intercellular spaces may prevent damage by anaerobiosis during periods of stomatal closure in the dark (see Williams and Barber, 1961). In view of results obtained during the present study this suggestion is clearly open to criticism since it seems unlikely that stomatal movements will restrict internal aeration. In addition, the re-growth of roots after 40h partial anoxia indicates that anaerobic metabolism may not exert the damaging effect commonly attributed to it; however, it is possible that in the field sub-optimal internal oxygen concentrations could be damaging to roots by restricting rhizosphere oxygenation. An investigation of the "reservoir function" of aerenchyma in E.angustifolium showed that internally-stored oxygen can maintain normal respiration at 23°C for no longer than 44 min; if a Q_{10} of 2 is assumed the corresponding time at 13°C would be only 88 min. After about 60 min oxygen in the internal atmosphere is completely exhausted. Full interpretation of the experimental results necessitated an electrical analogue simulation of the oxygen relations of submerged Eriophorum plants. It was shown that the gradient of oxygen concentration between leaves and roots persists after submergence, but oxygen is re-distributed within the plant as the major oxygen source for the basal regions of the plant is transferred from the base to apex of the leaves. The analogue simulation also indicated that once the C.O.P. occurred in the root apex the process of respiratory inhibition quickly spread to the aerial

parts.

There is abundant evidence in the literature that photosynthesis can enrich the internal atmospheres of submerged and semi-submerged plants with oxygen (e.g. Laing, 1940b; Hartman and Brown, 1967). In contrast, photosynthesis has little influence on the internal oxygen levels of plants with their aerial parts exposed to the atmosphere. Similarly, the photosynthetic effect in E.angustifolium was fouhd to be related to the degree of submergence. In the unsubmerged plant the effect is small; in this case, although photosynthesis may provide for the total oxygen demand of the plant, the negligible stomatal resistance allows excess gas to escape to the atmosphere as fast as it is generated and elevated internal concentrations are prevented. In the dark internal oxygen levels are depressed by all degrees of submergence above the root-shoot junction. In the light, without free CO_2 in the bathing medium, elevation of the internal oxygen regime depends upon the "jacketing" effect of submergence on the one hand, and the entry of adequate atmospheric CO_2 on the other. Thus at half-submergence and a radiant flux density of 100μE $m^{-2}s^{-1}$ the internal oxygen concentration in the root apex is 111% of that in the unsubmerged plant in the dark. At 3/4 and full submergence, however, the values are 102% and 66% respectively. Free CO_2 (but not HCO_3^-) in the bathing medium was shown to greatly increase the photosynthetic effect. At 100μE $m^{-2}s^{-1}$ and 1.0mM l^{-1} CO_2 the following values were obtained: 1/2 submerged, 124%; 3/4 submerged, 143%; fully submerged, 156%. At 500μE $m^{-2}s^{-1}$ and full submergence, CO_2 concentrations of 1.0 and 2.0mM l^{-1} raise the root apical oxygen concentration to respectively 274% and 308% of that in the darkened unsubmerged plant. These results suggest that in the field photosynthesis may considerably boost the internal oxygen regime of partially submerged Eriophorum plants. It is interesting to speculate as to whether, under such conditions, a diurnal variation in the dimensions of the oxygenated rhizosphere might occur.

The final part of the research described in this thesis, an

analogue investigation into the soil as a sink for oxygen diffusing from roots, must unfortunately be regarded as preliminary work. However, the results gave some indication of the extent to which the soil might influence the oxygen regime within the root. Increased soil oxygen demand produced a decrease in internal root oxygen concentration, and the effect is more severe the smaller the root radius. Potential rooting depth was shown to decrease with decreasing root radius, and with increasing respiration and soil oxygen demand; this is in agreement with observations that non-wetland plants commonly respond to flooding by producing new roots of greater radius and higher porosity (e.g. Yu et al., 1969). If root growth is arrested at an apical oxygen concentration of about 2%, it was predicted that even an "adapted" non-wetland root (of porosity 15%, respiratory rate 30ng $cm^{-3}s^{-1}$ and radius 0.05cm) could penetrate soil having a moderate rate of O_2 consumption of 4×10^{-6} cm^3O_2 $cm^{-3}s^{-1}$ to a maximum of only 17cm. Non-wetland roots having more normal characteristics (eg. porosity 7%, respiratory rate 120ng $cm^{-3}s^{-1}$, radius 0.05cm) could probably penetrate the same soil to only 7cm. In contrast, the wetland root, with its normally higher porosity and associated lower respiratory rate, and with oxygen leakage restricted to the apex, would be expected to attain greater depths. Using a mathematical model it was predicted that E.angustifolium could root to a depth of 40cm in a soil having the oxygen demand given above.

FUTURE RESEARCH

Although the internal transport of oxygen has been recognised for some time it is only comparatively recently that the mechanisms involved have begun to be studied in detail. The lack of convenient and reliable techniques must account in part for the gaps in our knowledge of internal plant aeration. The cylindrical platinum electrode technique provides an important tool for the characterisation of a number of factors likely to influence the internal oxygen status of the plant (Armstrong and Wright,

1975); its use in the future should facilitate progress in the field of internal aeration.

The work described in this thesis has suggested several lines for future research. In particular, C.O.P. studies could be made on mesophytes (grains and vegetable) and on woody species. The relationship between oxygen pressure and root growth requires further study, in both wetland and other species, and electron microscope work is required to follow the effects of low oxygen pressures at the ultrastructural level.

In addition to the present study the only other work known to the author in which internal resistances to oxygen diffusion have been characterised is that of Healy (1975). This aspect of the research could be extended to advantage to non-wetland and to dicotyledonous species; in the latter a study of stomatal effects may be of particular interest.

An experimental investigation is required to compliment the preliminary analogue study of the effect of the soil as an oxygen sink. It is envisaged that R.O.L. could be measured from the apices of standard silicone rubber "roots" which pass for most of their length through the soils under investigation. Comparison of the theoretical flux at zero soil oxygen consumption with the experimental fluxes should indicate the sink activity of the soils. Combination of flux data with measurements of soil oxygen consumption (membrane electrode) should enable calculations to be made of the diffusion coefficients of oxygen in the soils.

During the present study the electrical analogue proved an invaluable tool both for the analysis of experimental data and for investigations *per se*. It is anticipated that in the future use of the analogue will greatly facilitate analysis of the interaction between the many factors which influence internal plant aeration.

APPENDICES

APPENDIX 1: LIST OF SYMBOLS

A : Surface area (cm^2)

a (subscript): "in air"

A_x : Cross-sectional area (cm^2)

a-w (subscript): "in air-saturated water"

b (subscript): "of the boundary layer"

C : Concentration (difference) of oxygen (amount of O_2 per unit volume; eg. g cm^{-3})

C : Electrical capacitance (micro-Farad, μF)

D : Diffusion coefficient ($cm^2 s^{-1}$)

d : Diameter (cm)

d (subscript): "of the diaphragm"

Δ (delta) : "the difference in"

e (subscript): "of the electrode"

e (subscript): "effective"

end (subscript): "of the end correction"

ep (subscript): "of an elipse"

ex (subscript): "expected"

ϵ (epsilon): Porosity (%)

f : Diffusive flux of oxygen (amount of O_2 per unit area per unit time; eg. g $cm^{-2}s^{-1}$)

I : Electric current (Amperes)

i : Diffusion current (Amperes)

J : Diffusion rate of oxygen (amount of O_2 per unit time; eg. g s^{-1})

j (subscript): "of the root-shoot junction"

L : Distance or thickness (cm)

l (subscript): "of the leaf or leaf segment

lac (subscript): "of the lacuna or lacunae.

M : Rate of oxygen consumption (amount of O_2 per unit volume per unit time; eg. g $cm^{-3}s^{-1}$)

m (subscript): "of the stomatal mouth"

n : the number of

o (subscript): "of oxygen"

P : Fractional porosity (%)

p (subscript): "due to porosity or gas-space system"

Perm.: Permeability (cm s^{-1})

Q : Quantity (of diffusate) (eg. moles; g)

Q : Electrical charge (Coulombs)

R : Diffusive resistance (s cm^{-3})

R′ : Electrical resistance (ohms; Ω)

r : Radius (cm)

r (subscript): "of the root or root segment"

Resp.: Respiratory component (g O_2 s^{-1} cm^{-2} surface area)

s : Specific electrical resistance (ohm cm)

s (subscript): "of the liquid shell between root and electrode"

sm (subscript): "of the stem"

soil (subscript): "of (in) the soil"

st (subscript): "of the stoma or stomata"

t : time (s)

t (subscript): "at time t"

t (subscript): "total"

t (superscript): "at temperature t"

tb (subscript): "of the stomatal tube"

th (subscript): "of the stomatal throat"

τ (tau): Tortuosity factor (dimensionless)

V : Potential difference (volts)

V : Volume (cm^3)

V : Velocity (cm s^{-1})

W : Weight (g)

w (subscript): "in water"

wi (subscript): "of the wire"

wl (subscript): "at (of) the root wall"

x : Distance from the electrode surface (cm)

x : Length of the stomatal pore (cm)

y : Width of the stomatal pore (cm)

APPENDIX 2: OPERATION OF THE POLAROGRAPH

The polarograph circuitry (Armstrong and Wright, 1976a) is shown in Fig.A2.1; only those features relevant to the present study are described below.

The circuit comprises six units: (A) primary polarising circuit, (B) secondary polarising circuit, (C) automatic voltage regulator and timing unit, (D) electrometer unit, (E) amplifier, (F) mains or battery power supply.

One to five cathodes may be polarised simultaneously. Circuit (A) polarises one electrode at any one time and is used for the determination of current-voltage relationships and diffusion currents. Remaining cathodes are held polarised using the electrically isolated circuit (B) in which voltage is set manually and is indicated on meter M3. Each cathode may be switched into circuit (A) using switch S1 for measurements to be taken, current being read in μA on M1 or recorded on a chart recorder.

Polarising voltage in (A) is controlled by the automatic voltage regulator and timer (C), which may also be used manually if desired. The circuit supplies exactly 1.0V across a ten-turn linear resistor, employing a 1.5V battery. On automatic control a motor is triggered by the timer unit at a time interval preset using R1 (usually 2 min but variable between 1.5 and 2.5 min). When triggered the motor turns the voltage control one revolution and so alters the voltage by 0.1V. Polarising voltage in (A) may thus be varied automatically from 0 to 1.0V in steps of 0.1V, and in either a positive or negative direction depending upon the position of S3. When manual voltage control is required the push-button switch S2 shorts out the timing device and allows the motor to freely turn the voltage control. This is necessary in order to quickly return the voltage to zero or to re-set the plateau voltage. Any polarising voltage may be held by switching-off the motor circuit with S4.

FIG. A2.1 Circuit diagram of the polarograph

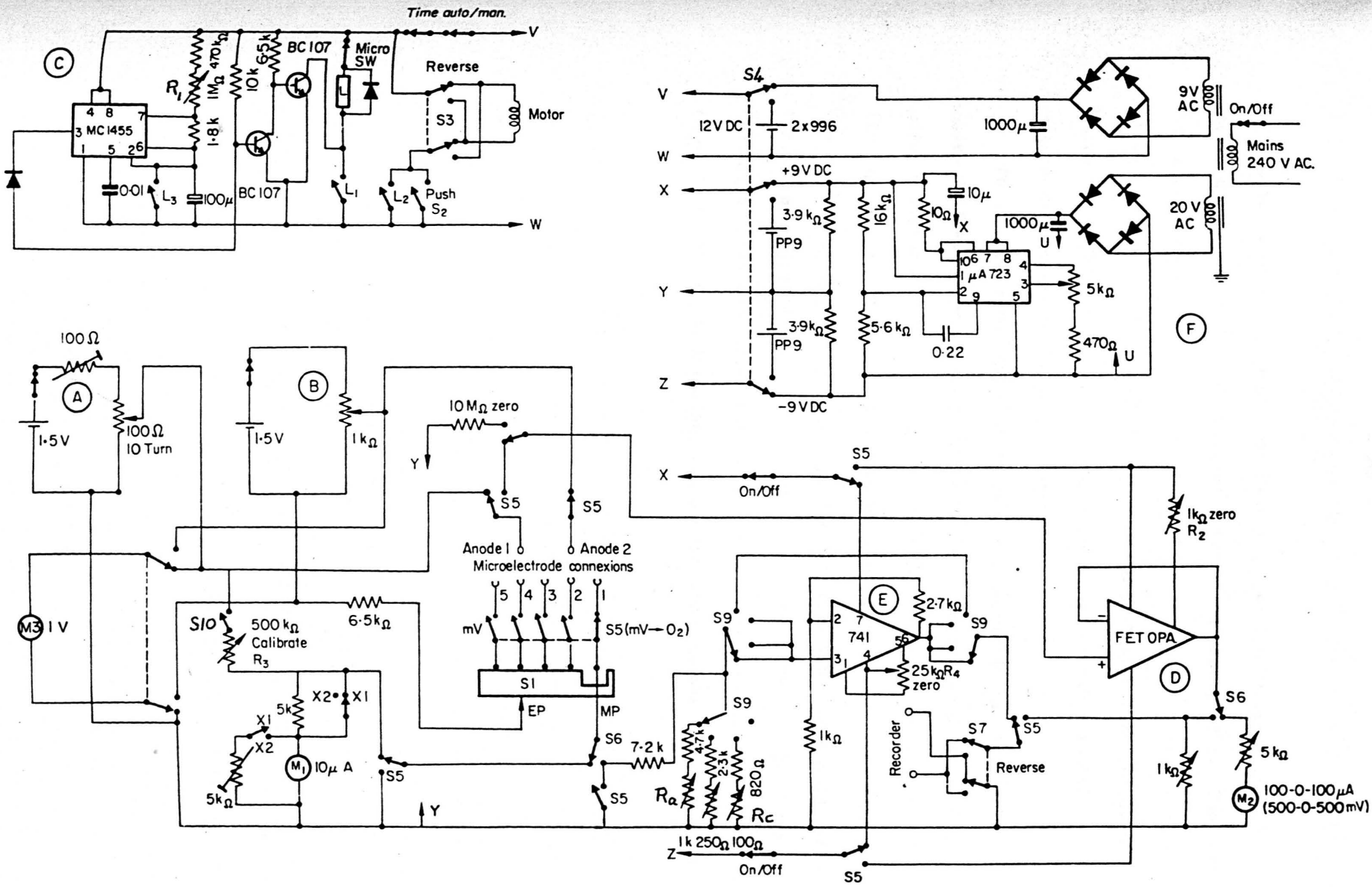
Time auto/man.
C
MC1455
R1
1MΩ
470kΩ
10k
6·5k
BC107
Micro SW
Reverse
S3
Motor
1·8k
0·01
L3
100μ
BC107
L1
L2
Push S2
V
W
S4
12V DC
2x996
1000μ
9V AC
On/Off
Mains 240 V AC.
+9V DC
3·9kΩ
PP9
16kΩ
10μ
10Ω
X
1000μ
U
20 V AC
μA723
5kΩ
Y
3·9kΩ
PP9
5·6kΩ
0·22
470Ω
U
F
Z
-9V DC
100Ω
A
1·5V
100Ω 10 Turn
B
1·5V
1kΩ
10MΩ zero
Y
S5
S5
Anode 1
Anode 2
Microelectrode connexions
5 4 3 2 1
mV
S5(mV—O2)
S1
EP
MP
M3 1V
S10
500kΩ Calibrate R3
6·5kΩ
X2
X1
5k
X1
X2
5kΩ
M1
10μ A
S5
S6
7·2k
S5
Y
S9
4·7k
2·3k
820Ω
Ra
Rc
X
On/Off
S5
E
741
2·7kΩ
S9
S9
25kΩ R4 zero
1kΩ
S9
1kΩ zero R2
FET OPA
D
S6
Recorder
S7
S5
Reverse
1kΩ
5kΩ
M2
100-0-100μA
(500-0-500mV)
Z
1k 250Ω 100Ω
On/Off
S5

Circuit unit (E) is an amplifier which enables current in (A) to be displayed on a chart recorder (Goerz "Multiscript 3"). The instrument has a six-centimetre scale graduated 0-50μA. The amplifier provides three further scales of 0-5, 0-10 and 0-25μA, which may be selected using S9. (The 0-5 and 0-10μA ranges were most suitable for the measurements made in the present study).

To calibrate the recorder the electrode pair in (A) is replaced (using S10) with a variable resistor R3. A potential applied in (A) now gives a current on M1 which can be set to the desired value using R3 (eg. 5μA for the 0-5μA range). The recorder zero is adjusted (R4), the current in (A) diverted through the recorder (S6) and the full-scale deflection adjusted using the appropriate control (Ra,Rb,Rc). This process of zero and f.s.d. adjustment is usually repeated once or twice to achieve correct calibration, and S10 returned to the "off" position.

APPENDIX 3: ELECTRICAL ANALOGUE : ADDITIONAL CIRCUIT DETAILS

VOLTMETERS

In order to remove any loading effect the voltmeters are high impedance "field effect transistor" systems. Fig. A3.1(i) shows the field effect transistor circuit (one per concentration voltmeter); Fig. A3.1(ii) is a circuit diagram of the central power supply for the field transistor units.

CONSTANT CURRENT DEVICES

Fig.A3.2 is a circuit diagram of the constant current device (one per analogue segment) which enables respiration rate to remain independent of oxygen concentration above about 0.3 - 0.4% (ie. the limit of operation of the transistor).

C.O.P. is programmed simply by opening switch S1 when the internal oxygen concentration has reached the desired value. The rate of decrease in respiratory rate below the C.O.P. may be varied using R1.

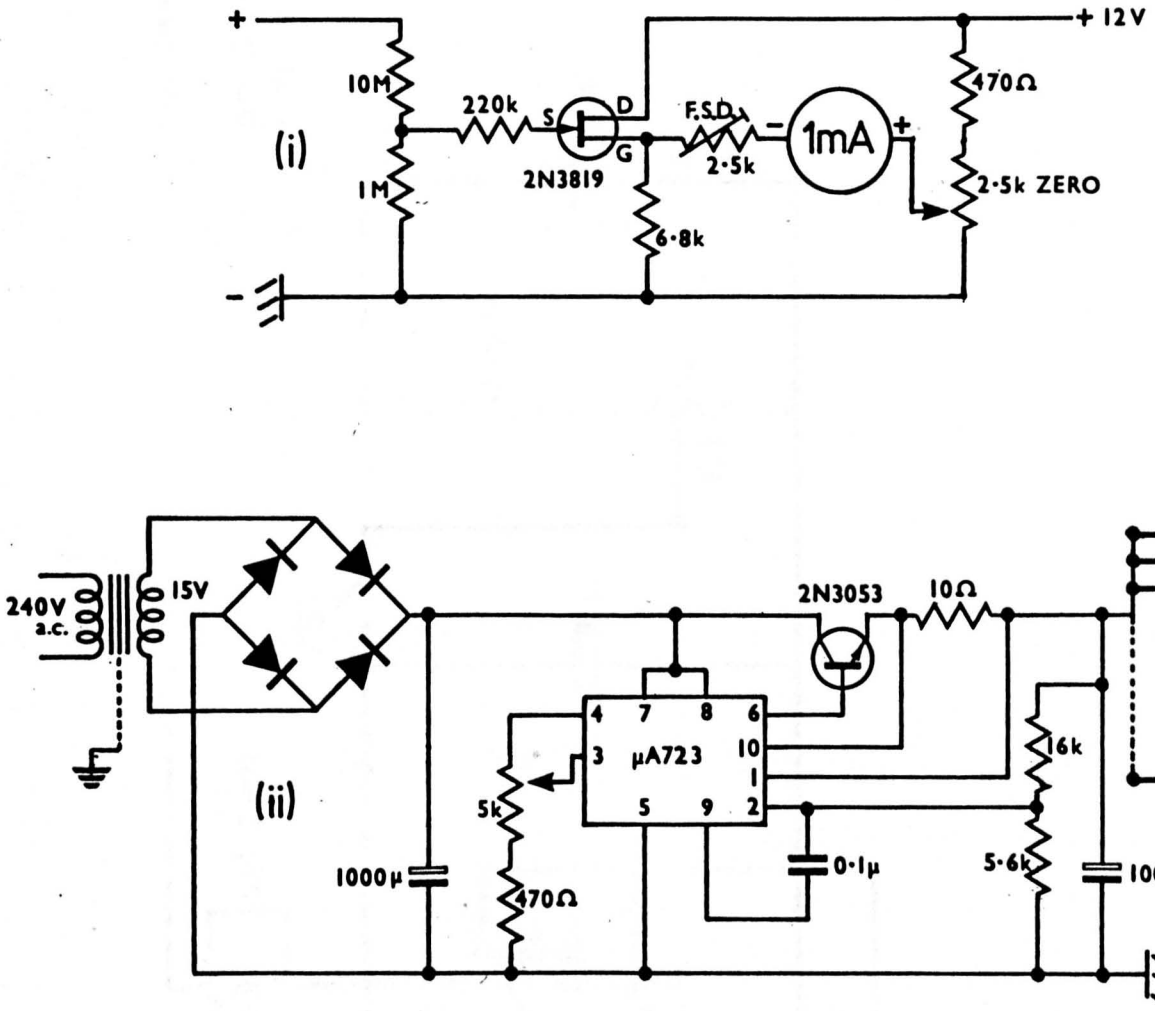

FIG. A3.1 Electrical analogue : additional circuit details

(i) field effect transistor unit

(ii) central power supply

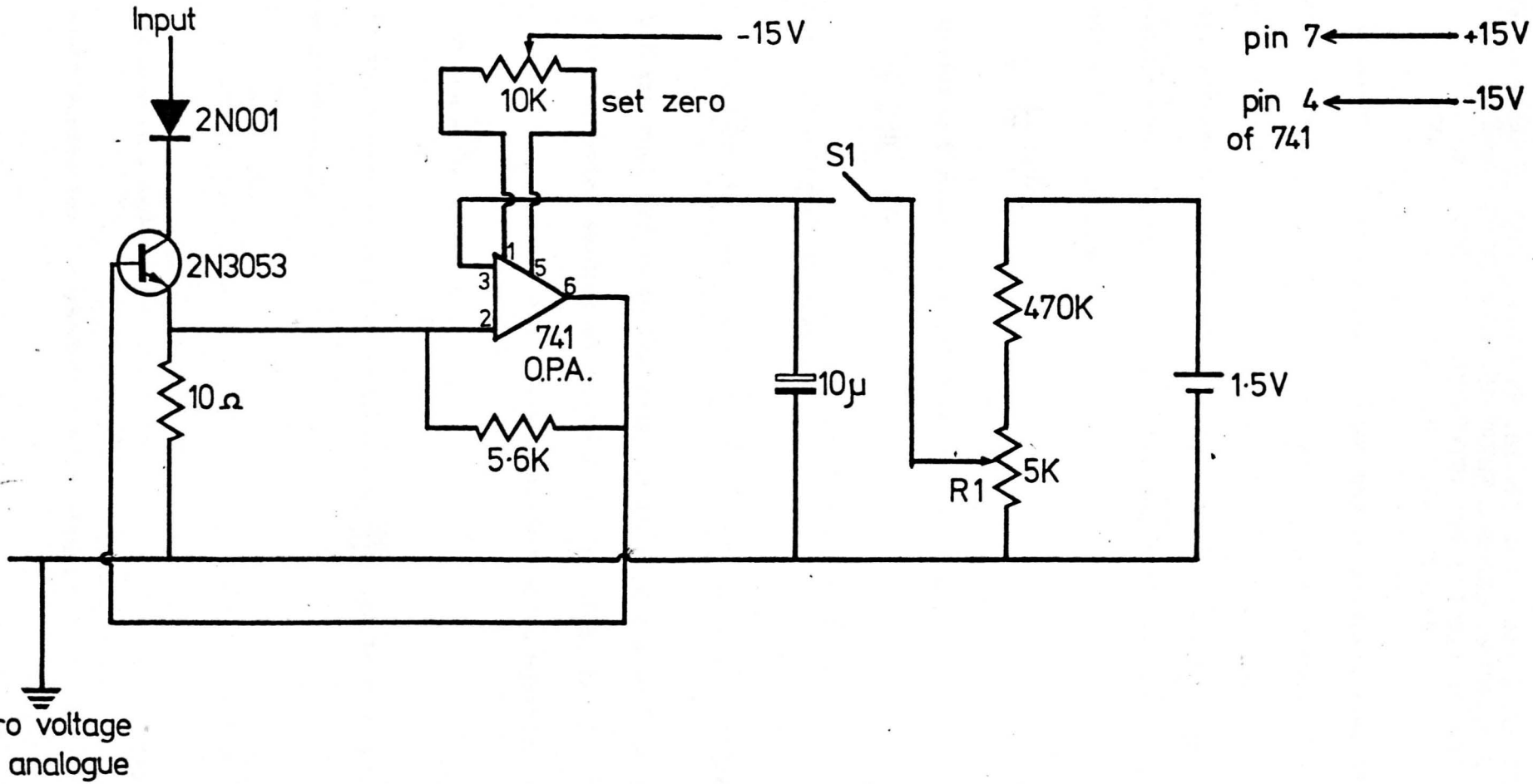

FIG. A3.2 Electrical analogue : additional circuit details. Constant current device

APPENDIX 4: AN EQUATION TO DEFINE THE OXYGEN CONCENTRATION DIFFERENCE BETWEEN THE INNER AND OUTER SURFACES OF THE ROOT WALL IN TERMS OF OXYGEN DIFFUSIVITY AND RESPIRATORY RATE IN THE WALL AND THE OXYGEN FLUX FROM THE ROOT.

Consider a root segment in which oxygen diffuses radially from the inner surface of the root wall to a sink (eg. an ensheathing electrode) external to the root. If the potential rate of oxygen consumption, M, and the effective diffusion coefficient for oxygen, D_e, are uniform throughout the root wall, the steady-state diffusion equation in cylindrical coordinates is:

$$\frac{1}{r}\frac{d}{dr}\left(r\frac{dC}{dr}\right) = \frac{M}{D_e} \qquad \text{(A4.1)}$$

Dividing through by r and integrating gives:

$$\frac{dC}{dr} = \frac{Mr}{2D_e} + \frac{A}{r} \qquad \text{(A4.2)}$$

and a second integration gives:

$$C = \frac{Mr^2}{4D_e} + A \log r + B \qquad \text{(A4.3)}$$

Let the root radius to the inner surface of the wall be r_i, and the radius to the outer surface of the wall be r_o; also, let $C = C_r$ on $r = r_i$ and $C = C_{wl}$ on $r = r_o$. Then, substituting in equation A4.3 gives:

$$C_{wl} = \frac{Mr_o^2}{4D_e} + A \log r_o + B \qquad \text{(A4.4)}$$

If the oxygen concentration gradient, $\frac{dC}{dr}$, equals P on $r = r_o$, then from equation A4.2:

$$P = \frac{Mr_o}{2D_e} + \frac{A}{r_o} \qquad \text{(A4.5)}$$

hence,

$$A = r_o\left(P - \frac{Mr_o}{2D_e}\right) \qquad \text{(A4.6)}$$

Substitution for A in equation A4.4 gives:

$$C_{wl} = \frac{Mr_o^2}{4D_e} + r_o \log r_o \left(P - \frac{Mr_o}{2D_e}\right) + B \qquad (A4.7)$$

from which B may be found:

$$B = C_{wl} - \frac{Mr_o^2}{4D_e} - r_o \log r_o \left(P - \frac{Mr_o}{2D_e}\right) \qquad (A4.8)$$

These expressions for A and B may now be substituted into the general equation A4.3. Applying the boundary condition $C = C_r$ on $r = r_i$, and re-arranging the resulting equation gives:

$$C_r - C_{wl} = \frac{M}{4D_e}(r_i^2 - r_o^2) + r_o \log \left(\frac{r_i}{r_o}\right)\left(P - \frac{Mr_o}{2D_e}\right) \qquad (A4.9)$$

or:

$$C_r - C_{wl} = \frac{Mr_o^2}{4D_e}\left[\frac{r_i^2}{r_o^2} + 2\log\left(\frac{r_o}{r_i}\right) - 1\right] + r_o \log \left(\frac{r_o}{r_i}\right) P \qquad (A4.10)$$

The concentration gradient, P, is given by

$P = \text{flux} \div D_e$; hence the final equation becomes:

$$C_r - C_{wl} = \frac{Mr_o^2}{4D_e}\left[\frac{r_i^2}{r_o^2} + 2\log\left(\frac{r_o}{r_i}\right) - 1\right] + r_o \log \left(\frac{r_o}{r_i}\right) \frac{f}{D_e} \qquad (A4.11)$$

SUMMARY

SUMMARY

The thesis describes a study of certain leaf, stem and root factors expected to influence internal aeration in the wetland plants Eriophorum angustifolium Honck. and Oryza sativa L. The effectiveness of the soil as an oxygen sink was also investigated.

Radial oxygen flux from roots was monitored polarographically and the data manipulated to calculate internal diffusive resistances and root apical oxygen concentration. Analysis of the internal atmosphere was carried out using a gas analyser constructed for this purpose. An existing electrical analogue system was modified and improved, and was used to interpret experimental data, and to carry out certain investigations per se.

Oxygen enters the Eriophorum plant exclusively by the stomata, which normally offer no resistance to oxygen diffusion; very few stomata at the leaf base are necessary for adequate aeration of the root system. Non-metabolic resistance is low in all organs, including the root-shoot junction and lacunar diaphragms; effective resistance was slightly higher due to respiration, but leakage effects were undetectable. Resistance in the apical root wall was significant. The concept of effective resistance was shown to be more complex than was realized previously.

Critical oxygen pressure (C.O.P.) for respiration in the intact plant was monitored in the cortical gas spaces of the root apex and was about 2-3%. Roots ceased elongation below the critical pressure but remained viable if the leaves were kept above the C.O.P. Results suggested that anaerobic respiration could maintain root viability but would not allow elongation.

In totally submerged plants in the dark internal oxygen is exhausted in about 1h. In submerged and partially submerged plants photosynthesis can considerably boost internal oxygen levels, the effect being related to CO_2 availability and the degree of submergence.

The soil was shown to be an effective sink for internal root oxygen, and the difference in potential rooting depths between wetland and non-wetland plants was demonstrated by modelling.

BIBLIOGRAPHY

BIBLIOGRAPHY

Adams, S.N., Dickson, D.A., and Cornforth I.S. (1972). Some effects of soil water tables on the growth of sitka spruce in Northern Ireland. Forestry, 45, 129-133.

Amoore, J.E. (1961a). Arrest of mitosis in roots by oxygen-lack or cyanide. Proc.R.Soc.B 154, 95-108.

Amoore, J.E. (1961b). Dependence of mitosis and respiration in roots upon oxygen tension. Proc.R.Soc. B 154, 109-129.

Arber, A. (1914) On root development in Stratiotes aloides L. Proc.Camb. Phil.Soc.Biol.Sci. 17, 369-379.

Arber, A. (1920) Water plants: A study of aquatic angiosperms. Cambridge.

Arikado, H. and Adachi, Y. (1955). Anatomical and ecological responses of barley and some forage crops to the flooding treatment. Bull.Fac.Agr.Mie Univ. (Japan) 11, 1-29.

Armstrong, W. (1964). Oxygen diffusion from the roots of some British bog plants. Nature, 204, 801-802.

Armstrong, W. (1967a) The relationship between oxidation-reduction potentials and oxygen diffusion levels in some waterlogged organic soils. J.Soil Sci. 18, 27-34.

Armstrong, W. (1967b). The use of polarography in the assay of oxygen diffusing from roots in anaerobic media. Physiol.Plant. 20, 540-553.

Armstrong, W. (1967c). The oxidising activity of roots in waterlogged soils. Physiol.Plant. 20, 920-926.

Armstrong, W. (1968). Oxygen diffusion from the roots of woody species. Physiol. Plant. 21, 539-543.

Armstrong, W. (1969). Rhizosphere oxidation in rice: An analysis of inter-varietal differences in oxygen flux from the roots. Physiol.Plant. 22, 296-303.

Armstrong, W. (1970). Rhizosphere oxidation in rice and other species: A mathematical model based on the oxygen flux component. Physiol.Plant. 23, 623-630.

Armstrong, W. (1971a). Radial oxygen losses from intact rice roots as affected by distance from the apex, respiration and water-logging. Physiol.Plant. 25, 192-197.

Armstrong, W. (1971b). Oxygen diffusion from the roots of rice grown under non-waterlogged conditions. Physiol.Plant. 24, 242-247.

Armstrong, W. (1972) A re-examination of the functional significance of aerenchyma. Physiol. Plant. 27, 173-177.

Armstrong, W. (1978). Root aeration in the wetland condition. In: Plant Life in Anaerobic Environments; ed. Hook, D.D. and Crawford, R.M.M.; Ann Arbor Science, Mich., U.S.A.

Armstrong, W. and Boatman, D.J. (1967). Some field observations relating the growth of bog plants to conditions of soil aeration. J.Ecol. 55, 101-110.

Armstrong, W. and Gaynard, T.J. (1976). The critical oxygen pressures for respiration in intact plants. Physiol.Plant. 37, 200-206.

Armstrong, W. and Read, D.J. (1972). Some observations on oxygen transport in conifer seedlings. New Phytol. 71, 55-62.

Armstrong, W. and Wright E.J. (1975). Radial oxygen loss from roots: the theoretical basis for the manipulation of flux data obtained by the cylindrical platinum electrode technique. Physiol. Plant. 35, 21-26.

Armstrong, W. and Wright, E.J. (1976a). A polarographic assembly for multiple sampling of soil oxygen flux in the field. J.Appl. Ecol. 13, 849-856.

Armstrong, W. and Wright E.J. (1976b). An electrical analogue to simulate the oxygen relations of roots in anaerobic media. Physiol. Plant. 36, 383-387.

Armstrong, W., Booth, T.C., Priestly, P. and Read, D.J. (1976). The relationship between soil aeration, stability and growth of sitka spruce (Picea sitchensis (Bong.) Carr.) on upland peaty gleys. J.Appl.Ecol. 13, 585-591.

Baba, I., Iwata, I., and Tajima, K. (1967). Physiological injury. In: "Theory and Practice of Growing Rice", ed. Matsubayashi, M., Fuji Publishing Co., Tokyo.

Baldwin, J.P., Tinker, P.B., and Nye P.H. (1972). Uptake of solutes by multiple root systems from soil. II. The theoretical effects of rooting density and pattern on uptake of nutrients from soil. Plant and Soil 36, 693-708.

Banath, C.L. and Monteith, N.H. (1966). Soil oxygen deficiency and sugar cane root growth. Plant and Soil 25, 143-149.

Barber, D.A. (1961). The physiology of Equisetum limosum and its environment. J.Exp.Bot. 12, 243-251.

Barber, D.A., Ebert, M. and Evans, N.T.S.(1962). Movement of ^{15}O through barley and rice plants. J.Exp.Bot. 13, 397-403.

Barthelemy, A. (1874) De la respiration et de la circulation des gaz dans les vegetaux. Annls. Sci.nat. (Bot.), Serie 5, 19, 131.

Bartlett, R.J. (1961). Iron oxidation proximate to plant roots. Soil Sci. 92, 372-379.

Berry, L.J. and Norris, W.E.(1949). Studies of onion root respiration. I. Velocity of oxygen consumption in different segments of root at different temperatures as a function of partial pressure of oxygen. Biochim. Biophys. Acta, 3, 593-606.

Bickford, E.D. and Dunn, S. (1972). Lighting for Plant Growth. Kent State Univ. Press, U.S.A.

* See p. 219

Birkle, D.E., Letey, J., Stolzy, L.H. and Szuszkiewicz, T.E. (1964). Measurements of oxygen diffusion rates with the platinum microelectrode. II. Factors influencing the measurement. Hilgardia, 35, 555-566.

Boatman, D.J. and Armstrong, W. (1968). A bog type in North-West Sutherland. J.Ecol. 56, 129-141.

Bockris, J.O'M. and Huq, A.K.M.S. (1956). The mechanism of the electrolytic evolution of oxygen on platinum. Proc.R.Soc. A. 237, 277-296.

Boggie, R. (1972). Effect of water table height on root development of Pinus contorta on deep peat in Scotland. Oikos, 23, 304-312.

Boulter, D., Coult, D.A. and Henslaw, G.G. (1963). Some effects of gas concentrations on metabolism of the rhizome of Iris pseudacorus L. Physiol. Plant. 16, 541-548.

Brown, R. (1947). The gaseous exchange between the root and shoot of the seedlings of Curcurbita pepo. Ann.Bot. 11, 417-437.

Cannon, W.A. (1932). Absorption of oxygen by roots when the shoot is in darkness or light. Pl.Physiol. 7, 673

Conway, V.M. (1937). Studies on the autecology of Cladium mariscus R.Br. III. The aeration of the subterranean parts of the plant. New Phytol. 36, 64-96.

Coult, D.A. (1964) Observations on gas movement in the rhizome of Menyanthes trifoliata L. with comments on the role of the endodermis. J.Exp.Bot. 15, 205-218.

Coult, D.A. and Vallance K.B. (1958) Observations on the gaseous exchanges which take place between Menyanthes trifoliata L. and its environment. II. J.Exp.Bot. 9, 384-402.

Covey, W. and Lemon, E.R. (1962). Soil aeration and plant root relations. IV. Testing the cylindrical shell model in the transient case. Soil Sci.Soc.Amer.Proc. 26, 526-530.

Crawford, R.M.M. (1966). The control of anaerobic respiration as a determining factor in the distribution of the genus Senecio. J.Ecol. 54, 403-413.

Crawford, R.M.M.(1967). Alcohol dehydrogenase activity in relation to flooding tolerance in roots. J.Exp.Bot. 18, 458-464.

Crawford, R.M.M. (1969). The physiological basis of flooding tolerance. Ber.dt.bot.Ges. 82, 111-114.

Crawford, R.M.M. and McManmon, M. (1968). Inductive responses of alcohol and malic dehydrogenases in relation to flooding tolerance in roots. J.Exp.Bot. 19, 435-441.

Crawford, R.M.M. and Tyler, P.D. (1969). Organic acid metabolism in relation to flooding tolerance in roots. J.Ecol. 57, 237-246.

- See p.219

Currie, J.A. (1961) Gaseous diffusion in the aeration of aggregated soils. Soil Sci. 92, 40-45.
*

Daneel, H. (1897) Über den durch diffundierende Gase hervorgerufenen Restrom. Z.Electrochem. 4,227-232.

Das, D.K. and Jat, R.L. (1977) Influence of threesoil-water regimes on root porosity and growth of four rice varieties. Agron.J. 69, 197-200.

Davies, D.D., Nascimento, K.H. and Patil, K.D. (1974). The distribution and properties of N.A.D.P. malic enzyme in flowering plants. Phytochemistry, 13, 2417-2425.

Davies, P.W. (1962). The oxygen cathode. In: Physical Techniques in Biological Research, Vo.IV, Special Methods.

De Bary, A. (1884) Comparative anatomy of the vegetative organs of the Phanaerogams and ferns. Oxford.

Doi, Y. (1952) Studies on the oxidising power of roots of crop plants. I. The difference with species of crop plants and wild grasses. Proc.Crop Sci.Soc., Japan, 21, 12-13.

El-Beltagy, A.S. and Hall,M.A. (1974) Effect of water stress upon endogenous ethylene levels in Vicia faba. New Phytol. 73, 47-60.

Engler, R.M. and Patrick, W.H. (1975). Stability of sulphides of manganese, iron, zinc, copper and mercury in flooded and non-flooded soil. Soil Sci. 119, 217-221.

Esau, K. (1965). Plant Anatomy, 2nd edn., Wiley, New York.

Etherington, J.R.(1975). Environment and Plant Ecology, Wiley, London.

Evans, N.T.S. and Ebert, M. (1960). Radioactive oxygen in the study of gas transport down the root of Vicia faba. J.Exp.Bot. 11 246-257.

Forrester, M.L., Krotkov, G. and Nelson, C.D. (1966). Effect of oxygen on photosynthesis, photorespiration and respiration in detached leaves. I. Soybean. Pl.Physiol. 41, 422-427.

Freudenberger, H. (1940). Die Reaktion der Schliesszellen auf Kohlensäure und Sauerstoff Entzug. Protoplasma, 35, 15-54.

Fukui, J. (1953). Studies on the adaptability of green manure and forage crops to paddy field conditions. Proc.Crop Sci.Soc. Japan 22, 110-112.

Fulton, J.M. and Erickson, A.E. (1964) Relation between soil aeration and ethyl alcohol accumulation in xylem exudate of tomatos. Soil Sci.Soc.Amer.Proc. 28, 610-614.

Gaastra, P. (1959). Photosynthesis of crop plants as influenced by light, carbon dioxide, temperature and stomatal diffusion resistance. Meded. LandbHoogesch. Wageningen, 59 1-68.

* See p.219

Geisler, G. (1967). Interactive effects of CO_2 and O_2 in soil on root and top growth of barley and peas. Plant Physiol. 42, 305-307.

Goto, Y. and Tai, K. (1957) On the differences of oxidising power of paddy rice seedling roots among some varieties. Soil and Plant Food, 2, 198-200.

Grable, A.R. (1966). Soil aeration and plant growth. Adv. Agron. 18, 57-106.

Grable, A.R. and Siemer, E.G.(1968). Effects of bulk density, aggregate size, and soil water suction on oxygen diffusion, redox potentials and elongation of corn roots. Soil Sci.Soc. Amer. Proc. 19, 7-16.

Green, M.S. and Etherington, J.R. (1977). Oxidation of ferrous iron by rice (Oryza sativa L.) roots: a mechanism for waterlogging tolerance? J.Exp.Bot. 28, 687-690.

Greenwood, D.J. (1963). Nitrogen transformations and the distribution of oxygen in soils. Chem. and Ind. No.20, 799-803.

Greenwood, D.J. (1967a) Studies on the transport of oxygen through the stems and roots of vegetable seedlings. New Phytol. 66, 337-347.

Greenwood, D.J. (1967b) Studies on oxygen transport through mustard seedlings (Sinapis alba L.). New Phytol. 66, 597-606.

Greenwood, D.J. (1968) Root growth and oxygen distribution in soil. Trans. 9th Int. Congr. Soil Sci. 1, 823-832.

Greenwood, D.J. (1969) Effect of oxygen distribution in the soil on plant growth. In: Root Growth, Butterworth, Oxford.

Greenwood, D.J. and Goodman, D. (1967) Direct measurements of the distribution of oxygen in soil aggregates and in columns of fine soil crumbs. J.Soil Sci. 18, 182-196.

Hartman, R.T. and Brown, D.L. (1967). Changes in the internal atmosphere of submersed vascular hydrophytes in relation to photosynthesis. Ecology 48, 252-258.

Healy, M.T. (1975). Oxygen transport in Pisum sativum L. Ph.D. thesis, Univ. of Hull.

Healy, M.T. and Armstrong, W. (1972). The effectiveness of internal oxygen transport in a mesophyte (Pisum sativum L.) Planta 103. 302-309.

Heath, O.V.S. (1948) Control of stomatal movement by a reduction in the normal carbon dioxide content of the air. Nature, 161, 179-181.

Heath, O.V.S. (1950). The role of carbon dioxide in the light - response of stomata. I. J.Exp.Bot. 1, 29-62.

Heath, O.V.S.(1969). The Physiological Aspects of Photosynthesis. Heineman, London.

Heath, O.V.S. and Milthorpe, F.L. (1950). The role of carbon dioxide in the light response of stomata. II. J.Exp.Bot. 1, 227-243.

Heath, O.V.S. and Russell, J. (1954). An investigation of the light responses of wheat stomata with the attempted elimination of control by the mesophyll. II. Interactions with carbon dioxide. J.Exp.Bot. 5, 269-292.

Heide H. van der, Raalte, M.H. van, and Boer-Bolt B.M.de (1963). The effect of low oxygen content of the medium on the roots of barley seedlings. Acta Bot.Neerl. 12, 131-147.

Heyrovsky, J. (1924). The processes at the mercury dropping cathode. Parts I and II. Trans. Faraday Soc. 19 692-702; 785-788.

Heyrovsky, J. and Shikata, M. (1925) Researches with the dropping mercury cathode. II The polarograph. Rec.Trav.Chim. 44 496-498.

Hoare, J.P. (1968) The Electrochemistry of Oxygen. Interscience Pubs., New York.

Hook, D.D., Brown, C.L. and Kormanik, P.O. (1971). Inductive flood tolerance in swamp tulepo. (Nyssa sylvatica var. biflora (Walt.) Sarg.). J.Exp. Bot. 22 78-89.

Huck, M.G. (1970) Variation in taproot elongation rate as influenced by composition of the soil air. Agron.J. 62, 815-818.

Humphries, W.J. (1926). International Critical Tables. Vol.1, p.393; McGraw-Hill Book Co., N.Y.

Hygen, G. and Midgaard, E. (1954). A re-investigation of the influence of varying air humidity on cuticular transpiration in Pinus sylvestris L. Physiol. Plant. 7, 128

Jackson, M.B. and Campbell, D.J. (1975a) Movement of ethylene from roots to shoots, a factor in the responses of tomato plants to waterlogged soil conditions. New Phytol. 74, 397-406.

Jackson, M.B, and Campbell D.J. (1975b) Ethylene and waterlogging effects in tomato. Ann.Appl.Biol. 81, 102-105.

James, W.O. (1971). Cell Respiration, English Univ.Press, London.

Jeffery, J.W.O. (1961) Defining the state of reduction of a paddy soil. J.Soil Sci. 12, 172-179.

Jensen, C.R., Luxmoore, R.J., Van Gundy, S.D. and Stolzy, L.H. (1969). Root air space measurements by a pycnometer method. Agron. J. 61, 474-475.

Jensen, C.R., Stolzy, L.H. and Letey, J. (1967). Tracer studies of oxygen diffusion through roots of barley, corn and rice. Soil Sci. 103, 23-29.

John C.D. and Greenway, H. (1976) Alcoholic fermentation and activity of some enzymes under anaerobiosis. Aust. J.Plant Physiol. 3 325-336.

Kawase, M. (1972) Effect of flooding on ethylene concentration in horticultural plants. J.Amer. Soc.Hort.Sci. 97, 584-588.

Kolthoff, I.M. and Laitinen H.A. (1940). The voltammetric determination of oxygen. Science 92, 152.

Kolthoff, I.M. and Lingane, J.J. (1952) Polarography. 2nd edn., Interscience Publishers, New York and London.

Kolthoff, I.M. and Miller, C.S. (1941). The reduction of oxygen at the dropping mercury electrode. J.Amer.Chem.Soc. 63, 1013-1017.

Kordan, H.A. (1974a) The rice root in relation to oxygen supply and root growth in seedlings germinating under water. New Phytol. 73, 695-697.

Kordan, H.A. (1974b). Patterns of shoot and root growth in rice seedlings germinating under water. J.Appl.Ecol. 11, 685-690.

Kordan, H.A. (1976). Adventious root initiation and growth in relation to oxygen supply in germinating rice seedlings. New Phytol. 76, 81-86.

Kramer, P.J. (1951) Causes of injury to plants resulting from flooding of soil. Pl. Physiol. 26, 722-735.

Kramer, P.J. (1966). Effects of deficient aeration on the roots of plants. Proc.Conf. on "Drainage for Efficient Crop Production", Amer.Soc.Agric. Eng., 13-14, 23.

Kristensen, K.J. and Lemon, E.R. (1964). Soil aeration and plant root relations. III.Physical aspects of oxygen diffusion in the liquid phase of the soil. Agron.J. 56, 295-301.

Laing, H.E. (1940a). Respiration of the rhizomes of Nuphar advenum and other water plants. Amer.J.Bot. 27, 574-581.

Laing, H.E. (1940b) The composition of the internal atmosphere of Nuphar advenum and other water plants. Amer.J.Bot. 27, 861-867.

Laitinen, H.A. and Kolthoff, I.M. (1941) Voltammetry with stationary electrodes of platinum wire. J.Phys.Chem. 45, 1061-1079.

Lemon, E.R. (1962) Soil aeration and plant root relations. I. Theory. Agron. J. 54, 167-170.

Lemon, E.R. and Wiegand, C.L. (1962). Soil aeration and plant root relations. II. Root respiration. Agron.J. 54, 171-175.

Leyton, L. and Rousseau, L.Z. (1958). Root growth of tree seedlings in relation to aeration. In: Physiology of Forest Trees 467-475, ed. Thimann, K.V., Ronald, N.Y.

Lingane, J.J. (1961). Chronopotentiometric study of oxygen reduction at a platinum wire cathode. J.Electroanal. Chem. 2, 296-309.

Luxmoore, R.J., Stolzy, L.H. and Letey, J. (1970a) Oxygen diffusion in the soil-plant system. I. A model. Agron. J. 62, 317-322.

Luxmoore, R.J., Stolzy, L.H. and Letey, J. (1970b). Oxygen diffusion in the soil-plant system. II. Respiration rate, permeability, and porosity of consecutive excised segments of maize and rice roots. Agron.J. 62, 322-324.

Luxmoore, R.J., Stolzy, L.H. and Letey, J. (1970c). Oxygen diffusion in the soil-plant system. III. Oxygen concentration profiles, respiration rates, and the significance of plant aeration predicted for maize roots. Agron. J. 62, 325-329.

Luxmoore, R.J., Stolzy, L.H. and Letey, J. (1970d) Oxygen diffusion in the soil-plant system. IV. Oxygen concentration profiles, respiration rates, and radial oxygen losses predicted for rice roots. Agron.J. 62, 329-332.

Luxmoore, R.J. and Stolzy, L.H. (1972a) Oxygen Diffusion in the soil-plant system. V. Oxygen concentration and temperature effects on oxygen relations predicted for maize roots. Agron.J. 64, 720-725.

Luxmoore, R.J. and Stolzy, L.H. (1972b) Oxygen diffusion in the soil-plant system. VI.A synopsis with commentary. Agron.J. 64, 725-729.

MacDowell, F.D.H. (1963) Midday closure of stomata in ageing tobacco leaves. Can.J.Bot. 41 1289-1300.

Mackereth, F.J.H. (1963) Water Analysis for Limnologists. Freshwater Bilogical Association, Publ'n No.21.

Mansfield, T.A. and Heath, O.V.S. (1963) Photoperiodic effects on rhythmic phenomena in stomata of Xanthium pennsylvanicum. J.Exp.Bot. 14, 334-352.

Martens, P. (1937) L'origine des espaces intercellulaires. Cellule 46 357-388.

Martens, P. (1938) Nouvelles recherches sur l'origine des espaces intercellulaires. Bot. Centbl. Beihefte, 58 349-364.

Martin, M.H. (1968) Conditions affecting the distribution of Mercurialis perennis L. in certain Cambridgeshire woodlands. J.Ecol. 56, 777-793.

McIntyre,D.S. (1970). The platinum microelectrode method for soil aeration measurement. Adv.Agron. 22, 235-283.

McManmon, M. and Crawford, R.M.M. (1971). A metabolic theory of flooding tolerance: the significance of enzyme distribution and behaviour. New Phytol. 70, 299-306.

Meidner, H. (1976). Vapour loss through stomatal pores with the mesophyll tissue excluded. J.Exp.Bot. 27 172-174.

Meidner, H. and Mansfield, T.A. (1968). Physiology of Stomata. McGraw-Hill, London.

Metcalfe, C.R.(1971). Anatomy of Monocotyledons. V. Cyperaceae, Oxford.

Molisch, H. (1926) Pflanzenbiologie in Japan, Jena.

Montgomery H.A.C., Thom, N.S. and Cockburn, A. (1964) Determination of dissolved oxygen by the Winkler method and the solubility of oxygen in pure water and sea water. J.Appl. Chem. 14 280-296.

Müller, L. and Nekrassow, L.N. (1965). Zum Mechanizmus der kathodischen Reduktion von Sauerstoff an einer glatten, aktiven Platinelektrode in alkalischen Lösung. J.Electroanal. Chem. 9, 282-289.

Nobel, P.S. (1974) Introduction to Biophysical Plant Physiology. W.H. Freeman, San Francisco.

Oden, S. (1962) Electrometric methods for oxygen studies in water and soil. IV. Fundamental problems involved with the design and use of oxygen diffusion electrodes. Grundfoerbattring, 3, 117-210 (English Translation, C.S.I.R.O. Aust. No.6480C).

Pallas, J.E. (1965) Transpiration and stomatal opening with changes in carbon dioxide content of the air. Science 147, 171-173.

Penman, H.L. and Schofield, R.K. (1951). Some physical aspects of assimilation and transpiration. S.E.B.Symp.V. 115-129.

Phillips, M.E. (1953) Studies in the quantitative morphology and ecology of Eriophorum angustifolium Roth. I. The rhizome system. J.Ecol. 41 295-318.

Phillips, M.E. (1954a) Studies in the quantitative morphology and ecology of Eriophorum angustifolium Roth. III. The leafy shoot. New Phytol. 53 312-343.

Phillips, M.E. (1954b) Eriophorum angustifolium Roth. J.Ecol. 42 612-622.

Ponnamperuma, F.N. (1955) Some aspects of the chemistry of rice soils. Tropical Agriculturist 3 92-101.

Ponnamperuma, F.N. (1972) The chemistry of submerged soils. Adv.Agron. 24 29-96.

Powell, R.W. (1940) Further experiments on the evaporation of water from saturated surfaces. Trans.Inst.Chem.Engnr's. 18, 36-50.

Raven, J.A. (1970) Exogenous inorganic carbon sources in plant photosynthesis. Biol. Rev. 45 167-221.

Raven, J.A. (1972) Endogenous inorganic carbon sources in plant photosynthesis. II. Comparison of total CO_2 production in the light with measured CO_2 evolution in the light. New Phytol. 71 995-1014.

Read, D.J. and Armstrong, W. (1972) A relationship between oxygen transport and the formation of the ectotrophic mycorrhizal sheath in conifer seedlings. New Phytol. 71 49-53.

Rickman, R.W., Letey, J., Aubertin, J.M. and Stolzy, L.H. (1968) Platinum microelectrode poisoning factors. Soil Sci.Soc. Amer.Proc. 32, 204-208.

Riddiford, A.C.(1961) Mechanisms for the evolution and ionisation of oxygen at platinum electrodes. Electrochim.Acta 4, 170-180.

Robards, A.W. (1970) Electron Microscopy and Plant Ultrastructure. McGraw-Hill, London.

Roughton, F.J.W. and Scholander, P.F. (1943). Micro-gasometric estimation of the blood gases. I. Oxygen. J.Biol. Chem. 148, 541-550.

Rowe, R.N. (1966) Anaerobic metabolism and cyanogenic glycoside hydrolysis in differential sensitivity of peach, plum and pear roots in water-saturated conditions. Ph.D. Thesis, Univ. of California.

Rowe, R.N. and Beardsell, D.V. (1973). Waterlogging of fruit trees. Horticultural Abst. 43, 534-548.

Sampson, J. (1961) A method of replicating dry or moist surfaces for examination by light microscopy. Nature 191, 932-933.

Sanders, F.E., Tinker, P.N. and Nye, P.H. (1970). Uptake of solutes by multiple root systems from soil. I. An electrical analog of diffusion to root systems. Pl.Soil 34 453-466.

Scarth, G.W. (1932) Mechanism of the action of light and other factors on stomatal movement. Pl. Physiol. 7 481-504.

Schenck, H. (1889) Uber das Aërenchym, ein dem Kork homologes Gewebe bei Sumpfpflanzen. Jb. wiss. Bot. 20 526-574.

Scholander, P.F., Claff, C.L., Teng, C.T. and Walters, V. (1951). Nitrogen tension in the swimbladder of marine fishes in relation to the depth. Biol. Bull. 101, 178-193.

Scholander, P.F., van Dam L. and Scholander, S.I. (1955) Gas exchange in the roots of mangroves. Amer.J.Bot. 42 92-98.

Scott, A.D. and Evans, D.D. (1955) Dissolved oxygen in saturated soil. Soil Sci.Soc.Amer.Proc. 19 7-16.

Scroggie, M.G. (1958) Foundations of Wireless. Iliffe and Sons, London.

Sculthorpe, C.D.(1967) The Biology of Aquatic Vascular Plants. Edward Arnold, London.

Shimshi, D. (1963a) Effect of chemical closure of stomata on transpiration in varied soil and atmospheric environments. Pl.Physiol. 38 709-712.

Shimshi, D. (1963b) Effect of soil moisture and phenylmercuric acetate upon stomatal aperture, transpiration and photosynthesis. Pl. Physiol. 38, 713-721.

Shoemaker, D.O., Garland, C.W. and Steinfeld, J.I. (1974) Experiments in Physical Chemistry. 3rd edn., McGraw-Hill, N.Y.

Sifton, H.B. (1945) Air space tissue in plants. Bot.Rev. 11, 108-143.

Slatyer, R.O. (1967) Plant-Water Relationships. Academic Press, London.

Sojka, R.E., Stolzy, L.H. and Kaufmann, M.R. (1975). Wheat growth related to rhizosphere temperature and oxygen levels. Agron.J. 67 591-596.

Sorokin, H.P. (1967) Distribution of intercellular material in the apical part of pea seedlings. Physiol. Plant. 20, 643-654.

Spurr, A.R. (1969) A low-viscosity epoxy resin embedding medium for electron microscopy. J.Ultrastruct. Res. 26 31.

Stålfelt, M.G. (1963) Diurnal dark reactions in the stomatal movements. Physiol. Plant. 16, 756-766.

Steeman Nielsen, E. (1960) Uptake of CO_2 by the plant. In: Encyclopedia of Plant Physiology, 5(i) 70-84.

Stiles, W. (1960) The composition of the atmosphere (oxygen content of air, water, soil, intercellular spaces, diffusion, carbon dioxide and oxygen tension). In: Encylopedia of Plant Physiology, 12(ii) 114-148, Springer-Verlag, Berlin.

Summerfield, R.J. and Rieley,J.O. (1974). Growth of Narthecium ossifragum in relation to the dissolved oxygen concentration of the rooting substrate. Pl. Soil 41 701-705.

Takai, Y. and Kamura, T. (1966) The mechanism of reduction in waterlogged paddy soil. Folia Microbiol. (Prague) 11 304-313.

Teal, J.M. and Kanwisher, J.W. (1961) Gas exchange in a Georgia salt marsh. Limnol. Oceanogr. 6 388-399.

Teal, J.M. and Kanwisher, J.W. (1966) Gas transport in the marsh grass Spartina alterniflora. J.Exp. Bot. 17 355-361.

Thomas, M., Ranson, S.L. and Richardson, J.A. (1973) Plant Physiology. 5th edition, Longman.

Turner, F.T. and Patrick, W.H. (1968) Chemical changes in waterlogged soils as a result of oxygen depletion. Trans. 9th Int. Congr. Soil Sci. 4 53-63.

Tyler, P.D. and Crawford, R.M.M. (1970) The role of shikimic acid in waterlogged roots and rhizomes of Iris pseudacorus L. J.Exp.Bot. 21 677-682.

Vallance, K.B. and Coult, D.A. (1951) Observations on the gaseous exchanges which take place between Menyanthes trifoliata L. and its environment. I. The composition of the internal gas of the plant. J.Exp.Bot. 2 212-222.

Vámos, R. and Köves, E. (1972) Role of the light in the prevention of the poisoning action of hydrogen sulphide in the rice plant. J.App.Ecol. 9 519-525.

Van Raalte, M.H. (1941) On the oxygen supply of rice roots. Annls. Bot. Gdns. Buitenzorg 51, 43-57.

Van Raalte, M.H. (1944) On the oxidation of the environment by the roots of rice (Oryza sativa L.). Hort.Bot.Bogoriensis, Java. Syokubutu - Iho 1 15-34.

Van Tieghem, P. (1866) Recherches sur la respiration des plantes submerges. Bull. Soc. bot. France 13, 411-421.

Vartapetian, B.B. (1973) Aeration of roots in relation to molecular oxygen transport in plants. Unesco symposium (Ecology and Conservation 5), Uppsala, 1975.

Vartapetian, B.B., Andreeva, I.N. and Kozlova, G.I. (1976) The resistance to anoxia and the mitochondrial fine structure of rice seedlings. Protoplasma 88 215-224.

Vartapetian, B.B., Andreeva, I.N., Kozlova, G.I. and Agapova, L.P. (1977) Mitochondrial ultrastructure in roots of mesophyte and hydrophyte at anoxia and after glucose feeding. Protoplasma 91 243-256.

Vartapetian, B.B., Andreeva, I.N., Maslova, I.P. and Davtian, N.G. (1970) The oxygen and ultrastructure of root cells. Agrochimica 15 1-19.

Vitek, V. (1933) Le dosage polarographique de l'oxygen contenu dans les eaux d'industrie. Chim. et Ind. (Paris) 29, Special No. 215-217.

Walker, D.A. and Zelitch, I. (1963) Some effects of metabolic inhibitors, temperature and anaerobic conditions on stomatal movement. Pl. Physiol. 38 390-396.

Weast, R.C. (1974) Handbook of Chemistry and Physics. 55th edn., C.R.C. Press, Cleveland, Ohio, U.S.A.

Williams, K.R. (1966) An Introduction to Fuel Cells. Elsevier, Amsterdam.

Williams, P.J. (1967) Replacement of water by air in soil pores. The Engineer, 223 293-298.

Williams, W.T. and Barber, D.A. (1961) The functional significance of aerenchyma in plants. S.E.B. Symp. 15 132-144.

Winzler, R.J. (1941) The respiration of baker's yeast at low oxygen tension. J.Cell. Comp.Physiol. 17 263-276.

Wium-Andersen, S. (1971) Photosynthetic uptake of free CO_2 by the roots of Lobelia dortmanna. Physiol. Plant. 25 245-248.

Wium-Anderson, S. and Andersen, J.M. (1972b) The influence of vegetation on the redox profile of Grane Langsø, a Danish Lobelia lake. Limnol. Oceanogr. 17 948-952.

Wium-Andersen, S. and Andersen, J.M. (1972a) Carbon dioxide content of the interstitial water in the sediment of Grane Langsø, a Danish Lobelia lake. Limn. Oceanogr. 17 943-947.

Wood, J.T. and Greenwood D.J. (1971) Distribution of carbon dioxide and oxygen in the gas phase of aerobic soils. J.Soil Sci. 22 281-288.

Yamada, N. and Ota,Y. (1958) Study on the respiration of crop plants. (7) Enzymatic oxidation of ferrous iron by root of rice plant. Proc.Crop Sci.Soc., Japan, 26 205-210.

Yocum, C.S. and Hackett, D.P. (1957). Participation of cytochromes in the respiration of the aroid spadix. Pl.Physiol. 32, 186-191.

Yoshida, S., Coronel, V., Parao, T. and de los Reyes, E. (1974). Soil carbon dioxide flux and rice photosynthesis. Soil Sci. Plant Nutr. 20 381-386.

Yu, P.T., Stolzy, L.H. and Letey, J. (1969). Survival of plants under prolonged flooded conditions. Agron. J. 61 844-847.

Yu, T.J. and Li, S.H. (1956) Studies on the oxidation-reduction processes in paddy soils. I. Conditions affecting redox potentials. Soil Sci.Soc. China, Reports to 6th Int.Congr. Soil Sci. (Inst.Soil Sci., Nanking).

Zelitch, I. (1965) Environmental and biochemical control of stomatal movement in leaves. Biol.Rev. 40 463-482.

Zelitch, I. and Waggoner, P.E. (1962) Effect of chemical control of stomata on transpiration of intact plants. Proc.Natn. Acad.Sci. U.S.A. 48 1297-1299.

Zentmeyer, G.A. (1966) Soil aeration and plant disease. Proc. Conf. on "Drainage for Efficient Crop Production", Amer.Soc. Agric.Eng., 15-16, 36.

Barber, D.A. (1956). The physiology of Equisetum limosum with special reference to its gaseous exchange. Ph.D. thesis, Univ. of Liverpool.

Currie, J.A. (1962) The importance of aeration in providing the right conditions for plant growth. J.Sci.Food Agric. 13 380-385.